U.S.NRC

United States Nuclear Regulatory Commission

Protecting People and the Environment

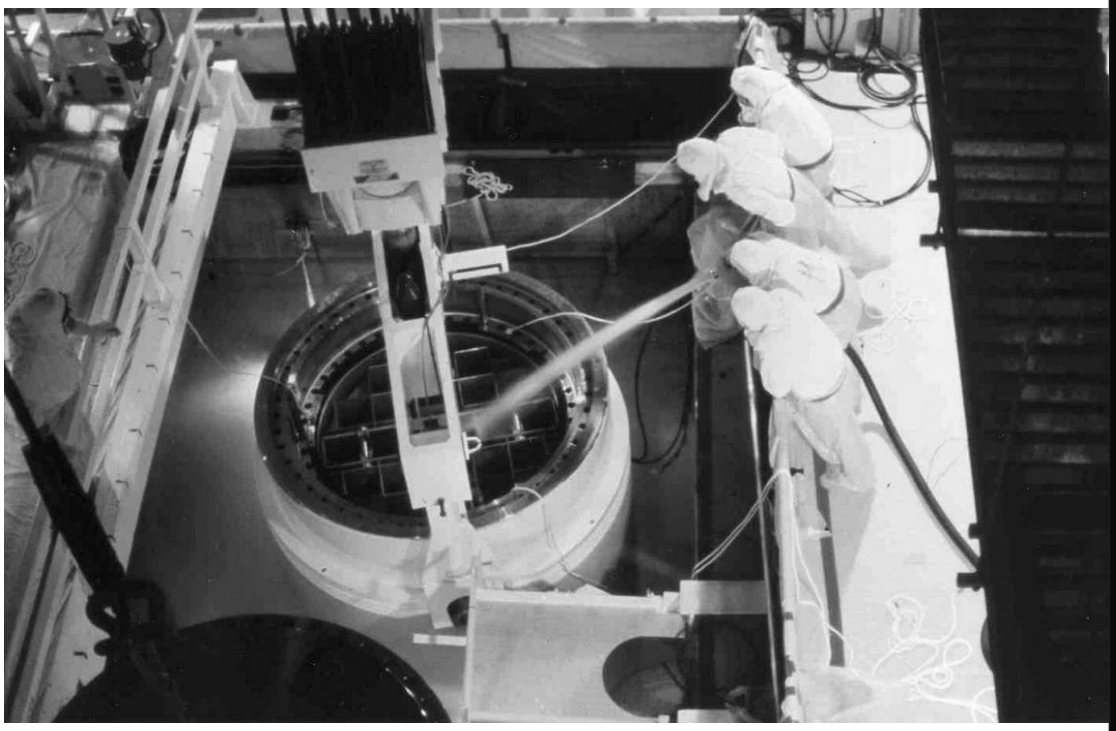

Sensitivity and Uncertainty Analysis of Commercial Reactor Criticals for Burnup Credit

Office of Nuclear Regulatory Research

AVAILABILITY OF REFERENCE MATERIALS IN NRC PUBLICATIONS

NRC Reference Material

As of November 1999, you may electronically access NUREG-series publications and other NRC records at NRC's Public Electronic Reading Room at http://www.nrc.gov/reading-rm.html. Publicly released records include, to name a few, NUREG-series publications; *Federal Register* notices; applicant, licensee, and vendor documents and correspondence; NRC correspondence and internal memoranda; bulletins and information notices; inspection and investigative reports; licensee event reports; and Commission papers and their attachments.

NRC publications in the NUREG series, NRC regulations, and *Title 10, Energy*, in the Code of *Federal Regulations* may also be purchased from one of these two sources:

1. The Superintendent of Documents
   U.S. Government Printing Office
   P.O. Box SSOP
   Washington, DC 20402–0001
   Internet: bookstore.gpo.gov
   Telephone: 202–512–1800
   Fax: 202-512-2250
2. The National Technical Information Service
   Springfield, VA 22161–0002
   www.ntis.gov
   1–800–553–6847 or, locally, 703–605–6000

A single copy of each NRC draft report for comment is available free, to the extent of supply, upon written request as follows:

Address: Office of the Chief Information Officer,
Reproduction and Distribution
Services Section
U.S. Nuclear Regulatory Commission
Washington, DC 20555–0001
E-mail: DISTRIBUTION@nrc.gov
Facsimile: 301–415–2289

Some publications in the NUREG series that are posted at NRC's Web site address http://www.nrc.gov/reading-rm/doc-collections/nuregs are updated periodically and may differ from the last printed version. Although references to material found on a Web site bear the date the material was accessed, the material available on the date cited may subsequently be removed from the site.

Non-NRC Reference Material

Documents available from public and special technical libraries include all open literature items, such as books, journal articles, and transactions, *Federal Register* notices, Federal and State legislation, and congressional reports. Such documents as theses, dissertations, foreign reports and translations, and non-NRC conference proceedings may be purchased from their sponsoring organization.

Copies of industry codes and standards used in a substantive manner in the NRC regulatory process are maintained at—

The NRC Technical Library
Two White Flint North
11545 Rockville Pike
Rockville, MD 20852–2738

These standards are available in the library for reference use by the public. Codes and standards are usually copyrighted and may be purchased from the originating organization or, if they are American National Standards, from—

American National Standards Institute
11 West 42nd Street
New York, NY 10036–8002
www.ansi.org
212–642–4900

Legally binding regulatory requirements are stated only in laws; NRC regulations; licenses, including technical specifications; or orders, not in NUREG-series publications. The views expressed in contractor-prepared publications in this series are not necessarily those of the NRC.

The NUREG series comprises (1) technical and administrative reports and books prepared by the staff (NUREG/XXXX) or agency contractors (NUREG/CR-XXXX), (2) proceedings of conferences (NUREG/CP-XXXX), (3) reports resulting from international agreements (NUREG/IA-XXXX), (4) brochures (NUREG/BR-XXXX), and (5) compilations of legal decisions and orders of the Commission and Atomic and Safety Licensing Boards and of Directors' decisions under Section 2.206 of NRC's regulations (NUREG-0750).

U.S.NRC
United States Nuclear Regulatory Commission
Protecting People and the Environment

Sensitivity and Uncertainty Analysis of Commercial Reactor Criticals for Burnup Credit

Manuscript Completed: October 2007
Date Published: January 2008

Prepared by
G. Radulescu, D. E. Mueller, and J. C. Wagner

Oak Ridge National Laboratory
Managed by UT-Battelle, LLC
Oak Ridge, TN 37831-6170

M. Aissa, NRC Project Manager

Prepared for
Division of Systems Analysis
Office of Nuclear Regulatory Research
U. S. Nuclear Regulatory Commission
Washington, DC 20555-0001
NRC Job Code Y6517

ABSTRACT

The purpose of this study is to provide insights into the neutronic similarities that may exist between a generic cask containing typical spent nuclear fuel assemblies and commercial reactor critical (CRC) state-points. Forty CRC state-points from five pressurized-water reactors were selected for the study and the type of CRC state-points that may be applicable for validation of burnup credit criticality safety calculations for spent fuel transport/storage/disposal systems are identified. The study employed cross-section sensitivity and uncertainty analysis methods developed at Oak Ridge National Laboratory and the TSUNAMI set of tools in the SCALE code system as a means to investigate system similarity on an integral and nuclide-reaction specific level. The results indicate that, except for the fresh fuel core configuration, all analyzed CRC state-points are either highly similar, similar, or marginally similar to a generic cask containing spent nuclear fuel assemblies with burnups ranging from 10 to 60 GWd/MTU. Based on the integral system parameter, c_k , approximately 30 of the 40 CRC state-points are applicable to validation of burnup credit in the generic cask containing typical spent fuel assemblies with burnups ranging from 10 to 60 GWd/MTU. The state-points providing the highest similarity (c_k>0.95) were attained at or near the end of a reactor cycle. The c_k values are dominated by neutron reactions with major actinides and hydrogen, as the sensitivities of these reactions are much higher than those of the minor actinides and fission products. On a nuclide-reaction specific level, the CRC state-points provide significant similarity for most of the actinides and fission products relevant to burnup credit. A comparison of energy-dependent sensitivity profiles shows a slight shift of the CRC k_{eff} sensitivity profiles toward higher energies in the thermal region as compared to the k_{eff} sensitivity profile of the generic cask. Parameters representing coverage of the application by the CRCs on an energy-dependent, nuclide-reaction specific level (i.e., effectiveness of the CRCs for validating the cross sections as used in the application) were also examined. Based on the CRCs with c_k>0.8 and an assumed relative standard deviation for uncovered covariance data of 25%, the relative standard deviation of k_{eff} due to uncovered sensitivity data varies from 0.79% to 0.95% for cask burnups ranging from 10 to 60 GWd/MTU. As expected, this uncertainty in k_{eff} is largely dominated by noncoverage of sensitivities from major actinides and hydrogen. The contributions from fission products and minor actinides are very small and comparable to statistical uncertainties in k_{eff} results. These results (again, assuming a 25% uncertainty for uncovered covariance data) indicate that there could be approximately 1% uncertainty in the calculated application k_{eff} due to incomplete neutronic testing (validation) of the software by the CRCs. However, this conclusion also assumes all other uncertainties in the complex CRC configurations (e.g., isotopic compositions of burned fuel, operation history, data) are well known. To accomplish this, an evaluation and quantification of the uncertainties in the CRC configurations is needed prior to the use of CRCs for code validation (i.e., quantifying code bias and bias uncertainty).

FOREWORD

In 1999 the United States Nuclear Regulatory Commission (U.S. NRC) issued initial recommended guidance for using reactivity credit due to fuel irradiation (i.e., burnup credit) in the criticality safety analysis of spent pressurized-water-reactor (PWR) fuel in storage and transportation packages. This guidance was issued by the NRC Spent Fuel Project Office (SFPO) as Revision 1 to Interim Staff Guidance 8 (ISG8R1) and published in the *Standard Review Plan for Transportation Packages for Spent Nuclear Fuel*, NUREG-1617 (March 2000). With this initial guidance as a basis, the NRC Office of Nuclear Regulatory Research initiated a program to provide the SFPO with technical information that would:

- enable realistic estimates of the subcritical margin for systems with spent nuclear fuel (SNF) and an increased understanding of the phenomena and parameters that impact the margin, and
- support the development of technical bases and recommendations for effective implementation of burnup credit and provide realistic SNF acceptance criteria while maintaining an adequate margin of safety.

An outcome of the research program was Revision 2 to Interim Staff Guidance 8 (ISG8R2), which expand the guidance to: (1) extend the range of allowed burnup and cooling time; (2) allow loading of assemblies exposed to burnable absorbers; (3) removing the loading offset for initial ^{235}U enrichments between 4 and 5 percent; and (4) indicate an acceptable source for selecting a bounding axial burnup profile(s). The Recommendation that burnup credit be based on only the actinide compositions remained unchanged, and hence a focus of current work is to investigate the technical basis for enabling credit for fission products. A significant number of domestic and international studies have been performed to help understand the components that influence the negative reactivity available with burnup credit, including the presence of the fission product nuclides. However, the availability of adequate experimental benchmark data for validation has continued to be an issue. The purpose of this study was to provide insights into the neutronic similarities that may exist between a transportation cask containing typical spent nuclear fuel assemblies and commercial reactor critical (CRC) state-points, which have been proposed by applicant for criticality validation. The study employed cross-section sensitivity and uncertainty analysis methods developed at Oak Ridge National Laboratory and the TSUNAMI set of tools in the SCALE code system as a means to investigate system similarity on an integral and nuclide-reaction specific level. The results indicate that the CRC configurations attained at or near the end of a reactor cycle are highly similar neutronically to a cask loaded with spent fuel, and therefore applicable to validation of burnup credit criticality calculations. However, it is also noted that the CRC state-points are complex configurations that include considerable uncertainty (e.g., isotopic compositions of the burned fuel, operating history, data). Hence, while this work addressed the issue of neutronic similarity, future work is suggested to evaluate and better understand the uncertainties in the CRC configurations that should be considered in their use as part of code validation.

Farouk Eltawila, Director
Division of Systems Analysis

CONTENTS

Page

LIST OF FIGURES

LIST OF FIGURES (continued)

LIST OF FIGURES (continued)

Figure **Page**

LIST OF TABLES

ACKNOWLEDGMENTS

This work was performed under contract with the Office of Nuclear Regulatory Research, U.S. Nuclear Regulatory Commission (NRC). The authors acknowledge useful questions and comments from Carl J. Withee of the NRC Division of Spent Fuel Storage and Transportation (SFST) during the process of this study and the review comments and suggestions provided by staff of SFST and the Office of Nuclear Regulatory Research. The authors gratefully acknowledge John M. Scaglione of the Yucca Mountain Project for his invaluable contribution to this report by supplying MCNP input files for the Crystal River Unit 3 CRCs. The authors would like to thank Bryan L. Broadhead and Mark D. DeHart for their peer review of this document and Cynthia C. Southmayd for her careful editing of the final report.

1 INTRODUCTION

A commercial reactor critical (CRC) state-point is either a hot zero-power critical condition attained after sufficient cooling time to allow the fission product xenon inventory to decay or at-power equilibrium critical condition where xenon worth has reached a fairly stable value. Due primarily to the differences in physical characteristics between CRC state-points and spent nuclear fuel in storage and transport casks, the applicability of CRC state-points to validation of burnup credit criticality safety calculations has been repeatedly called into question. A number of studies have been previously carried out to compare general problem characteristics between the two types of systems to support the case for applicability, but a conclusive demonstration of applicability has not been performed.[1, 2, 3] These studies focused on neutron spectra comparisons, determining trends in calculated k_{eff} values and assessing the effects on k_{eff} of specific system characteristics such as material temperatures. A concern has been raised that the reactivity of the CRCs is driven by the low-burnup fuel, which would render CRC experiments inappropriate for burnup credit validation studies.[4] The development and release of the Tools for Sensitivity and Uncertainty Analysis Methodology Implementation (TSUNAMI) (Refs. 5, 6, and 7) in the Standardized Computer Analyses for Licensing Evaluation (SCALE) 5 (Ref. 8) provides an ability to calculate and compare detailed information on the physics of the CRCs and applications of interest.

This report provides an evaluation of the neutronic similarities between a generic high-capacity, rail-type, burnup credit cask containing typical spent fuel and 40 CRC state-points based on indices and parameters computed with the TSUNAMI tools and identifies the state-points that are most similar to the generic cask. Integral and nuclide-reaction specific indices indicative of k_{eff} sensitivity to cross sections and to cross-section uncertainties are used to assess the similarities of the two types of systems. The set of nuclides considered in sensitivity evaluations consist of actinides and major fission products that are important for burnup credit criticality calculations for spent fuel casks. The analysis evaluates 40 critical configurations from five pressurized-water reactors (PWRs); Crystal River Unit 3 (33 configurations), Sequoyah Unit 2 (three configurations), Surry Unit 1 (two configurations), Three Mile Island (TMI) Unit 1 (a single configuration), and North Anna Unit 1 (a single configuration). These state-points are deemed to be representative of the available CRC state-points and were expected to be at least marginally applicable to burnup credit criticality safety validation. A series of Yucca Mountain Project (YMP) studies that provide descriptions, isotopic evaluations, and criticality calculations for additional CRC state-points from commercial reactors McGuire, Sequoyah, Three Mile Island, Quad Cities, and LaSalle, were not evaluated in this report. Note that the CRC data evaluated in the YMP studies were taken before most of the nuclear industry moved to extended cycles (18- and 24-month cycles) and reactor uprates. Currently, most of the commercial reactors use higher enrichments (many close to the 5 wt% limit) and some use complex fuel designs such as axial and asymmetric enrichments. Gathering data for more recent CRCs may be necessary to provide adequate benchmarks for burnup credit validation of systems designed for modern spent fuel types.

The objective of this analysis report is limited to determination of neutronic similarity between the generic cask and the evaluated CRCs using the TSUNAMI methodology. The applicability of a set of benchmark experiments to validation of burnup credit calculations for a design system may be based on the similarities of material compositions and neutron spectra of the two types of systems.[9] However, there are other characteristics, such as material and environmental condition uncertainties, that should also be considered in the process of selecting experiments for use in bias determination. Information regarding uncertainties in operating parameters of the nuclear reactors or in material compositions of the CRC configurations is not available in the YMP studies. Therefore, use of CRCs as a component of the benchmarking methodology requires additional evaluations to determine whether the data collection process for the CRCs is of benchmark quality, particularly in view of the caveat in standard ANS-19.4[10] regarding data acquisition methods, and to determine isotopic uncertainties or k_{eff} penalties for conservatively bounding such uncertainties.

Note that the term “applicability” is used throughout this report to indicate that sufficient neutronic similarity between an evaluated CRC state-point and the generic cask has been determined so that the CRC state-point could be used as a component of the benchmarking methodology, providing the CRCs satisfy benchmark quality requirements.

The structure of this report is the following. Section 2 describes the theoretical bases and the tools of cross-section sensitivity and uncertainty (S/U) analysis methods. Descriptions of a generic spent fuel cask that serves as the application system, the CRC configurations, and required calculations for the S/U analysis are presented in Sect. 3. An analysis of the TSUNAMI results is provided in Sect. 4. Conclusions and recommendations are presented in Sect. 5.

2 SENSITIVITY/UNCERTAINTY ANALYSIS METHOD

Sensitivity/uncertainty analysis methods can be used to demonstrate that nuclear systems with similar physical characteristics, including material compositions, geometry, and neutron flux spectra, exhibit similar sensitivities of the effective neutron multiplication factor, k_{eff}, to perturbations in the neutron cross-section data on an energy-dependent, nuclide-reaction specific level. The assessment of system similarities and shared variance, due to cross-section uncertainties, in the computed values of k_{eff} is particularly useful in determining applicability of critical experiments to be used to determine bias and uncertainty of criticality safety calculations. The Oak Ridge National Laboratory (ORNL) has formulated the theoretical bases for use of S/U analysis methods in criticality safety validation[11] and developed the software tools needed to implement the methodology in the SCALE code system.[5, 6, 7] A set of indices has been defined for use in S/U analyses that provide a measure of the neutronic similarity between a design system and a critical experiment. Methodologies for determining first-order-linear perturbation theory sensitivity coefficients with multigroup Monte Carlo methods in SCALE employ both forward and adjoint neutron fluxes.[12]

The analyses presented in this report are limited to system similarity evaluations and are based on results obtained with cross-section S/U analysis tools in SCALE 5.1, including TSUNAMI-3D (Tools for Sensitivity and Uncertainty Analysis Methodology Implementation in Three Dimensions) and TSUNAMI-IP (Tools for Sensitivity and Uncertainty Analysis Methodology Implementation - Indices and Parameters). SCALE 238-GROUP ENDF/B-V library (235GROUPNDF5) was used in cross-section processing and transport calculations and the SCALE 44-GROUP ENDF/B-V recommended covariance library (44GROUPV5REC) was used in S/U calculations. The TSUNAMI-3D calculations for the analyses invoke functional modules SENLIB, BONAMIST, NITAWLST, KENO V.a, and SAMS to determine the sensitivity of the calculated value of k_{eff} to the nuclear data used in the calculation as a function of nuclide, reaction type, and energy. TSUNAMI-IP produces a set of integral and nuclide-reaction specific indices indicative of similarity of nuclear systems. These analyses use sensitivity coefficients and energy-dependent sensitivity profiles,[11] integral index c_k,[11] and the nuclide-reaction specific integral index g[13] to assess the similarities of a generic spent fuel cask and CRC state-points. Integral index c_k is generally used to assess neutronic similarity between systems since a c_k value is based on uncertainty correlations from all nuclides in the systems. The global similarity criteria require the major sensitivity components of each system pair to match. Reference 11 demonstrates that c_k values of 0.80 or higher constitute systems that are similar to the extent that they are useful in the determination of bias and associate uncertainty. Further, Ref. 11 recommends that the validation methodology should include about 15 to 20 very correlated systems (c_k of 0.90 or higher) or 25 to 40 moderately correlated systems (c_k of 0.80 or higher).

2.1 SENSITIVITY COEFFICIENTS, S_K

The sensitivity of k_{eff} to a particular nuclide-reaction pair macroscopic cross section Σ_x^n, referred to as sensitivity coefficient, provides a measure of the first-order effect of perturbations in nuclear reaction x for nuclide n upon k_{eff}. Nuclear data for which sensitivity coefficients are computed in a TSUNAMI calculation include total, scatter, capture and fission cross sections, $\bar{\nu}$ (average number of neutrons per fission event), and χ (distribution function of fission neutrons). The sensitivity coefficient has been defined in Ref. 11 as:

$$S_{k,\Sigma_x^n} = \frac{\delta k_{eff} / k_{eff}}{\delta \Sigma_x^n / \Sigma_x^n} \quad . \tag{1}$$

A sensitivity coefficient is computed as the sum over all energy groups of the sensitivities of k_{eff} to group-wise cross-section data. The sensitivity coefficient expressed as a function of energy,

$$S_{k,\Sigma_{x,j}^n} = \frac{\delta k_{eff} / k_{eff}}{\delta \Sigma_{x,j}^n / \Sigma_{x,j}^n}, \quad (2)$$

where j denotes an energy group, is referred to as an energy-dependent sensitivity profile. In addition to an explicit change in the affected nuclide reaction rate, perturbations of $\sum_{x,j}^n$ produce secondary effects on the resonance-shielded values of some cross sections, which in turn affect k_{eff}. Therefore, a complete sensitivity coefficient consists of two components referred to as explicit and implicit sensitivity coefficients. The implicit sensitivity component is the cumulative sensitivity of k_{eff} to all processes that are influenced by the perturbations in the value of $\sum_x^n$. TSUNAMI-3D computes sensitivity profiles in a SCALE energy group structure. A graphical representation of sensitivity per unit lethargy as a function of neutron energy can be generated with the Javapeño plotting package of the SCALE code system (Ref. 14).

2.2 INTEGRAL INDEX c_k

The effects of uncertainties in nuclear data on the k_{eff} values of systems with the same materials and similar spectra are correlated. Integral index c_k is a measure of similarity of two systems in terms of their common components of uncertainty in k_{eff} due to cross-section uncertainties. A c_k value represents the correlation coefficient between sensitivity weighted uncertainties in the design system (application) and an experiment. The definition and intended use of the integral index c_k are documented in Refs. 7 and 11.

Relative uncertainties in cross-section data can be represented as the elements of an $M \times M$ matrix, $C_{\alpha,\alpha} \equiv \left[\frac{cov(\alpha_n, \alpha_m)}{\alpha_n \alpha_m} \right]$, where M is the product of the number of nuclide-reaction pairs and the number of energy groups, $\alpha \equiv (\alpha_n)$ is a variable array containing the cross-sections of nuclide-reaction-energy group triplets. The $C_{\alpha,\alpha}$ matrix contains covariance data that provide a measure of how strong the correlation of uncertainty is between two nuclide-reaction-energy group triplets. An individual element of the covariance matrix, c_{nm}, is the ratio of the covariance of cross-section uncertainties to the product of cross-section expectation values for nuclide-reaction-energy group triplets n and m. In a TSUNAMI-IP calculation, the covariance data are propagated to relative changes in the calculated k_{eff} value of a given system via the sensitivity coefficients. An uncertainty matrix is computed for the system k_{eff} values, $C_{kk} = S_k C_{\alpha,\alpha} S_k^\dagger$, where S_k and $S_k^\dagger$ are the matrix and the transpose matrix, respectively, containing sensitivities of the calculated k_{eff} values of critical systems to the α parameters. S_k is an $I \times M$ matrix defined as:

$$S_k \equiv \left[\frac{\alpha_m}{k_i} \frac{\partial k_i}{\partial \alpha_m} \right], \text{ i = 1, 2, …, } I\text{; } m = 1, 2, \ldots, M,$$

where I is the number of critical systems being considered.

The diagonal elements of the C_{kk} matrix represent the relative variance values, η_i^2, for each of the systems under consideration, and the off-diagonal elements, η_{ij}^2, represent the common variance between two systems. A correlation coefficient is defined as:

$$c_k = \frac{\eta_{ij}^2}{(\eta_i \eta_j)}, \tag{3}$$

such that the single c_k value represents the correlation coefficient between sensitivity weighted uncertainties in system *i* and system *j*. The interpretation of the correlation coefficient is the following: a value of 0.0 represents no correlation between the systems, a value of 1.0 represents full correlation between the systems, and a value of -1.0 represents a full anticorrelation.

Covariance data for some nuclide-reaction pairs are not available.[7] In the TSUNAMI-IP calculations for this analysis, the default value of 0.05 was used for the fractional standard deviation in cross-section data for nuclide-reaction pairs for which covariance data are not available. This value is deemed to be a conservative estimation for fractional standard deviation in cross-section data in the thermal and epithermal energy regions and is based on the fractional standard deviation in cross-section data for nuclide-reaction pairs for which covariance data are available.[15]

2.3 INTEGRAL INDEX *G* AND NUCLIDE-REACTION SPECIFIC INTEGRAL INDEX *g*

The *G* index provides a measure of the similarity of two systems based on normalized differences in the energy-dependent sensitivity data for fission, capture, and scatter reactions, as appropriate for each nuclide. Differences in energy-dependent sensitivity profiles are indicative of the coverage of the application by an experiment (i.e., the effectiveness of the experiment for validating the cross-sections as used in the application). The definitions of the integral index *G* and nuclide-reaction specific integral index *g* are documented in Refs. 7 and 13. An example of analysis that utilizes the integral index *g* to assess the similarity between an application and a set of experiments on a nuclide-reaction specific level is available in Ref. 16.

The *G* index is defined as

$$G = 1 - \frac{\sum_n \sum_x \sum_j \left(S_{x,j}^{a,n} - S_{x,j}^{e',n} \right)}{\sum_n \sum_x \sum_j S_{x,j}^{a,n}},$$

where

$$S_{x,j}^{e',n} = \begin{cases} S_{x,j}^{e,n}, where & \left|S_{x,j}^{a,n}\right| \geq \left|S_{x,j}^{e,n}\right| \ and \ \dfrac{S_{x,j}^{a,n}}{\left|S_{x,j}^{a,n}\right|} = \dfrac{S_{x,j}^{e,n}}{\left|S_{x,j}^{e,n}\right|} \\ S_{x,j}^{a,n}, where & \left|S_{x,j}^{a,n}\right| < \left|S_{x,j}^{e,n}\right| \ and \ \dfrac{S_{x,j}^{a,n}}{\left|S_{x,j}^{a,n}\right|} = \dfrac{S_{x,j}^{e,n}}{\left|S_{x,j}^{e,n}\right|} \\ 0, & otherwise \end{cases}$$

Superscripts *a* and *e* denote the application and an experiment, respectively; the *n* summation is performed over all nuclides present in the application system; the *x* summation is performed over fission, capture, and scatter reactions, as appropriate for each nuclide; and the *j* summation is performed over all energy groups.

A *G* value of 1.0 indicates complete coverage of the application by the experiment for the particular nuclide-reaction pair, while a *G* value of 0.0 indicates no coverage of the application by the experiment for the particular nuclide-reaction pair.

The nuclide-reaction specific integral index *g* provides a measure of the intersection area of the application and the experiment sensitivity profiles. It is defined in terms of the normalized differences of the group-wise sensitivity coefficients for a particular nuclide *n* and reaction *x*, summed over all energy groups *j*, as:

$$g_x^n = 1 - \frac{\sum_j \left(S_{x,j}^{a,n} - S_{x,j}^{e',n} \right)}{\sum_j S_{x,j}^{a,n}} , \qquad (4)$$

A *g* value of 1.0 indicates complete coverage of the application by the experiment for the particular nuclide-reaction pair, while a *g* value of 0.0 indicates no coverage of the application by the experiment for the particular nuclide-reaction pair.

2.4 UNCERTAINTY ESTIMATE FOR NON-COVERED SENSITIVITY DATA

A method is available in TSUNAMI-IP to assess the impact, or penalty for non-covered sensitivity data, when sufficient critical experiments are not available to provide complete coverage for an application.[7] This quantity is intended to represent the uncertainty in the calculated value of k_{eff} due to inadequate validation coverage or when an extension of the range of applicability is required.[7] However, the k_{eff} penalty for non-covered sensitivity data computed in a TSUNAMI-IP calculation has not been validated in comparative studies that use a different method of calculation. Therefore, in this report the penalty for non-covered sensitivity data is used only as a measure of non-similarity between the composite set of the CRCs and the generic cask and it will be referred to as "relative standard deviation of k_{eff} due to uncovered sensitivity data" in the other report sections.

The definition of penalty for non-covered sensitivity data and the technique to be used in penalty calculation are described in Refs. 7 and 16. The penalty is estimated as:

$$\Delta k_{eff} / k_{eff} = \sqrt{Z_a C_{\alpha,\alpha} Z_a^{\dagger}} \qquad (5)$$

where $C_{\alpha,\alpha}$ is the matrix of the cross-section-covariance data defined in Section 2.2, $\dagger$ indicates a transpose, and Z_a is a vector of minimum differences in the sensitivity coefficients for the application with respect to all experiments. The elements of vector Z_a are computed as:

$$Z_{x,j}^{a,n} = S_{x,j}^{a,n} - C_{x,j}^{a,n}$$

where

$C_{x,j}^{a,n}$ is a composite of the best available sensitivity data from all experiments and is defined as $C_{x,j}^{a,n} = S_{x,j}^{e',n}$ for the experiment that satisfies $\min\left|S_{x,j}^{a,n} - S_{x,j}^{e',n}\right|$

$$S_{x,j}^{e',n} = \begin{cases} S_{x,j}^{e,n}, \text{ where } \left|S_{x,j}^{a,n}\right| \geq \left|S_{x,j}^{e,n}\right| \text{ and } \dfrac{S_{x,j}^{a,n}}{\left|S_{x,j}^{a,n}\right|} = \dfrac{S_{x,j}^{e,n}}{\left|S_{x,j}^{e,n}\right|} \\ S_{x,j}^{a,n}, \text{ where } \left|S_{x,j}^{a,n}\right| < \left|S_{x,j}^{e,n}\right| \text{ and } \dfrac{S_{x,j}^{a,n}}{\left|S_{x,j}^{a,n}\right|} = \dfrac{S_{x,j}^{e,n}}{\left|S_{x,j}^{e,n}\right|} \\ 0, \qquad \text{otherwise} \end{cases}$$

Superscripts *a* and *e* or e' denote the application and an experiment, respectively; *n* represents a particular nuclide present in the application system; *x* represents a particular reaction (fission, capture, and scatter reactions, as appropriate for each nuclide); and *j* represents a particular energy group.

Only experiments that exhibit a certain degree of similarity to the application, based on *g* integral index and/or a global integral index, can be used in a penalty calculation. Use of minimum differences in group-wise nuclide-reaction specific sensitivity coefficients from the most similar experiments ensures that only uncovered sensitivity data is used in the penalty calculations. Note that in the limit that no relevant validation experiments are used in penalty calculation, the penalty assessed is simply the uncertainty in the application's criticality calculation due to cross-section covariance data.

2.5 DIRECT PERTURBATION CALCULATIONS

The direst perturbation method is used to assess the quality of the sensitivity coefficients obtained in a TSUNAMI-3D calculation that could be affected by the quality of the neutron fluxes from forward and adjoint Monte Carlo calculations with KENO V.a. Factors that determine the quality of neutron flux estimates are related to the number and quality of sample neutron tracks or to the size of the unit volumes used in a track-length estimation of the flux.

The macroscopic cross section of a nuclide-reaction pair can be perturbed by changing either the nuclide atom density or the microscopic cross section for the neutron reaction with the nuclide. The direct perturbation method employs variations of nuclide atom density that result in small k_{eff} variations consistent with the linear-perturbation approximation. Applications of this method require k_{eff} results for the nominal system and for the perturbed system with the concentration of the nuclide of interest increased or decreased by the same percentage. The direct total perturbation sensitivity coefficient of k_{eff} to some input quantity is determined as

$$S_k = \frac{\alpha}{k} \times \frac{dk}{d\alpha} = \frac{\alpha}{k} \times \frac{k_{\alpha^+} - k_{\alpha^-}}{\alpha^+ - \alpha^-} \ , \tag{6}$$

where α^+ and α^- represent the increased and decreased values of the input quantity, α, respectively, and k_{α^+} and k_{α^-} represent the corresponding values of k_{eff}. The standard deviation of a direct perturbation sensitivity coefficient is determined as

$$\sigma_S = \left(\left(\frac{\left(\sigma_{k^+}^2 + \sigma_{k^-}^2\right)}{\left(k^+ - k^-\right)^2} + \frac{\sigma_k^2}{k^2} \right) \times \left(\frac{k^+ - k^-}{k} \right)^2 \right)^{1/2} \times \frac{\alpha}{\alpha^+ - \alpha^-} \ . \quad (7)$$

3 CALCULATIONS

The application system for the S/U analysis in this report is a conceptual high-capacity spent fuel cask containing typical PWR spent fuel assemblies. This system will be compared with 40 CRC state-points from various PWRs. A brief description of the physical characteristics of these systems and the set of required calculations for an S/U analysis are presented in this section.

3.1 GENERIC BURNUP CREDIT CASK GBC-32

A generic burnup credit cask design, referred to as GBC-32 cask, has been proposed as a reference configuration for burnup credit studies.[17] The generic cask, which can accommodate 32 PWR assemblies, uses Boral® panels containing ^{10}B as a fixed neutron poison dispersed uniformly with an areal density of 0.0225 g $^{10}B/cm^2$. The strong neutron-absorbing effect of ^{10}B in the Boral® panels reduces neutronic interaction between adjacent fuel assemblies.

3.1.1 Description of Calculations for GBC-32 Cask

CSAS25/KENO V.a (Ref. 18) and TSUNAMI-3D calculations were performed for the GBC-32 cask to validate KENO V.a cask modeling and determine sensitivity profiles in the SCALE 238-energy group structure. The KENO V.a cask model consists of identical spent fuel assemblies of Westinghouse 17×17 OFA type. Pin geometry contains 18 equal-length axial regions that allow specifications of different fuel compositions corresponding to a fuel burnup axial profile. Nodal spent fuel compositions for spent fuel with assembly-average burnup ranging from 10 GWd/MTU to 60 GWd/MTU and a 5-year cooling time were computed using control module STARBUCS in the SCALE code system.[19] A built-in bounding burnup-dependent axial profile was used to automatically generate the spent fuel compositions. Reference 20 has demonstrated that this burnup-dependent axial profile adequately bounds the axial-profile database documented in Ref. 21 and that the database provides an adequate representation of discharged U.S. PWR spent nuclear fuel assembly designs with initial enrichments up to 4.0 wt % ^{235}U and burnups up to 40 GWd/MTU. The nuclides included in fuel compositions consist of the following actinides and major fission products that have been identified in Ref. 4 as being important for burnup credit criticality calculations: ^{234}U, ^{235}U, ^{236}U, ^{238}U, ^{238}Pu through ^{242}Pu, ^{241}Am, ^{243}Am, ^{237}Np, ^{95}Mo, ^{99}Tc, ^{101}Ru, ^{103}Rh, ^{109}Ag, ^{133}Cs, ^{147}Sm, ^{149}Sm through ^{152}Sm, ^{143}Nd, ^{145}Nd, ^{151}Eu, ^{153}Eu, and ^{155}Gd. The mesh option was used in TSUNAMI-3D calculations to generate smaller volumes for accumulation of flux moments to assure accuracy of the sensitivity coefficient calculations. The results of the CSAS25 calculations, i.e., k_{eff} and associated standard deviation (σ), are presented in Table 3.1, along with calculated energy of average lethargy causing fission (EALF). A cutaway view of the KENO V.a cask model is shown in Figure 3.1. Note that the fuel initial enrichments used in the calculations are typical for the selected burnup values. Therefore, the S/U analysis presented in this report is limited to a generic cask containing spent fuel assemblies with the characteristics presented in Table 3.1.

Table 3.1 k_{eff} for GBC-32 cask as a function of spent fuel burnup

Case identifier	Average burnup (GWd/MTU)	Initial enrichment (wt% ^{235}U)	Fuel temperature (K)	EALF (eV)	k_{eff}	σ
GBC10	10	1.9972	293	2.09E-01	0.8975	0.0005
GBC20	20	2.5563	293	2.42E-01	0.8854	0.0006
GBC30	30	3.2025	293	2.67E-01	0.8807	0.0005
GBC40	40	3.7777	293	2.84E-01	0.8776	0.0004
GBC50	50	4.3427	293	2.99E-01	0.8755	0.0006
GBC60	60	4.8819	293	3.14E-01	0.8703	0.0005

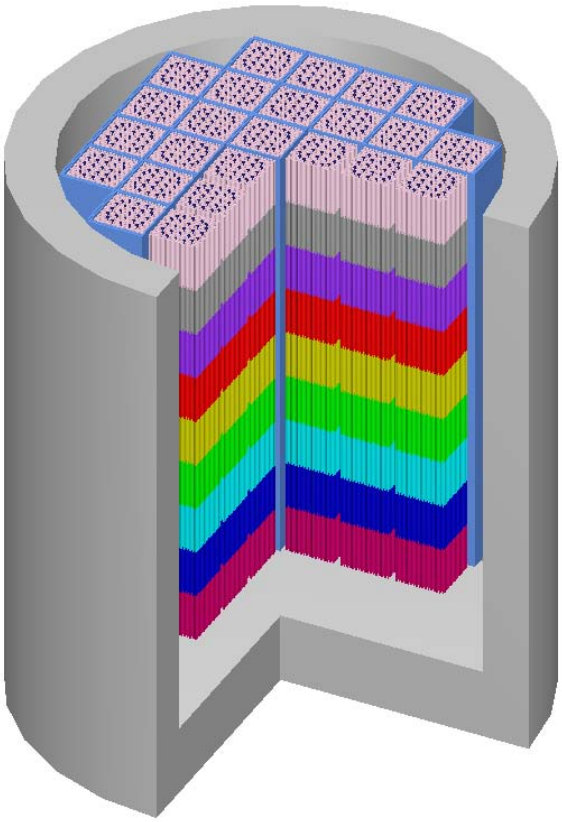

Fig. 3.1 Cutaway view of the KENO V.a model for GBC-32 cask showing the cask bottom half with a quarter of the model removed.

3.2 COMMERCIAL REACTOR CRITICALS

The CRCs evaluated in this analysis are comprised of 40 state-points from various PWRs, including Crystal River Unit 3, Sequoyah Unit 2, Surry Unit 1, TMI Unit 1, and North Anna Unit 1. These state-points are deemed to be representative of the available CRC configurations and are expected to be at least marginally applicable for burnup credit calculation validation. The CRC state-points consist of 37 hot zero-power (HZP) reactor start-up critical conditions and three hot full-power (HFP) critical configurations, and include beginning-of-life (BOL), beginning-of-cycle (BOC), middle-of-cycle (MOC), and end-of-cycle (EOC) reactor core configurations containing either Babcock and Wilcox (B&W) fuel or Westinghouse fuel types.

3.2.1 Description of Crystal River Unit 3 State-Points

Thirty-three Crystal River Unit 3 state-points were evaluated in the S/U analysis. The state-points were HZP startup critical configurations attained during Cycles 1 through 10 of reactor operation. Crystal River Unit 3 is a B&W reactor core design of 177 15×15 fuel assemblies. During Cycles 1 through 10, the reactor used fuel assemblies from 15 fuel batches representing 6 different fuel assembly designs. Each fuel assembly contains 16 guide tubes and 1 instrument tube. Cycles 1A and 4 through 10 used burnable poison rod assemblies (BPRAs) with B_4C-Al_2O_3 as the absorber material. The Crystal River Unit 3 reactor, Cycles 1 through 10, used three rod cluster control assembly (RCCA) banks and one axial power shaping rod assembly (APSRA) bank during startup and operation. The RCCA guide tubes contain 16 control rods made of Ag-In-Cd alloy. The APSRA guide tubes contain 16 axial power shaping rods made of Ag-In-Cd alloy during Cycles 1 through 5 and of stainless steel 304 during Cycles 6 through 10. The insertion heights varied with reactor cycle from completely inserted to completely withdrawn. State-point characteristics, including effective full-power days, the fraction of fuel assemblies in BOC cores, fuel initial enrichments and temperature, core average burnup, soluble boron concentrations and moderator density, are presented in Table 3.2. A detailed description of the Crystal River Unit 3 critical configurations and fuel compositions is available in Refs. 22 and 23.

3.2.2 Description of Sequoyah Unit 2 State-Points

Three Sequoyah Unit 2 Cycle 3 state-points were evaluated in the S/U analysis. The reactor core consisted of 193 Westinghouse fuel assemblies, each comprised of a 17×17 lattice containing 264 fuel rods, 24 control guide tubes, and 1 instrument tube. At-power reactivity control was maintained using four control banks and two shutdown banks of full-length Ag-In-Cd control rod clusters, 44 BPR clusters, containing a total of 656 BPRs, and soluble boron. The critical configurations modeled are based on HZP and HFP conditions at BOC-3 and HFP conditions at the MOC-3 restart. State-point characteristics, including effective full-power days, the fraction of fuel assemblies in BOC cores, fuel initial enrichments and temperature, core average burnup, soluble boron concentrations and moderator density, are presented in Table 3.2. A detailed description of the Sequoyah Unit 2 critical configurations and fuel compositions is available in Ref. 24. Note that a HFP state-point is characterized by high fuel temperatures and equilibrium Xe poison concentrations.

3.2.3 Description of Surry Unit 1 State-Points

Two Surry Unit 1 Cycle 2 state-points were evaluated in the S/U analysis. The reactor core consisted of 157 Westinghouse fuel assemblies, each comprised of a 15×15 lattice containing 204 fuel rods, 20 control rod guide tubes, and 1 instrument tube. At-power reactivity control was maintained using 4 control banks, 28 BPR clusters, containing a total of 320 fresh and 48 depleted BPRs, and soluble boron. The critical configurations modeled are based on HZP conditions at BOC-2 and HFP conditions at EOC-2. State-point characteristics, including effective full-power days, the fraction of fuel assemblies in the BOC core, fuel

initial enrichments and temperature, core average burnup, soluble boron concentration and moderator density, are presented in Table 3.2. A detailed description of the Surry Unit 1 critical configurations and fuel compositions is available in Ref. 25.

3.2.4 Description of TMI Unit 1 State-Points

A single TMI Unit 1 Cycle 5 state-point was evaluated in the S/U analysis. The reactor core consisted of 177 B&W fuel assemblies, each comprised of a 15×15 lattice containing 208 fuel rods, 16 control/safety rod guide tubes, and 1 instrument tube. At-power reactivity control was maintained using 24 full-length Ag-In-Cd control rod clusters and soluble boron. Eight partial-length Ag-In-Cd axial power shape rod clusters were used to control the axial power distribution. The critical configuration modeled is based on HZP startup testing for BOC-5. Cycle-5 startup occurred after a downtime of 6.63 years, and the core consisted primarily of burned fuel, with all fresh fuel loaded on the core outer periphery. State-point characteristics, including effective full-power days, the fraction of fuel assemblies in the BOC core, fuel initial enrichments and temperature, core average burnup, soluble boron concentration and moderator density, are presented in Table 3.2. A detailed description of the TMI Unit 1 critical configuration and fuel compositions is available in Ref. 26.

3.2.5 Description of North Anna Unit 1 State-Points

A single North Anna Unit 1 Cycle 5 state-point was evaluated in the S/U analysis. The reactor core consisted of 157 Westinghouse fuel assemblies, each comprised of a 17×17 lattice containing 264 fuel rods, 24 control rod guide tubes, and 1 instrument tube. At-power reactivity control was maintained using four control banks and two shutdown banks of full-length Ag-In-Cd control rod clusters, 68 BPR clusters containing a total of 912 fresh and 192 depleted BPRs, and soluble boron. The critical configuration modeled in this report is based on HZP startup testing for BOC-5. State-point characteristics, including effective full-power days, the fraction of fuel assemblies in the BOC core, fuel initial enrichments and temperature, core average burnup, soluble boron concentration, and moderator density, are presented in Table 3.2. A detailed description of the critical configuration and fuel compositions is available in Ref. 27.

3.2.6 Description of Calculations for the CRC State-Points

CSAS25/KENO V.a and TSUNAMI-3D calculations were performed for the CRC state-points to validate the KENO V.a reactor core models and compute sensitivity profiles in the SCALE 238-energy group structure for use in a TSUNAMI-IP calculation. Due to the large amount of input data describing a reactor critical configuration, a computer program was developed to generate CSAS25/KENO V.a input files automatically. The input data for these files were extracted from the CSASN (SCALE 4) or MCNP 4B (Ref. 28) input files and reactor core descriptions available in Refs. 22 through 27. KENO V.a pin geometry for Sequoyah, Surry, TMI, and North Anna critical configurations consists of a single mixture composition based on average assembly burnup. The KENO V.a core model for Crystal River is much more complex. It includes an 18-zone and a 17-zone axial profile for fuel rods and burnable poison rods, respectively, control rods and axial power shaping rods, spacer grids, and homogenized assembly hardware regions. The majority of the configurations had eighth-core symmetry, which requires modeling for only 29 different fuel assemblies. A horizontal and a partial vertical cross section of the KENO V.a geometry for a Crystal River state-point is illustrated in Figure 3.2. Table 3.3 presents a comparison of the k_{eff} results of the CSAS25 validation calculations and the k_{eff} results documented in Refs. 22 through 27. Generally, the CSAS25 results are in good agreement with the results described in the referenced documents, indicating that the mixture compositions and geometry models are consistent between the current and previous calculations. Only the results for the last two Crystal River state-points are significantly lower than the comparison MCNP calculation results (see Table 3.3). The largest difference

is observed in the case of Crystal River state-point 32, which has the highest coolant boron concentration (2326 ppm). The ORNL staff has thoroughly verified CSAS25/KENO V.a material compositions and geometry modeling against the YMP MCNP input files, but could not identify any differences between the inputs to the two computational methods. Considering the complexity of the CRC configurations, modeling errors in the CSAS25 input files for the two Crystal River state-points may exist. However, the impact on sensitivity coefficients is expected to be less important because these coefficients are defined in terms of relative values (see Eq. 1). Further exploration of the k_{eff} deviation exhibited by these two state-point models would be necessary prior to using them in bias determination analysis.

To reduce the computer time of a TSUNAMI-3D calculation using the SCALE 238-energy group library for a Crystal River state-point, the total number of nuclides in KENO V.a fuel mixtures was reduced from more than 40,000 to approximately 20,000 by including in fuel compositions only the actinides and the major fission products that have been identified as being important to burnup credit criticality calculations (see Sect. 3.1.1). While this approach significantly reduced the required computer time, it had minimal effects on the accuracy of the sensitivity coefficients because these coefficients are defined in terms of relative values.

Table 3.2 Summary of CRC state-point characteristics

State point	Reactor cycle	FFFA[a]	EFPD[b]	Average core burnup[c] (GWd/MTU)	Initial enrichment (wt% ^{235}U)	Fuel temperature (K)	Soluble boron (ppm)	Moderator density (g/cm^3)
Crystal River Unit 3								
1	1A	1.0	0	0	1.93 – 2.83	551	1403	0.7682
2	1B	0	268.8	8.09	1.93 – 2.83	551	1106	0.7686
3	1B	0	411	12.34	1.93 – 2.83	553	493	0.7653
4	2	0.32	0	8.67	2.54 – 2.83	551	1294	0.7682
5	3	0.32	0	7.50	2.54 – 2.83	551	1428	0.7682
6	3	0	168.5	12.54	2.54 – 2.83	553	737	0.7653
7	3	0	250	14.98	2.54 – 2.83	554	562	0.7633
8	4	0.38	0	6.92	2.62 – 2.95	551	1384	0.7682
9	4	0	228.1	14.00	2.62 – 2.95	551	705	0.7682
10	4	0	253	14.77	2.62 – 2.95	554	502	0.7633
11	5	0.43	0	7.08	2.62 – 3.29	551	1540	0.7682
12	5	0	388.5	19.12	2.62 – 3.29	554	605	0.7633
13	6	0.34	0	12.01	2.62 – 3.49	551	1574	0.7682
14	6	0	96	14.99	2.62 – 3.49	552	1211	0.7662
15	6	0	400	24.41	2.62 – 3.49	553	390	0.7653
16	7	0.45	0	10.02	2.54 – 3.84	551	2033	0.7682
17	7	0	260.3	18.09	2.54 – 3.84	551	1223	0.7682
18	7	0	291	19.04	2.54 – 3.84	553	1149	0.7643
19	7	0	319	19.91	2.54 – 3.84	551	1048	0.7682
20	7	0	462.3	24.35	2.54 – 3.84	550	563	0.7691
21	7	0	479	24.87	2.54 – 3.84	553	520	0.7691
22	8	0.41	0	12.26	1.93 – 3.94	551	2101	0.7682
23	8	0	97.6	15.27	1.93 – 3.94	553	1751	0.7653
24	8	0	139.8	16.58	1.93 – 3.94	553	1612	0.7653
25	8	0	404	24.74	1.93 – 3.94	553	865	0.7643
26	8	0	409.6	24.91	1.93 – 3.94	553	865	0.7643
27	8	0	515.5	28.19	1.93 – 3.94	553	675	0.7643
28	9	0.36	0	14.18	1.93 – 3.94	551	2212	0.7682
29	9	0	158.8	19.10	1.93 – 3.94	553	1572	0.7683
30	9	0	219	20.96	1.93 – 3.94	553	1481	0.7653
31	9	0	363.1	25.42	1.93 – 3.94	555	963	0.7614
32	10	0.41	0	15.24	3.84 – 4.167	551	2326	0.7682
33	10	0	573.7	33.00	3.84 – 4.167	553	516	0.7643
Sequoyah Unit 2								
1	3	0.35	0	11.00	2.6 – 3.8	559	1685	0.7540
2	3	0.35	0	11.15	2.6 – 3.8	901	1150	0.7149
3[d]	3	0	205	19.25	2.6 – 3.8	901	475	0.7149
Surry Unit 1								
1	2	0.54	0	6.93	1.9 – 3.3	559	1030	0.7540
2	2	0	204	13.85	1.9 - 3.3	910	123	0.7327
TMI Unit 1								
1[e]	5	0.29	0	11.44	2.6 - 2.9	551	1182	0.7540
North Anna Unit 1								
1	5	0.43	0	11.07	3.2 - 3.6	559	1836	0.7540

[a]Fraction of fresh fuel assemblies in the reactor core.
[b]Effective full-power days.
[c]Core average burnup for Crystal River Unit 3 is provided in Ref. 29.
[d]Startup after a downtime of 2.73 years.
[e]Startup after a downtime of 6.63 years.

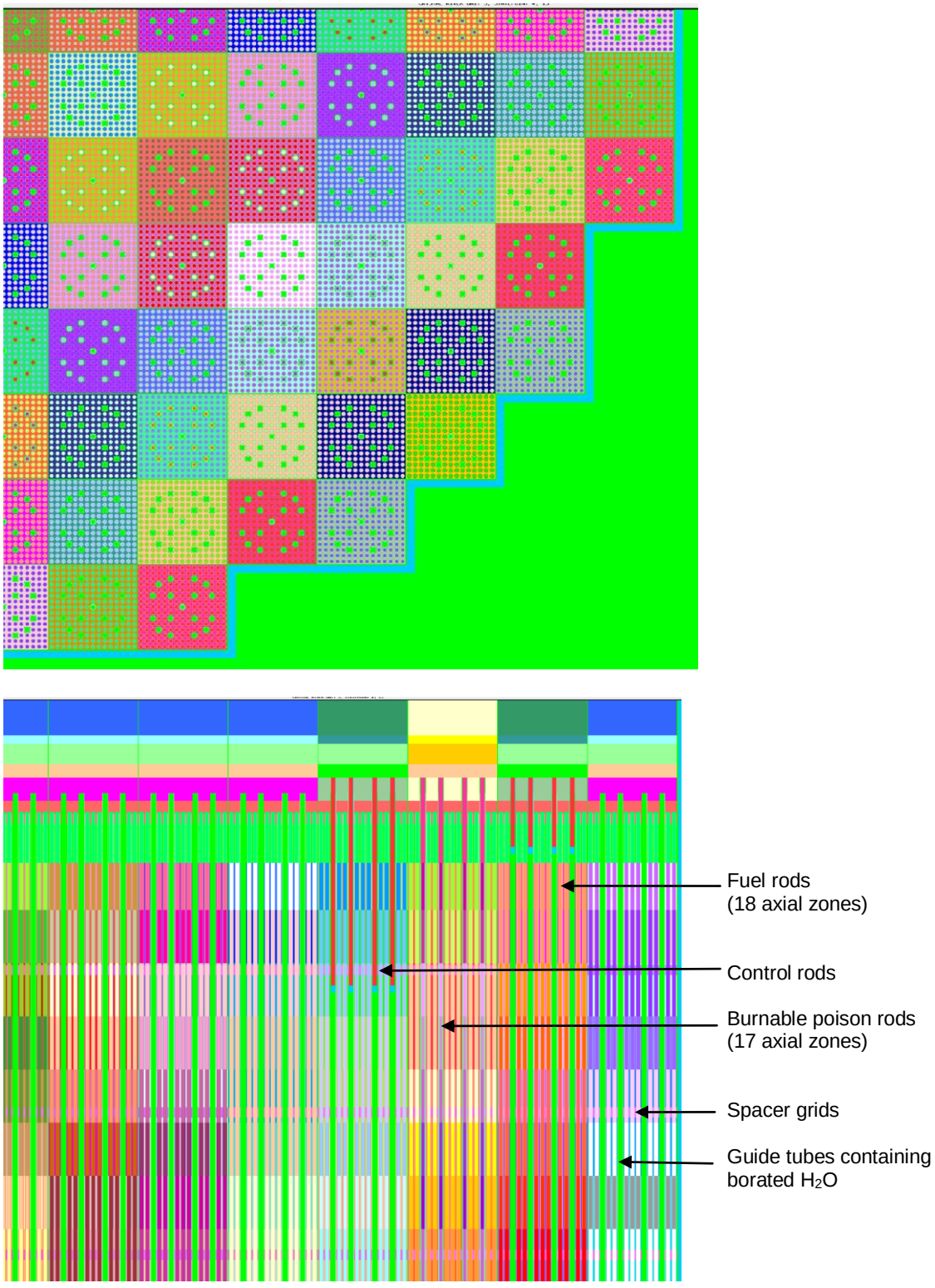

Fig. 3.2 Horizontal and partial vertical cross sections of KENO V.a geometry for a Crystal River Unit 3 state-point.

Table 3.3 k_{eff} results for CRCs

State point	Case identifier	EALF (eV)	CSAS25[a]		Comparison calculations[b]		% Difference[c]
			k_{eff}	σ	k_{eff}	σ	
Crystal River Unit 3							
1	CR3SP1	5.58E-01	0.9938	0.0004	0.9960	0.0004	0.22
2	CR3SP2	6.28E-01	0.9925	0.0004	0.9929	0.0004	0.04
3	CR3SP3	6.09E-01	0.9946	0.0005	0.9950	0.0005	0.04
4	CR3SP4	6.28E-01	0.9920	0.0004	0.9928	0.0004	0.08
5	CR3SP5	6.58E-01	0.9924	0.0004	0.9941	0.0005	0.17
6	CR3SP6	6.46E-01	0.9919	0.0004	0.9930	0.0005	0.11
7	CR3SP7	6.43E-01	0.9893	0.0005	0.9907	0.0005	0.14
8	CR3SP8	6.62E-01	0.9915	0.0004	0.9913	0.0005	-0.02
9	CR3SP9	6.35E-01	0.9890	0.0004	0.9915	0.0005	0.25
10	CR3SP10	6.64E-01	0.9956	0.0004	0.9960	0.0005	0.04
11	CR3SP11	7.24E-01	0.9952	0.0004	0.9948	0.0005	-0.04
12	CR3SP12	7.08E-01	0.9960	0.0004	0.9981	0.0005	0.21
13	CR3SP13	7.88E-01	0.9940	0.0004	0.9956	0.0004	0.16
14	CR3SP14	7.80E-01	0.9948	0.0004	0.9958	0.0005	0.10
15	CR3SP15	7.36E-01	0.9899	0.0003	0.9927	0.0004	0.28
16	CR3SP16	8.74E-01	0.9923	0.0004	0.9932	0.0005	0.09
17	CR3SP17	8.40E-01	0.9902	0.0003	0.9908	0.0005	0.06
18	CR3SP18	8.46E-01	0.9906	0.0003	0.9922	0.0005	0.16
19	CR3SP19	8.27E-01	0.9895	0.0004	0.9899	0.0005	0.04
20	CR3SP20	7.78E-01	0.9912	0.0005	0.9932	0.0004	0.20
21	CR3SP21	7.83E-01	0.9899	0.0003	0.9925	0.0005	0.26
22	CR3SP22	9.39E-01	0.9905	0.0004	0.9904	0.0004	-0.01
23	CR3SP23	9.42E-01	0.9903	0.0004	0.9902	0.0005	-0.01
24	CR3SP24	9.34E-01	0.9916	0.0004	0.9906	0.0005	-0.10
25	CR3SP25	8.52E-01	0.9910	0.0005	0.9905	0.0004	-0.05
26	CR3SP26	8.37E-01	0.9910	0.0005	0.9907	0.0005	-0.03
27	CR3SP27	8.20E-01	0.9873	0.0004	0.9877	0.0004	0.04
28	CR3SP28	9.60E-01	0.9895	0.0004	0.9921	0.0004	0.26
29	CR3SP29	9.32E-01	0.9919	0.0004	0.9931	0.0005	0.12
30	CR3SP30	9.23E-01	0.9897	0.0004	0.9908	0.0005	0.11
31	CR3SP31	8.81E-01	0.9861	0.0004	0.9884	0.0005	0.23
32	CR3SP32	1.04E+00	0.9811	0.0005	0.9916	0.0005	1.06
33	CR3SP33	8.60E-01	0.9807	0.0005	0.9873	0.0005	0.67
Sequoyah Unit 2							
1	SQ2C3BZ	8.65E-01	1.0054	0.0002	1.0039	0.0005	-0.15
2	SQ2C3BF[d]	9.58E-01	1.0076	0.0002	1.0067	0.0005	-0.09
3	SQ2C3M[d]	9.47E-01	1.0054	0.0003	1.0046	0.0005	-0.08
Surry Unit 1							
1	SU1C2B	6.19E-01	1.0035	0.0002	1.0014	0.0005	-0.21
2	SU1C2E[d]	6.72E-01	1.0107	0.0002	1.0113	0.0005	0.06
TMI Unit 1							
1	TMI1C5B	7.28E-01	1.0017	0.0002	0.9978	0.0004	-0.39
North Anna Unit 1							
1	NA1C5B	9.17E-01	1.0041	0.0002	1.0040	0.0005	-0.03

[a]Irradiated fuel compositions for the Crystal River Unit 3 state-points consist of oxygen and up to 85 nuclides (Ref. 22), while irradiated fuel compositions for the other state-points consist of 48 nuclides (Refs. 24 through 27).

[b]Criticality calculations for Crystal River Unit 3, Sequoyah Unit 2, Surry Unit 1, TMI Unit 1, and North Anna Unit 1 are provided in Refs. 22, 24, 25, 26, and 27, respectively.

[c]100x(Comparison calculation k_{eff} – CSAS25 k_{eff})/Comparison calculation k_{eff}.

[d]Hot full-power critical configuration.

3.3 DIRECT PERTURBATION CALCULATIONS

Direct perturbation calculations were performed for the GBC-32 cask loaded with fuel burned to 40 GWd/MTU using the method described in Sect. 2.4 (Eqs. 6 and 7), and fission-product reactivity worth calculations were performed for Crystal River Unit 3 state-point 27 to verify the quality of the sensitivity coefficients computed with TSUNAMI-3D. A reactivity-worth calculation is adequate for individual fission products because the effect on k_{eff} of removing a fission product from the fuel composition is small. A comparison of the TSUNAMI-3D sensitivity coefficients and the change in k_{eff} due to direct perturbations in ^{149}Sm, ^{143}Nd, ^{103}Rh, ^{133}Cs, ^{151}Sm, and ^{155}Gd compositions is shown in Table 3.4.

Table 3.4 Direct perturbation results

	GBC40					CR3SP27				
	Direct perturbation		TSUNAMI-3D		% Difference[a]	Direct perturbation		TSUNAMI-3D		% Difference[a]
	S_k	σ_s	$S_{k,\Sigma}$	σ		S_k	σ_s	$S_{k,\Sigma}$	σ	
^{149}Sm	-0.0156	1.2E-03	-0.0156	8.3E-05	0.6	-0.0150	6.2E-04	-0.0139	1.3E-05	-7.3
^{143}Nd	-0.0114	3.1E-04	-0.0112	6.3E-05	-2.1	-0.0103	5.6E-04	-0.0109	8.0E-06	6.4
^{103}Rh	-0.0089	3.3E-04	-0.0087	6.3E-05	-2.8	-0.0101	5.7E-04	-0.0099	7.6E-06	-1.3
^{151}Sm	-0.0092	4.1E-04	-0.0084	5.5E-05	-9.2	-0.0050	6.1E-04	-0.0054	4.4E-06	7.9
^{133}Cs	-0.0040	1.9E-04	-0.0038	4.3E-05	-5.3	-0.0057	6.1E-04	-0.0050	6.3E-06	-12.2
^{155}Gd	-0.0038	1.9E-04	-0.0038	2.5E-05	-1.9	-	-	-	-	-

[a] $100x(S_{k,\Sigma}-S_k)/S_k$

4 SENSITIVITY AND UNCERTAINTY ANALYSIS

The GBC-32 cask and a CRC state-point are physically similar because the two systems contain spent nuclear fuel assemblies placed in lattice configurations with light water as the neutron moderator. However, differences in isotopic compositions and neutron spectra may exist due to differences in fuel burnup, temperature, and cooling time, moderator density and temperature, and boron concentration and form (plates versus soluble). Additionally, the CRCs contain a number of materials (e.g., boron in BPRAs and Ag-In-Cd in RCCAs) that are not present in the GBC-32 cask. For state-points at or near reactor EOC however, the amount of neutron absorbers is significantly reduced since control and power shaping rods are almost entirely withdrawn, burnable boron is depleted due to neutron capture, and the soluble boron concentration is low to maintain a critical state. As indicated by the EALF values presented in Tables 3.1 and 3.3, the CRC state-points have harder neutron spectra than the GBC-32 cask. Spectral differences between the two systems are the result of different water temperatures and densities and different fuel temperatures. Further, soluble boron, burnable poison rods, and control rods used to balance the reactor core excess reactivity decrease the thermal neutron population within the fuel lattice cell, while the Boral® panels placed between fuel assemblies in GBC-32 cask absorb most of the thermal neutrons crossing fuel assembly boundaries. Similarities of the GBC-32 cask and the CRC state-points will be rigorously examined using the calculated values for the set of indices described in Sect. 2, including sensitivity coefficients (Eq. 1), integral index c_k (Eq. 3), and nuclide-reaction specific integral index g (Eq. 4). Further, the relative standard deviation of k_{eff} due to uncovered sensitivity data will be evaluated (Eq. 5).

4.1 SENSITIVITY COEFFICIENTS

Energy- and region-integrated k_{eff} sensitivity to nuclide total cross sections for the GBC-32 cask is presented in Table 4.1. The sensitivity coefficients are shown for the actinide and major fission product nuclides important for burnup credit criticality calculations (see Sect. 3.1.1), and for ^{1}H and ^{10}B, which also can cause significant reactivity changes. The values are presented starting with the lowest negative sensitivity coefficient, which corresponds to the nuclide with the greatest negative effect on reactivity, and ending with the highest positive sensitivity coefficient, which corresponds to the nuclide with the greatest positive effect on reactivity. Sensitivity coefficients with the absolute value greater than 1.0E-05 for the CRC state-points are listed in Appendix A, Table A.1. Comparisons of energy-and region-integrated k_{eff} sensitivities to relevant nuclides are illustrated in Figures A.1 through A.29, Appendix A.

As can be seen in Tables 4.1 and A.1, the main neutron absorbers include actinide nuclides ^{238}U, ^{240}Pu, ^{241}Am, ^{237}Np, and ^{236}U, the neutron absorber ^{10}B, and the following six fission product nuclides ^{149}Sm, ^{143}Nd, ^{103}Rh, ^{151}Sm, ^{133}Cs, and ^{155}Gd. These fission product nuclides are stable except for ^{151}Sm, which has a half-life of 90 years. Their concentrations in spent fuel compositions increase after fuel discharge, as main precursors ^{149}Pm, ^{143}Pr, ^{103}Ru, ^{151}Pm, ^{133}Xe, and ^{155}Eu, decay by negative beta-emission with half-lives of 2.212 days, 13.57 days, 39.27 days, 1.183 days, 5.243 days, and 4.75 years, respectively.[30] The decay process mainly affects ^{155}Gd and, to a lesser extent, ^{149}Sm concentrations. These two fission product nuclides have very large thermal neutron absorption cross sections and exist in small concentrations during fuel irradiation. However, ^{155}Gd and ^{149}Sm concentrations in spent fuel with a 5-year cooling time are approximately 100 times and 2 times, respectively, those of discharge spent fuel compositions. Investigation of the energy-dependent sensitivity profiles for the aforementioned six high-reactivity worth fission product nuclides is provided in Section 4.3.

For each of the nuclides listed in Table 4.1, Appendix A provides a plot comparing the k_{eff} sensitivities in each of the CRC state-points and the GBC-32 cask. With the exception of a few nuclides that build in after discharge (e.g., ^{155}Gd, ^{241}Am, and to a lesser extent ^{147}Sm), the sensitivities are quite comparable between the GBC-32 cask and many of the CRC state-points. This is an important finding that addresses long-standing questions related to the influence of the various nuclides on the k_{eff} of these systems.

Table 4.1 Energy-and region-integrated k_{eff} sensitivity to nuclide total cross section for GBC-32 cask

Spent nuclear fuel burnup (GWd/MTU) and initial enrichment (wt% ^{235}U)											
10/1.9972		**20/2.5563**		**30/3.2025**		**40/3.7777**		**50/4.3427**		**60/4.8819**	
^{238}U	-1.38E-01	^{238}U	-1.19E-01	^{238}U	-1.06E-01	^{238}U	-9.88E-02	^{238}U	-9.10E-02	^{238}U	-8.59E-02
^{10}B	-3.25E-02	^{10}B	-3.24E-02	^{240}Pu	-3.63E-02	^{240}Pu	-3.78E-02	^{240}Pu	-3.89E-02	^{240}Pu	-4.03E-02
^{240}Pu	-1.94E-02	^{240}Pu	-3.12E-02	^{10}B	-3.26E-02	^{10}B	-3.19E-02	^{10}B	-3.18E-02	^{10}B	-3.13E-02
^{149}Sm	-1.28E-02	^{149}Sm	-1.52E-02	^{149}Sm	-1.58E-02	^{149}Sm	-1.56E-02	^{149}Sm	-1.52E-02	^{149}Sm	-1.53E-02
^{151}Sm	-4.93E-03	^{143}Nd	-7.66E-03	^{143}Nd	-9.93E-03	^{143}Nd	-1.12E-02	^{143}Nd	-1.21E-02	^{143}Nd	-1.34E-02
^{143}Nd	-4.26E-03	^{151}Sm	-6.67E-03	^{103}Rh	-7.75E-03	^{103}Rh	-8.66E-03	^{103}Rh	-9.33E-03	^{103}Rh	-1.02E-02
^{103}Rh	-3.06E-03	^{103}Rh	-5.94E-03	^{151}Sm	-7.74E-03	^{151}Sm	-8.38E-03	^{151}Sm	-8.81E-03	^{151}Sm	-9.44E-03
^{236}U	-1.71E-03	^{241}Am	-4.69E-03	^{241}Am	-6.66E-03	^{241}Am	-7.69E-03	^{241}Am	-8.44E-03	^{241}Am	-9.42E-03
^{241}Am	-1.64E-03	^{236}U	-2.74E-03	^{236}U	-3.38E-03	^{236}U	-3.86E-03	^{237}Np	-4.39E-03	^{237}Np	-5.30E-03
^{133}Cs	-1.24E-03	^{133}Cs	-2.43E-03	^{133}Cs	-3.26E-03	^{133}Cs	-3.78E-03	^{155}Gd	-4.29E-03	^{155}Gd	-5.02E-03
^{234}U	-1.08E-03	^{155}Gd	-2.16E-03	^{155}Gd	-3.16E-03	^{155}Gd	-3.77E-03	^{236}U	-4.18E-03	^{133}Cs	-4.68E-03
^{155}Gd	-1.03E-03	^{152}Sm	-1.92E-03	^{237}Np	-2.86E-03	^{237}Np	-3.65E-03	^{133}Cs	-4.17E-03	^{236}U	-4.53E-03
^{152}Sm	-9.36E-04	^{99}Tc	-1.79E-03	^{152}Sm	-2.61E-03	^{152}Sm	-2.92E-03	^{152}Sm	-3.20E-03	^{99}Tc	-3.57E-03
^{99}Tc	-9.11E-04	^{237}Np	-1.78E-03	^{99}Tc	-2.39E-03	^{99}Tc	-2.88E-03	^{99}Tc	-3.18E-03	^{152}Sm	-3.52E-03
^{145}Nd	-6.88E-04	^{145}Nd	-1.35E-03	^{145}Nd	-1.84E-03	^{145}Nd	-2.15E-03	^{145}Nd	-2.42E-03	^{153}Eu	-2.74E-03
^{237}Np	-6.81E-04	^{147}Sm	-1.13E-03	^{153}Eu	-1.67E-03	^{153}Eu	-2.04E-03	^{153}Eu	-2.35E-03	^{145}Nd	-2.71E-03
^{147}Sm	-6.23E-04	^{234}U	-1.09E-03	^{242}Pu	-1.53E-03	^{242}Pu	-1.94E-03	^{242}Pu	-2.26E-03	^{242}Pu	-2.60E-03
^{95}Mo	-4.59E-04	^{153}Eu	-1.08E-03	^{147}Sm	-1.47E-03	^{147}Sm	-1.68E-03	^{147}Sm	-1.85E-03	^{238}Pu	-2.41E-03
^{153}Eu	-3.95E-04	^{95}Mo	-9.05E-04	^{95}Mo	-1.24E-03	^{95}Mo	-1.45E-03	^{238}Pu	-1.80E-03	^{147}Sm	-2.05E-03
^{150}Sm	-3.62E-04	^{242}Pu	-8.88E-04	^{234}U	-1.13E-03	^{238}Pu	-1.36E-03	^{95}Mo	-1.60E-03	^{95}Mo	-1.78E-03
^{109}Ag	-2.56E-04	^{150}Sm	-8.01E-04	^{150}Sm	-1.13E-03	^{150}Sm	-1.31E-03	^{150}Sm	-1.45E-03	^{150}Sm	-1.63E-03
^{101}Ru	-2.42E-04	^{109}Ag	-6.69E-04	^{109}Ag	-9.63E-04	^{234}U	-1.22E-03	^{234}U	-1.27E-03	^{109}Ag	-1.43E-03
^{242}Pu	-1.62E-04	^{101}Ru	-5.28E-04	^{238}Pu	-9.35E-04	^{109}Ag	-1.13E-03	^{109}Ag	-1.26E-03	^{234}U	-1.31E-03
^{151}Eu	-1.48E-04	^{238}Pu	-4.50E-04	^{101}Ru	-7.75E-04	^{101}Ru	-9.35E-04	^{101}Ru	-1.07E-03	^{101}Ru	-1.25E-03
^{238}Pu	-9.02E-05	^{151}Eu	-2.06E-04	^{243}Am	-4.63E-04	^{243}Am	-6.86E-04	^{243}Am	-9.13E-04	^{243}Am	-1.21E-03
^{243}Am	-1.73E-05	^{243}Am	-1.93E-04	^{151}Eu	-2.46E-04	^{151}Eu	-2.72E-04	^{151}Eu	-2.91E-04	^{151}Eu	-3.16E-04
^{241}Pu	7.42E-03	^{241}Pu	1.99E-02	^{241}Pu	2.71E-02	^{241}Pu	2.93E-02	^{241}Pu	3.13E-02	^{241}Pu	3.39E-02
^{239}Pu	1.07E-01	^{239}Pu	1.28E-01	^{239}Pu	1.32E-01	^{239}Pu	1.26E-01	^{239}Pu	1.24E-01	^{239}Pu	1.23E-01
^{1}H	1.56E-01	^{1}H	1.85E-01	^{235}U	1.72E-01	^{235}U	1.64E-01	^{235}U	1.64E-01	^{235}U	1.58E-01
^{235}U	2.31E-01	^{235}U	1.87E-01	^{1}H	1.98E-01	^{1}H	2.20E-01	^{1}H	2.27E-01	^{1}H	2.31E-01

4.2 INTEGRAL INDEX c_k

Integral c_k values for the GBC-32 cask containing spent fuel assemblies of 10, 20, 30, 40, 50, and 60 GWd/MTU burnup are presented in Table 4.2. As described in Sect. 2, an integral c_k value of 1.0 indicates complete correlation between the effects of cross-section uncertainties on the k_{eff} values of two systems, while a value of 0.0 indicates no correlation between these effects. Hence, the integral c_k value for the GBC-32 cask is 1.0, and the integral c_k value for a CRC state-point depends on its neutronic similarity to the cask. Table 4.2 also provides the number of CRC state-points that exceed threshold c_k values deemed to be indicative of the degree of system similarity. A c_k value of 0.90 or higher indicates similar systems, and a value of 0.80 or higher indicates marginally similar systems.[11]

The analysis will focus next on the TSUNAMI-IP results for the GBC-32 cask containing spent fuel assemblies of 40-GWd/MTU burnup and 3.78 wt% initial enrichment, which is a typical spent fuel assembly in the current commercial waste stream. The integral c_k values vary from 0.6726 to 0.9620, with the lowest value corresponding to Crystal River Unit 3 BOL state-point (CR3SP1) and the highest value corresponding to Crystal River Unit 3 Cycle 10 EOC state-point (CR3SP33). Except for the Crystal River Unit 3 fresh core, a CRC state-point is either similar or marginally similar to the generic spent fuel cask. Thirty CRC state-points, or 75% of the total CRC state-points evaluated in this study, have integral c_k values greater than 0.90. Among these, 16 Crystal River Unit 3 state-points have c_k values greater than 0.95. These state-points are highly similar to the generic spent fuel cask. Except for the BOC core configurations with fresh fuel assemblies located at core periphery, such as the Crystal River Unit 3 BOC-2 (CR3SP4) and BOC-3 (CR3SP5) and TMI Unit 1 BOC-5 (TMI1C5B) core configurations, the BOC CRCs are only marginally similar to the GBC-32 cask due to their fresh fuel contents and lower average burnups.

A grouping of the CRC state-points based on the degree of similarity, core average burnup, soluble boron concentrations, and EALF, is presented in Table 4.3. A graphical representation of the integral index c_k as a function of core average burnup is shown in Fig. 4.1. Integral index c_k exhibits an ascending trend with increasing core average burnup within a given reactor cycle. However, integral c_k values greater than 0.95 exist for a large range of reactor core burnup (12.34–33.00 GWd/MTU). This is an indication that the integral index c_k varies with initial fuel enrichment and core average burnup. As can be seen in Table 3.2, fresh fuel enrichment at the beginning of a Crystal River Unit 3 cycle was increased, as compared with that of the previous cycle, to achieve higher burnups. The higher fuel reactivity excess was balanced by adjusting the position of control rods and by adding boron to the reactor coolant.

Figure 4.2 shows integral index c_k as a function of burnup for Crystal River Unit 3 state-points with similar soluble boron concentrations. In the figure, the first (~500 ppm), second (~1000 ppm), and fourth (~2000 ppm) data series from the top show a slight linear variation with burnup for state-points at or near EOC, MOC, and BOC, respectively, while the third data series (~1500 ppm) shows a steeper linear variation for BOC and MOC state-points with similar soluble boron concentrations. The variation in the third data series is expected since the state-points consist of BOC configurations containing a large amount of fresh fuel and MOC configurations containing irradiated fuel. Similar trends are observed when the CRC state-points are compared with the GBC-32 cask containing spent fuel of various burnups, as shown in Fig. 4.3.

Table 4.2 Integral c_k values

Case identifier	Application burnup (GWd/MTU) and initial enrichment (wt% ^{235}U)					
	10/1.9972	**20/2.5563**	**30/3.2025**	**40/3.7777**	**50/4.3427**	**60/4.8819**
GBC-32	1.0000	1.0000	1.0000	1.0000	1.0000	1.0000
CR3SP1	0.8091	0.7128	0.6782	0.6726	0.6682	0.6574
CR3SP2	0.9579	0.9576	0.9485	0.9442	0.9375	0.9330
CR3SP3	0.9383	0.9629	0.9624	0.9593	0.9536	0.9516
CR3SP4	0.9559	0.9508	0.9413	0.9374	0.9317	0.9273
CR3SP5	0.9527	0.9378	0.9253	0.9211	0.9150	0.9100
CR3SP6	0.9482	0.9617	0.9582	0.9552	0.9498	0.9471
CR3SP7	0.9370	0.9614	0.9617	0.9594	0.9544	0.9528
CR3SP8	0.9415	0.9084	0.8911	0.8867	0.8810	0.8747
CR3SP9	0.9366	0.9587	0.9580	0.9554	0.9499	0.9480
CR3SP10	0.9340	0.9578	0.9578	0.9554	0.9502	0.9485
CR3SP11	0.9292	0.8882	0.8689	0.8649	0.8597	0.8531
CR3SP12	0.9157	0.9536	0.9588	0.9577	0.9530	0.9531
CR3SP13	0.9372	0.9092	0.8945	0.8916	0.8871	0.8819
CR3SP14	0.9465	0.9435	0.9359	0.9335	0.9289	0.9255
CR3SP15	0.9114	0.9531	0.9604	0.9602	0.9564	0.9573
CR3SP16	0.9162	0.8752	0.8571	0.8545	0.8506	0.8447
CR3SP17	0.9400	0.9516	0.9488	0.9473	0.9431	0.9411
CR3SP18	0.9351	0.9522	0.9513	0.9501	0.9459	0.9445
CR3SP19	0.9361	0.9551	0.9548	0.9537	0.9496	0.9483
CR3SP20	0.9185	0.9540	0.9595	0.9592	0.9556	0.9559
CR3SP21	0.9185	0.9548	0.9605	0.9604	0.9568	0.9573
CR3SP22	0.9151	0.8776	0.8607	0.8584	0.8545	0.8489
CR3SP23	0.9358	0.9238	0.9139	0.9120	0.9077	0.9039
CR3SP24	0.9396	0.9337	0.9257	0.9240	0.9198	0.9165
CR3SP25	0.9212	0.9507	0.9542	0.9539	0.9503	0.9502
CR3SP26	0.9208	0.9503	0.9538	0.9536	0.9501	0.9500
CR3SP27	0.9074	0.9479	0.9553	0.9558	0.9524	0.9536
CR3SP28	0.9138	0.8769	0.8603	0.8581	0.8545	0.8490
CR3SP29	0.9379	0.9359	0.9292	0.9275	0.9234	0.9205
CR3SP30	0.9344	0.9444	0.9413	0.9401	0.9359	0.9341
CR3SP31	0.9188	0.9482	0.9517	0.9513	0.9476	0.9476
CR3SP32	0.9062	0.8677	0.8510	0.8493	0.8460	0.8407
CR3SP33	0.9129	0.9533	0.9609	0.9620	0.9593	0.9605
SQ2C3BZ	0.9379	0.9163	0.9030	0.9010	0.8961	0.8912
SQ2C3BF	0.9239	0.9029	0.8900	0.8881	0.8833	0.8785
SQ2C3M	0.9170	0.9399	0.9399	0.9391	0.9339	0.9326
SU1C2B	0.9518	0.9220	0.9052	0.9016	0.8955	0.8892
SU1C2E	0.9271	0.9497	0.9491	0.9472	0.9416	0.9397
TMI1C5B	0.9534	0.9462	0.9356	0.9324	0.9259	0.9212
NA1C5B	0.9131	0.8708	0.8517	0.8493	0.8446	0.8383
Integral c_k values	**Number of CRCs**					
0.95-1	5	17	16	16	11	9
0.9-0.95	34	16	14	14	17	19
0.8-0.9	1	6	9	9	11	11
0-0.8	0	1	1	1	1	1

Table 4.3 CRC state-point grouping based on the degree of similarity to GBC-32 cask

Integral index c_k	Number of CRC state-points	CRC state-points	Average core burnup (GWd/MTU)	Soluble B concentration (ppm)	EALF (eV)
0.95-0.9726	16	Crystal River Unit 3 state-points 3, 6, 7, 9, 10, 12, 15, 18, 19, 20, 21, 25, 26, 27, 31, and 33.	12.34-33.00	390-1149	0.61-0.88
0.90-0.95	14	Crystal River Unit 3 state-points 2, 4, 5, 14, 17, 23, 24, 29, and 30. Sequoyah Unit 2 state-points 1 and 3. Surry Unit 1 state-points 1 and 2. TMI Unit 1 state-point 1.	6.93-20.96	123-1751	0.62-0.95
0.85-0.90	7	Crystal River Unit 3 state-points 8, 11, 13, 16, 22 and 28. Sequoyah Unit 2 state-point 2.	6.92-12.26	1150-2212	0.66-0.96
0.80-0.85	2	Crystal River Unit 3 state-point 32. North Anna Unit 1 state-point 1.	15.24, 11.07	2326, 1836	1.04, 0.92
0.6726	1	Crystal River Unit 3 state-point 1.	0	1403	0.56

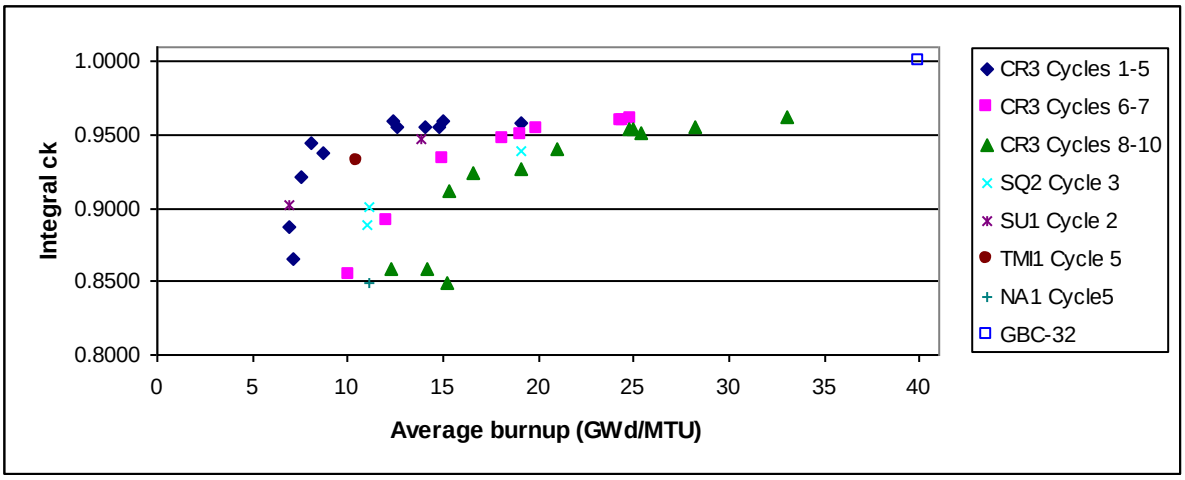

Fig. 4.1 Integral c_k index as a function of CRC average burnup.

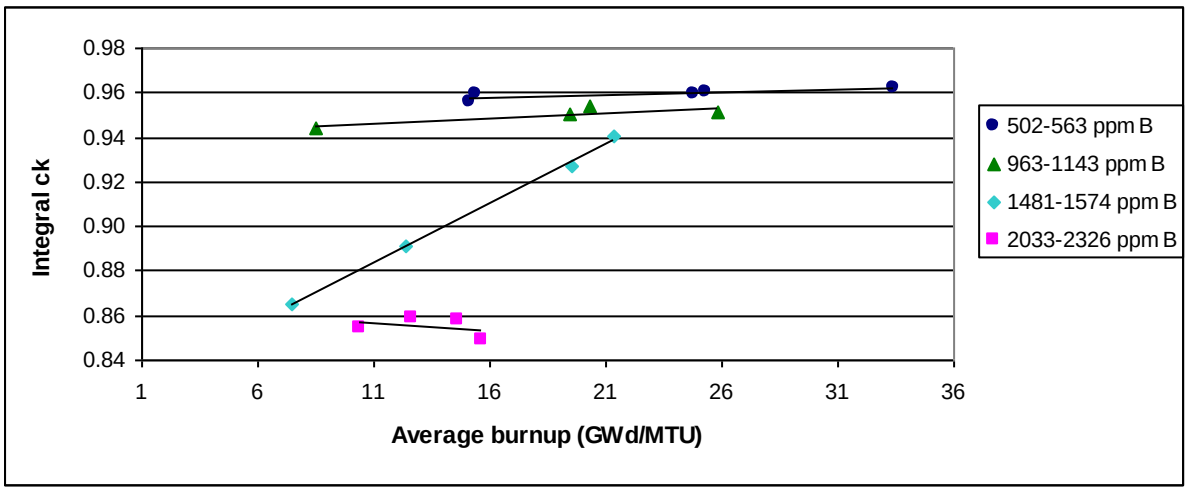

Fig. 4.2 Integral index c_k as a function of burnup: CRC state-points with similar soluble boron concentrations.

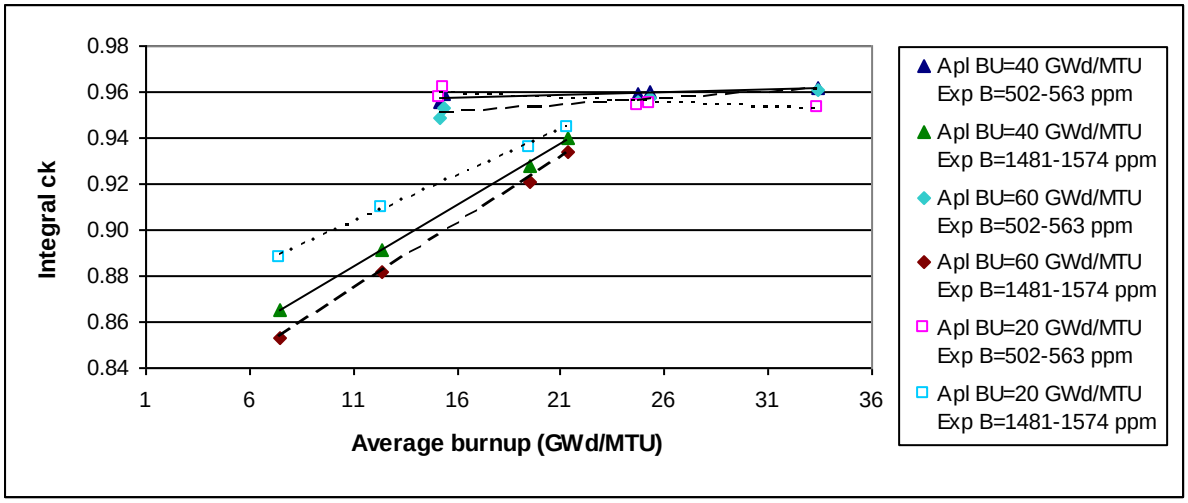

Fig. 4.3 Integral index c_k as a function of CRC average burnup for various application burnups.

The EALF is often used as a parameter in trending analyses. Figures 4.4 and 4.5 show integral index c_k as a function of EALF for Crystal River Unit 3 state-points with similar burnup and similar soluble boron concentrations, respectively. The range of EALF values for integral c_k values greater than 0.95 increases with increasing burnup and/or decreasing soluble boron concentrations, which characterize CRC configurations at or near the end of reactor cycle (i.e., configurations with low reactivity excess). Note that the EALF values for the GBC-32 cask with burnup and enrichment combinations representative of an anticipated loading curve are in the 0.21-0.31 eV range (see Table 3.1). These values are notably lower than the values for the CRCs, which are in the 0.56-1.0 eV range (see Table 3.3).

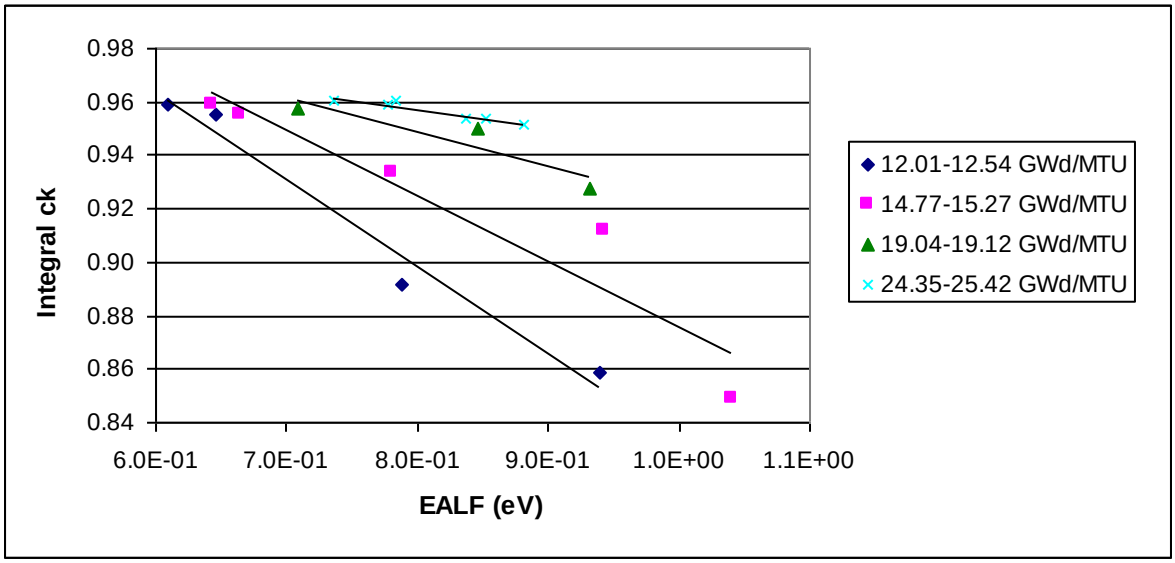

Fig. 4.4 Integral index c_k as a function of EALF: CRC state-points with similar burnup.

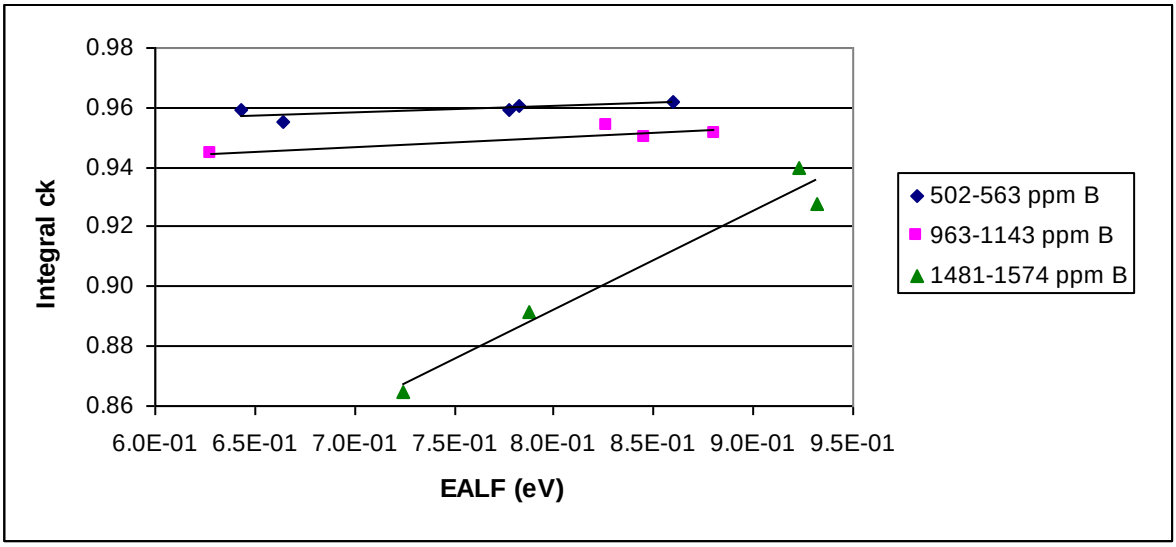

Fig. 4.5 Integral index c_k as a function of EALF: CRC state-points with similar soluble boron concentrations.

In summary, the integral index, c_k, values indicate that 30 of the 40 CRC state-points considered in the analysis are highly similar ($c_k > 0.90$) to the GBC-32 cask loaded with representative spent fuel, and hence meet the neutronic similarity criteria for being useful in bias determination. As expected, the CRC state-points with higher average burnup have higher c_k values, and hence are more similar to the GBC-32 cask. Only one of the CRC state-points (Crystal River BOL state-point with all fresh fuel) had a c_k value below the suggested threshold for being moderately similar (e.g., 0.80).

4.3 SENSITIVITY PROFILES

To further evaluate system similarities, selected sensitivity profiles representing k_{eff} sensitivity to total cross sections of the six highest worth fission products (^{149}Sm, ^{143}Nd, ^{103}Rh, ^{151}Sm, ^{133}Cs, and ^{155}Gd) as a function of neutron energy (see Eq. 2), are shown in Figs. 4.6 through 4.12. Sensitivity profiles for actinides and other relevant nuclides are included in Appendix B, Figs. B.1 through B.16. Comparison of the sensitivity profiles from the GBC-32 cask and the CRCs indicates that the energy-dependent sensitivities are quite similar between the cask model and many of the CRC state-points for the fission products and actinides relevant to burnup credit. The differences between the sensitivity profiles of the two systems result from the differences in the sensitivity coefficients (see Tables 4.1 and A.1) and a slight displacement between the sensitivity profiles of the two systems. As indicated by the values in Table 4.1, CRC state-points with higher average burnup tend to have higher sensitivity coefficients, and the state-points at or near the end of reactor cycle provide better similarity for the same burnup than the other state-points. This can be illustrated in the case of ^{149}Sm. Figure 4.6 shows a comparison of the ^{149}Sm sensitivity profiles for the GBC-32 cask and Crystal River Unit 3 EOC state-points of various burnup values (boron concentrations ~500 ppm, burnup values 12−33 GWd/MTU). Although the average burnups vary greatly, the CRC sensitivity profiles in the figure are almost identical, indicating the same degree of similarity seen with integral index c_k for these state-points and the good coverage (i.e., the effectiveness for validating cross sections as used in the application) of these CRC state-points. Figure 4.7 shows a comparison of the ^{149}Sm sensitivity profiles for the GBC-32 cask and Crystal River Unit 3 state-points 12 and 29, which have a core average burnup of approximately 19-GWd/MTU and boron concentrations of 605 ppm and 1572 ppm, respectively. The CRC sensitivity profile shift toward slightly higher energies in the thermal region is better seen in the case of nuclides with total cross sections inversely proportional to neutron velocity, such as ^{143}Nd (see Fig. 4.8). Note that similar trends are seen in Figures 4.9 through 4.11. Sensitivity profile displacement can be explained by the differences in the thermal spectra of the two types of systems, i.e., the difference in temperature between the reactor criticals and the cask. Note that only TMI Unit1 Cycle 5 BOC (6.63-year downtime) and Sequoyah Unit 2 Cycle 3 MOC (2.73-year downtime) configurations are similar to the GBC-32 cask in regard to ^{155}Gd contents, as seen in Fig. 4.12, since only these systems contain comparable ^{155}Gd concentrations as a result of ^{155}Eu decay after fuel discharge.

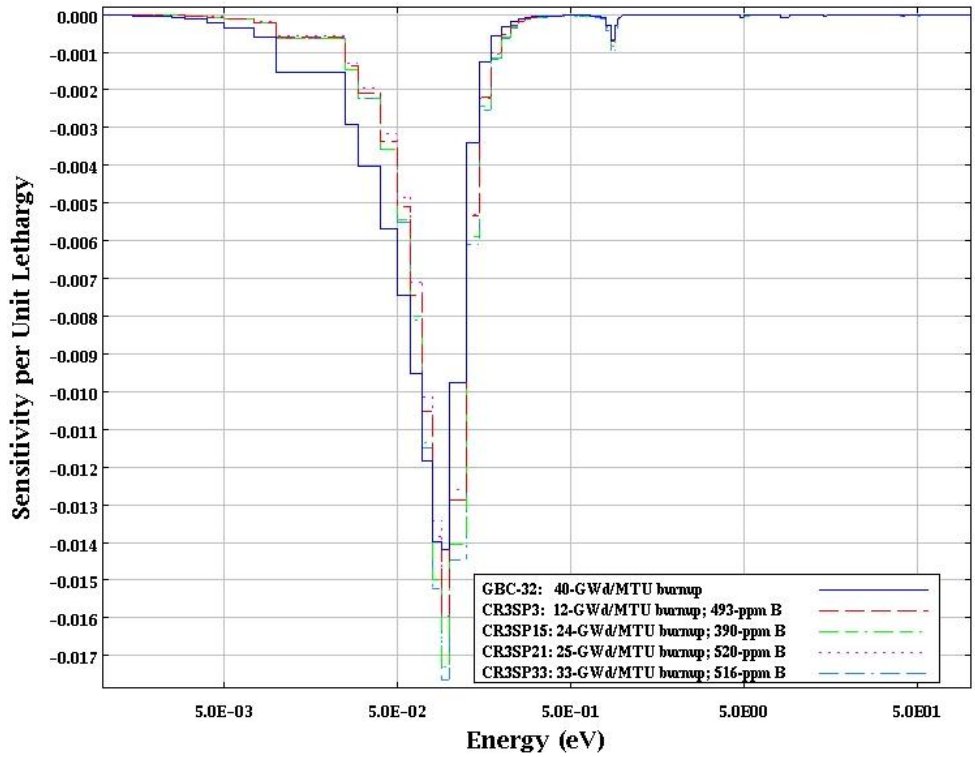

Fig. 4.6 k_{eff} sensitivity profile to ^{149}Sm total cross section: CRC state-points with similar soluble boron concentrations.

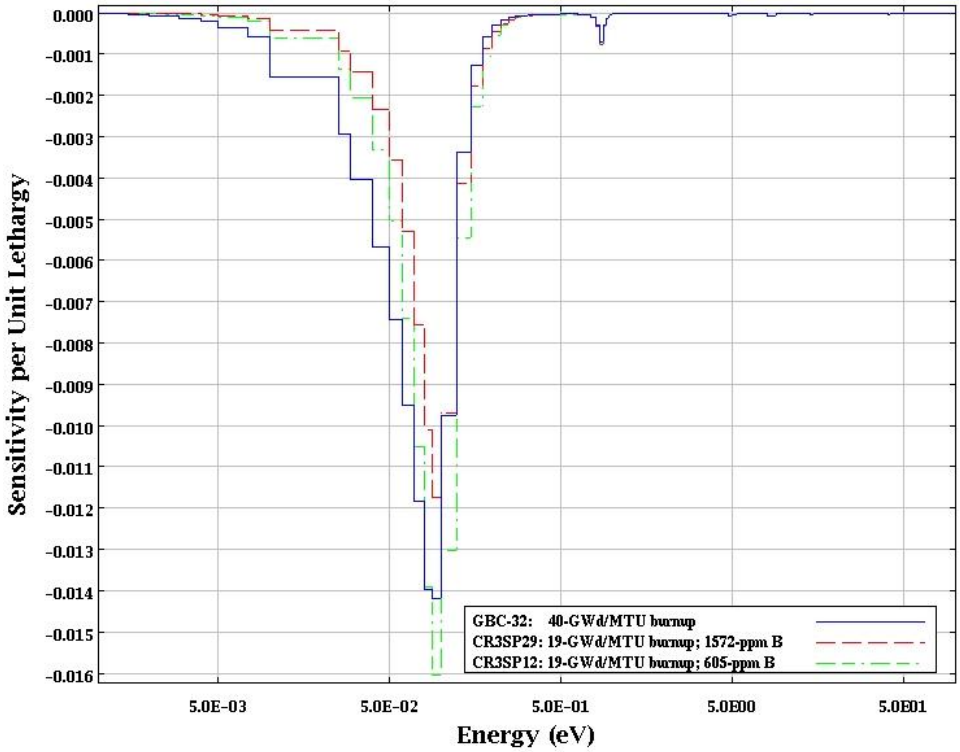

Fig. 4.7 k_{eff} sensitivity profile to ^{149}Sm total cross section: CRC state-points with similar burnup and different soluble boron concentrations.

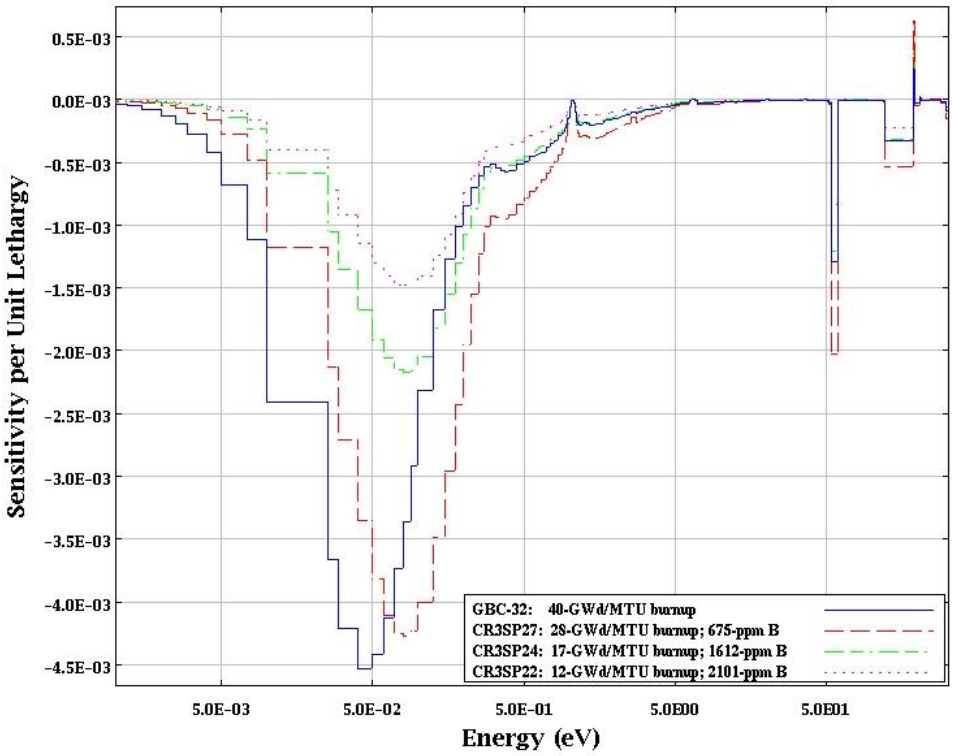

Fig. 4.8 Comparison of ^{143}Nd sensitivity profiles for GBC40, CR3SP27, CR3SP24, and CR3SP22.

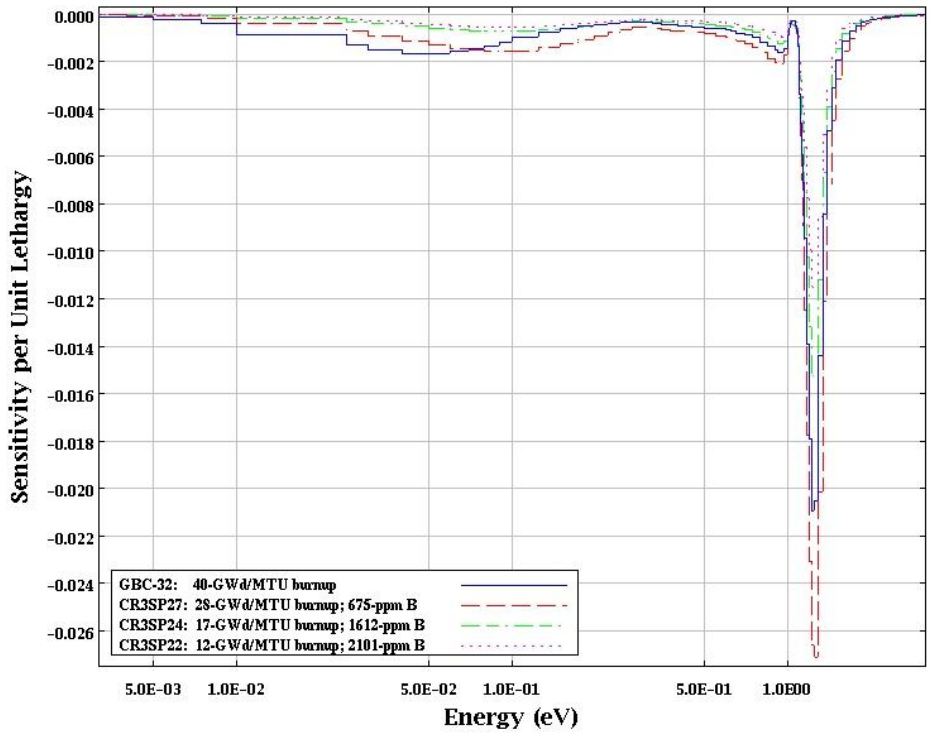

Fig. 4.9 Comparison of ^{103}Rh sensitivity profiles for GBC40, CR3SP27, CR3SP24, and CR3SP22.

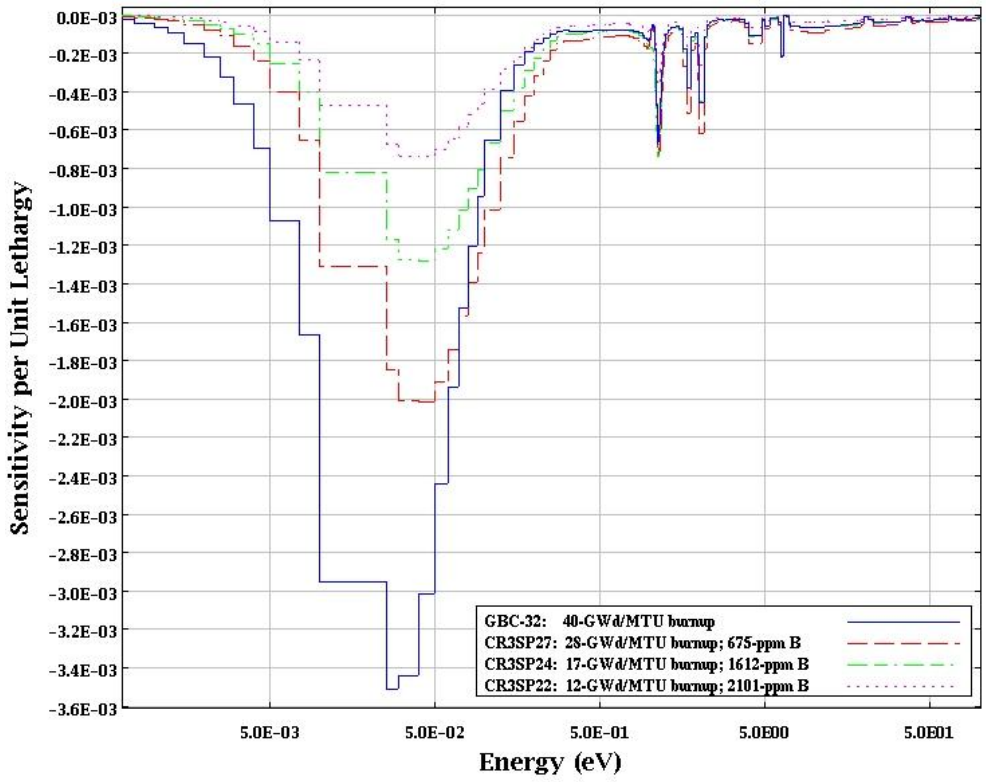

Fig. 4.10 Comparison of ^{151}Sm sensitivity profiles for GBC40, CR3SP27, CR3SP24, and CR3SP22.

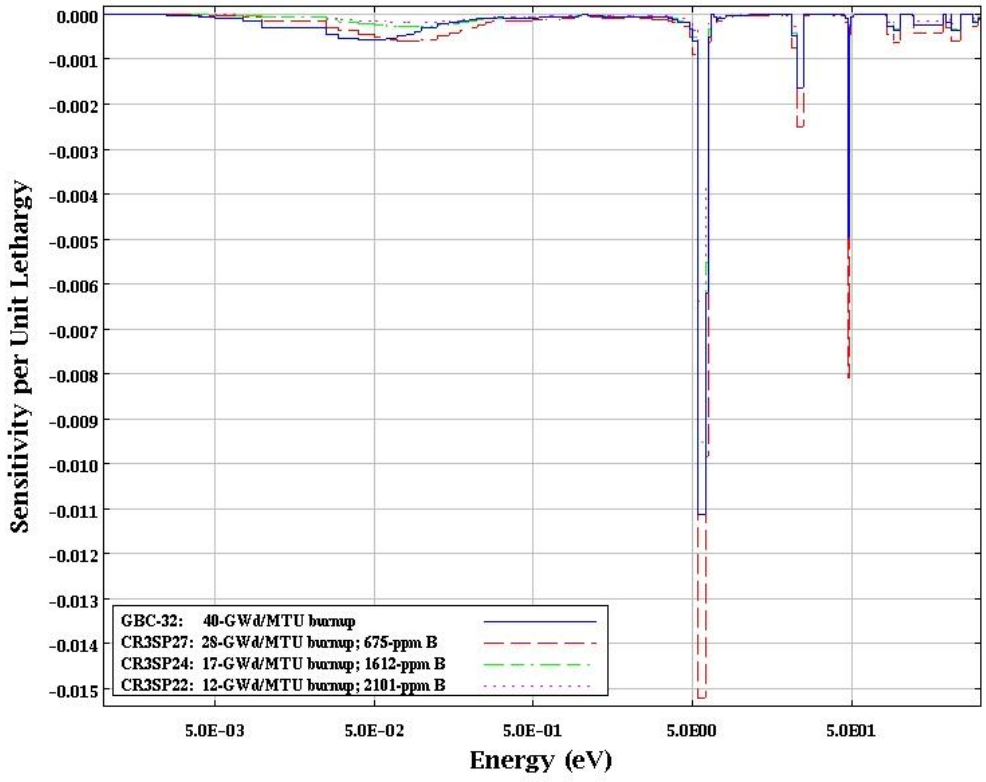

Fig. 4.11 Comparison of ^{133}Cs sensitivity profiles for GBC40, CR3SP27, CR3SP24, and CR3SP22.

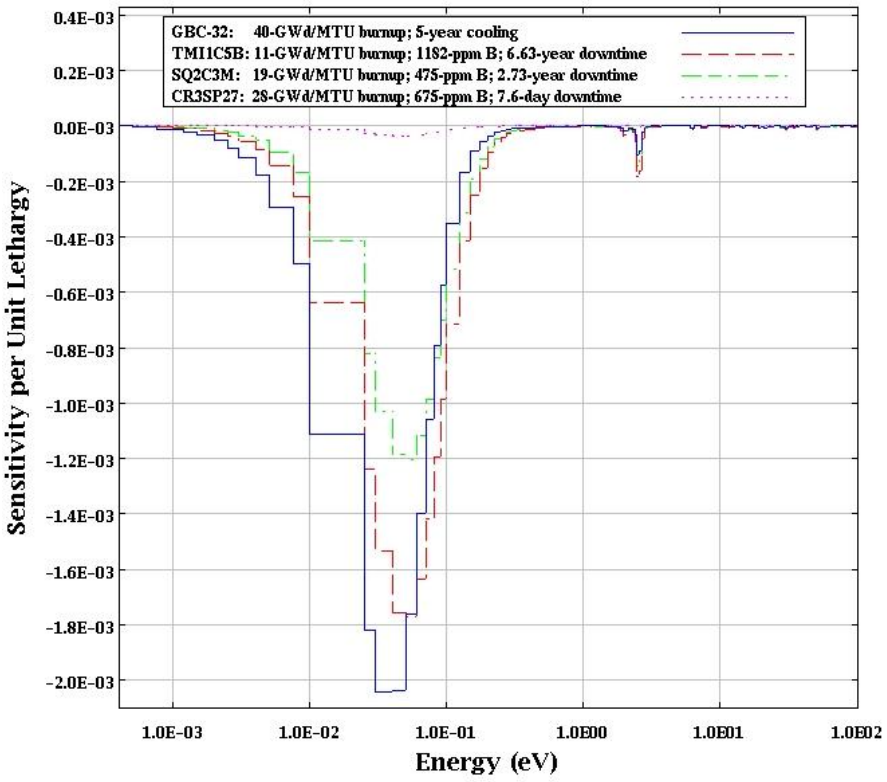

Fig. 4.12 Comparison of ^{155}Gd sensitivity profiles for GBC40, TMI1C5B, SQ2C3M, and CR3SP27.

4.4 NUCLIDE-REACTION SPECIFIC INTEGRAL INDEX *g*

As suggested by the sensitivity profiles illustrated in Figures 4.6 through 4.12 and B.1 through B.16, use of sensitivity coefficients is not sufficient in assessing system similarities on a nuclide-reaction specific level because systems with similar sensitivity coefficients may have very different sensitivity profiles. Therefore, the concept of coverage of an application by an experiment can be used to assess system similarities on an energy-dependent, nuclide-reaction specific level. Nuclide-reaction integral index *g*, representing the fraction of the application sensitivity profile area that also pertains to the area delimited by the sensitivity profile of the experiment, provides a measure of this coverage (see Sect. 2.3). Nuclide-reaction integral index g values for the actinides and major fission products relevant for burnup credit in the GBC-32 cask in relation to the CRC state-points are presented in Appendix C, Tables C.1 through C.6. Note that the GBC-32 model did not include adjustments to account for measured versus calculated isotope compositions.

The EOC state-points provide better coverage of the cask's k_{eff} sensitivities to ^{149}Sm, ^{143}Nd, ^{103}Rh, ^{151}Sm, and ^{133}Cs than the other state-points, and the integral-*g* index values do not vary significantly with the burnup of an EOC state-point, as shown in Fig. 4.13. As expected, only TMI Unit 1 BOC and Sequoyah Unit 2 MOC provide coverage of the cask's k_{eff} sensitivities to nuclides that significantly build in after fuel discharge, such as ^{155}Gd, ^{241}Am, and ^{147}Sm. The highest *g*-index values were obtained for nuclides with greater reactivity worth in a critical reactor core than in the generic cask, such as ^{235}U, ^{236}U, ^{238}U, ^{240}Pu, ^{242}Pu, ^{243}Am, ^{99}Tc, ^{101}Ru, ^{109}Ag, ^{133}Cs, and ^{152}Sm. The maximum coverage of the cask's sensitivities to ^{149}Sm, ^{143}Nd, ^{103}Rh, ^{151}Sm, ^{133}Cs, and ^{155}Gd provided by the CRC state-points is 81%, 78%, 89%, 60%, 92%, and 75%, respectively. The CRC state-points that provide significant coverage are summarized in Table 4.4.

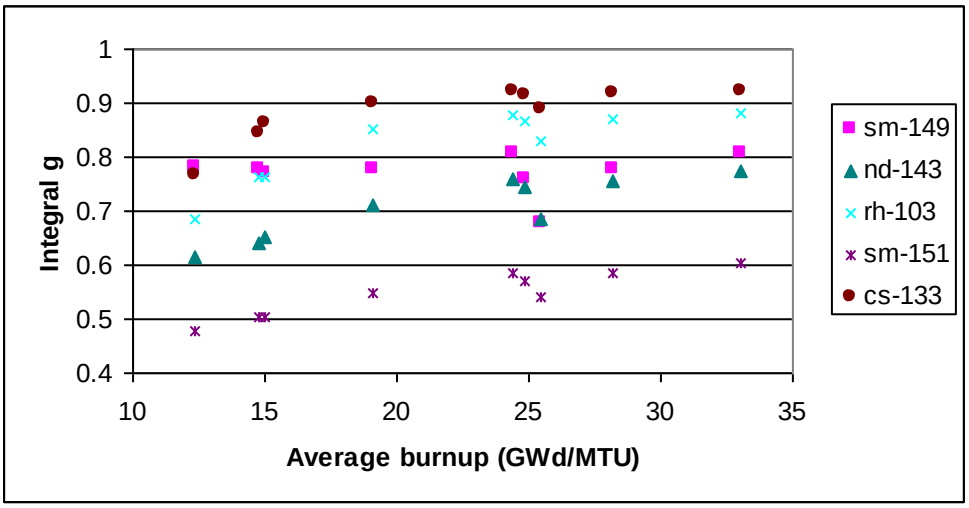

Fig. 4.13 Nuclide-reaction integral index *g* for Crystal River Unit 3 EOC state-points.

Table 4.4 Summary of CRC state-points providing significant coverage for the cask's k_{eff} sensitivities to ^{149}Sm, ^{143}Nd, ^{103}Rh, ^{151}Sm, ^{133}Cs, and ^{155}Gd

Fission product	Integral *g* index interval	CRC state-points
^{149}Sm	0.7-0.81	Crystal River Unit 3 state-points 2, 3, 6, 7, 9, 10, 12, 14, 15, 17, 18, 19, 20, 21, 25, 27, 30, and 33
^{143}Nd	0.6-0.78	Crystal River Unit 3 state-points 3, 7, 9, 10, 12, 15, 18, 19, 20, 21, 25, 26, 27, 31, and 33. Sequoyah Unit 2, state-point 3
^{103}Rh	0.7-0.89	Crystal River Unit 3 state-points 7, 9, 10, 12, 15, 18, 19, 20, 21, 25, 26, 27, 30, 31, and 33. Sequoyah Unit 2, state-point 3
^{151}Sm	0.5-0.6	Crystal River Unit 3 state-points 7, 10, 12, 15, 20, 21, 25, 26, 27, 31, and 33
^{133}Cs	0.8-0.92	Crystal River Unit 3 state-points 7, 9, 10, 12, 15, 17, 18, 19, 20, 21, 25, 26, 27, 30, 31, and 33. Sequoyah Unit 2, state-point 3
^{155}Gd	0.7493	TMI Unit 1 state-point 1

4.5 RELATIVE STANDARD DEVIATION OF k_{eff} DUE TO UNCOVERED SENSITIVITY DATA

The relative standard deviation of k_{eff} due to uncovered sensitivity data by all CRC state-points with c_k>0.8 was evaluated using the TSUNAMI-IP methodology (see Section 2.4). Contributions to uncertainty in k_{eff} (% $\Delta k_{eff}/k_{eff}$) by individual energy covariance matrices are listed in Appendix C, Tables C.7 through C.12, for cask burnups ranging from 10 to 60 GWd/MTU. Note that only contributions larger than 1.0E-04 are listed in the tables. The relative standard deviation of k_{eff} due to uncovered sensitivity data and contributions by nuclide groups are summarized in Table 4.5. The values shown in the tables are based on an assumed relative standard deviation for unknown covariance data of 25% and vary from 0.79% to 0.95% $\Delta k_{eff}/k_{eff}$ for cask burnups ranging from 10 to 60 GWd/MTU. Major actinides dominate the relative standard deviation of k_{eff} due to uncovered sensitivities, while the total contribution due to noncoverage of fission-product cross sections varies from approximately 0.02% to 0.08% $\Delta k_{eff}/k_{eff}$ for cask burnups ranging from 10 to 60 GWd/MTU. Note that the contributions from individual fission products are comparable to statistical uncertainties in k_{eff} results (see Table 3.1).

Table 4.5 Relative standard deviation of k_{eff} (% $\Delta k_{eff}/k_{eff}$) due to uncovered sensitivity data[a]

	Cask burnup (GWd/MTU)					
Nuclide group	10	20	30	40	50	60
Major actinides[b]	0.7540	0.8295	0.8763	0.8913	0.9004	0.9173
Minor actinides[c]	0.0093	0.0168	0.0213	0.0283	0.0333	0.0386
Fission products[d]	0.0210	0.0444	0.0560	0.0631	0.0688	0.0761
^{1}H	0.2095	0.2194	0.2201	0.2272	0.2280	0.2261
^{16}O	0.0389	0.0401	0.0413	0.0420	0.0433	0.0430
^{10}B	0.0076	0.0076	0.0077	0.0075	0.0075	0.0074
Total[e]	0.7877	0.8639	0.9099	0.9268[f]	0.9364	0.9529

[a] Assumed relative standard deviation for unknown covariance data is 25%.

[b] ^{234}U, ^{235}U, ^{238}U, ^{238}Pu, ^{239}Pu, ^{240}Pu, ^{241}Pu, ^{242}Pu, and ^{241}Am.

[c] ^{236}U, ^{237}Np , and ^{243}Am.

[d] ^{95}Mo, ^{99}Tc, ^{101}Ru, ^{103}Rh, ^{109}Ag, ^{133}Cs, ^{147}Sm, ^{149}Sm, ^{150}Sm, ^{151}Sm, ^{152}Sm, ^{143}Nd, ^{145}Nd, ^{151}Eu, ^{153}Eu, and ^{155}Gd.

[e] Quadrature sum of total contributions.

[f] For comparison purposes, the value is 0.7895 when assuming a relative standard deviation for unknown covariance data of 5% (instead of 25%).

5 CONCLUSIONS

This report provides an analysis of similarities between a generic spent fuel cask and a set of 40 critical state-points achieved at BOC, MOC, and EOC of various PWR reactors, including Crystal River Unit 3, Sequoyah Unit 2, Surry Unit 1, TMI Unit 1, and North Anna Unit 1. The analysis uses the cross-section S/U analysis methods developed at ORNL and the TSUNAMI set of tools in the SCALE code system. Material and neutron spectrum similarities between the two types of systems are examined using a set of indices that provide a measure of similarity on an integral and on an energy-dependent and nuclide-reaction specific level. The CSAS25/KENO V.a models for the CRC state-points used in TSUNAMI-3D calculations were automatically generated and were validated by comparing the CSAS25 results with criticality calculation results previously published, as described in Sect. 3.2.6.

The CRC state-points present various degrees of similarity with the GBC-32 cask, as summarized in Table 4.3. Thus, 30 CRC state-points are highly similar (c_k>0.90), and 39 state-points are moderately similar (c_k>0.80) to the GBC-32 cask containing typical spent fuel assemblies of 3.78 wt% ^{235}U initial enrichment, 40-GWd/MTU burnup, and 5-year cooling time. The state-points providing the highest similarity (c_k>0.95) were attained at or near the end of a reactor cycle. Except for the TMI Unit 1 state-point, the BOC state-points are only moderately similar to the GBC-32 cask due to their fresh fuel contents and lower average burnup. The correlation coefficient (c_k) exhibits an ascending trend with increasing average burnup within a given reactor cycle. It varies linearly with burnup for state-points with similar soluble boron concentrations, regardless of cycle, and the rate of change increases with increasing boron concentrations, as illustrated in the set of graphs provided in Sect. 4.2.

On a nuclide-reaction specific level, the CRC state-points provide significant similarity for most of the actinides and fission products relevant to burnup credit. A comparison of energy-dependent sensitivity profiles shows a slight shift of the CRC k_{eff} sensitivity profiles toward higher energies in the thermal region as compared to k_{eff} sensitivity profile of the GBC-32 cask. The profile displacement reduces the number of energy groups for which coverage is provided by a CRC state-point. Based on CRCs with c_k>0.80 and assuming a relative standard deviation for uncovered covariance data of 25%, the relative standard deviation of k_{eff} due to uncovered sensitivity data varies from 0.79% to 0.95% for cask burnups ranging from 10 to 60 GWd/MTU. This uncertainty is largely dominated by contributions from major actinides. The contributions from minor actinides and fission products are small and comparable to statistical uncertainties in the k_{eff} results.

Based on the recommended applicability criterion in Ref. 11 (i.e., c_k>0.9 indicates applicability), 30 of the 40 CRC state-points are applicable and can contribute to the validation of burnup credit in the GBC-32 cask loaded with fuel burned to 40 GWd/MTU. Hence, in principle, these CRC state-points could be part of a set of benchmark experiments for determining a bias in calculated k_{eff} of a spent fuel transport/storage/disposal system due to approximations in computational methods and uncertainties in parameters and nuclear data. The use of the methods described in Ref. 11 is recommended to determine the bias and bias uncertainty. However, a CRC state-point model is much more complex than a typical burnup credit cask model, requires a large amount of data for comprehensive modeling (e.g., physical characteristics of reactor core components and assembly irradiation histories), and the available CRC documentation does not provide uncertainties associated with various modeling parameters. Therefore, additional evaluations should be included in the burnup credit validation methodology if the CRCs are selected as a component of the benchmarking methodology.

6 REFERENCES

1. J. J. Sapyta, C. W. Mays, and J. W. Pegram, Jr., "Use of Reactor-Follow Data to Determine Biases and Uncertainties for PWR Spent Nuclear Fuel," *Trans. Am. Nucl. Soc.* **83**, 137 (2000).

2. W. J. Anderson, P. M. O'Leary, and J. M. Scaglione, "Selection of Reactor Criticals as Benchmarks for Spent Nuclear Fuels," *Trans. Am. Nucl. Soc.* **83**, 140 (2000).

3. J. M. Scaglione, D. P. Henderson, J. R. Worsham, and W. J. Anderson, "Applicability of CRC Benchmark Experiments for Burnup Credit Validation," *Trans. Am. Nucl. Soc.* **83**, 138 (2000).

4. C. V. Parks, M. D. DeHart, and J. C. Wagner, *Review and Prioritization of Technical Issues Related to Burnup Credit for LWR Fuel*, NUREG/CR-6665 (ORNL/TM-1999/303), U.S. Nuclear Regulatory Commission, Oak Ridge National Laboratory, February 2000.

5. B. T. Rearden, "TSUNAMI-1D: Control Module for One-Dimensional Cross-Section Sensitivity and Uncertainty Analysis for Criticality," Vol. I, Book 2, Sect. C8 in *SCALE: A Modular Code System for Performing Standardized Computer Analyses for Licensing Evaluations*, ORNL/TM-2005/39, Version 5.1, Vols. I-III, November 2006. Available from Radiation Safety Information Computational Center at Oak Ridge National Laboratory as CCC-732.

6. B. T. Rearden, "TSUNAMI-3D: Control Module for Three-Dimensional Cross-Section Sensitivity and Uncertainty Analysis for Criticality," Vol. I, Book 2, Sect. C9 in *SCALE: A Modular Code System for Performing Standardized Computer Analyses for Licensing Evaluations*, ORNL/TM-2005/39, Version 5.1, Vols. I-III, November 2006. Available from Radiation Safety Information Computational Center at Oak Ridge National Laboratory as CCC-732.

7. B. T. Rearden, "Sensitivity Utility Modules," Vol. III, Book 3, Sect. M18 in *SCALE: A Modular Code System for Performing Standardized Computer Analyses for Licensing Evaluations*, ORNL/TM-2005/39, Version 5.1, Vols. I-III, November 2006. Available from Radiation Safety Information Computational Center at Oak Ridge National Laboratory as CCC-732.

8. "*SCALE: A Modular Code System for Performing Standardized Computer Analyses for Licensing Evaluations*," ORNL/TM-2005/39, Version 5.1, Vols. I-III, November 2006. Available from Radiation Safety Information Computational Center at Oak Ridge National Laboratory as CCC-732.

9. K. R. Elam and B. T. Rearden, "Use of Sensitivity and Uncertainty Analysis to Select Benchmark Experiments for the Validation of Computer Codes and Data," *Nucl. Sci. Eng.* **145**, 196-212 (2003).

10. American Nuclear Society, A Guide for Acquisition and Documentation of Reference Power Reactor Physics Measurements for Nuclear Analysis Verification, ANS-19.4, ANSI N652-1976, Hinsdale, Illinois, 1976.

11. B. L. Broadhead, B. T. Rearden, C. M. Hopper, J. J. Wagschal, and C. V. Parks, "Sensitivity- and Uncertainty-Based Criticality Safety Validation Techniques," *Nuc. Sci. Eng.* **146,** 340-366 (2004).

12. B. T. Rearden, "Perturbation Theory Eigenvalue Sensitivity Analysis with Monte Carlo Techniques," *Nuc. Sci. Eng.* **146**, 367-382 (2004).

13. S. Goluoglu, C. M. Hopper, and B. T. Rearden, "Extended Interpretation of Sensitivity Data for Benchmark Areas of Applicability," *Trans. Am. Nucl. Soc.* **88**, 77-79 (2003).

14. B. T. Rearden and A. M. Fleckenstein "JAVAPEÑO," Vol. III, Book 3, Sect. M20 in *SCALE: A Modular Code System for Performing Standardized Computer Analyses for Licensing Evaluations*, ORNL/TM-2005/39, Version 5.1, Vols. I-III, November 2006. Available from Radiation Safety Information Computational Center at Oak Ridge National Laboratory as CCC-732.

15. S. F. Mughabghab, *Atlas of Nuclear Resonances*, Elsevier Publisher 2006.

16. S. Goluoglu, K. R. Elam, B. T. Rearden, B. L. Broadhead, and C. M. Hopper, *Sensitivity Analysis Applied to the Validation of the ^{10}B Capture Reaction in Nuclear Fuel Casks*, NUREG/CR-6845 (ORNL/TM-2004/48), U.S. Nuclear Regulatory Commission,

17. J. C. Wagner, *Computational Benchmark for Estimation of Reactivity Margin from Fission Products and Minor Actinides in PWR Burnup Credit*, NUREG/CR-6747 (ORNL/TM-2000/306), U.S. Nuclear Regulatory Commission, Oak Ridge National Laboratory, October 2001.

18. S. Goluoglu, N. F. Landers, L. M. Petrie, and D. F. Hollenbach, "CSAS: Control Module for Enhanced Criticality Safety Analysis Sequences," Vol. II, Book 1, Sect. C4 in *SCALE: A Modular Code System for Performing Standardized Computer Analyses for Licensing Evaluations*, ORNL/TM-2005/39, Version 5.1, Vols. I-III, November 2006. Available from Radiation Safety Information Computational Center at Oak Ridge National Laboratory as CCC-732.

19. I. C. Gauld and G. Radulescu, "STARBUCS: A SCALE Control Module for Automated Criticality Analyses Using Burnup Credit," Vol. I, Book 2, Sect. C10 in *SCALE: A Modular Code System for Performing Standardized Computer Analyses for Licensing Evaluations*, ORNL/TM-2005/39, Version 5, Vols. I-III, November 2006. Available from Radiation Safety Information Computational Center at Oak Ridge National Laboratory as CCC-732.

20. J. C. Wagner, M. D. DeHart, and C. V. Parks, *Recommendations for Addressing Axial Burnup in PWR Burnup Credit Analyses*, NUREG/CR-6801 (ORNL/TM-2001/273), U.S. Nuclear Regulatory Commission, Oak Ridge National Laboratory, March 2003.

21. R. J. Cacciapouti and S. Van Volkinburg, "Axial Burnup Profile Database for Pressurized Water Reactors," YAEC-1937, Yankee Atomic Electric Company (May 1997). Available from Radiation Safety Information Computational Center at Oak Ridge National Laboratory as DLC-201.

22. *CRC Reactivity Calculations for Crystal River Unit 3*, B00000000-01717-0210-00002 REV 00, CRWMS M&O, Las Vegas, Nevada, 1998.

23. *Summary Report of Commercial Reactor Criticality Data for Crystal River Unit 3*, B00000000-01717-5705-00060 REV 01, CRWMS M&O, Las Vegas, Nevada, 1998.

24. S. M. Bowman, O. W. Herman, and M. C. Brady, *Scale-4 Analysis of Pressurized Water Reactor Critical Configurations: Volume 2 – Sequoyah Unit 2 Cycle 3*, ORNL/TM-12294/V2, Lockheed Martin Energy Research Corporation, Oak Ridge National Laboratory, March 1995.

25. S. M. Bowman and O. W. Herman, *Scale-4 Analysis of Pressurized Water Reactor Critical Configurations: Volume 3 – Surry Unit 1 Cycle 2*, ORNL/TM-12294/V3, Lockheed Martin Energy Research Corporation, Oak Ridge National Laboratory, March 1995.

26. M. D. DeHart, *Scale-4 Analysis of Pressurized Water Reactor Critical Configurations: Volume 4–Three Mile Island Unit 1 Cycle 5*, ORNL/TM-12294/V4, Lockheed Martin Energy Research Corporation, Oak Ridge National Laboratory, March 1995.

27. S. M. Bowman and T. Suto, *Scale-4 Analysis of Pressurized Water Reactor Critical Configurations: Volume 5 – North Anna Unit 1 Cycle 5*, ORNL/TM-12294/V5, Lockheed Martin Energy Research Corporation, Oak Ridge National Laboratory, October 1996.

28. J. F. Briesmeister (ed), "MCNP – A General Monte Carlo N-Particle Transport Code," Version 4B, LA-12625-M, Los Alamos National Laboratory, 1997.

29. *Criticality Model*, CAL-DS0-NU-000003 REV 00A, Bechtel SAIC Company, Las Vegas, Nevada, 2004.

30. J. R. Parrington, H. D. Knox, S. L. Breneman, E. M. Baum, and F. Feiner, "Nuclides and Isotopes," 15th Ed., General Electric Co. and KAPL, Inc., 1996.

APPENDIX A

ENERGY- AND REGION-INTEGRATED CRC k_{eff} SENSITIVITIES TO NUCLIDE TOTAL CROSS SECTIONS

Table A.1 Energy- and region-integrated sensitivity coefficients for CRC state-points

CR3SP1		CR3SP2		CR3SP3		CR3SP4		CR3SP5	
b-10	-1.72E-01	u-238	-1.58E-01	u-238	-1.65E-01	u-238	-1.51E-01	u-238	-1.55E-01
u-238	-1.69E-01	b-10	-1.13E-01	b-10	-5.47E-02	b-10	-1.23E-01	b-10	-1.34E-01
zr	-1.12E-02	pu-240	-2.73E-02	pu-240	-3.80E-02	pu-240	-2.76E-02	pu-240	-2.39E-02
o-16	-9.86E-03	sm-149	-1.24E-02	sm-149	-1.37E-02	sm-149	-1.01E-02	o-16	-1.24E-02
ni	-3.37E-03	zr	-1.05E-02	zr	-1.03E-02	zr	-9.96E-03	zr	-1.10E-02
ta-181	-1.62E-03	o-16	-9.92E-03	o-16	-8.69E-03	o-16	-9.80E-03	sm-149	-1.02E-02
u-234	-1.61E-03	nd-143	-5.01E-03	nd-143	-7.41E-03	nd-143	-5.43E-03	nd-143	-4.90E-03
cr	-1.04E-03	rh-103	-4.63E-03	rh-103	-6.10E-03	rh-103	-5.01E-03	rh-103	-4.59E-03
co-59	-6.58E-04	sm-151	-3.36E-03	ag-109	-4.79E-03	sm-151	-3.23E-03	ni	-3.07E-03
fe	-6.39E-04	ni	-3.24E-03	sm-151	-4.11E-03	ni	-3.17E-03	sm-151	-2.97E-03
ag-107	-4.44E-04	u-236	-3.03E-03	u-236	-3.79E-03	u-236	-2.63E-03	u-236	-2.38E-03
al-27	-3.00E-04	cs-133	-2.02E-03	ni	-3.33E-03	cs-133	-2.28E-03	cs-133	-2.09E-03
u-236	-2.95E-04	sm-152	-1.61E-03	cs-133	-2.98E-03	sm-152	-1.86E-03	sm-152	-1.66E-03
ag-109	-2.34E-04	ta-181	-1.61E-03	sm-152	-2.51E-03	tc-99	-1.71E-03	ta-181	-1.58E-03
mo	-2.31E-04	tc-99	-1.51E-03	tc-99	-2.23E-03	ta-181	-1.61E-03	tc-99	-1.57E-03
sn-117	-1.42E-04	u-234	-1.28E-03	np-237	-1.75E-03	u-234	-1.40E-03	u-234	-1.44E-03
mn-55	-1.26E-04	nd-145	-1.06E-03	nd-145	-1.61E-03	np-237	-1.29E-03	np-237	-1.20E-03
sn-118	-1.19E-04	np-237	-1.02E-03	ta-181	-1.57E-03	nd-145	-1.22E-03	nd-145	-1.12E-03
sn-116	-1.19E-04	cr	-9.94E-04	u-234	-1.22E-03	cr	-1.07E-03	cr	-9.69E-04
ti	-8.91E-05	mo-95	-6.92E-04	eu-153	-1.15E-03	fe	-1.01E-03	ag-109	-8.97E-04
nb-93	-8.12E-05	co-59	-6.38E-04	pu-242	-1.05E-03	eu-153	-7.95E-04	eu-153	-7.49E-04
sn-119	-7.23E-05	fe	-6.33E-04	cr	-1.05E-03	ag-109	-7.78E-04	fe	-7.48E-04
sn-115	-4.93E-05	eu-153	-6.24E-04	mo-95	-8.64E-04	mo-95	-7.66E-04	mo-95	-7.31E-04
cd	-4.60E-05	ag-109	-5.43E-04	sm-150	-7.70E-04	pu-242	-6.43E-04	pu-242	-6.23E-04
sn-120	-4.54E-05	sm-150	-4.65E-04	fe	-7.18E-04	co-59	-6.12E-04	ag-107	-6.05E-04
sn-124	-3.04E-05	ru-101	-4.52E-04	ru-101	-6.95E-04	ru-101	-5.39E-04	co-59	-6.02E-04
sn-112	-2.34E-05	am-	-4.32E-04	co-59	-6.45E-04	sm-150	-5.31E-04	am-241	-5.33E-04
cu	-1.72E-05	pu-242	-3.86E-04	am-241	-5.34E-04	am-241	-4.93E-04	ru-101	-5.02E-04
si	1.05E-05	sm-147	-3.00E-04	sm-147	-4.16E-04	sm-147	-4.08E-04	sm-150	-4.82E-04
in-115	3.12E-04	mo	-2.27E-04	in-115	-3.36E-04	ag-107	-3.72E-04	sm-147	-4.10E-04
h-1	1.13E-01	gd-155	-1.43E-04	pu-238	-2.98E-04	mo	-2.24E-04	mo	-2.21E-04
u-235	3.34E-01	sn-117	-1.32E-04	mo	-2.21E-04	pu-238	-1.90E-04	pu-238	-1.92E-04
		mn-55	-1.15E-04	mn-55	-1.65E-04	sn-117	-1.29E-04	sn-117	-1.29E-04
		sn-116	-1.13E-04	am-243	-1.59E-04	mn-55	-1.16E-04	gd-155	-1.20E-04
		sn-118	-1.12E-04	sn-117	-1.37E-04	sn-116	-1.12E-04	sn-118	-1.14E-04
		pu-238	-1.12E-04	sn-116	-1.14E-04	sn-118	-1.11E-04	sn-116	-1.14E-04
		ti	-8.50E-05	sn-118	-1.12E-04	am-243	-9.78E-05	am-243	-1.07E-04
		nb-93	-8.02E-05	ti	-8.72E-05	gd-155	-8.30E-05	mn-55	-1.00E-04
		sn-119	-6.66E-05	nb-93	-7.82E-05	ti	-8.10E-05	ti	-7.96E-05
		sn-115	-4.51E-05	sn-119	-7.04E-05	nb-93	-7.98E-05	nb-93	-7.88E-05
		in-115	-4.41E-05	sn-115	-4.90E-05	sn-119	-6.34E-05	cd	-6.54E-05
		sn-120	-4.19E-05	sn-120	-4.08E-05	sn-115	-4.25E-05	sn-119	-6.41E-05
		am-	-4.10E-05	gd-155	-3.31E-05	sn-120	-4.01E-05	sn-120	-4.40E-05
		sn-124	-2.85E-05	sn-124	-2.85E-05	sn-124	-2.81E-05	sn-115	-4.20E-05
		sn-112	-2.20E-05	sn-112	-2.24E-05	cd	-2.73E-05	sn-124	-2.88E-05
		eu-151	-1.97E-05	cu	-1.68E-05	sn-112	-2.16E-05	sn-112	-2.18E-05
		cu	-1.66E-05	pu-241	2.09E-02	cu	-1.60E-05	cu	-1.58E-05
		pu-241	1.15E-02	pu-239	1.10E-01	eu-151	-1.31E-05	eu-151	-1.45E-05
		pu-239	9.96E-02	u-235	1.53E-01	pu-241	1.40E-02	pu-241	1.26E-02
		h-1	1.32E-01	h-1	1.58E-01	pu-239	9.07E-02	pu-239	8.37E-02
		u-235	1.95E-01			h-1	1.32E-01	h-1	1.24E-01
						u-235	2.01E-01	u-235	2.16E-01

Table A.1 Energy- and region-integrated sensitivity coefficients for CRC state-points (continued)

CR3SP6		CR3SP7		CR3SP8		CR3SP9		CR3SP10	
u-238	-1.57E-01	u-238	-1.57E-01	u-238	-1.60E-01	u-238	-1.60E-01	u-238	-1.61E-01
b-10	-7.46E-02	b-10	-5.83E-02	b-10	-1.44E-01	b-10	-7.19E-02	b-10	-5.20E-02
pu-240	-3.38E-02	pu-240	-3.84E-02	pu-240	-1.99E-02	pu-240	-3.70E-02	pu-240	-3.82E-02
sm-149	-1.32E-02	sm-149	-1.35E-02	o-16	-1.22E-02	sm-149	-1.40E-02	sm-149	-1.37E-02
zr	-1.02E-02	zr	-9.97E-03	zr	-1.14E-02	o-16	-1.14E-02	zr	-1.08E-02
o-16	-9.14E-03	o-16	-8.98E-03	sm-149	-7.24E-03	zr	-1.13E-02	o-16	-1.00E-02
nd-143	-7.07E-03	nd-143	-8.08E-03	nd-143	-3.98E-03	nd-143	-7.49E-03	nd-143	-7.85E-03
rh-103	-5.88E-03	rh-103	-6.85E-03	rh-103	-3.67E-03	rh-103	-6.36E-03	rh-103	-6.88E-03
ag-109	-5.65E-03	ag-107	-4.60E-03	ni	-3.13E-03	sm-151	-4.24E-03	ag-107	-5.57E-03
sm-151	-3.97E-03	sm-151	-4.39E-03	u-236	-2.41E-03	u-236	-4.03E-03	sm-151	-4.37E-03
u-236	-3.85E-03	u-236	-4.15E-03	sm-151	-2.17E-03	ag-107	-3.44E-03	u-236	-4.11E-03
ni	-3.11E-03	cs-133	-3.41E-03	cs-133	-1.70E-03	ni	-3.26E-03	ni	-3.33E-03
cs-133	-2.99E-03	ni	-3.36E-03	ta-181	-1.61E-03	cs-133	-3.22E-03	cs-133	-3.32E-03
sm-152	-2.43E-03	sm-152	-2.79E-03	u-234	-1.48E-03	sm-152	-2.64E-03	sm-152	-2.72E-03
tc-99	-2.24E-03	tc-99	-2.54E-03	sm-152	-1.40E-03	ag-109	-2.60E-03	tc-99	-2.48E-03
np-237	-1.90E-03	np-237	-2.30E-03	tc-99	-1.27E-03	tc-99	-2.41E-03	np-237	-2.22E-03
nd-145	-1.62E-03	nd-145	-1.86E-03	cr	-1.00E-03	np-237	-2.12E-03	nd-145	-1.80E-03
ta-181	-1.57E-03	ag-109	-1.70E-03	np-237	-9.97E-04	nd-145	-1.75E-03	ag-109	-1.75E-03
u-234	-1.33E-03	ta-181	-1.62E-03	nd-145	-9.07E-04	ta-181	-1.61E-03	ta-181	-1.63E-03
eu-153	-1.23E-03	pu-242	-1.55E-03	ag-109	-8.70E-04	pu-242	-1.45E-03	pu-242	-1.52E-03
pu-242	-1.18E-03	eu-153	-1.49E-03	fe	-8.19E-04	eu-153	-1.39E-03	eu-153	-1.45E-03
cr	-9.61E-04	u-234	-1.29E-03	eu-153	-6.38E-04	u-234	-1.29E-03	u-234	-1.30E-03
mo-95	-8.57E-04	cr	-1.14E-03	ag-107	-6.19E-04	cr	-1.12E-03	fe	-1.25E-03
sm-150	-7.51E-04	fe	-1.01E-03	co-59	-6.16E-04	fe	-1.11E-03	cr	-1.19E-03
ru-101	-7.27E-04	mo-95	-1.01E-03	pu-242	-5.64E-04	mo-95	-8.95E-04	mo-95	-9.91E-04
co-59	-6.13E-04	sm-150	-8.92E-04	mo-95	-5.45E-04	sm-150	-8.40E-04	sm-150	-8.74E-04
fe	-6.11E-04	ru-101	-8.43E-04	al-27	-4.43E-04	ru-101	-7.98E-04	ru-101	-8.22E-04
am-241	-5.94E-04	am-241	-7.10E-04	sm-150	-4.11E-04	co-59	-6.22E-04	cd	-6.95E-04
sm-147	-4.72E-04	co-59	-6.39E-04	ru-101	-4.10E-04	al-27	-5.64E-04	co-59	-6.31E-04
pu-238	-3.90E-04	cd	-5.78E-04	am-241	-2.91E-04	am-241	-5.15E-04	am-241	-6.18E-04
in-115	-3.50E-04	sm-147	-5.36E-04	sm-147	-2.42E-04	pu-238	-4.49E-04	al-27	-5.79E-04
am-243	-2.65E-04	pu-238	-5.27E-04	mo	-2.26E-04	sm-147	-3.95E-04	pu-238	-4.89E-04
mo	-2.17E-04	am-243	-3.79E-04	pu-238	-1.55E-04	am-243	-3.56E-04	sm-147	-4.41E-04
sn-117	-1.32E-04	mo	-2.25E-04	sn-117	-1.38E-04	cd	-3.03E-04	am-243	-3.86E-04
mn-55	-1.27E-04	mn-55	-1.94E-04	sn-118	-1.21E-04	mo	-2.25E-04	mo	-2.26E-04
sn-116	-1.13E-04	sn-117	-1.33E-04	sn-116	-1.20E-04	sn-117	-1.41E-04	mn-55	-1.84E-04
sn-118	-1.12E-04	sn-116	-1.14E-04	am-243	-8.87E-05	mn-55	-1.25E-04	sn-117	-1.42E-04
ti	-8.19E-05	sn-118	-1.12E-04	mn-55	-8.36E-05	sn-116	-1.20E-04	sn-116	-1.20E-04
nb-93	-7.75E-05	ti	-8.58E-05	ti	-8.14E-05	sn-118	-1.20E-04	sn-118	-1.19E-04
sn-119	-6.62E-05	nb-93	-8.00E-05	nb-93	-8.03E-05	ti	-8.31E-05	ti	-8.39E-05
sn-115	-4.50E-05	sn-119	-6.70E-05	sn-119	-6.83E-05	nb-93	-8.03E-05	nb-93	-8.09E-05
sn-120	-4.09E-05	in-113	-4.63E-05	gd-155	-5.48E-05	sn-119	-7.04E-05	sn-119	-7.10E-05
gd-155	-3.82E-05	sn-115	-4.60E-05	cd	-5.33E-05	sn-115	-4.71E-05	gd-155	-5.82E-05
sn-124	-2.85E-05	gd-155	-4.25E-05	sn-120	-4.65E-05	sn-120	-4.58E-05	in-113	-5.45E-05
sn-112	-2.21E-05	sn-120	-4.02E-05	sn-115	-4.48E-05	gd-155	-4.01E-05	sn-115	-4.81E-05
cu	-1.60E-05	sn-124	-2.85E-05	sn-124	-3.07E-05	sn-124	-3.07E-05	sn-120	-4.42E-05
pu-241	1.97E-02	sn-112	-2.21E-05	sn-112	-2.33E-05	sn-112	-2.36E-05	sn-124	-3.08E-05
pu-239	9.88E-02	cu	-1.67E-05	cu	-1.61E-05	in-113	-2.00E-05	sn-112	-2.37E-05
h-1	1.58E-01	pu-241	2.39E-02	pu-241	1.15E-02	cu	-1.63E-05	cu	-1.65E-05
u-235	1.69E-01	pu-239	1.05E-01	pu-239	6.59E-02	pu-241	2.32E-02	pu-241	2.34E-02
		u-235	1.53E-01	h-1	1.29E-01	pu-239	1.06E-01	pu-239	1.04E-01
		h-1	1.64E-01	u-235	2.37E-01	u-235	1.56E-01	u-235	1.50E-01
						h-1	1.58E-01	h-1	1.66E-01

Table A.1 Energy- and region-integrated sensitivity coefficients for CRC state-points (continued)

CR3SP11		CR3SP12		CR3SP13		CR3SP14		CR3SP15	
b-10	-1.55E-01	u-238	-1.56E-01	b-10	-1.47E-01	u-238	-1.43E-01	u-238	-1.50E-01
u-238	-1.50E-01	b-10	-6.04E-02	u-238	-1.43E-01	b-10	-1.15E-01	pu-240	-4.69E-02
pu-240	-1.75E-02	pu-240	-4.48E-02	pu-240	-2.20E-02	pu-240	-2.81E-02	b-10	-3.86E-02
o-16	-1.14E-02	sm-149	-1.38E-02	o-16	-1.18E-02	sm-149	-1.22E-02	sm-149	-1.48E-02
zr	-1.08E-02	o-16	-1.25E-02	zr	-1.06E-02	o-16	-1.07E-02	o-16	-1.15E-02
sm-149	-5.77E-03	zr	-1.14E-02	sm-149	-6.94E-03	zr	-1.03E-02	zr	-1.08E-02
nd-143	-3.35E-03	nd-143	-9.41E-03	nd-143	-4.56E-03	nd-143	-6.13E-03	nd-143	-1.07E-02
rh-103	-3.22E-03	rh-103	-8.29E-03	rh-103	-4.55E-03	rh-103	-6.02E-03	rh-103	-9.43E-03
ni	-2.86E-03	sm-151	-4.86E-03	ni	-3.38E-03	u-236	-3.74E-03	ag-109	-6.81E-03
u-236	-2.19E-03	u-236	-4.82E-03	u-236	-2.81E-03	sm-151	-3.53E-03	sm-151	-5.28E-03
sm-151	-1.82E-03	cs-133	-4.14E-03	sm-151	-2.27E-03	ni	-3.08E-03	u-236	-5.25E-03
u-234	-1.61E-03	sm-152	-3.45E-03	cs-133	-2.06E-03	cs-133	-2.77E-03	cs-133	-4.72E-03
ta-181	-1.55E-03	ni	-3.15E-03	ta-181	-1.73E-03	ag-107	-2.31E-03	sm-152	-3.88E-03
cs-133	-1.46E-03	tc-99	-3.10E-03	sm-152	-1.71E-03	sm-152	-2.19E-03	np-237	-3.87E-03
sm-152	-1.19E-03	np-237	-3.04E-03	u-234	-1.64E-03	tc-99	-2.07E-03	tc-99	-3.52E-03
tc-99	-1.09E-03	pu-242	-2.30E-03	tc-99	-1.54E-03	ag-109	-2.07E-03	ni	-3.02E-03
cr	-9.01E-04	nd-145	-2.29E-03	np-237	-1.41E-03	np-237	-1.89E-03	pu-242	-2.88E-03
np-237	-8.19E-04	eu-153	-2.00E-03	nd-145	-1.11E-03	ta-181	-1.63E-03	nd-145	-2.63E-03
ag-107	-7.85E-04	ta-181	-1.63E-03	cr	-1.07E-03	u-234	-1.55E-03	eu-153	-2.45E-03
nd-145	-7.73E-04	ag-109	-1.51E-03	fe	-9.26E-04	nd-145	-1.49E-03	ta-181	-1.56E-03
ag-109	-7.48E-04	u-234	-1.29E-03	pu-242	-8.95E-04	pu-242	-1.24E-03	mo-95	-1.49E-03
fe	-6.65E-04	mo-95	-1.23E-03	eu-153	-8.68E-04	eu-153	-1.17E-03	u-234	-1.34E-03
co-59	-5.71E-04	sm-150	-1.14E-03	mo-95	-7.44E-04	am-241	-1.10E-03	sm-150	-1.32E-03
eu-153	-5.21E-04	ru-101	-1.07E-03	am-241	-7.18E-04	mo-95	-9.97E-04	ru-101	-1.27E-03
mo-95	-5.01E-04	cr	-1.00E-03	ag-109	-6.95E-04	cr	-9.78E-04	am-241	-1.26E-03
pu-242	-4.25E-04	fe	-7.79E-04	co-59	-6.44E-04	fe	-7.93E-04	pu-238	-1.16E-03
ru-101	-3.49E-04	am-241	-7.77E-04	ru-101	-5.31E-04	ru-101	-7.11E-04	cr	-9.96E-04
am-241	-3.47E-04	pu-238	-7.56E-04	sm-150	-5.09E-04	sm-150	-6.76E-04	am-243	-9.80E-04
sm-150	-3.38E-04	am-243	-6.37E-04	sm-147	-4.09E-04	sm-147	-6.15E-04	fe	-8.55E-04
al-27	-3.14E-04	co-59	-6.22E-04	pu-238	-2.55E-04	co-59	-6.00E-04	sm-147	-8.46E-04
sm-147	-2.51E-04	sm-147	-5.61E-04	mo	-2.55E-04	pu-238	-3.95E-04	co-59	-5.92E-04
mo	-2.17E-04	al-27	-5.26E-04	al-27	-2.32E-04	am-243	-2.94E-04	al-27	-3.96E-04
sn-117	-1.33E-04	mo	-2.25E-04	am-243	-1.73E-04	al-27	-2.68E-04	in-115	-2.64E-04
sn-118	-1.19E-04	ag-107	-2.11E-04	gd-155	-1.49E-04	mo	-2.33E-04	mo	-2.14E-04
sn-116	-1.18E-04	sn-117	-1.39E-04	sn-117	-1.28E-04	gd-155	-1.78E-04	sn-117	-1.36E-04
pu-238	-1.16E-04	sn-118	-1.21E-04	mn-55	-1.22E-04	cd	-1.38E-04	mn-55	-1.19E-04
mn-55	-1.04E-04	sn-116	-1.21E-04	sn-118	-1.17E-04	sn-117	-1.29E-04	sn-116	-1.19E-04
nb-93	-7.73E-05	mn-55	-1.02E-04	sn-116	-1.17E-04	sn-116	-1.18E-04	sn-118	-1.18E-04
cd	-7.66E-05	ti	-8.20E-05	nb-93	-9.29E-05	sn-118	-1.17E-04	ti	-7.77E-05
ti	-7.37E-05	nb-93	-8.14E-05	ag-107	-9.10E-05	mn-55	-1.11E-04	nb-93	-7.48E-05
gd-155	-6.51E-05	sn-119	-6.90E-05	ti	-8.41E-05	nb-93	-8.33E-05	sn-119	-6.66E-05
sn-119	-6.33E-05	sn-120	-4.64E-05	sn-119	-6.00E-05	ti	-7.82E-05	gd-155	-6.63E-05
am-243	-5.75E-05	sn-115	-4.55E-05	sn-120	-4.39E-05	sn-119	-6.06E-05	sn-120	-4.42E-05
sn-120	-4.48E-05	gd-155	-3.91E-05	sn-115	-3.76E-05	sn-120	-4.27E-05	sn-115	-4.40E-05
sn-115	-4.06E-05	sn-124	-3.10E-05	sn-124	-2.98E-05	sn-115	-3.86E-05	sn-124	-3.03E-05
sn-124	-3.03E-05	cd	-2.65E-05	sn-112	-2.25E-05	sn-124	-2.97E-05	sn-112	-2.31E-05
sn-112	-2.29E-05	sn-112	-2.36E-05	cu	-1.76E-05	sn-112	-2.26E-05	cu	-1.54E-05
cu	-1.49E-05	cu	-1.63E-05	eu-151	-1.43E-05	eu-151	-1.96E-05	pu-241	3.45E-02
pu-241	9.58E-03	pu-241	3.14E-02	pu-241	1.46E-02	cu	-1.61E-05	pu-239	1.09E-01
pu-239	5.87E-02	pu-239	1.12E-01	pu-239	6.62E-02	pu-241	1.80E-02	u-235	1.25E-01
h-1	1.33E-01	u-235	1.33E-01	h-1	1.37E-01	pu-239	8.51E-02	h-1	1.76E-01
u-235	2.43E-01	h-1	1.63E-01	u-235	2.24E-01	h-1	1.50E-01		
						u-235	1.89E-01		

Table A.1 Energy- and region-integrated sensitivity coefficients for CRC state-points (continued)

CR3SP16		CR3SP17		CR3SP18		CR3SP19		CR3SP20	
b-10	-1.68E-01	u-238	-1.38E-01	u-238	-1.39E-01	u-238	-1.39E-01	u-238	-1.44E-01
u-238	-1.35E-01	b-10	-1.03E-01	b-10	-9.59E-02	b-10	-8.91E-02	b-10	-5.11E-02
pu-240	-1.79E-02	pu-240	-3.41E-02	pu-240	-3.62E-02	pu-240	-3.71E-02	pu-240	-4.44E-02
zr	-9.84E-03	sm-149	-1.24E-02	sm-149	-1.26E-02	sm-149	-1.25E-02	sm-149	-1.17E-02
o-16	-9.76E-03	o-16	-9.90E-03	o-16	-1.11E-02	zr	-9.91E-03	o-16	-1.05E-02
sm-149	-5.21E-03	zr	-9.77E-03	zr	-1.03E-02	o-16	-9.85E-03	zr	-1.03E-02
zr-93	-3.87E-03	nd-143	-7.36E-03	nd-143	-7.90E-03	nd-143	-8.32E-03	nd-143	-1.03E-02
rh-103	-3.70E-03	rh-103	-6.69E-03	rh-103	-7.50E-03	rh-103	-8.10E-03	rh-103	-9.09E-03
nd-143	-3.67E-03	u-236	-4.54E-03	u-236	-4.78E-03	u-236	-4.83E-03	in-115	-6.48E-03
u-236	-2.51E-03	sm-151	-4.11E-03	sm-151	-4.32E-03	sm-151	-4.42E-03	u-236	-5.36E-03
sm-151	-1.84E-03	zr-93	-3.79E-03	zr-93	-3.97E-03	zr-93	-3.82E-03	sm-151	-5.15E-03
u-234	-1.79E-03	cs-133	-3.45E-03	cs-133	-3.69E-03	cs-133	-3.80E-03	cs-133	-4.61E-03
cs-133	-1.73E-03	sm-152	-2.73E-03	sm-152	-2.93E-03	sm-152	-3.02E-03	np-237	-3.81E-03
ni	-1.72E-03	tc-99	-2.58E-03	np-237	-2.78E-03	np-237	-2.88E-03	zr-93	-3.79E-03
sm-152	-1.42E-03	np-237	-2.51E-03	tc-99	-2.76E-03	tc-99	-2.84E-03	sm-152	-3.75E-03
tc-99	-1.29E-03	ag-109	-2.11E-03	ag-107	-2.46E-03	ag-109	-2.11E-03	ag-109	-3.70E-03[a]
np-237	-1.19E-03	ag-107	-2.01E-03	nd-145	-2.01E-03	ag-107	-2.11E-03	tc-99	-3.45E-03
nd-145	-9.29E-04	nd-145	-1.88E-03	ag-109	-1.86E-03	nd-145	-2.08E-03	pu-242	-2.67E-03
am-241	-9.02E-04	pu-242	-1.61E-03	ni	-1.79E-03	pu-242	-1.86E-03	nd-145	-2.61E-03
ta-181	-8.70E-04	u-234	-1.55E-03	pu-242	-1.78E-03	eu-153	-1.74E-03	eu-153	-2.36E-03
pu-242	-7.13E-04	eu-153	-1.53E-03	eu-153	-1.67E-03	u-234	-1.52E-03	ni	-1.72E-03
eu-153	-7.10E-04	ni	-1.45E-03	u-234	-1.53E-03	ni	-1.52E-03	mo-95	-1.55E-03
mo-95	-6.12E-04	mo-95	-1.05E-03	mo-95	-1.20E-03	am-241	-1.44E-03	am-241	-1.47E-03
cr	-5.90E-04	am-241	-9.72E-04	am-241	-1.06E-03	mo-95	-1.37E-03	u-234	-1.44E-03
ag-109	-5.17E-04	ru-101	-9.15E-04	ru-101	-9.88E-04	ru-101	-1.02E-03	ru-101	-1.27E-03
fe	-5.08E-04	sm-150	-8.38E-04	sm-150	-9.02E-04	sm-150	-9.42E-04	sm-150	-1.25E-03
ru-101	-4.54E-04	ta-181	-7.55E-04	ta-181	-8.56E-04	sm-147	-8.58E-04	pu-238	-1.18E-03
sm-147	-4.19E-04	sm-147	-6.37E-04	sm-147	-6.93E-04	ta-181	-7.68E-04	sm-147	-9.75E-04
sm-150	-4.05E-04	pu-238	-6.03E-04	pu-238	-6.77E-04	pu-238	-7.54E-04	am-243	-9.48E-04
co-59	-3.23E-04	cr	-5.11E-04	cr	-6.41E-04	am-243	-5.84E-04	ta-181	-7.91E-04
al-27	-3.19E-04	am-243	-4.87E-04	fe	-6.01E-04	cr	-5.43E-04	cr	-6.60E-04
pu-238	-2.10E-04	al-27	-4.48E-04	am-243	-5.51E-04	al-27	-4.70E-04	fe	-6.54E-04
gd-155	-1.69E-04	fe	-3.74E-04	al-27	-4.41E-04	fe	-4.23E-04	al-27	-5.19E-04
am-243	-1.43E-04	co-59	-2.81E-04	co-59	-3.27E-04	co-59	-2.90E-04	co-59	-3.15E-04
mo	-1.31E-04	cd	-1.74E-04	sn-117	-1.33E-04	cd	-2.04E-04	sn-117	-1.37E-04
sn-117	-1.29E-04	sn-117	-1.32E-04	mo	-1.28E-04	gd-155	-1.95E-04	cd	-1.34E-04
sn-118	-1.20E-04	sn-118	-1.20E-04	sn-118	-1.22E-04	sn-117	-1.33E-04	mn-55	-1.22E-04
sn-116	-1.18E-04	sn-116	-1.19E-04	sn-116	-1.21E-04	sn-118	-1.20E-04	sn-118	-1.20E-04
mn-55	-8.53E-05	mo	-1.08E-04	mn-55	-1.06E-04	sn-116	-1.19E-04	sn-116	-1.19E-04
sn-119	-5.81E-05	mn-55	-7.94E-05	gd-155	-8.62E-05	mo	-1.11E-04	mo	-1.15E-04
nb-93	-4.95E-05	sn-119	-6.10E-05	sn-119	-6.18E-05	mn-55	-9.21E-05	sn-119	-6.55E-05
sn-120	-4.26E-05	gd-155	-5.15E-05	nb-93	-4.85E-05	sn-119	-6.20E-05	gd-155	-5.12E-05
ti	-4.23E-05	sn-120	-4.21E-05	sn-120	-4.44E-05	sn-120	-4.24E-05	sn-120	-4.34E-05
sn-115	-3.59E-05	nb-93	-3.94E-05	ti	-4.40E-05	nb-93	-4.00E-05	sn-115	-4.28E-05
sn-124	-3.04E-05	sn-115	-3.89E-05	sn-115	-3.89E-05	sn-115	-3.97E-05	nb-93	-4.26E-05
sn-112	-2.29E-05	ti	-3.70E-05	sn-124	-3.11E-05	ti	-3.85E-05	ti	-4.26E-05
eu-151	-1.92E-05	sn-124	-3.05E-05	sn-112	-2.35E-05	sn-124	-3.06E-05	sn-124	-3.08E-05
pu-241	1.13E-02	sn-112	-2.32E-05	eu-151	-1.11E-05	sn-112	-2.33E-05	sn-112	-2.35E-05
pu-239	5.48E-02	in-113	-1.24E-05	pu-241	2.38E-02	eu-151	-2.06E-05	pu-241	3.16E-02
h-1	1.42E-01	pu-241	2.21E-02	pu-239	9.44E-02	in-113	-1.53E-05	pu-239	1.01E-01
u-235	2.37E-01	pu-239	9.16E-02	u-235	1.58E-01	pu-241	2.43E-02	u-235	1.31E-01
		u-235	1.65E-01	h-1	1.69E-01	pu-239	9.55E-02	h-1	1.79E-01
		h-1	1.66E-01			u-235	1.56E-01		
						h-1	1.72E-01		

[a] Value determined using the direct perturbation method.

Table A.1 Energy- and region-integrated sensitivity coefficients for CRC state-points (continued)

CR3SP21		CR3SP22		CR3SP23		CR3SP24		CR3SP25	
u-238	-1.45E-01	b-10	-1.68E-01	b-10	-1.41E-01	b-10	-1.32E-01	u-238	-1.37E-01
b-10	-4.73E-02	u-238	-1.31E-01	u-238	-1.31E-01	u-238	-1.31E-01	b-10	-7.42E-02
pu-240	-4.49E-02	pu-240	-1.86E-02	pu-240	-2.47E-02	pu-240	-2.72E-02	pu-240	-4.12E-02
sm-149	-1.33E-02	o-16	-1.14E-02	o-16	-1.17E-02	sm-149	-1.09E-02	sm-149	-1.38E-02
nd-143	-1.05E-02	zr	-1.02E-02	sm-149	-1.12E-02	o-16	-1.06E-02	o-16	-1.10E-02
o-16	-1.01E-02	zr-93	-6.59E-03	zr	-1.03E-02	zr	-9.76E-03	zr	-1.00E-02
zr	-1.00E-02	sm-149	-5.85E-03	zr-93	-6.71E-03	zr-93	-6.48E-03	nd-143	-9.58E-03
rh-103	-9.32E-03	rh-103	-3.96E-03	nd-143	-5.25E-03	nd-143	-5.72E-03	rh-103	-8.96E-03
ag-109	-5.59E-03	nd-143	-3.92E-03	rh-103	-4.87E-03	rh-103	-5.28E-03	zr-93	-6.70E-03
u-236	-5.42E-03	u-236	-2.78E-03	u-236	-3.82E-03	u-236	-4.08E-03	u-236	-5.35E-03
sm-151	-5.19E-03	sm-151	-2.04E-03	sm-151	-3.29E-03	sm-151	-3.56E-03	sm-151	-4.88E-03
cs-133	-4.71E-03	cs-133	-1.88E-03	ag-109	-3.06E-03	ag-109	-3.47E-03	cs-133	-4.40E-03
np-237	-3.91E-03	u-234	-1.80E-03	cs-133	-2.60E-03	cs-133	-2.81E-03	np-237	-3.69E-03
sm-152	-3.82E-03	sm-152	-1.52E-03	sm-152	-2.01E-03	sm-152	-2.20E-03	sm-152	-3.52E-03
zr-93	-3.73E-03	tc-99	-1.42E-03	tc-99	-1.97E-03	tc-99	-2.13E-03	tc-99	-3.28E-03
tc-99	-3.52E-03	np-237	-1.34E-03	np-237	-1.84E-03	np-237	-2.00E-03	ag-107	-3.12E-03
pu-242	-2.73E-03	nd-145	-1.02E-03	u-234	-1.69E-03	u-234	-1.66E-03	nd-145	-2.44E-03
nd-145	-2.64E-03	am-241	-9.55E-04	nd-145	-1.41E-03	nd-145	-1.54E-03	ag-109	-2.39E-03
eu-153	-2.41E-03	ni	-8.09E-04	eu-153	-1.06E-03	eu-153	-1.16E-03	pu-242	-2.39E-03
ni	-1.70E-03	eu-153	-7.65E-04	pu-242	-1.05E-03	pu-242	-1.15E-03	eu-153	-2.14E-03
mo-95	-1.57E-03	pu-242	-7.36E-04	am-241	-8.76E-04	am-241	-8.59E-04	u-234	-1.48E-03
am-241	-1.49E-03	mo-95	-6.68E-04	mo-95	-7.88E-04	mo-95	-8.47E-04	mo-95	-1.47E-03
u-234	-1.43E-03	ag-109	-5.42E-04	ni	-7.46E-04	ru-101	-7.57E-04	ru-101	-1.22E-03
ru-101	-1.29E-03	ru-101	-5.01E-04	ru-101	-6.95E-04	sm-150	-6.47E-04	am-241	-1.21E-03
sm-150	-1.27E-03	sm-147	-4.48E-04	sm-150	-5.88E-04	sm-147	-5.25E-04	sm-150	-1.13E-03
pu-238	-1.20E-03	sm-150	-4.32E-04	sm-147	-5.00E-04	ni	-4.82E-04	pu-238	-9.47E-04
sm-147	-9.94E-04	cr	-3.39E-04	fe	-3.62E-04	pu-238	-3.77E-04	sm-147	-8.09E-04
am-243	-9.70E-04	fe	-3.38E-04	pu-238	-3.30E-04	am-243	-2.84E-04	am-243	-7.58E-04
ta-181	-7.76E-04	ta-181	-3.10E-04	cr	-3.29E-04	cr	-2.40E-04	ni	-6.75E-04
fe	-6.95E-04	pu-238	-2.20E-04	ta-181	-2.79E-04	fe	-2.21E-04	fe	-4.53E-04
cr	-6.76E-04	al-27	-1.92E-04	in-115	-2.46E-04	ta-181	-2.03E-04	cr	-3.61E-04
al-27	-4.93E-04	gd-155	-1.89E-04	am-243	-2.46E-04	al-27	-1.98E-04	al-27	-3.25E-04
in-115	-3.68E-04	am-243	-1.47E-04	al-27	-2.13E-04	in-115	-1.71E-04	ta-181	-2.42E-04
co-59	-3.12E-04	sn-117	-1.27E-04	sn-117	-1.28E-04	sn-117	-1.28E-04	sn-117	-1.33E-04
mn-55	-1.37E-04	co-59	-1.26E-04	sn-118	-1.22E-04	sn-118	-1.21E-04	sn-118	-1.21E-04
sn-117	-1.37E-04	sn-118	-1.21E-04	sn-116	-1.19E-04	sn-116	-1.18E-04	sn-116	-1.20E-04
sn-116	-1.20E-04	sn-116	-1.17E-04	co-59	-1.19E-04	co-59	-8.28E-05	gd-155	-1.14E-04
sn-118	-1.20E-04	mn-55	-5.96E-05	mn-55	-5.93E-05	sn-119	-5.73E-05	co-59	-1.05E-04
mo	-1.14E-04	sn-119	-5.67E-05	sn-119	-5.73E-05	mn-55	-4.53E-05	mn-55	-8.40E-05
sn-119	-6.55E-05	mo	-5.52E-05	mo	-4.96E-05	sn-120	-4.29E-05	sn-119	-6.20E-05
gd-155	-6.34E-05	sn-120	-4.44E-05	sn-120	-4.51E-05	sn-115	-3.50E-05	sn-120	-4.37E-05
sn-115	-4.31E-05	sn-115	-3.40E-05	sn-115	-3.43E-05	mo	-3.40E-05	mo	-4.28E-05
sn-120	-4.25E-05	sn-124	-3.04E-05	gd-155	-3.16E-05	sn-124	-3.04E-05	sn-115	-3.92E-05
ti	-4.20E-05	nb-93	-2.36E-05	sn-124	-3.09E-05	gd-155	-2.77E-05	sn-124	-3.10E-05
nb-93	-4.19E-05	sn-112	-2.28E-05	sn-112	-2.30E-05	sn-112	-2.30E-05	sn-112	-2.35E-05
sn-124	-3.08E-05	eu-151	-2.03E-05	nb-93	-2.21E-05	nb-93	-1.44E-05	nb-93	-1.79E-05
sn-112	-2.36E-05	ti	-1.89E-05	ti	-1.71E-05	ti	-1.14E-05	ti	-1.54E-05
pu-241	3.19E-02	pu-241	1.14E-02	pu-241	1.52E-02	pu-241	1.64E-02	eu-151	-1.19E-05
pu-239	1.01E-01	pu-239	5.54E-02	pu-239	7.60E-02	pu-239	7.93E-02	pu-241	2.85E-02
u-235	1.29E-01	h-1	1.39E-01	h-1	1.48E-01	h-1	1.55E-01	pu-239	9.76E-02
h-1	1.87E-01	u-235	2.38E-01	u-235	2.04E-01	u-235	1.93E-01	u-235	1.42E-01
								h-1	1.79E-01

Table A.1 Energy- and region-integrated sensitivity coefficients for CRC state-points (continued)

CR3SP26		CR3SP27		CR3SP28		CR3SP29		CR3SP30	
u-238	-1.37E-01	u-238	-1.40E-01	b-10	-1.72E-01	u-238	-1.31E-01	u-238	-1.32E-01
b-10	-7.42E-02	b-10	-5.93E-02	u-238	-1.30E-01	b-10	-1.27E-01	b-10	-1.20E-01
pu-240	-4.12E-02	pu-240	-4.63E-02	pu-240	-1.89E-02	pu-240	-2.90E-02	pu-240	-3.31E-02
sm-149	-1.38E-02	sm-149	-1.39E-02	o-16	-1.11E-02	sm-149	-1.00E-02	sm-149	-1.26E-02
o-16	-1.10E-02	o-16	-1.19E-02	zr	-1.00E-02	o-16	-9.86E-03	o-16	-1.15E-02
zr	-1.00E-02	nd-143	-1.09E-02	zr-93	-7.09E-03	zr	-9.39E-03	zr	-1.00E-02
nd-143	-9.58E-03	zr	-1.04E-02	sm-149	-5.88E-03	zr-93	-6.67E-03	nd-143	-7.36E-03
rh-103	-8.96E-03	rh-103	-9.94E-03	rh-103	-4.08E-03	nd-143	-6.15E-03	rh-103	-7.04E-03
zr-93	-6.70E-03	zr-93	-6.90E-03	nd-143	-4.03E-03	rh-103	-5.54E-03	zr-93	-6.99E-03
u-236	-5.35E-03	u-236	-5.70E-03	u-236	-2.90E-03	u-236	-4.32E-03	u-236	-4.73E-03
sm-151	-4.88E-03	sm-151	-5.42E-03	sm-151	-2.11E-03	sm-151	-3.75E-03	sm-151	-4.13E-03
cs-133	-4.40E-03	cs-133	-5.01E-03	cs-133	-1.96E-03	ag-109	-3.28E-03	ag-109	-3.58E-03
np-237	-3.69E-03	np-237	-4.46E-03	u-234	-1.81E-03	cs-133	-3.01E-03	cs-133	-3.50E-03
sm-152	-3.52E-03	sm-152	-4.05E-03	sm-152	-1.57E-03	sm-152	-2.37E-03	sm-152	-2.74E-03
ag-107	-3.28E-03	tc-99	-3.74E-03	tc-99	-1.47E-03	tc-99	-2.28E-03	np-237	-2.73E-03
tc-99	-3.12E-03	pu-242	-3.07E-03	np-237	-1.41E-03	np-237	-2.21E-03	tc-99	-2.63E-03
ag-109	-2.44E-03	nd-145	-2.82E-03	nd-145	-1.06E-03	u-234	-1.67E-03	nd-145	-1.92E-03
nd-145	-2.39E-03	eu-153	-2.65E-03	eu-153	-7.91E-04	nd-145	-1.67E-03	u-234	-1.59E-03
pu-242	-2.39E-03	ag-109	-2.54E-03	pu-242	-7.37E-04	eu-153	-1.28E-03	pu-242	-1.57E-03
eu-153	-2.14E-03	ag-107	-2.25E-03	mo-95	-7.00E-04	pu-242	-1.26E-03	eu-153	-1.54E-03
mo-95	-1.48E-03	mo-95	-1.69E-03	am-241	-6.71E-04	mo-95	-8.92E-04	mo-95	-1.13E-03
u-234	-1.47E-03	am-241	-1.43E-03	ag-109	-5.44E-04	ru-101	-8.18E-04	am-241	-9.59E-04
am-241	-1.22E-03	ru-101	-1.42E-03	ni	-5.39E-04	am-241	-7.56E-04	ru-101	-9.53E-04
ru-101	-1.21E-03	u-234	-1.41E-03	ru-101	-5.27E-04	sm-150	-7.06E-04	sm-150	-8.31E-04
sm-150	-1.13E-03	sm-150	-1.36E-03	sm-150	-4.44E-04	sm-147	-5.63E-04	sm-147	-6.75E-04
pu-238	-9.47E-04	pu-238	-1.33E-03	sm-147	-4.34E-04	pu-238	-4.44E-04	pu-238	-5.92E-04
ni	-8.09E-04	am-243	-1.10E-03	fe	-3.22E-04	am-243	-3.33E-04	am-243	-4.54E-04
sm-147	-7.58E-04	sm-147	-9.40E-04	cr	-2.71E-04	al-27	-1.97E-04	al-27	-2.47E-04
am-243	-6.75E-04	al-27	-3.91E-04	al-27	-2.35E-04	ni	-1.59E-04	ni	-2.31E-04
fe	-4.53E-04	fe	-2.60E-04	pu-238	-2.32E-04	in-115	-1.49E-04	fe	-2.16E-04
cr	-3.61E-04	ni	-2.35E-04	ta-181	-1.67E-04	cr	-1.47E-04	cr	-1.81E-04
al-27	-3.25E-04	cr	-2.08E-04	am-243	-1.52E-04	sn-117	-1.27E-04	in-115	-1.31E-04
ta-181	-2.42E-04	sn-117	-1.36E-04	sn-117	-1.27E-04	fe	-1.22E-04	sn-117	-1.29E-04
sn-117	-1.33E-04	sn-118	-1.23E-04	sn-118	-1.22E-04	sn-118	-1.19E-04	sn-118	-1.21E-04
co-59	-1.21E-04	sn-116	-1.20E-04	sn-116	-1.18E-04	sn-116	-1.16E-04	sn-116	-1.18E-04
sn-118	-1.20E-04	ta-181	-1.14E-04	gd-155	-1.03E-04	ta-181	-6.93E-05	gd-155	-8.71E-05
sn-116	-1.14E-04	gd-155	-6.81E-05	co-59	-7.71E-05	sn-119	-5.67E-05	ta-181	-8.10E-05
mn-55	-1.05E-04	sn-119	-6.45E-05	sn-119	-5.62E-05	sn-120	-4.11E-05	sn-119	-5.81E-05
gd-155	-8.40E-05	mn-55	-4.88E-05	mn-55	-4.58E-05	sn-115	-3.50E-05	sn-120	-4.38E-05
sn-119	-6.20E-05	sn-120	-4.52E-05	sn-120	-4.41E-05	mn-55	-3.32E-05	co-59	-3.68E-05
mo	-4.37E-05	co-59	-4.23E-05	mo	-3.50E-05	co-59	-3.08E-05	sn-115	-3.55E-05
sn-120	-4.28E-05	sn-115	-4.13E-05	sn-115	-3.35E-05	sn-124	-2.99E-05	mn-55	-3.35E-05
sn-115	-3.92E-05	sn-124	-3.14E-05	sn-124	-3.07E-05	gd-155	-2.52E-05	sn-124	-3.07E-05
sn-124	-3.10E-05	sn-112	-2.37E-05	sn-112	-2.28E-05	sn-112	-2.27E-05	sn-112	-2.30E-05
sn-112	-2.35E-05	mo	-1.59E-05	nb-93	-1.68E-05	mo	-1.18E-05	mo	-1.50E-05
nb-93	-1.79E-05	pu-241	3.41E-02	eu-151	-1.62E-05	pu-241	1.73E-02	eu-151	-1.13E-05
ti	-1.54E-05	pu-239	1.03E-01	ti	-1.20E-05	pu-239	7.97E-02	pu-241	2.09E-02
eu-151	-1.19E-05	u-235	1.28E-01	pu-241	1.14E-02	h-1	1.54E-01	pu-239	8.87E-02
pu-241	2.85E-02	h-1	1.85E-01	pu-239	5.42E-02	u-235	1.88E-01	h-1	1.59E-01
pu-239	9.76E-02			h-1	1.41E-01			u-235	1.75E-01
u-235	1.42E-01			u-235	2.38E-01				
h-1	1.79E-01								

Table A.1 Energy- and region-integrated sensitivity coefficients for CRC state-points (continued)

CR3SP31		CR3SP32		CR3SP33		SQ2C3BZ		SQ2C3BF	
u-238	-1.37E-01	b-10	-1.73E-01	u-238	-1.35E-01	b-10	-1.45E-01	u-238	-1.45E-01
b-10	-8.11E-02	u-238	-1.26E-01	pu-240	-4.59E-02	u-238	-1.40E-01	b-10	-1.01E-01
pu-240	-4.12E-02	pu-240	-1.81E-02	b-10	-4.33E-02	pu-240	-2.24E-02	xe-135	-2.72E-02
o-16	-1.16E-02	zr-93	-1.01E-02	sm-149	-1.51E-02	o-16	-1.02E-02	pu-240	-2.35E-02
sm-149	-1.13E-02	o-16	-9.98E-03	nd-143	-1.16E-02	zr	-8.61E-03	o-16	-1.10E-02
zr	-1.03E-02	zr	-9.31E-03	rh-103	-1.04E-02	sm-149	-8.58E-03	zr	-8.85E-03
nd-143	-9.31E-03	sm-149	-5.78E-03	zr	-8.70E-03	rh-103	-4.58E-03	sm-149	-5.94E-03
rh-103	-8.40E-03	rh-103	-3.91E-03	o-16	-8.18E-03	nd-143	-4.50E-03	rh-103	-4.61E-03
zr-93	-7.19E-03	nd-143	-3.89E-03	zr-93	-6.38E-03	u-236	-3.06E-03	nd-143	-4.42E-03
u-236	-5.43E-03	u-236	-2.78E-03	u-236	-5.88E-03	xe-131	-2.80E-03	u-236	-3.34E-03
sm-151	-4.93E-03	sm-151	-1.94E-03	sm-151	-5.65E-03	sm-151	-2.58E-03	xe-131	-2.86E-03
cs-133	-4.38E-03	cs-133	-1.92E-03	cs-133	-5.21E-03	pm-147	-2.15E-03	sm-151	-2.47E-03
np-237	-3.73E-03	u-234	-1.87E-03	np-237	-4.90E-03	cs-133	-2.10E-03	pm-147	-2.17E-03
sm-152	-3.52E-03	sm-152	-1.56E-03	sm-152	-4.17E-03	eu-155	-1.95E-03	cs-133	-2.14E-03
tc-99	-3.29E-03	np-237	-1.47E-03	tc-99	-3.88E-03	sm-152	-1.71E-03	eu-155	-2.04E-03
in-115	-2.88E-03	tc-99	-1.44E-03	pu-242	-3.23E-03	u-234	-1.67E-03	sm-152	-1.76E-03
nd-145	-2.47E-03	nd-145	-1.05E-03	nd-145	-2.97E-03	np-237	-1.60E-03	u-234	-1.71E-03
pu-242	-2.38E-03	pu-242	-8.53E-04	eu-153	-2.83E-03	tc-99	-1.57E-03	np-237	-1.62E-03
eu-153	-2.16E-03	eu-153	-8.28E-04	ag-109	-2.57E-03	nd-145	-1.15E-03	tc-99	-1.61E-03
ag-109	-1.87E-03	mo-95	-6.44E-04	ag-107	-2.22E-03	eu-154	-8.70E-04	nd-145	-1.18E-03
u-234	-1.49E-03	ag-109	-5.74E-04	mo-95	-1.77E-03	eu-153	-8.30E-04	eu-154	-8.90E-04
mo-95	-1.41E-03	ru-101	-5.28E-04	ru-101	-1.49E-03	mo-95	-7.65E-04	eu-153	-8.38E-04
ru-101	-1.23E-03	sm-150	-4.51E-04	u-234	-1.47E-03	pu-242	-7.56E-04	pu-242	-8.05E-04
sm-150	-1.13E-03	am-241	-3.87E-04	sm-150	-1.47E-03	am-241	-6.17E-04	mo-95	-7.81E-04
am-241	-1.12E-03	sm-147	-2.94E-04	pu-238	-1.46E-03	ag-109	-5.95E-04	rh-105	-7.67E-04
pu-238	-9.84E-04	pu-238	-2.51E-04	am-241	-1.30E-03	hf	-5.50E-04	am-241	-6.29E-04
sm-147	-8.20E-04	al-27	-2.30E-04	am-243	-1.24E-03	ru-101	-5.49E-04	ag-109	-6.08E-04
am-243	-7.90E-04	ni	-2.19E-04	sm-147	-8.83E-04	sm-150	-5.43E-04	hf	-5.68E-04
cd	-4.96E-04	am-243	-1.88E-04	al-27	-3.46E-04	sm-147	-4.12E-04	ru-101	-5.65E-04
al-27	-3.12E-04	cr	-1.46E-04	fe	-2.92E-04	kr-83	-2.93E-04	sm-150	-5.39E-04
fe	-3.07E-04	sn-117	-1.27E-04	cr	-2.29E-04	pd-105	-2.91E-04	sm-147	-4.21E-04
ni	-2.68E-04	sn-118	-1.22E-04	sn-117	-1.32E-04	pr-141	-2.80E-04	pd-105	-2.97E-04
cr	-2.19E-04	sn-116	-1.17E-04	sn-118	-1.16E-04	gd-155	-2.64E-04	kr-83	-2.95E-04
sn-117	-1.32E-04	fe	-9.93E-05	sn-116	-1.16E-04	pu-238	-2.63E-04	pr-141	-2.79E-04
sn-118	-1.22E-04	ta-181	-8.44E-05	ni	-1.07E-04	zr-93	-2.01E-04	pu-238	-2.56E-04
sn-116	-1.20E-04	sn-119	-5.52E-05	mn-55	-1.07E-04	cs-134	-1.85E-04	zr-93	-2.06E-04
ta-181	-8.52E-05	sn-120	-4.23E-05	gd-155	-9.30E-05	am-243	-1.66E-04	gd-155	-2.02E-04
sn-119	-6.13E-05	gd-155	-4.12E-05	sn-119	-6.14E-05	pd-108	-1.65E-04	cs-134	-1.88E-04
in-113	-4.51E-05	co-59	-3.69E-05	ta-181	-5.52E-05	cs-135	-1.58E-04	am-243	-1.73E-04
sn-120	-4.45E-05	sn-115	-3.29E-05	sn-115	-4.04E-05	sn-117	-1.23E-04	pd-108	-1.70E-04
gd-155	-4.25E-05	sn-124	-3.06E-05	sn-120	-3.81E-05	sn-118	-1.12E-04	pm-148	-1.66E-04
mn-55	-3.97E-05	mn-55	-2.71E-05	sn-124	-2.97E-05	sn-116	-1.11E-04	cs-135	-1.62E-04
co-59	-3.91E-05	sn-112	-2.31E-05	sn-112	-2.32E-05	mn-55	-8.18E-05	sn-117	-1.27E-04
sn-115	-3.84E-05	mo	-1.68E-05	co-59	-2.15E-05	sn-119	-5.62E-05	sn-118	-1.18E-04
sn-124	-3.11E-05	pu-241	1.27E-02	eu-151	-1.03E-05	nd-148	-4.35E-05	sn-116	-1.16E-04
sn-112	-2.33E-05	pu-239	5.29E-02	pu-241	3.41E-02	sn-120	-4.17E-05	mn-55	-8.03E-05
mo	-1.57E-05	h-1	1.45E-01	pu-239	9.81E-02	sn-115	-3.47E-05	sn-119	-5.73E-05
pu-241	2.84E-02	u-235	2.39E-01	u-235	1.24E-01	sn-124	-2.91E-05	sn-120	-4.32E-05
pu-239	9.61E-02			h-1	1.97E-01	sn-112	-2.18E-05	nd-148	-4.27E-05
u-235	1.44E-01					ni	-1.17E-05	pm-149	-4.26E-05
h-1	1.72E-01					pu-241	1.42E-02	sn-115	-3.50E-05
						pu-239	6.70E-02	sn-124	-3.01E-05
						h-1	1.53E-01	pu-241	1.42E-02
						u-235	2.13E-01	pu-239	6.49E-02
								h-1	1.61E-01
								u-235	2.10E-01

Table A.1 Energy- and region-integrated sensitivity coefficients for CRC state-points (continued)

SQ2C3M		SU1C2B		SU1C2E		TMI1C5B		NA1C5B	
u-238	-1.47E-01	u-238	-1.65E-01	u-238	-1.68E-01	u-238	-1.56E-01	b-10	-1.63E-01
b-10	-4.50E-02	b-10	-1.21E-01	pu-240	-3.74E-02	b-10	-1.10E-01	u-238	-1.38E-01
pu-240	-3.88E-02	pu-240	-1.99E-02	xe-135	-2.99E-02	pu-240	-2.71E-02	pu-240	-1.63E-02
xe-135	-2.82E-02	zr	-9.65E-03	b-10	-2.05E-02	o-16	-1.04E-02	o-16	-9.85E-03
o-16	-1.23E-02	o-16	-9.34E-03	zr	-9.66E-03	sm-149	-1.00E-02	zr	-8.38E-03
sm-149	-9.64E-03	sm-149	-6.10E-03	o-16	-9.30E-03	zr	-9.62E-03	sm-149	-5.66E-03
zr	-9.27E-03	nd-143	-4.04E-03	sm-149	-8.84E-03	nd-143	-5.69E-03	rh-103	-3.30E-03
rh-103	-8.07E-03	rh-103	-3.71E-03	nd-143	-7.20E-03	rh-103	-5.47E-03	nd-143	-3.25E-03
nd-143	-7.81E-03	xe-131	-2.19E-03	rh-103	-5.90E-03	am-241	-4.79E-03	u-236	-2.49E-03
u-236	-5.17E-03	u-236	-2.17E-03	xe-131	-4.05E-03	u-236	-3.41E-03	xe-131	-2.06E-03
xe-131	-4.89E-03	sm-151	-2.07E-03	sm-151	-4.03E-03	xe-131	-3.29E-03	sm-151	-1.86E-03
sm-151	-4.22E-03	pm-147	-1.73E-03	u-236	-3.91E-03	gd-155	-3.20E-03	u-234	-1.80E-03
am-241	-4.07E-03	cs-133	-1.62E-03	eu-155	-3.34E-03	sm-151	-3.06E-03	cs-133	-1.54E-03
cs-133	-3.74E-03	u-234	-1.43E-03	pm-147	-3.25E-03	cs-133	-2.47E-03	pm-147	-1.52E-03
np-237	-3.20E-03	sm-152	-1.37E-03	cs-133	-3.02E-03	sm-152	-2.01E-03	sm-152	-1.23E-03
eu-155	-3.16E-03	eu-155	-1.37E-03	sm-152	-2.61E-03	tc-99	-1.84E-03	eu-155	-1.22E-03
sm-152	-3.07E-03	tc-99	-1.20E-03	tc-99	-2.26E-03	np-237	-1.74E-03	tc-99	-1.15E-03
tc-99	-2.80E-03	np-237	-1.18E-03	np-237	-2.22E-03	u-234	-1.49E-03	np-237	-1.13E-03
gd-155	-2.19E-03	nd-145	-8.96E-04	eu-154	-1.78E-03	sm-147	-1.43E-03	fe	-8.52E-04
nd-145	-2.07E-03	eu-154	-6.96E-04	nd-145	-1.72E-03	nd-145	-1.36E-03	nd-145	-8.39E-04
pm-147	-1.98E-03	eu-153	-6.35E-04	pu-242	-1.47E-03	mo-95	-9.53E-04	mo-95	-5.70E-04
pu-242	-1.84E-03	hf	-6.23E-04	rh-105	-1.46E-03	eu-153	-9.50E-04	eu-153	-5.59E-04
eu-154	-1.72E-03	mo-95	-5.71E-04	eu-153	-1.30E-03	pu-242	-8.74E-04	hf	-5.55E-04
eu-153	-1.64E-03	pu-242	-5.67E-04	u-234	-1.27E-03	eu-155	-8.73E-04	am-241	-5.35E-04
sm-147	-1.53E-03	ag-109	-5.02E-04	ag-109	-1.01E-03	ag-109	-8.67E-04	eu-154	-5.09E-04
u-234	-1.49E-03	sm-150	-4.43E-04	fe	-9.14E-04	sm-150	-6.50E-04	pu-242	-4.25E-04
mo-95	-1.46E-03	am-241	-4.43E-04	sm-150	-9.14E-04	eu-154	-6.26E-04	ru-101	-3.99E-04
ag-109	-1.18E-03	ru-101	-3.91E-04	mo-95	-8.50E-04	ru-101	-6.21E-04	ag-109	-3.92E-04
rh-105	-1.03E-03	sm-147	-2.82E-04	ru-101	-7.58E-04	hf	-6.08E-04	cr	-3.74E-04
sm-150	-1.02E-03	kr-83	-2.54E-04	hf	-6.16E-04	pm-147	-5.32E-04	sm-150	-3.62E-04
ru-101	-1.01E-03	pr-141	-2.34E-04	am-241	-5.28E-04	kr-83	-3.65E-04	sm-147	-3.42E-04
pu-238	-6.79E-04	pd-105	-2.32E-04	kr-83	-4.81E-04	pr-141	-3.45E-04	ni	-2.86E-04
pd-105	-5.72E-04	pu-238	-1.86E-04	pu-238	-4.81E-04	pd-105	-3.42E-04	gd-155	-2.51E-04
hf	-5.52E-04	mn-55	-1.71E-04	pm-148	-4.78E-04	in-115	-3.08E-04	kr-83	-2.15E-04
am-243	-5.20E-04	gd-155	-1.56E-04	pd-105	-4.71E-04	pu-238	-2.96E-04	pr-141	-1.99E-04
kr-83	-5.12E-04	cs-134	-1.46E-04	cr	-4.18E-04	cs-135	-1.96E-04	pd-105	-1.99E-04
pr-141	-5.10E-04	zr-93	-1.46E-04	pr-141	-4.10E-04	pd-108	-1.88E-04	mn-55	-1.58E-04
zr-93	-3.63E-04	sn-117	-1.41E-04	sm-147	-3.94E-04	am-243	-1.81E-04	pu-238	-1.54E-04
pd-108	-3.41E-04	ni	-1.39E-04	ni	-3.84E-04	zr-93	-1.52E-04	cs-135	-1.43E-04
cs-135	-2.92E-04	cs-135	-1.34E-04	cs-134	-3.75E-04	sn-117	-1.39E-04	sn-117	-1.22E-04
cs-134	-1.96E-04	cr	-1.32E-04	am-243	-3.34E-04	cd	-1.34E-04	sn-118	-1.13E-04
cr	-1.51E-04	pd-108	-1.28E-04	mn-55	-2.78E-04	sn-118	-1.19E-04	sn-116	-1.12E-04
pm-148	-1.50E-04	sn-118	-1.14E-04	zr-93	-2.77E-04	sn-116	-1.19E-04	cs-134	-1.11E-04
mn-55	-1.41E-04	sn-116	-1.12E-04	pd-108	-2.76E-04	ag-107	-1.08E-04	pd-108	-1.06E-04
ni	-1.31E-04	am-243	-8.54E-05	cs-135	-2.30E-04	sn-119	-6.74E-05	zr-93	-9.77E-05
sn-117	-1.29E-04	sn-119	-7.19E-05	sn-117	-1.44E-04	ni	-5.64E-05	am-243	-7.47E-05
sn-118	-1.18E-04	sn-115	-4.88E-05	sn-118	-1.16E-04	nd-148	-5.00E-05	sn-119	-5.45E-05
sn-116	-1.17E-04	sn-120	-4.52E-05	sn-116	-1.16E-04	mn-55	-4.94E-05	sn-120	-4.09E-05
nd-148	-7.83E-05	nd-148	-3.18E-05	pm-149	-1.01E-04	sn-120	-4.57E-05	sn-115	-3.31E-05
sn-119	-5.92E-05	sn-124	-3.02E-05	cm-244	-8.86E-05	sn-115	-4.39E-05	nd-148	-3.05E-05
fe	-4.60E-05	sn-112	-2.30E-05	ru-103	-8.21E-05	sn-124	-3.11E-05	sn-124	-2.88E-05
pm-149	-4.46E-05	pu-241	1.38E-02	nd-147	-8.21E-05	cs-134	-2.68E-05	sn-112	-2.19E-05
sn-120	-4.43E-05	pu-239	6.80E-02	sn-119	-7.33E-05	in-113	-2.41E-05	pu-241	8.88E-03
sn-115	-3.65E-05	h-1	1.35E-01	nd-148	-6.26E-05	pu-241	1.25E-02	pu-239	4.82E-02
pu-241	2.31E-02	u-235	2.26E-01	pu-241	2.52E-02	pu-239	8.71E-02	h-1	1.45E-01
pu-239	9.68E-02			pu-239	1.03E-01	h-1	1.53E-01	u-235	2.46E-01
u-235	1.50E-01			u-235	1.49E-01	u-235	1.95E-01		
h-1	1.82E-01			h-1	1.68E-01				

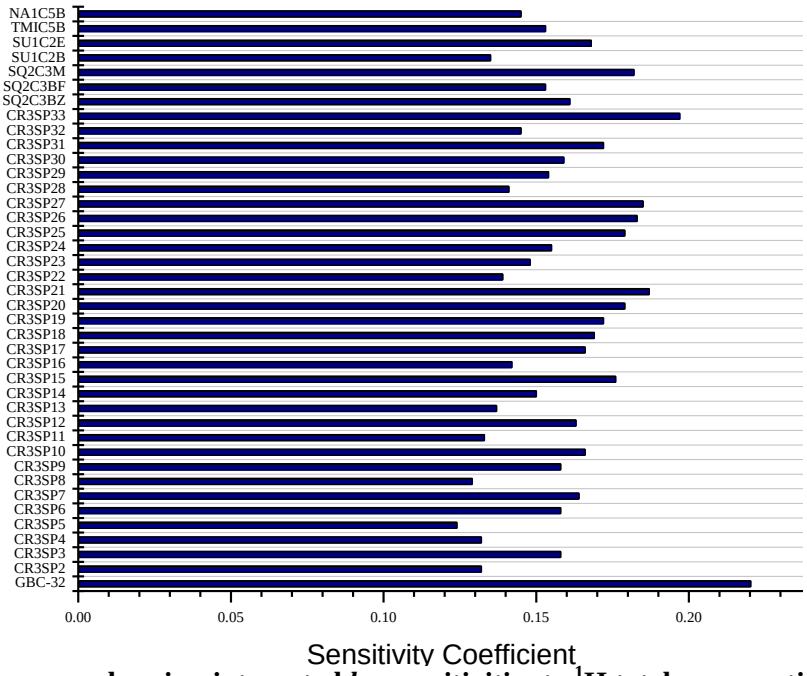

Fig. A.1 Energy- and region-integrated k_{eff} sensitivities to ^{1}H total cross section.

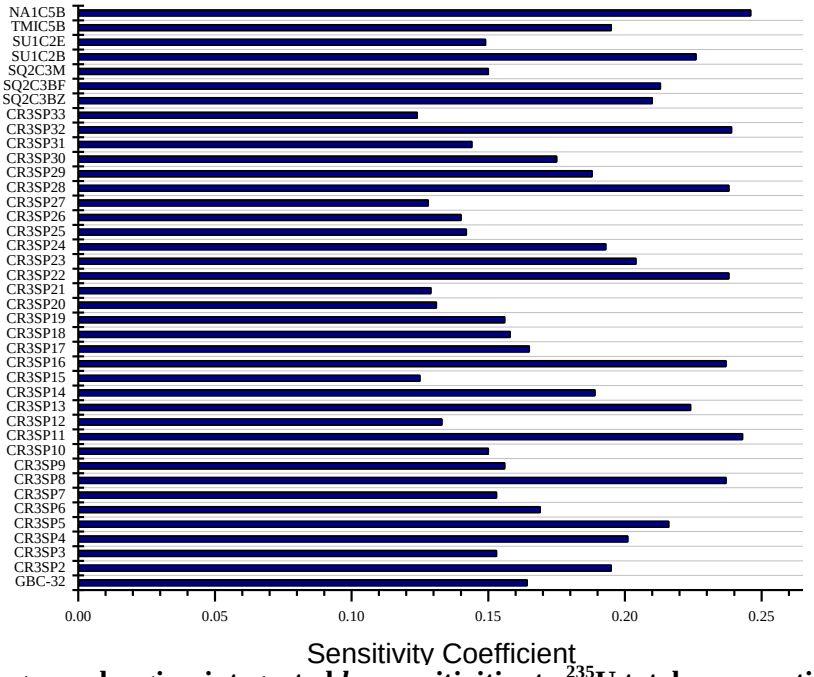

Fig. A.2 Energy- and region-integrated k_{eff} sensitivities to ^{235}U total cross section.

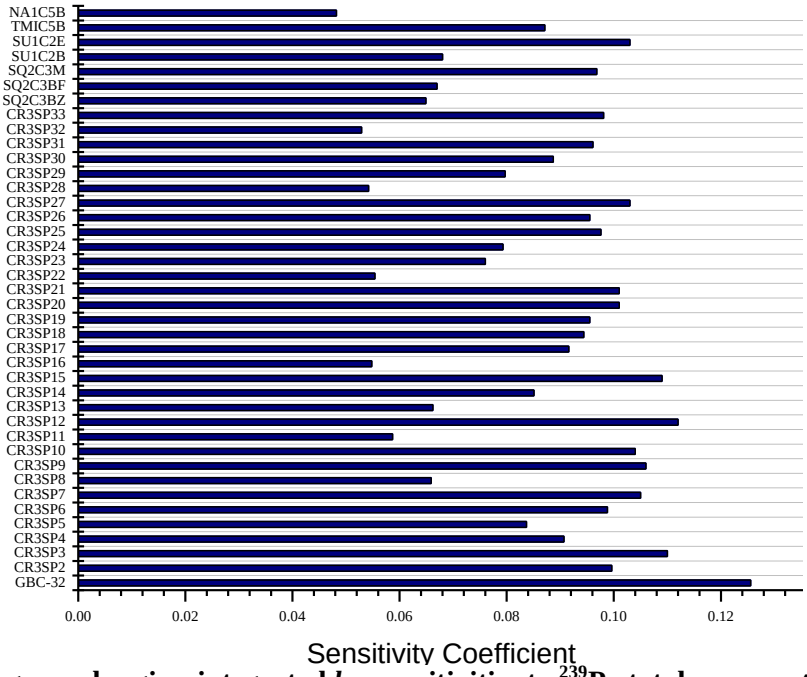

Fig. A.3 Energy- and region-integrated k_{eff} sensitivities to ^{239}Pu total cross section.

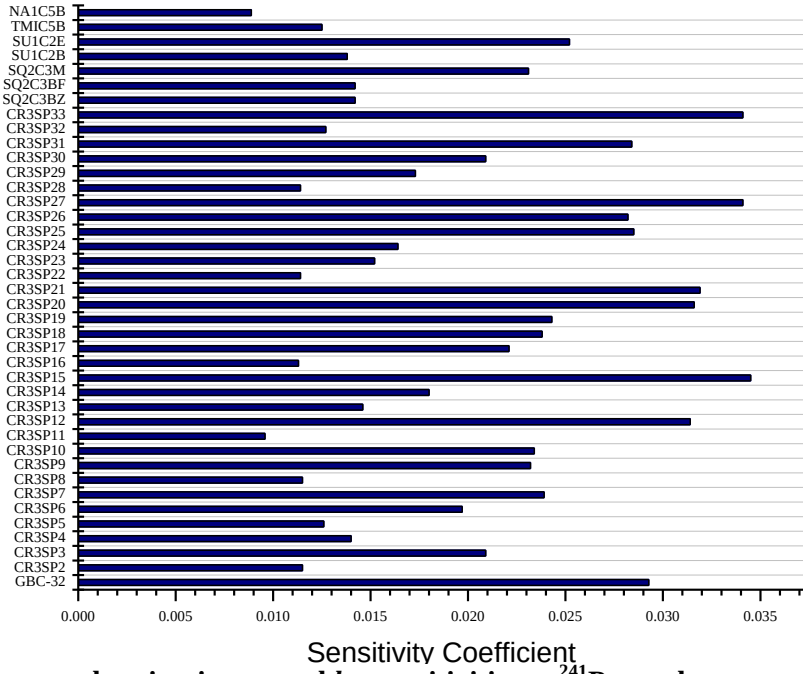

Fig. A.4 Energy- and region-integrated k_{eff} sensitivities to ^{241}Pu total cross section.

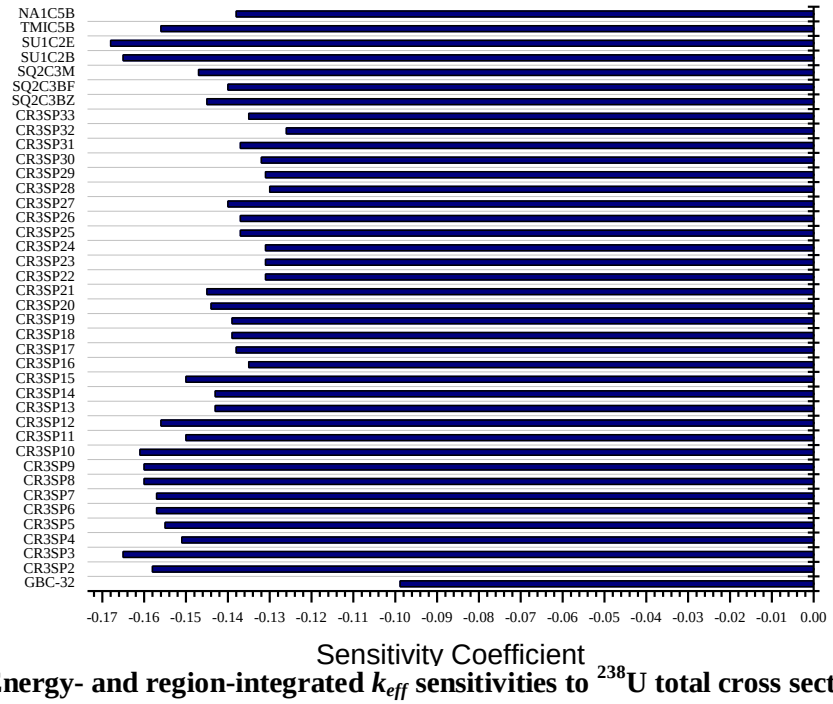

Fig. A.5 Energy- and region-integrated k_{eff} sensitivities to ^{238}U total cross section.

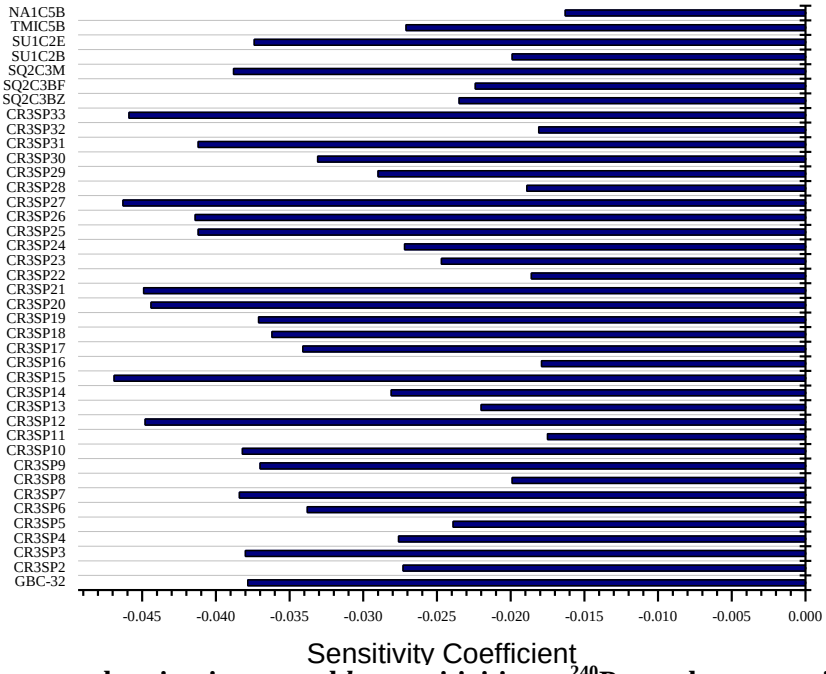

Fig. A.6 Energy- and region-integrated k_{eff} sensitivities to ^{240}Pu total cross section.

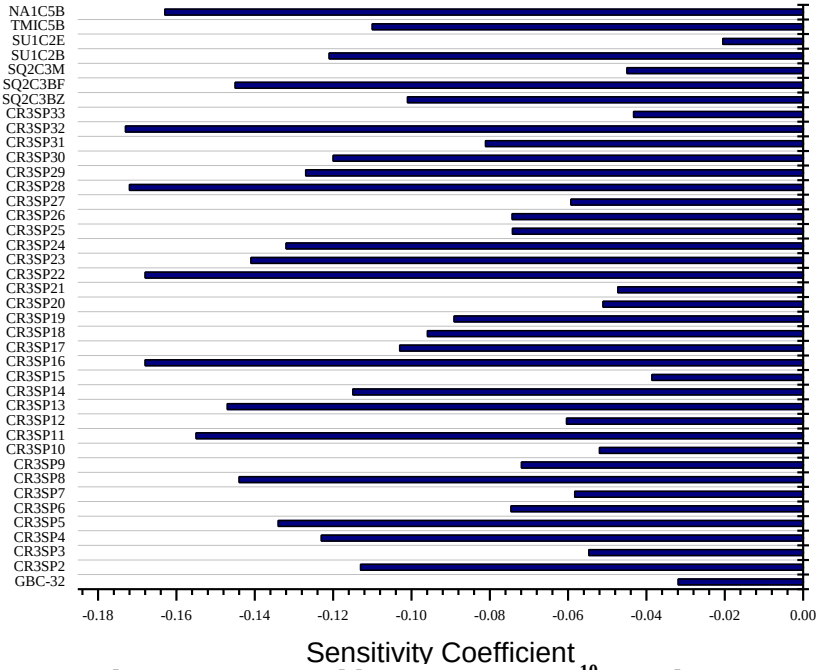

Fig. A.7 Energy- and region-integrated k_{eff} sensitivities to ^{10}B total cross section.

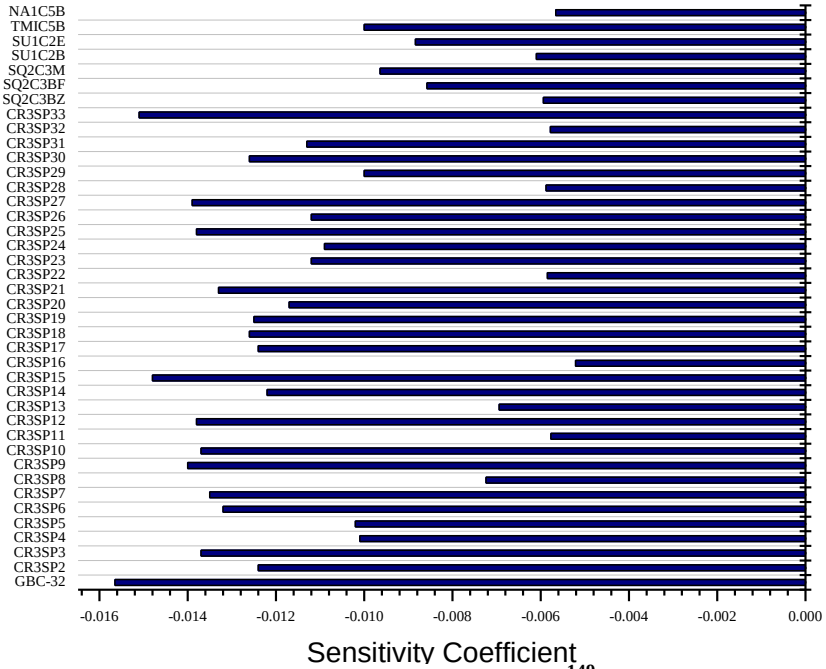

Fig. A.8 Energy- and region-integrated k_{eff} sensitivities to ^{149}Sm total cross section.

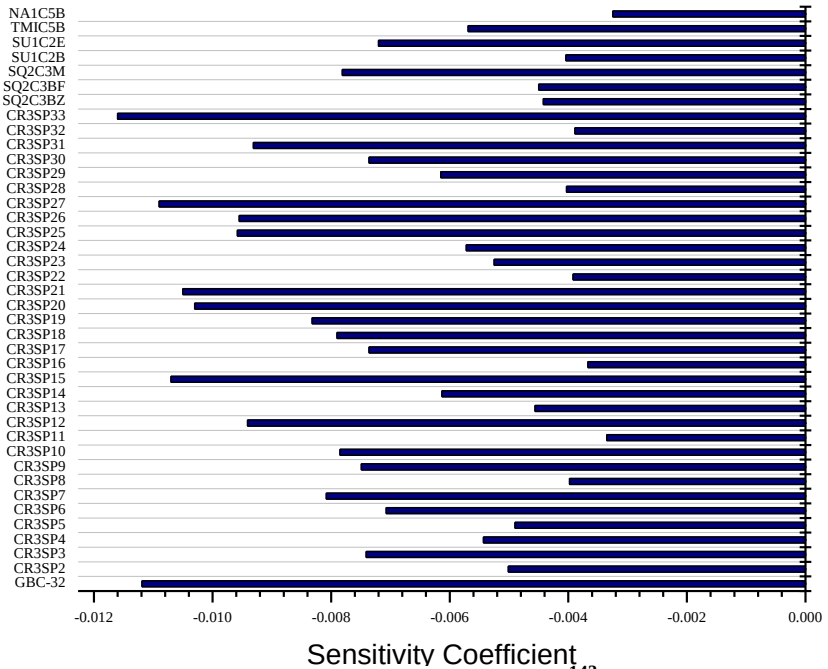

Fig. A.9 Energy- and region-integrated k_{eff} sensitivities to ^{143}Nd total cross section.

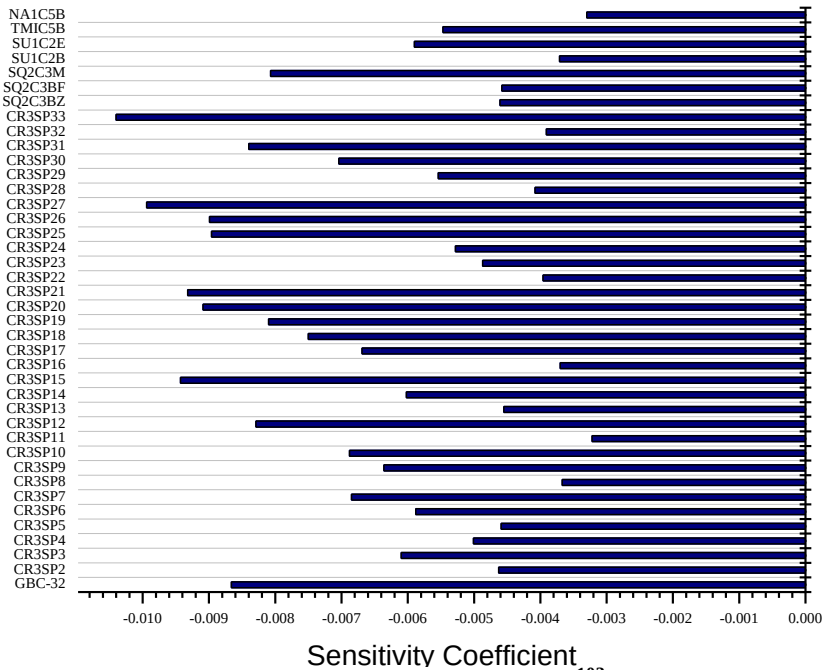

Fig. A.10 Energy- and region-integrated k_{eff} sensitivities to ^{103}Rh total cross section.

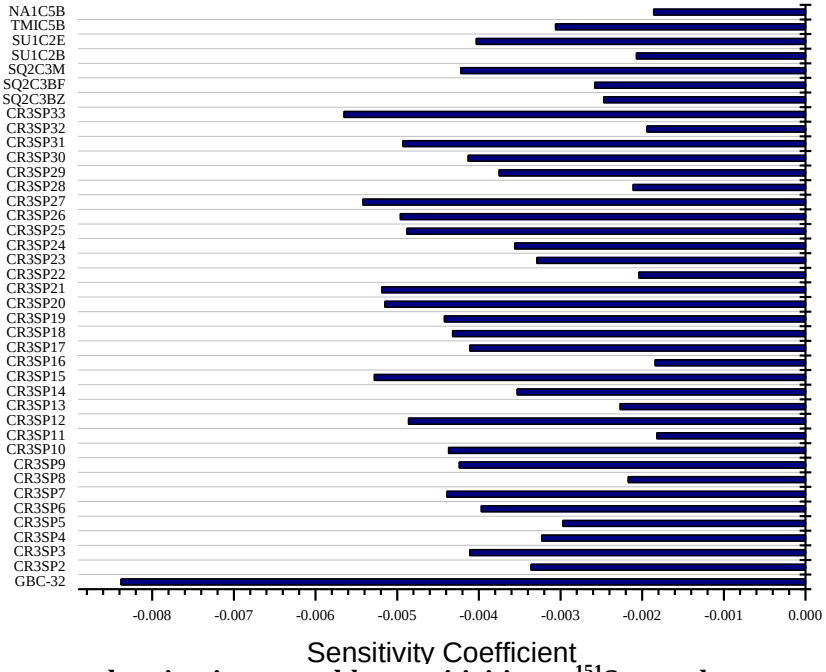

Fig. A.11 Energy- and region-integrated k_{eff} sensitivities to ^{151}Sm total cross section.

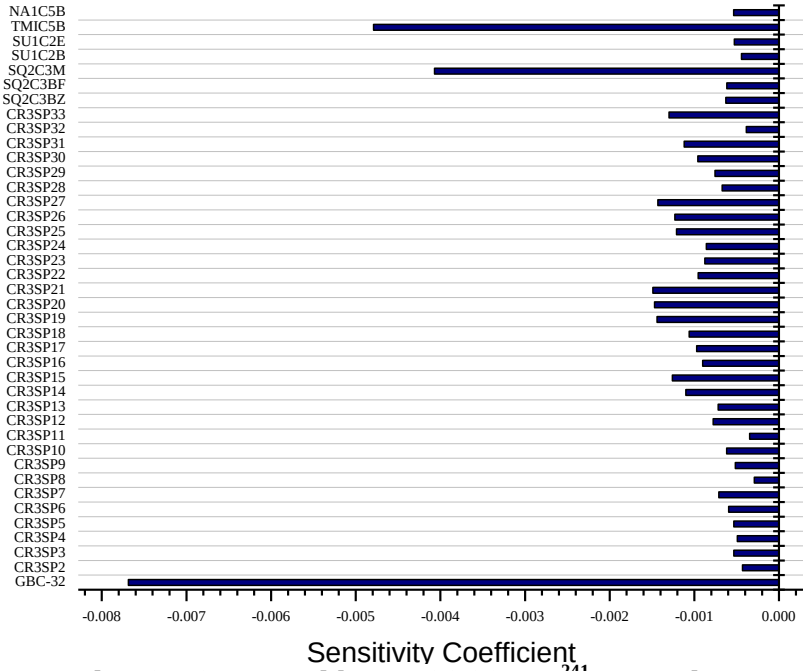

Fig. A.12 Energy- and region-integrated k_{eff} sensitivities to ^{241}Am total cross section.

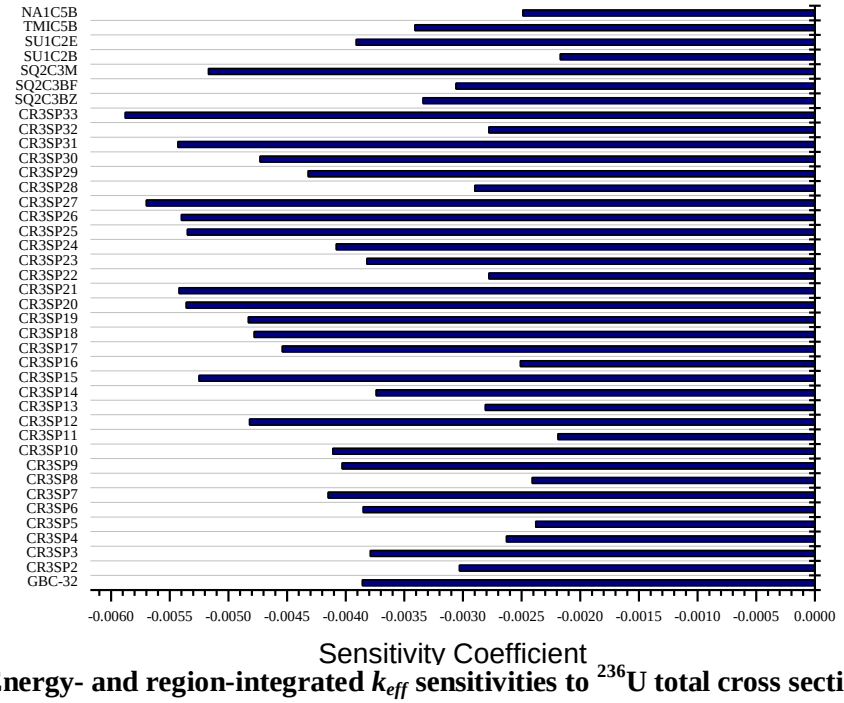

Fig. A.13 Energy- and region-integrated k_{eff} sensitivities to ^{236}U total cross section.

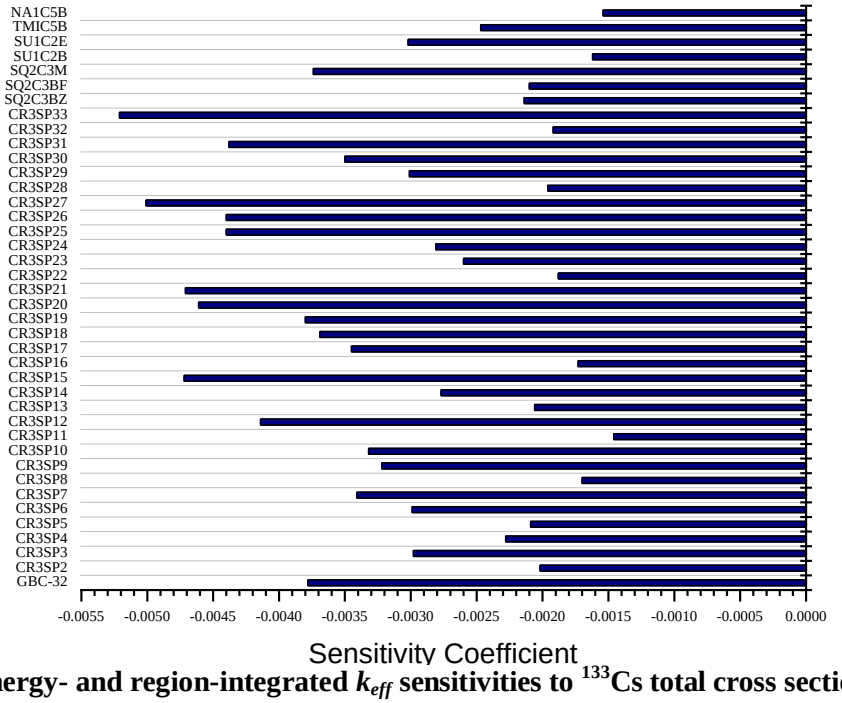

Fig. A.14 Energy- and region-integrated k_{eff} sensitivities to ^{133}Cs total cross section.

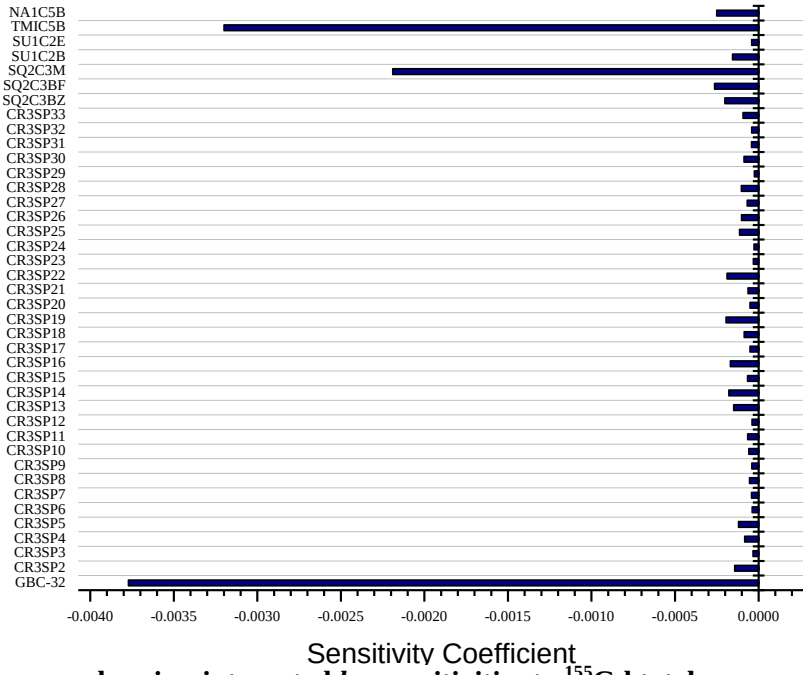

Fig. A.15 Energy- and region-integrated k_{eff} sensitivities to ^{155}Gd total cross section.

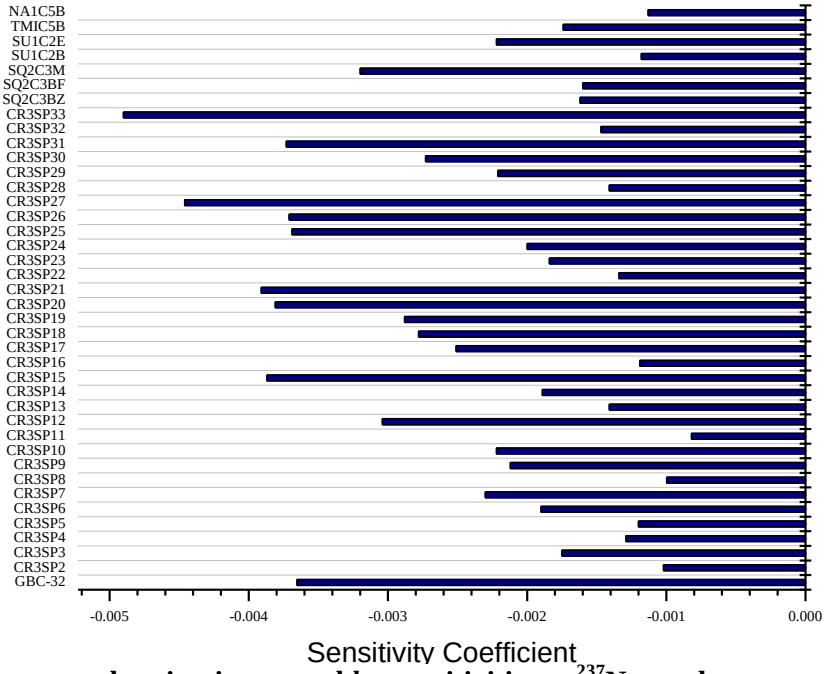

Fig. A.16 Energy- and region-integrated k_{eff} sensitivities to ^{237}Np total cross section.

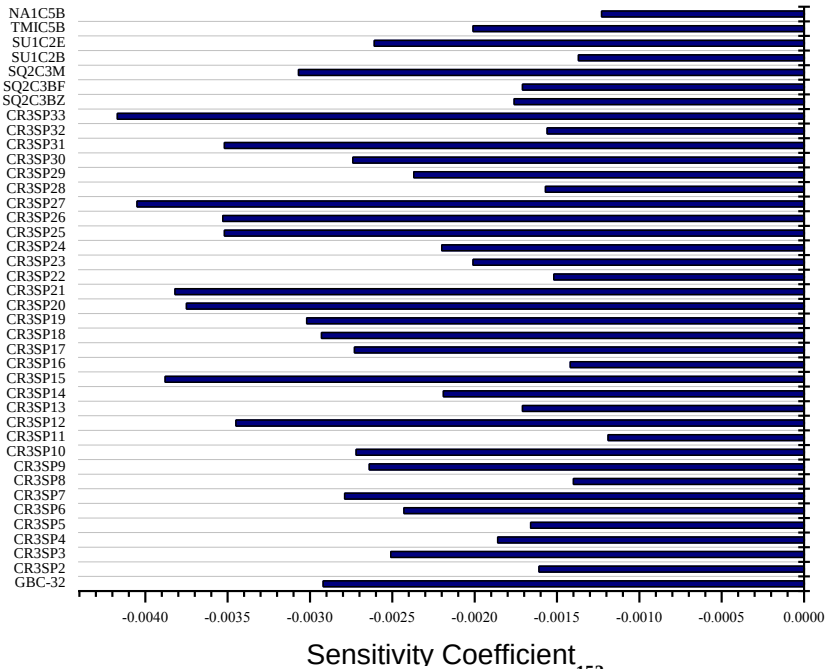

Fig. A.17 Energy- and region-integrated k_{eff} sensitivities to ^{152}Sm total cross section.

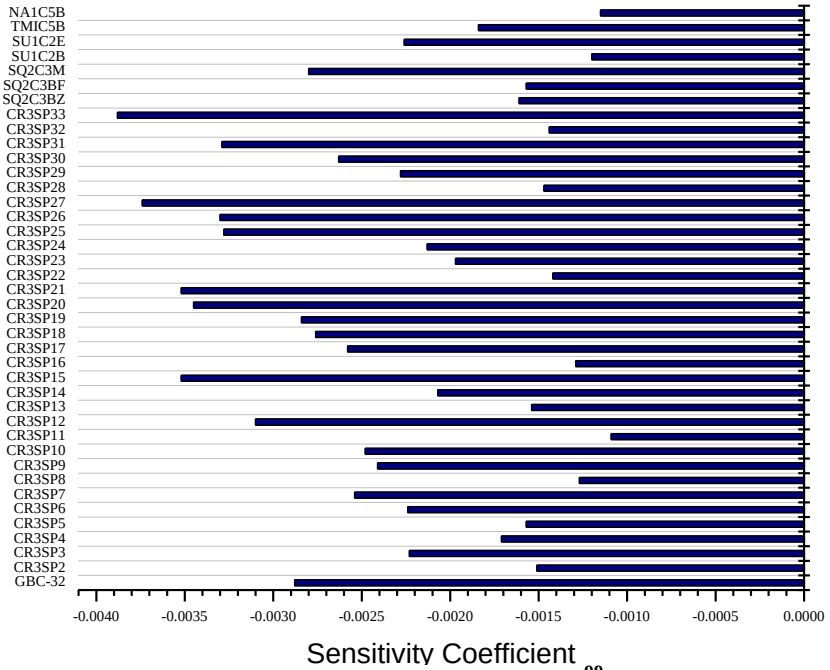

Fig. A.18 Energy- and region-integrated k_{eff} sensitivities to ^{99}Tc total cross section.

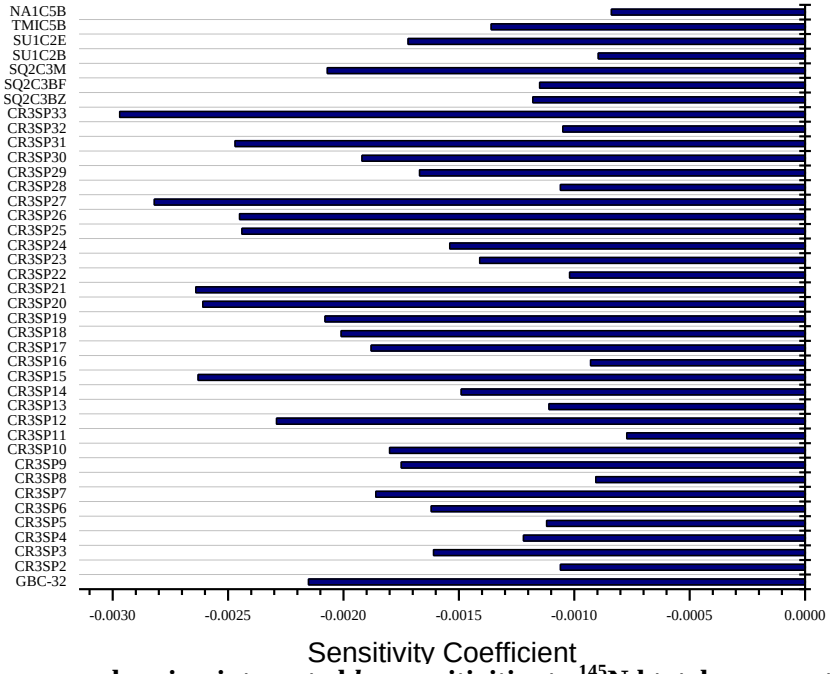

Fig. A.19 Energy- and region-integrated k_{eff} sensitivities to ^{145}Nd total cross section.

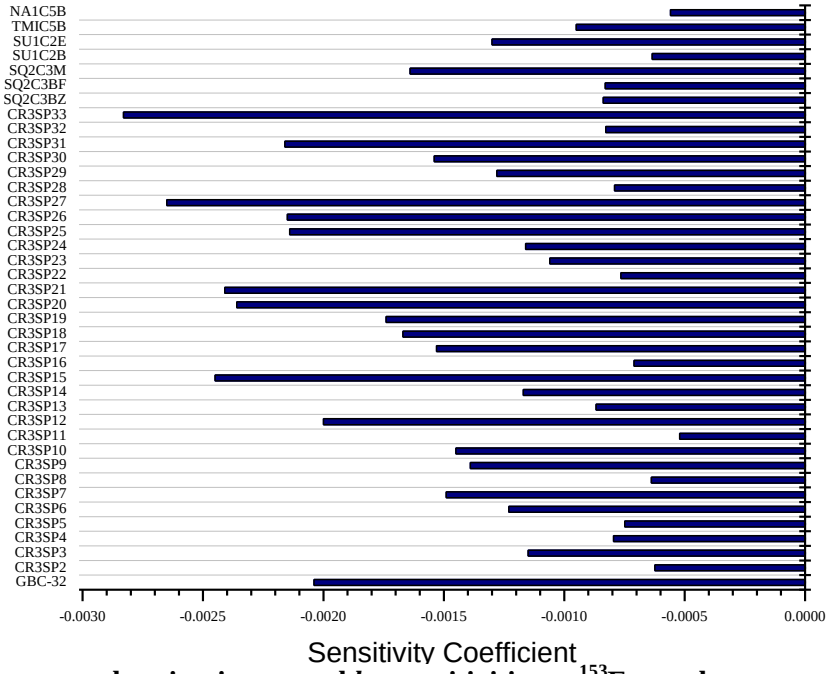

Fig. A.20 Energy- and region-integrated k_{eff} sensitivities to ^{153}Eu total cross section.

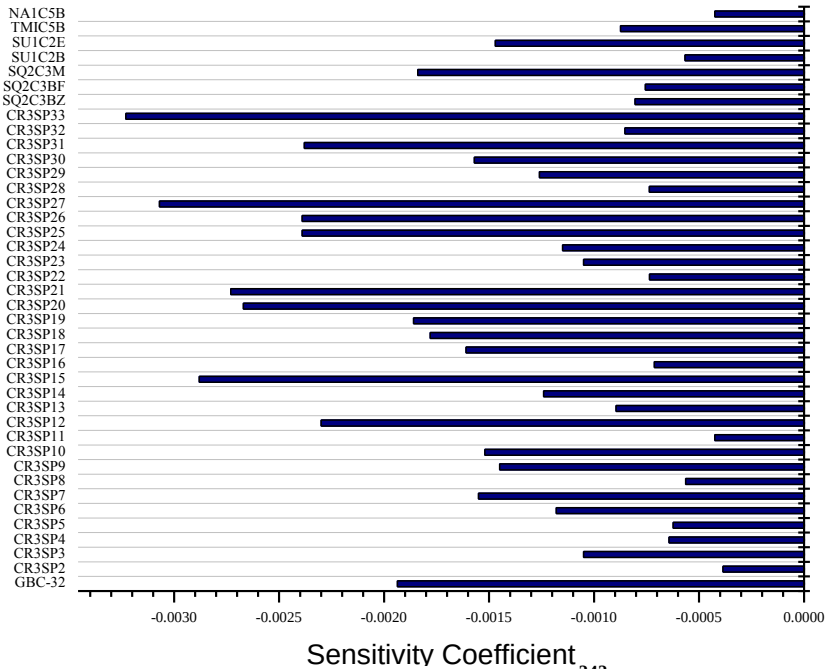

Fig. A.21 Energy- and region-integrated k_{eff} sensitivities to ^{242}Pu total cross section.

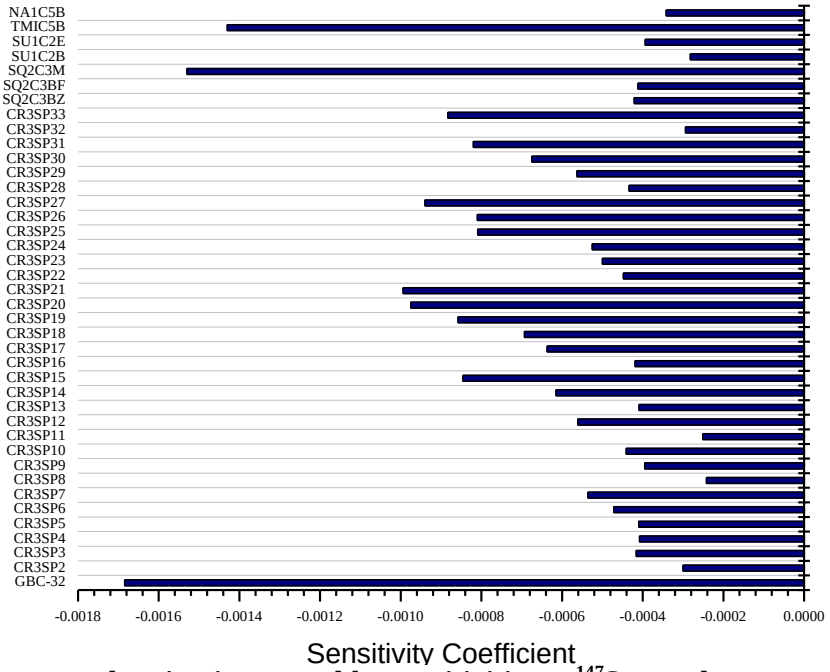

Fig. A.22 Energy- and region-integrated k_{eff} sensitivities to ^{147}Sm total cross section.

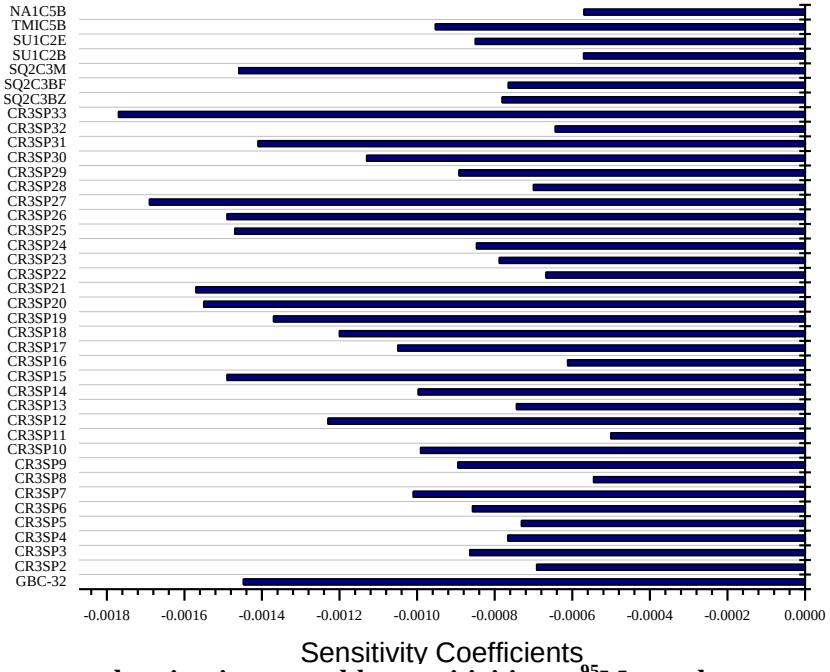

Fig. A.23 Energy- and region-integrated k_{eff} sensitivities to ^{95}Mo total cross section.

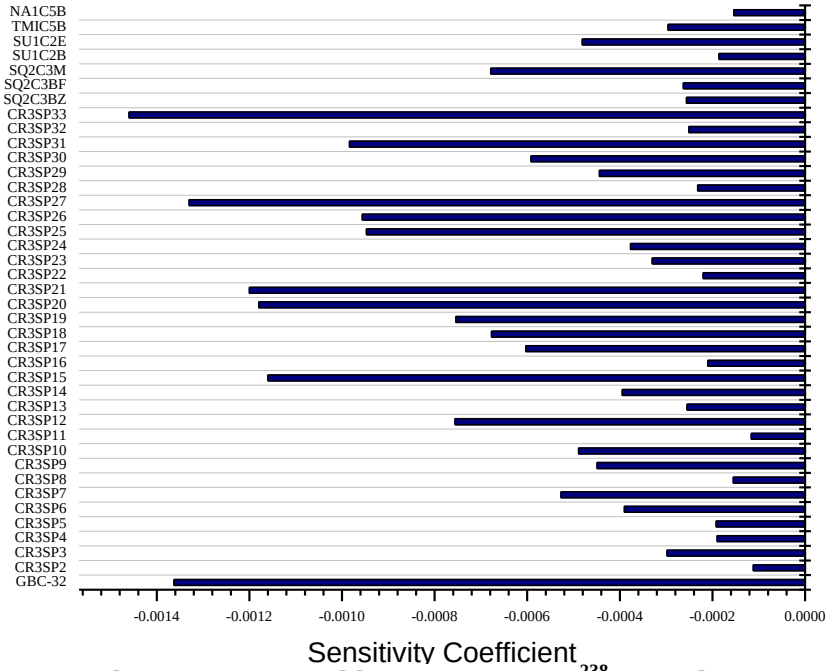

Fig. A.24 Energy- and region-integrated k_{eff} sensitivities to ^{238}Pu total cross section.

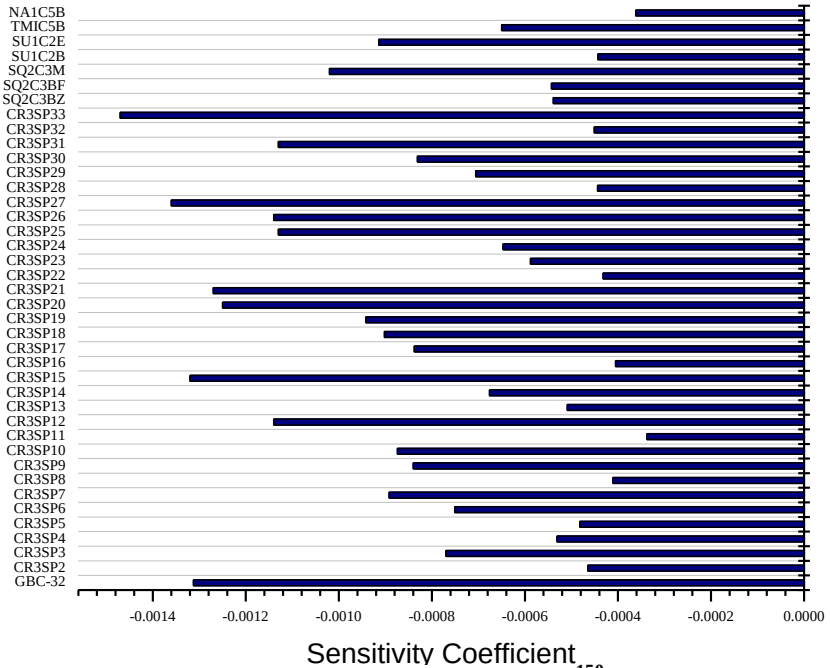

Fig. A.25 Energy- and region-integrated k_{eff} sensitivities to ^{150}Sm total cross section.

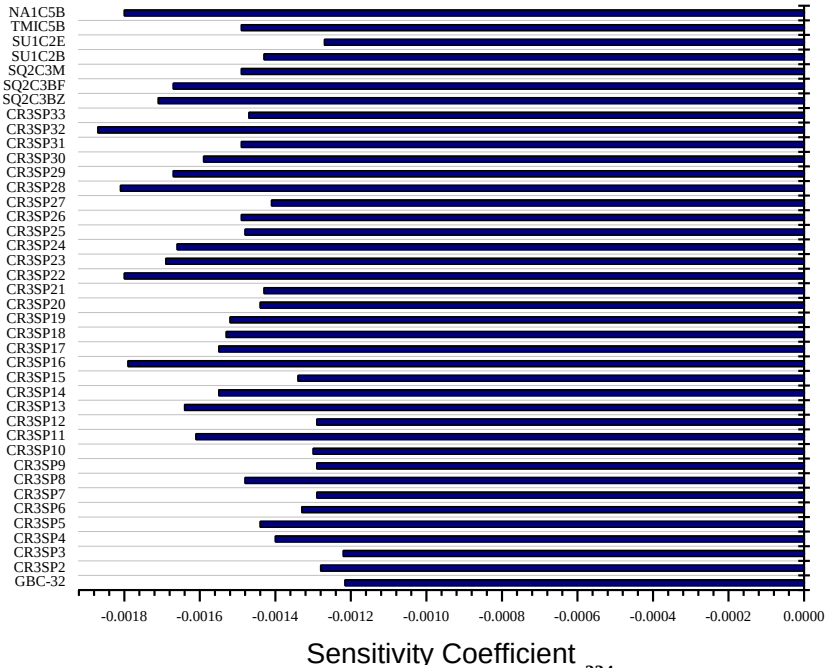

Fig. A.26 Energy- and region-integrated k_{eff} sensitivities to ^{234}U total cross section.

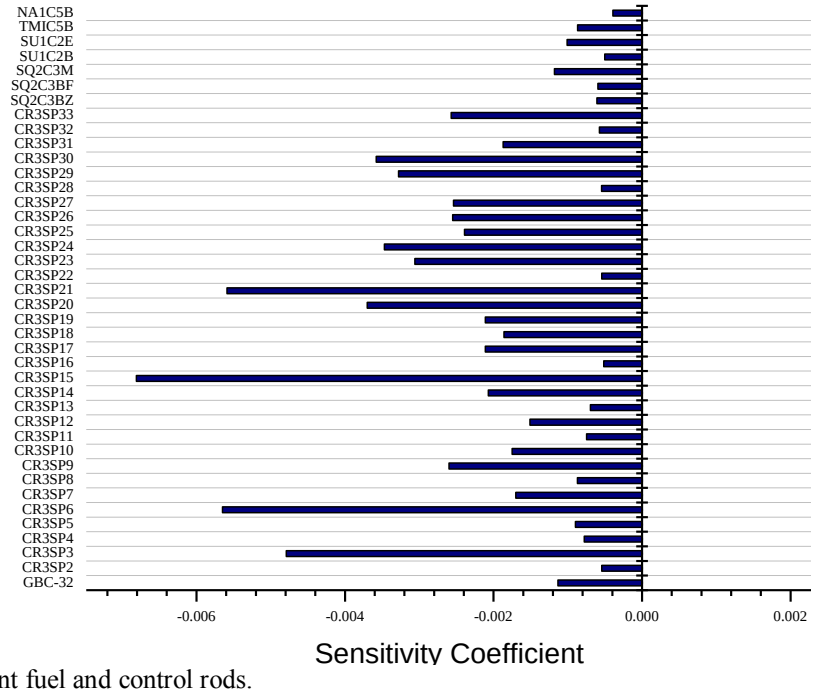

Note: ^{109}Ag exists in spent fuel and control rods.

Fig. A.27 Energy- and region-integrated k_{eff} sensitivities to ^{109}Ag total cross section.

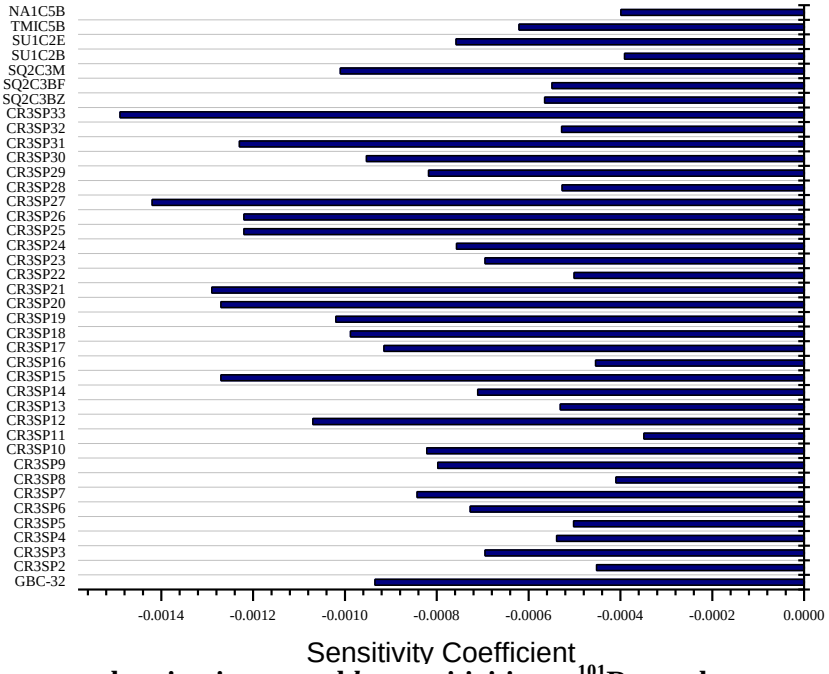

Fig. A.28 Energy- and region-integrated k_{eff} sensitivities to ^{101}Ru total cross section.

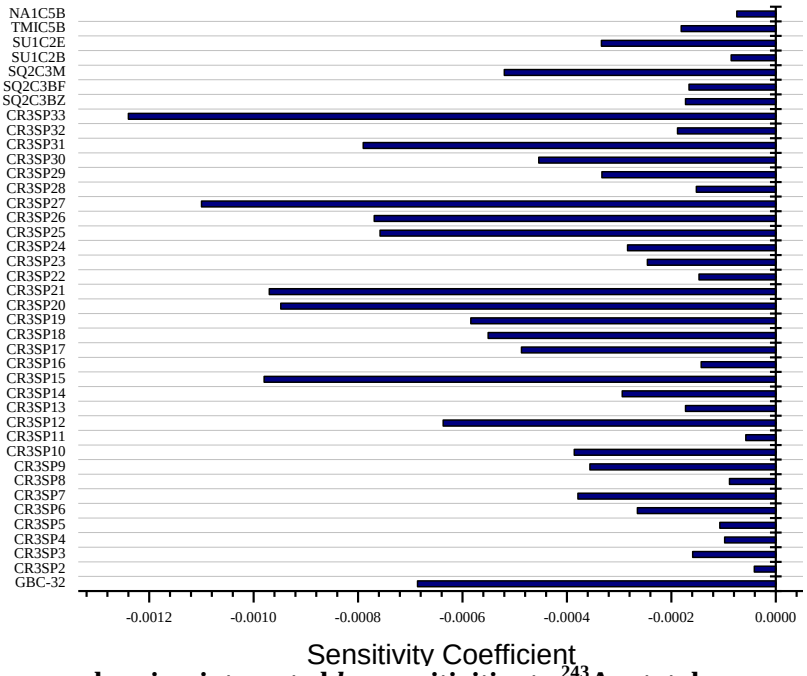

Fig. A.29 Energy- and region-integrated k_{eff} sensitivities to ^{243}Am total cross section.

APPENDIX B

ADDITIONAL SENSITIVITY PROFILES

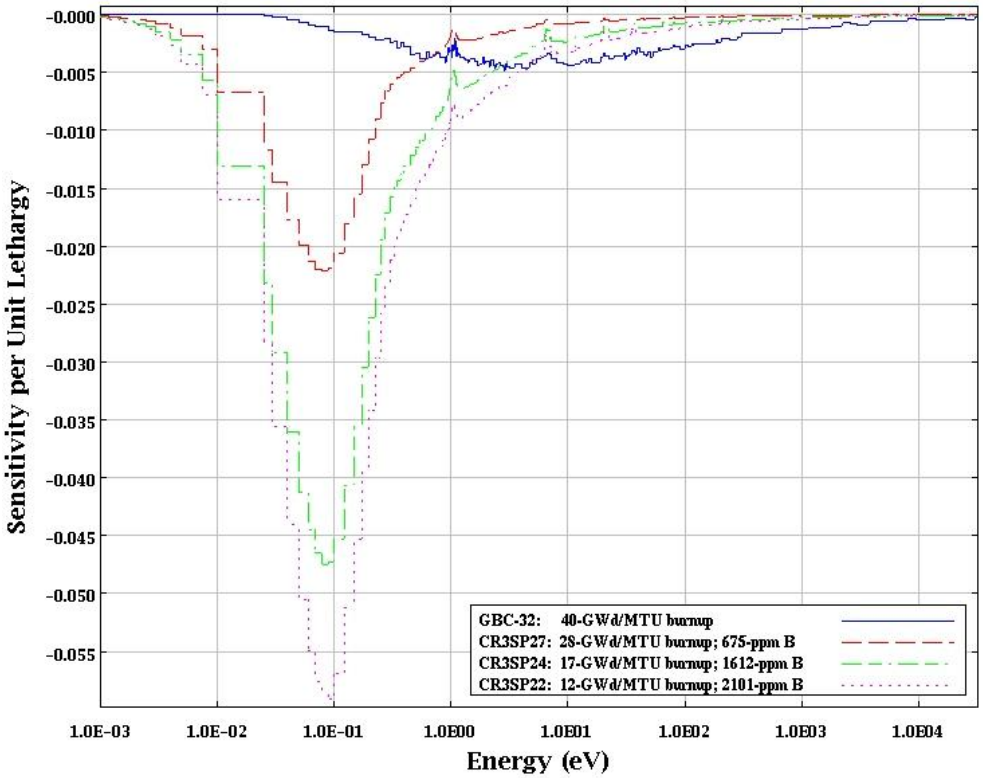

Fig. B.1 Comparison of ^{10}B sensitivity profiles for GBC40, CR3SP27, CR3SP24, and CR3SP22.

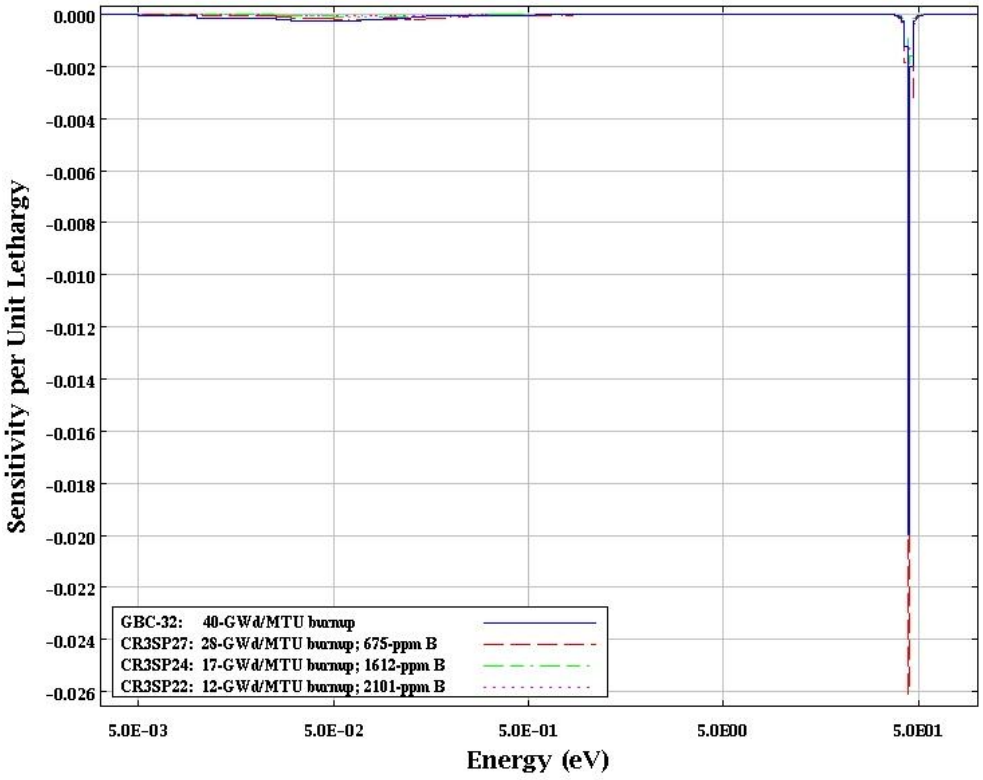

Fig. B.2 Comparison of ^{95}Mo sensitivity profiles for GBC40, CR3SP27, CR3SP24, and CR3SP22.

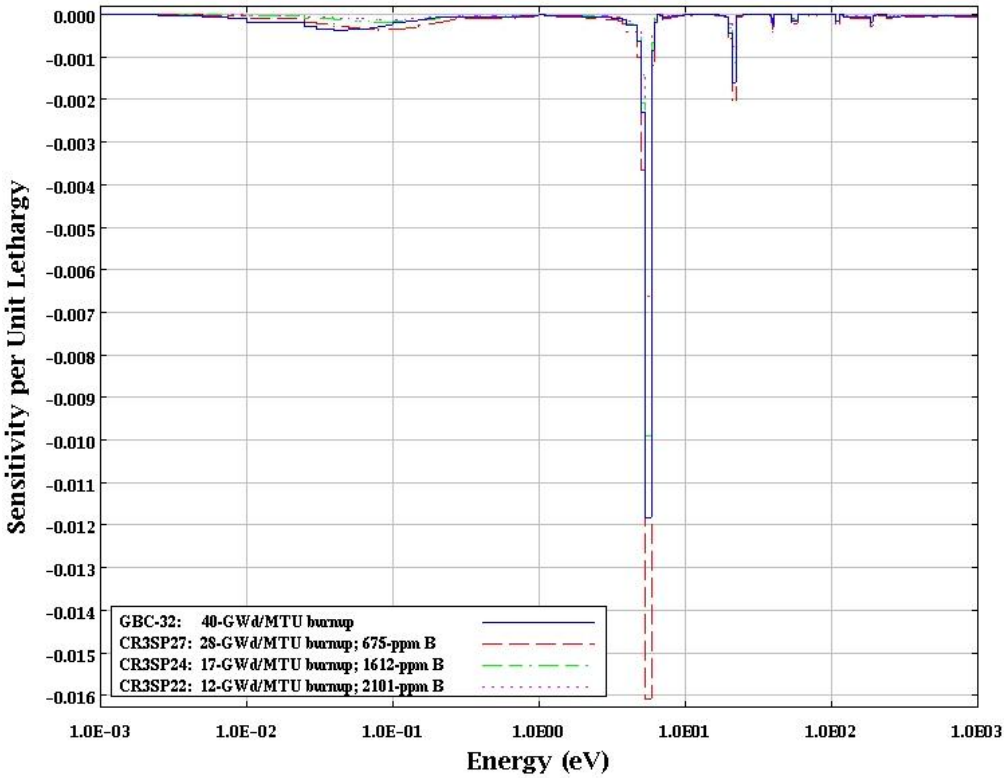

Fig. B.3 Comparison of ^{99}Tc sensitivity profiles for GBC40, CR3SP27, CR3SP24, and CR3SP22.

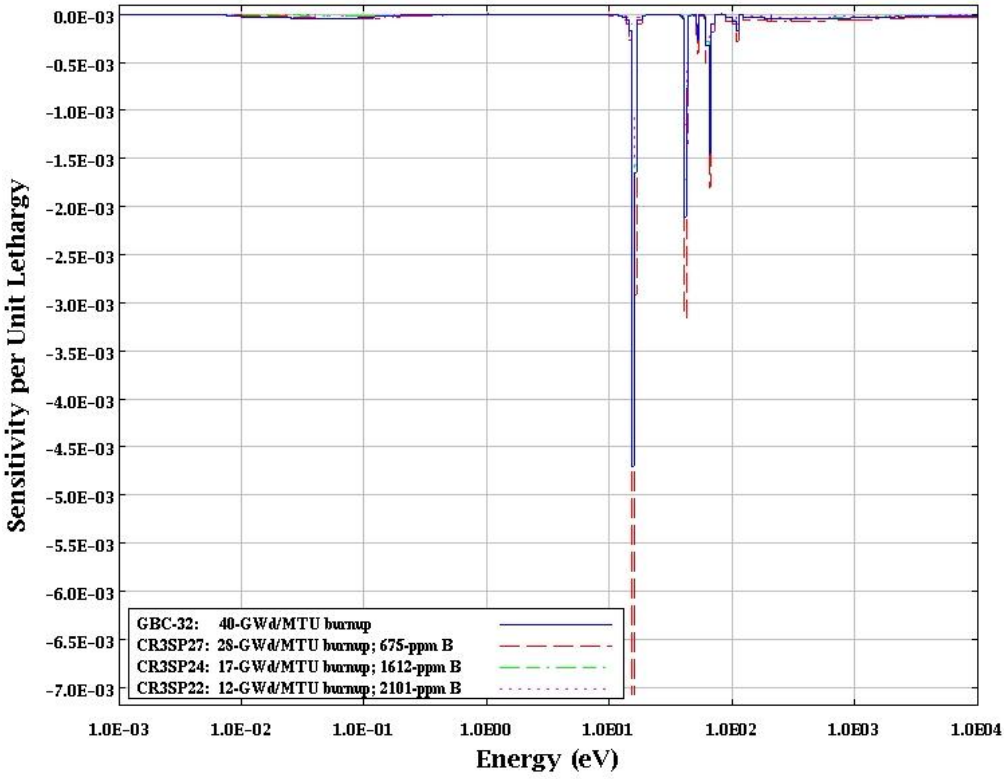

Fig. B.4 Comparison of ^{101}Ru sensitivity profiles for GBC40, CR3SP27, CR3SP24, and CR3SP22.

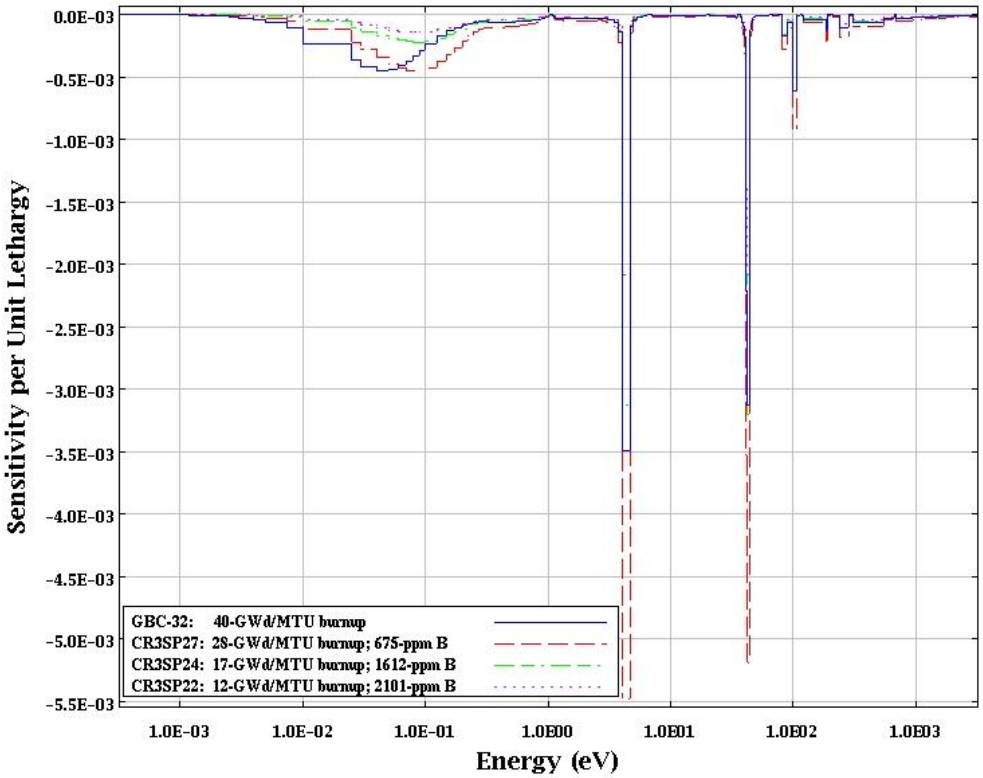

Fig. B.5 Comparison of ^{145}Nd sensitivity profiles for GBC40, CR3SP27, CR3SP24, and CR3SP22.

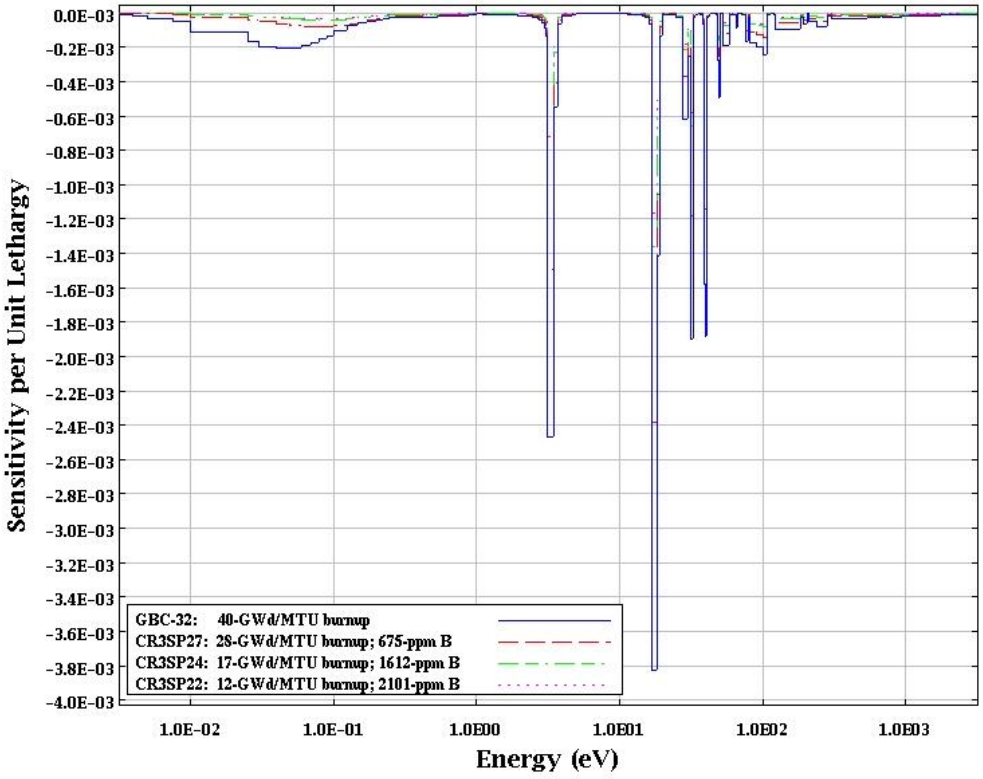

Fig. B.6 Comparison of ^{147}Sm sensitivity profiles for GBC40, CR3SP27, CR3SP24, and CR3SP22.

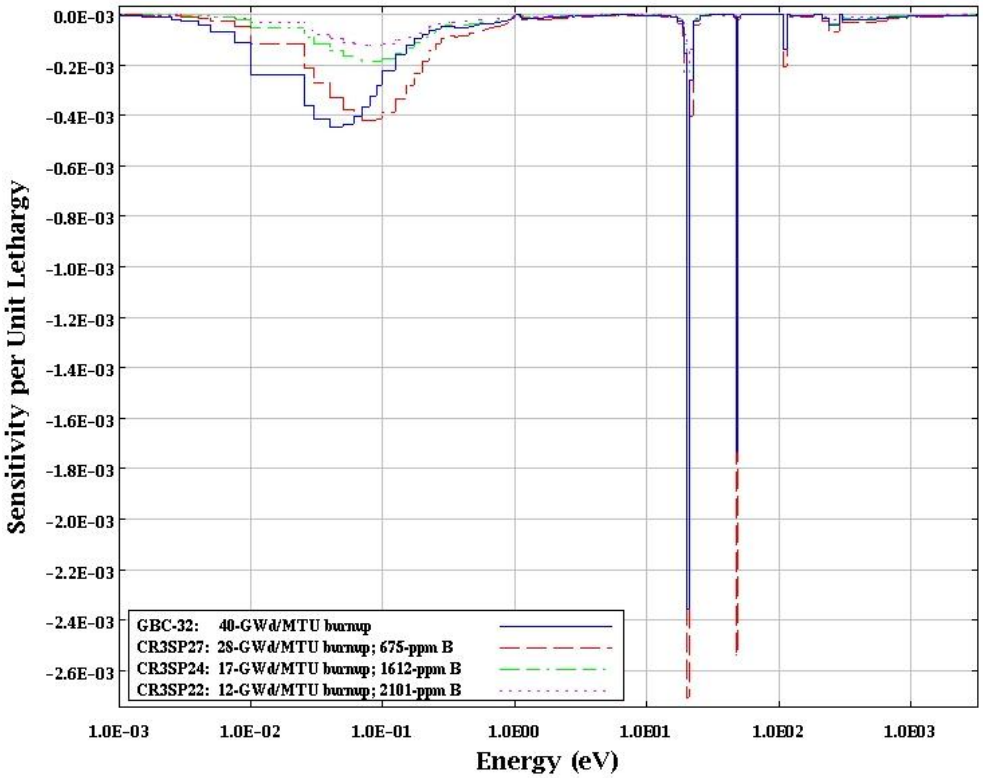

Fig. B.7 Comparison of ^{150}Sm sensitivity profiles for GBC40, CR3SP27, CR3SP24, and CR3SP22.

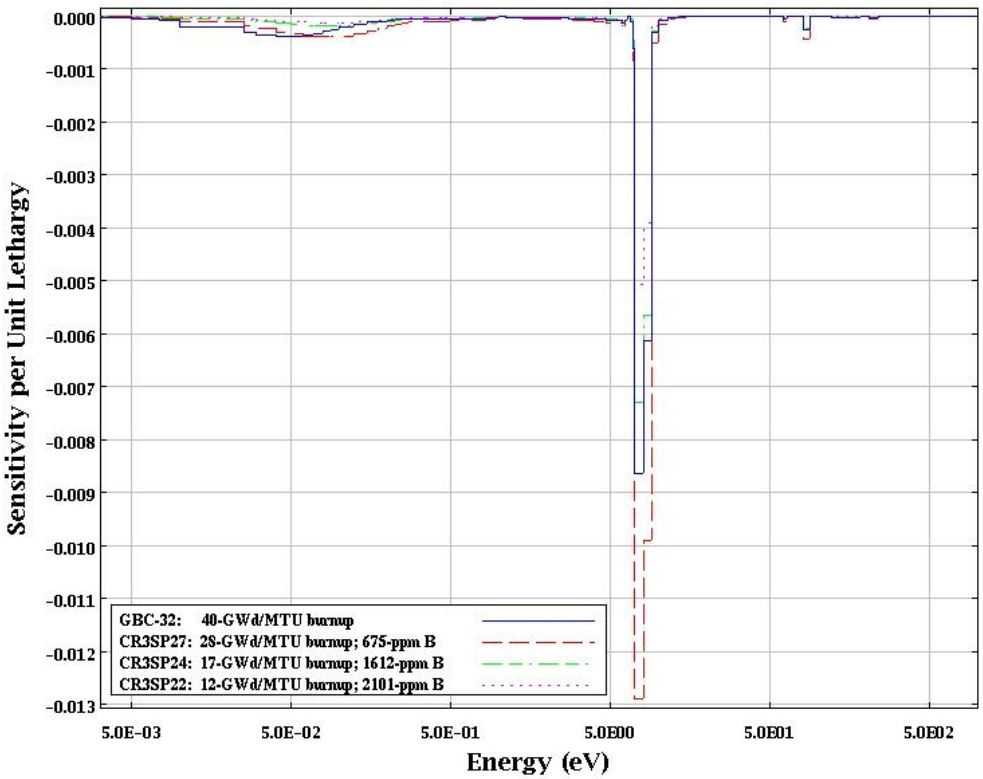

Fig. B.8 Comparison of ^{152}Sm sensitivity profiles for GBC40, CR3SP27, CR3SP24, and CR3SP22.

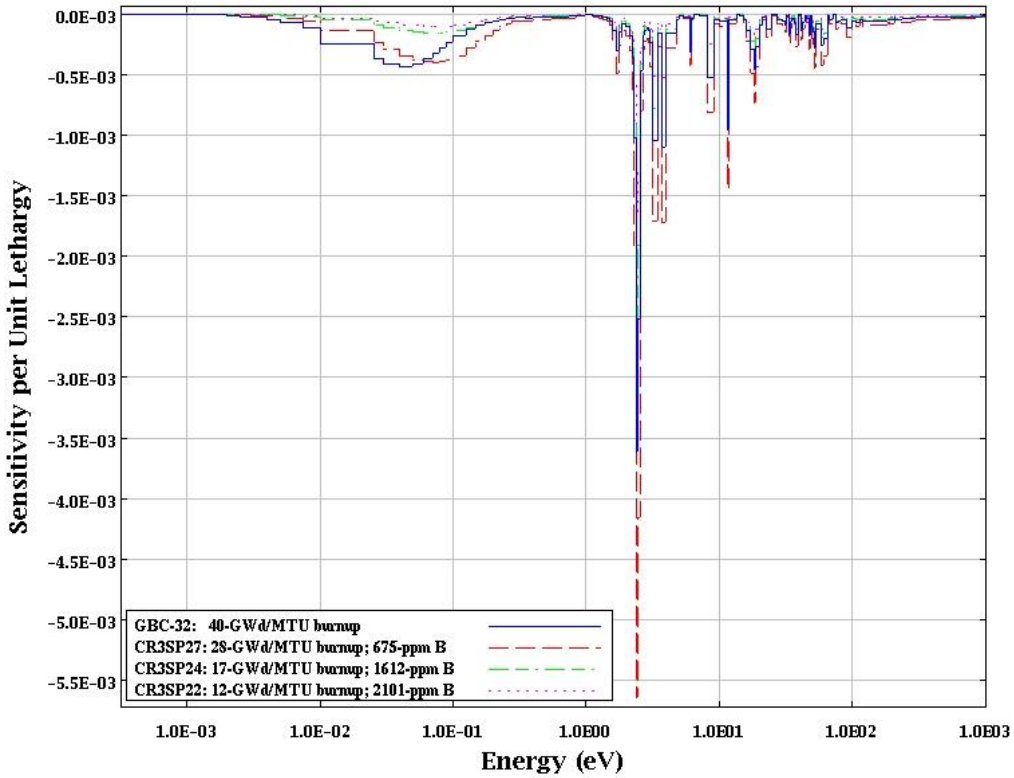

Fig. B.9 Comparison of ^{153}Eu sensitivity profiles for GBC40, CR3SP27, CR3SP24, and CR3SP22.

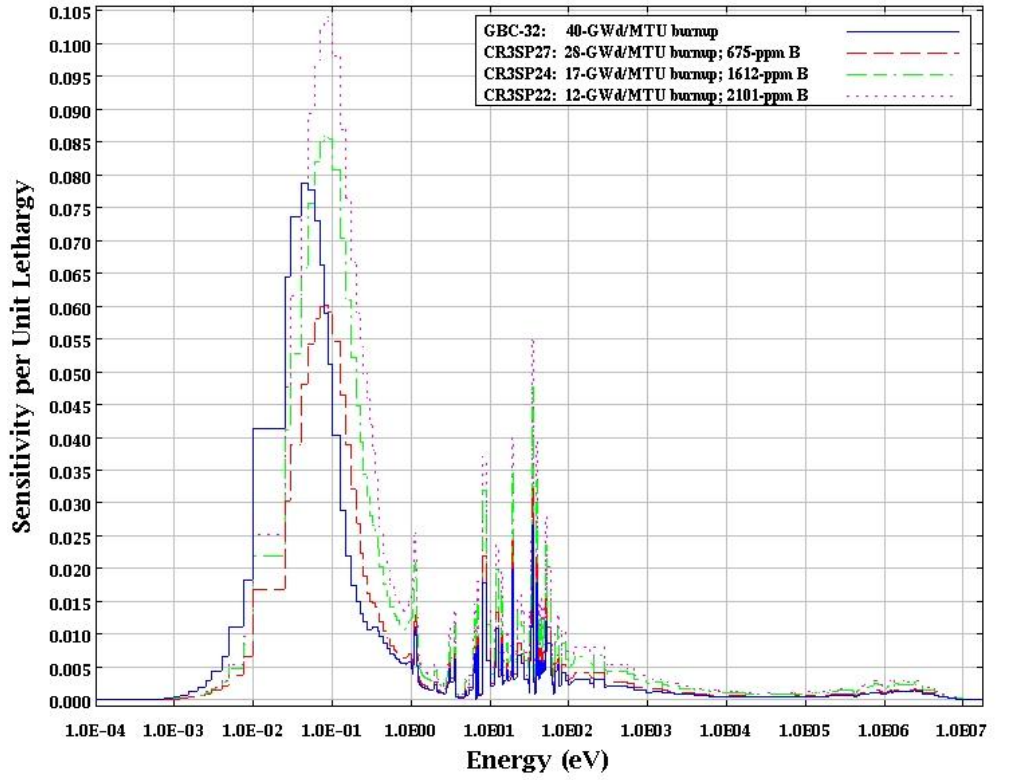

Fig. B.10 Comparison of ^{235}U-fission sensitivity profiles for GBC40, CR3SP27, CR3SP24, and CR3SP22.

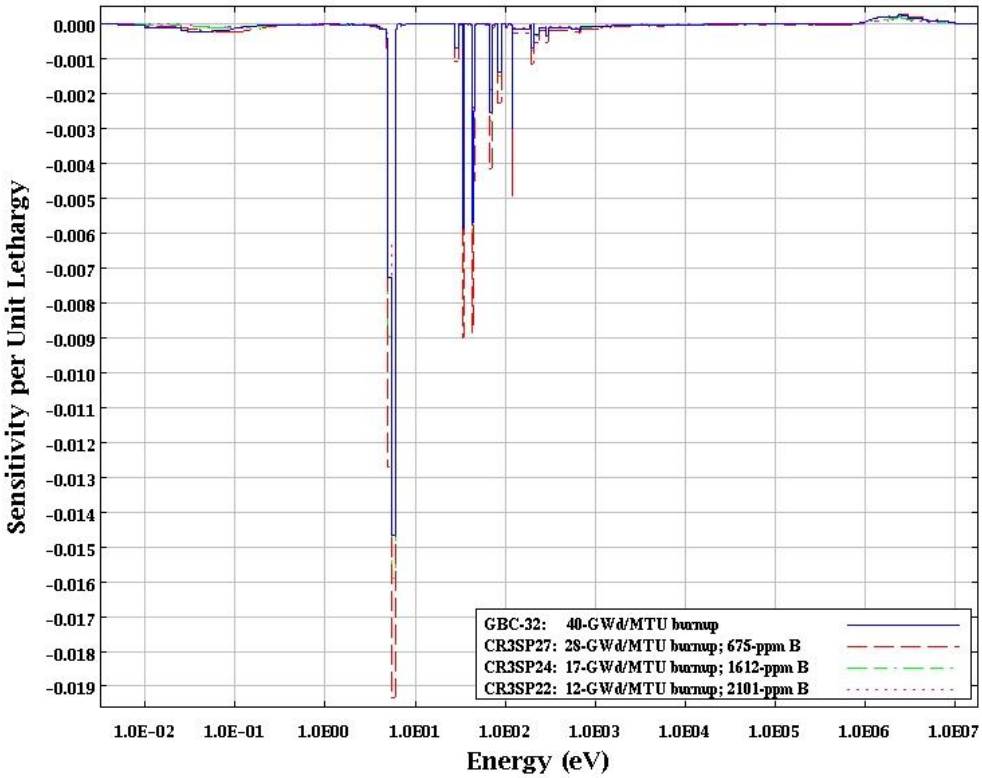

Fig. B.11 Comparison of ^{236}U sensitivity profiles for GBC40, CR3SP27, CR3SP24, and CR3SP22.

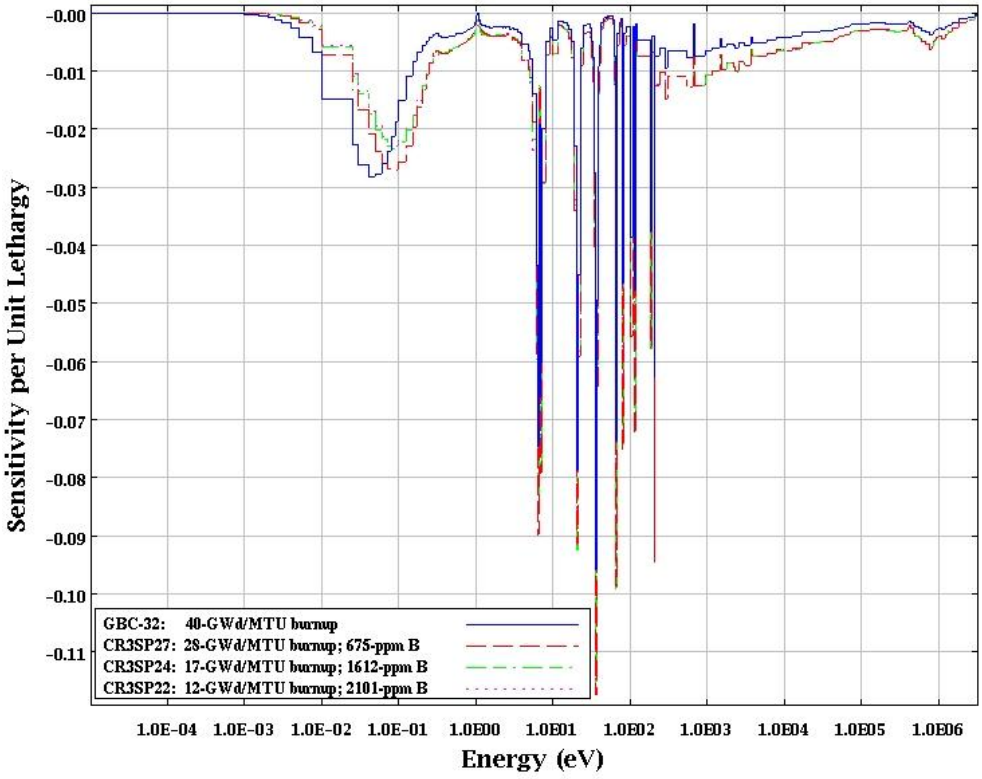

Fig. B.12 Comparison of ^{238}U-capture sensitivity profiles for GBC40, CR3SP27, CR3SP24, and CR3SP22.

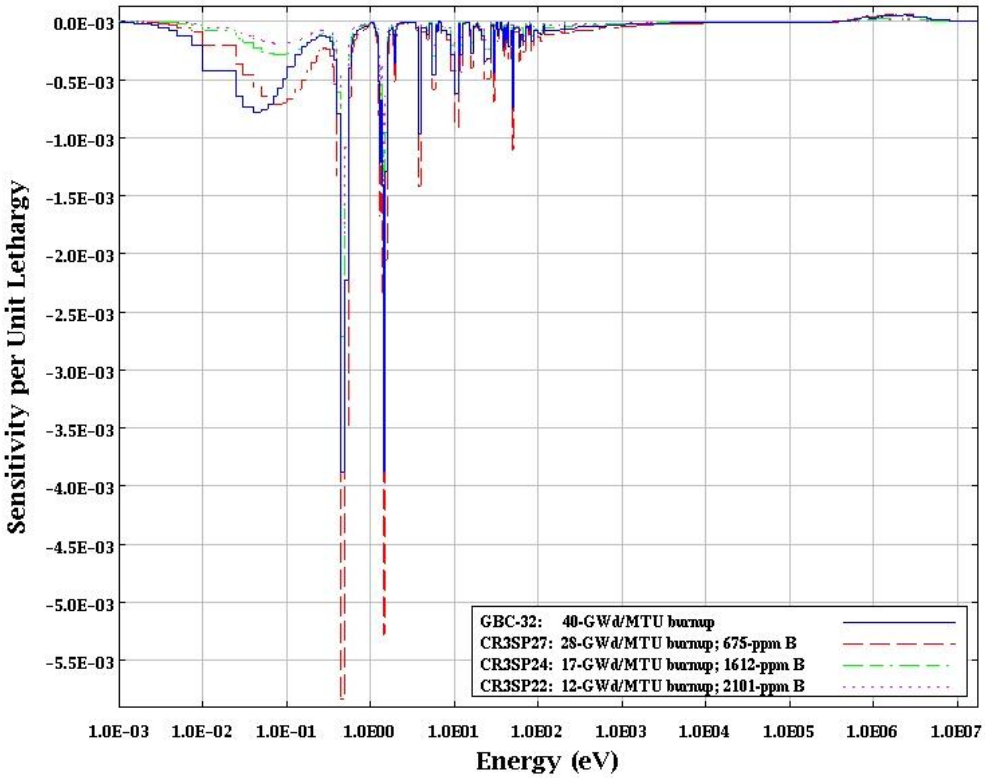

Fig. B.13 Comparison of ^{237}Np sensitivity profiles for GBC40, CR3SP27, CR3SP24, and CR3SP22.

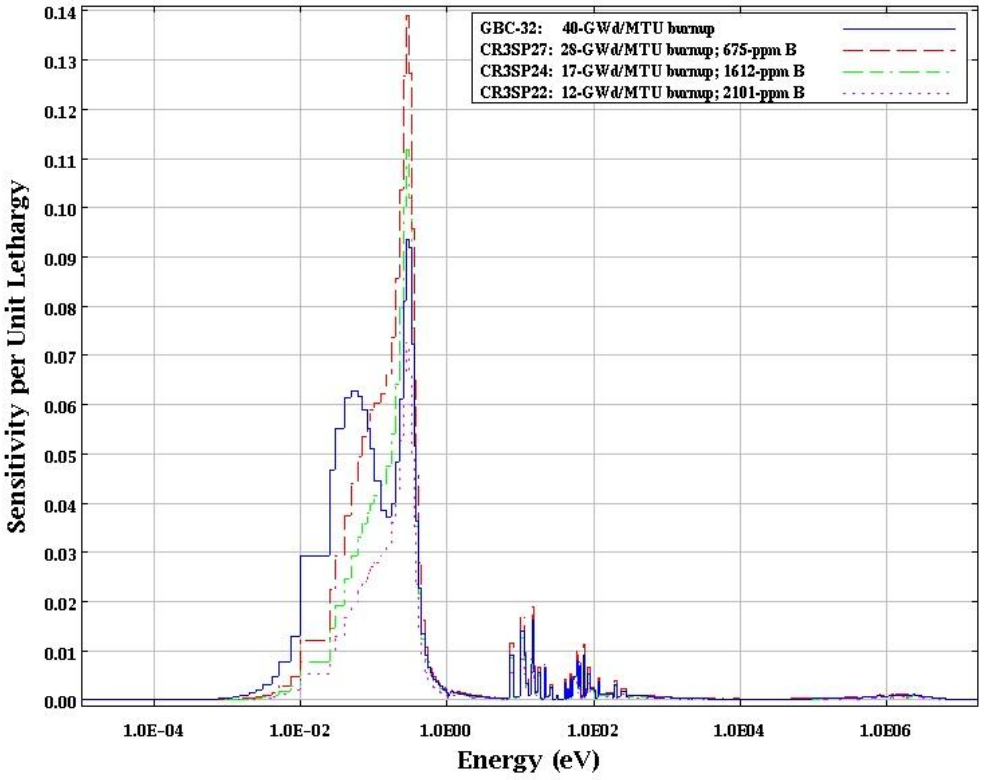

Fig. B.14 Comparison of ^{239}Pu-fission sensitivity profiles for GBC40, CR3SP27, CR3SP24, and CR3SP22.

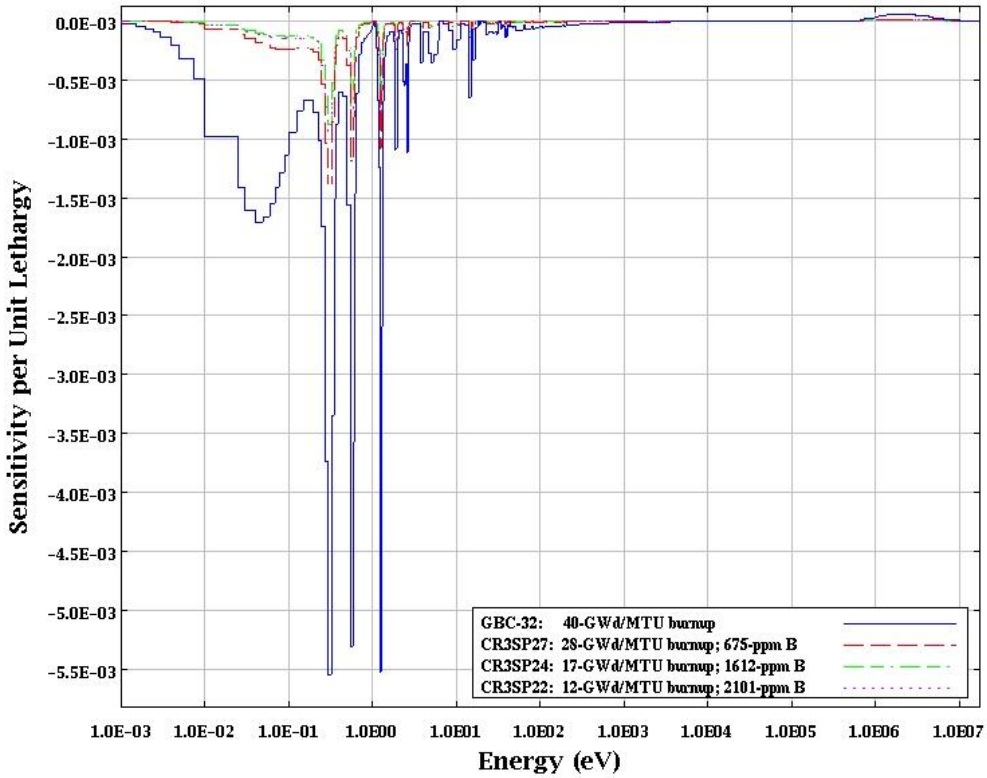

Fig. B.15 Comparison of ^{241}Am sensitivity profiles for GBC40, CR3SP27, CR3SP24, and CR3SP22.

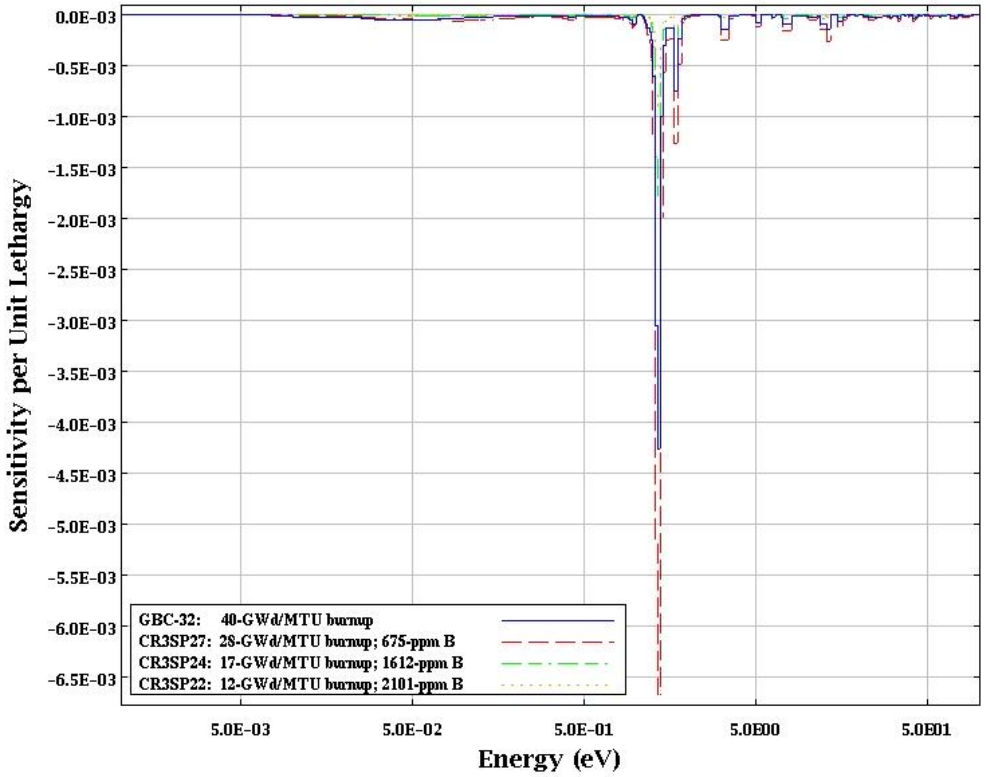

Fig. B.16 Comparison of ^{243}Am sensitivity profiles for GBC40, CR3SP27, CR3SP24, and CR3SP22.

APPENDIX C

NUCLIDE-TOTAL REACTION SPECIFIC INTEGRAL INDEX g

Table C.1 Nuclide-reaction specific *g* index for GBC10

CRC state-points	^{234}U	^{235}U	^{236}U	^{238}U	^{238}Pu	^{239}Pu	^{240}Pu	^{241}Pu	^{242}Pu	^{237}Np
CR3SP1	0.8886	0.8794	0.1668	0.8645	0.0000	0.0000	0.0000	0.0000	0.0000	0.0000
CR3SP2	0.8391	0.7008	0.9774	0.8505	0.8654	0.7479	0.9323	0.9025	0.9901	0.8834
CR3SP3	0.8435	0.6182	0.9928	0.8688	1.0000	0.8046	0.9916	1.0000	1.0000	0.9914
CR3SP4	0.8481	0.7027	0.9695	0.8343	0.9943	0.7105	0.9395	0.9434	0.9992	0.9219
CR3SP5	0.8507	0.7253	0.9651	0.8306	0.9948	0.6803	0.9016	0.9157	0.9989	0.9025
CR3SP6	0.8510	0.6441	0.9914	0.8483	1.0000	0.7542	0.9764	0.9974	1.0000	0.9914
CR3SP7	0.8477	0.6101	0.9953	0.8526	1.0000	0.7804	0.9913	1.0000	1.0000	0.9993
CR3SP8	0.8589	0.7532	0.9673	0.8390	0.9674	0.5957	0.8125	0.8923	0.9980	0.8669
CR3SP9	0.8418	0.6145	0.9928	0.8469	1.0000	0.7810	0.9859	1.0000	1.0000	0.9967
CR3SP10	0.8435	0.6007	0.9937	0.8505	1.0000	0.7780	0.9895	1.0000	1.0000	0.9984
CR3SP11	0.8584	0.7391	0.9596	0.8158	0.8727	0.5415	0.7696	0.8299	0.9895	0.8163
CR3SP12	0.8351	0.5536	0.9981	0.8346	1.0000	0.8046	0.9893	1.0000	1.0000	1.0000
CR3SP13	0.8529	0.6972	0.9723	0.7992	0.9999	0.5966	0.8019	0.9434	0.9999	0.9232
CR3SP14	0.8467	0.6467	0.9849	0.8033	1.0000	0.6836	0.9182	0.9891	1.0000	0.9760
CR3SP15	0.8431	0.5261	0.9993	0.8288	1.0000	0.7946	0.9776	1.0000	1.0000	1.0000
CR3SP16	0.8533	0.6973	0.9626	0.7806	0.9968	0.5123	0.7342	0.8605	0.9986	0.8718
CR3SP17	0.8436	0.5985	0.9916	0.7953	1.0000	0.7080	0.9670	0.9985	1.0000	0.9967
CR3SP18	0.8388	0.5831	0.9930	0.7932	1.0000	0.7174	0.9719	0.9996	1.0000	0.9990
CR3SP19	0.8437	0.5821	0.9947	0.7995	1.0000	0.7266	0.9755	0.9999	1.0000	0.9996
CR3SP20	0.8481	0.5355	0.9990	0.8128	1.0000	0.7636	0.9794	1.0000	1.0000	1.0000
CR3SP21	0.8480	0.5301	0.9991	0.8144	1.0000	0.7625	0.9795	1.0000	1.0000	1.0000
CR3SP22	0.8477	0.6896	0.9655	0.7674	0.9973	0.5171	0.7469	0.8496	0.9980	0.8853
CR3SP23	0.8371	0.6460	0.9793	0.7675	1.0000	0.6263	0.8684	0.9326	1.0000	0.9500
CR3SP24	0.8391	0.6329	0.9834	0.7737	1.0000	0.6421	0.9092	0.9508	1.0000	0.9650
CR3SP25	0.8388	0.5509	0.9980	0.7929	1.0000	0.7328	0.9728	1.0000	1.0000	1.0000
CR3SP26	0.8387	0.5464	0.9979	0.7926	1.0000	0.7272	0.9724	1.0000	1.0000	1.0000
CR3SP27	0.8385	0.5218	0.9992	0.8009	1.0000	0.7622	0.9660	1.0000	1.0000	1.0000
CR3SP28	0.8470	0.6872	0.9671	0.7660	0.9986	0.5066	0.7526	0.8439	0.9969	0.8905
CR3SP29	0.8422	0.6263	0.9869	0.7734	1.0000	0.6466	0.9273	0.9595	1.0000	0.9807
CR3SP30	0.8361	0.6046	0.9910	0.7750	1.0000	0.6820	0.9518	0.9902	1.0000	0.9960
CR3SP31	0.8374	0.5520	0.9979	0.7870	1.0000	0.7259	0.9740	0.9999	1.0000	1.0000
CR3SP32	0.8448	0.6783	0.9651	0.7605	0.9994	0.4963	0.7166	0.8759	0.9988	0.8970
CR3SP33	0.8447	0.5091	0.9995	0.8008	1.0000	0.7482	0.9647	1.0000	1.0000	1.0000
SQ2C3BZ	0.8440	0.6692	0.9705	0.7849	0.9999	0.5943	0.8437	0.9248	0.9990	0.9325
SQ2C3BF	0.8339	0.6502	0.9682	0.7784	0.9997	0.5765	0.8450	0.9109	0.9986	0.9182
SQ2C3M	0.8188	0.5566	0.9900	0.7850	1.0000	0.7158	0.9657	0.9986	1.0000	0.9994
SU1C2B	0.8630	0.7425	0.9673	0.8558	0.9939	0.6105	0.8086	0.9512	0.9990	0.9071
SU1C2E	0.8383	0.5923	0.9911	0.8529	1.0000	0.7742	0.9862	1.0000	1.0000	0.9986
TMI1C5B	0.8552	0.6761	0.9819	0.8313	1.0000	0.6959	0.9250	0.9143	1.0000	0.9664
NA1C5B	0.8488	0.7061	0.9580	0.7763	0.9430	0.4552	0.7422	0.7678	0.9817	0.8466

Table C.1 Nuclide-reaction specific *g* index for GBC10 (continued)

CRC state-points	^{241}Am	^{243}Am	^{1}H	^{16}O	^{10}B	^{95}Mo	^{99}Tc	^{101}Ru	^{103}Rh	^{109}Ag[a]
CR3SP1	0.0000	0.0000	0.6022	0.6096	0.6146	0.0000	0.0000	0.0000	0.0000	0.1248
CR3SP2	0.2639	0.9814	0.6782	0.7067	0.4701	0.8954	0.9397	0.9649	0.8999	0.9484
CR3SP3	0.3259	1.0000	0.7242	0.7267	0.3093	0.9496	0.9915	0.9944	0.9634	0.9816
CR3SP4	0.3017	1.0000	0.6651	0.6991	0.5030	0.9039	0.9505	0.9712	0.9069	0.9635
CR3SP5	0.3261	1.0000	0.6532	0.6770	0.5291	0.8922	0.9376	0.9644	0.8874	0.9547
CR3SP6	0.3632	1.0000	0.7075	0.7226	0.3799	0.9359	0.9854	0.9912	0.9477	0.9812
CR3SP7	0.4340	1.0000	0.7155	0.7241	0.3289	0.9663	0.9957	0.9971	0.9733	0.9807
CR3SP8	0.1777	1.0000	0.6603	0.6787	0.5554	0.8400	0.9149	0.9523	0.8465	0.9437
CR3SP9	0.3147	1.0000	0.7032	0.7002	0.3758	0.9446	0.9924	0.9955	0.9609	0.9872
CR3SP10	0.3777	1.0000	0.7131	0.7140	0.3145	0.9608	0.9946	0.9966	0.9720	0.9807
CR3SP11	0.2125	0.9938	0.6597	0.6822	0.6257	0.8190	0.8890	0.9382	0.8129	0.9196
CR3SP12	0.4750	1.0000	0.6909	0.6899	0.3482	0.9871	0.9992	0.9991	0.9922	0.9873
CR3SP13	0.4400	1.0000	0.6581	0.6786	0.6250	0.8857	0.9296	0.9613	0.8746	0.9604
CR3SP14	0.6457	1.0000	0.6768	0.6995	0.5405	0.9414	0.9669	0.9815	0.9328	0.9713
CR3SP15	0.7005	1.0000	0.7081	0.7015	0.2748	0.9971	0.9997	0.9993	0.9967	0.9842
CR3SP16	0.5494	1.0000	0.6478	0.6899	0.6650	0.8335	0.8962	0.9432	0.8194	0.9333
CR3SP17	0.5873	1.0000	0.6805	0.7122	0.5001	0.9446	0.9836	0.9910	0.9458	0.9864
CR3SP18	0.6324	1.0000	0.6890	0.7061	0.4824	0.9626	0.9884	0.9938	0.9608	0.9811
CR3SP19	0.7219	1.0000	0.6955	0.7140	0.4567	0.9836	0.9937	0.9962	0.9740	0.9871
CR3SP20	0.7374	1.0000	0.6983	0.7080	0.3274	0.9962	0.9994	0.9992	0.9933	0.9763
CR3SP21	0.7396	1.0000	0.7171	0.7256	0.3142	0.9968	0.9995	0.9992	0.9943	0.9842
CR3SP22	0.5782	1.0000	0.6439	0.6827	0.7086	0.8396	0.9006	0.9454	0.8244	0.9325
CR3SP23	0.5366	1.0000	0.6554	0.6907	0.6404	0.8711	0.9417	0.9676	0.8681	0.9588
CR3SP24	0.5262	1.0000	0.6645	0.6923	0.6107	0.8888	0.9542	0.9746	0.8860	0.9667
CR3SP25	0.6772	1.0000	0.6968	0.7061	0.4186	0.9892	0.9969	0.9980	0.9844	0.9814
CR3SP26	0.6799	1.0000	0.6948	0.7003	0.4196	0.9898	0.9967	0.9980	0.9842	0.9814
CR3SP27	0.7225	1.0000	0.7033	0.6957	0.3621	0.9971	0.9995	0.9992	0.9944	0.9817
CR3SP28	0.4120	1.0000	0.6457	0.6838	0.7165	0.8412	0.9022	0.9462	0.8242	0.9290
CR3SP29	0.4636	1.0000	0.6618	0.7074	0.5940	0.9004	0.9633	0.9798	0.8964	0.9719
CR3SP30	0.5820	1.0000	0.6618	0.6920	0.5686	0.9443	0.9775	0.9875	0.9401	0.9803
CR3SP31	0.6534	1.0000	0.6806	0.6944	0.4432	0.9823	0.9964	0.9979	0.9747	0.9830
CR3SP32	0.2376	1.0000	0.6434	0.6937	0.7155	0.8226	0.8988	0.9449	0.8130	0.9310
CR3SP33	0.6985	1.0000	0.7149	0.7369	0.3067	0.9983	0.9996	0.9993	0.9962	0.9817
SQ2C3BZ	0.3785	1.0000	0.6649	0.7004	0.6500	0.8695	0.9185	0.9558	0.8596	0.9536
SQ2C3BF	0.3857	1.0000	0.6664	0.7212	0.5775	0.8587	0.9111	0.9524	0.8473	0.9468
SQ2C3M	0.2704	1.0000	0.6887	0.7250	0.5296	0.8633	0.9193	0.9560	0.8599	0.9656
SU1C2B	0.3222	1.0000	0.7124	0.7302	0.2167	0.9366	0.9899	0.9953	0.9530	1.0000
SU1C2E	0.9298	1.0000	0.6826	0.7080	0.3468	0.9711	0.9799	0.9897	0.9568	0.9989
TMI1C5B	0.9840	1.0000	0.6914	0.7135	0.4895	0.9357	0.9551	0.9755	0.9168	0.9603
NA1C5B	0.3281	0.9949	0.6397	0.6873	0.7331	0.8043	0.8714	0.9301	0.7849	0.8935

[a] ^{109}Ag exists in spent fuel and/or control rods.

Table C.1 Nuclide-reaction specific *g* index for GBC10 (continued)

CRC state-points	^{133}Cs	^{143}Nd	^{145}Nd	^{147}Sm	^{149}Sm	^{150}Sm	^{151}Sm	^{152}Sm	^{153}Eu	^{155}Gd
CR3SP1	0.0000	0.0000	0.0000	0.0000	0.0000	0.0000	0.0000	0.0000	0.0000	0.0000
CR3SP2	0.9272	0.8090	0.8931	0.4812	0.7973	0.8424	0.6024	0.9389	0.8928	0.1381
CR3SP3	0.9897	0.9478	0.9814	0.6620	0.8341	0.9871	0.7068	0.9953	0.9985	0.0321
CR3SP4	0.9400	0.8318	0.9109	0.6509	0.7101	0.8749	0.5788	0.9504	0.9347	0.0804
CR3SP5	0.9244	0.7900	0.8891	0.6539	0.7151	0.8386	0.5401	0.9338	0.9159	0.1158
CR3SP6	0.9821	0.9271	0.9713	0.7434	0.8170	0.9733	0.6821	0.9868	0.9970	0.0370
CR3SP7	0.9948	0.9647	0.9914	0.8246	0.8253	0.9942	0.7349	0.9965	1.0000	0.0411
CR3SP8	0.8969	0.7112	0.8484	0.3876	0.5564	0.7897	0.4207	0.9137	0.8838	0.0531
CR3SP9	0.9906	0.9436	0.9825	0.6310	0.8391	0.9893	0.7149	0.9943	0.9997	0.0388
CR3SP10	0.9935	0.9557	0.9883	0.7002	0.8307	0.9924	0.7315	0.9954	0.9998	0.0564
CR3SP11	0.8655	0.6398	0.8046	0.4028	0.4509	0.7165	0.3620	0.8866	0.8282	0.0631
CR3SP12	0.9991	0.9873	0.9981	0.8319	0.8298	0.9998	0.7806	0.9997	1.0000	0.0379
CR3SP13	0.9146	0.7523	0.8733	0.6547	0.5349	0.8436	0.4315	0.9293	0.9329	0.1444
CR3SP14	0.9597	0.8660	0.9377	0.8292	0.7813	0.9311	0.6091	0.9649	0.9883	0.1723
CR3SP15	0.9997	0.9960	0.9996	0.8869	0.8538	0.9999	0.8214	0.9999	1.0000	0.0642
CR3SP16	0.8741	0.6567	0.8171	0.6696	0.4077	0.7498	0.3581	0.8915	0.8694	0.1635
CR3SP17	0.9798	0.9188	0.9683	0.8315	0.7874	0.9750	0.6772	0.9814	0.9988	0.0499
CR3SP18	0.9856	0.9367	0.9761	0.8389	0.7916	0.9852	0.7011	0.9865	0.9995	0.0835
CR3SP19	0.9923	0.9525	0.9859	0.8713	0.7910	0.9893	0.7152	0.9930	0.9998	0.1888
CR3SP20	0.9994	0.9908	0.9991	0.9007	0.7704	0.9998	0.8013	0.9997	1.0000	0.0496
CR3SP21	0.9995	0.9928	0.9992	0.9024	0.8143	0.9998	0.8048	0.9997	1.0000	0.0614
CR3SP22	0.8787	0.6745	0.8249	0.7100	0.4557	0.7611	0.3864	0.8932	0.8735	0.1829
CR3SP23	0.9282	0.7877	0.8958	0.7761	0.7430	0.8647	0.5619	0.9321	0.9454	0.0306
CR3SP24	0.9429	0.8215	0.9180	0.7954	0.7346	0.8968	0.5986	0.9467	0.9643	0.0268
CR3SP25	0.9962	0.9820	0.9936	0.8575	0.8230	0.9982	0.7636	0.9965	1.0000	0.1101
CR3SP26	0.9959	0.9814	0.9934	0.8569	0.7494	0.9978	0.7699	0.9963	1.0000	0.0989
CR3SP27	0.9995	0.9935	0.9992	0.8850	0.8284	0.9999	0.8222	0.9997	1.0000	0.0660
CR3SP28	0.8812	0.6809	0.8285	0.6914	0.4578	0.7631	0.3957	0.8934	0.8727	0.0996
CR3SP29	0.9538	0.8486	0.9345	0.8040	0.6976	0.9199	0.6229	0.9562	0.9802	0.0244
CR3SP30	0.9726	0.9081	0.9587	0.8260	0.7895	0.9584	0.6703	0.9728	0.9948	0.0844
CR3SP31	0.9954	0.9774	0.9930	0.8585	0.7493	0.9972	0.7663	0.9958	1.0000	0.0412
CR3SP32	0.8769	0.6662	0.8220	0.4719	0.4500	0.7664	0.3682	0.8910	0.8800	0.0400
CR3SP33	0.9996	0.9960	0.9994	0.8753	0.8535	0.9999	0.8372	0.9997	1.0000	0.0901
SQ2C3BZ	0.9019	0.7242	0.8580	0.4516	0.4758	0.8275	0.4067	0.9233	0.8994	0.1507
SQ2C3BF	0.9864	0.9274	0.9809	0.6225	0.6467	0.9953	0.6847	0.9944	0.9994	0.0406
SQ2C3M	0.8920	0.7083	0.8482	0.6609	0.4604	0.8257	0.4463	0.9062	0.8880	0.1957
SU1C2B	0.9015	0.7321	0.8593	0.6583	0.6306	0.8443	0.4705	0.9132	0.9036	0.2552
SU1C2E	0.9753	0.9154	0.9647	0.9313	0.6743	0.9883	0.6752	0.9791	0.9969	0.9992
TMI1C5B	0.9463	0.8427	0.9219	0.9506	0.7062	0.9248	0.5503	0.9547	0.9559	1.0000
NA1C5B	0.8451	0.6018	0.7805	0.5475	0.4411	0.6965	0.3571	0.8606	0.7966	0.2430

Table C.2 Nuclide-reaction specific *g* index for GBC20

CRC state-points	^{234}U	^{235}U	^{236}U	^{238}U	^{238}Pu	^{239}Pu	^{240}Pu	^{241}Pu	^{242}Pu	^{237}Np
CR3SP1	0.8886	0.8794	0.1668	0.8645	0.0000	0.0000	0.0000	0.0000	0.0000	0.0000
CR3SP2	0.8391	0.7008	0.9774	0.8505	0.8654	0.7479	0.9323	0.9025	0.9901	0.8834
CR3SP3	0.8435	0.6182	0.9928	0.8688	1.0000	0.8046	0.9916	1.0000	1.0000	0.9914
CR3SP4	0.8481	0.7027	0.9695	0.8343	0.9943	0.7105	0.9395	0.9434	0.9992	0.9219
CR3SP5	0.8507	0.7253	0.9651	0.8306	0.9948	0.6803	0.9016	0.9157	0.9989	0.9025
CR3SP6	0.8510	0.6441	0.9914	0.8483	1.0000	0.7542	0.9764	0.9974	1.0000	0.9914
CR3SP7	0.8477	0.6101	0.9953	0.8526	1.0000	0.7804	0.9913	1.0000	1.0000	0.9993
CR3SP8	0.8589	0.7532	0.9673	0.8390	0.9674	0.5957	0.8125	0.8923	0.9980	0.8669
CR3SP9	0.8418	0.6145	0.9928	0.8469	1.0000	0.7810	0.9859	1.0000	1.0000	0.9967
CR3SP10	0.8435	0.6007	0.9937	0.8505	1.0000	0.7780	0.9895	1.0000	1.0000	0.9984
CR3SP11	0.8584	0.7391	0.9596	0.8158	0.8727	0.5415	0.7696	0.8299	0.9895	0.8163
CR3SP12	0.8351	0.5536	0.9981	0.8346	1.0000	0.8046	0.9893	1.0000	1.0000	1.0000
CR3SP13	0.8529	0.6972	0.9723	0.7992	0.9999	0.5966	0.8019	0.9434	0.9999	0.9232
CR3SP14	0.8467	0.6467	0.9849	0.8033	1.0000	0.6836	0.9182	0.9891	1.0000	0.9760
CR3SP15	0.8431	0.5261	0.9993	0.8288	1.0000	0.7946	0.9776	1.0000	1.0000	1.0000
CR3SP16	0.8533	0.6973	0.9626	0.7806	0.9968	0.5123	0.7342	0.8605	0.9986	0.8718
CR3SP17	0.8436	0.5985	0.9916	0.7953	1.0000	0.7080	0.9670	0.9985	1.0000	0.9967
CR3SP18	0.8388	0.5831	0.9930	0.7932	1.0000	0.7174	0.9719	0.9996	1.0000	0.9990
CR3SP19	0.8437	0.5821	0.9947	0.7995	1.0000	0.7266	0.9755	0.9999	1.0000	0.9996
CR3SP20	0.8481	0.5355	0.9990	0.8128	1.0000	0.7636	0.9794	1.0000	1.0000	1.0000
CR3SP21	0.8480	0.5301	0.9991	0.8144	1.0000	0.7625	0.9795	1.0000	1.0000	1.0000
CR3SP22	0.8477	0.6896	0.9655	0.7674	0.9973	0.5171	0.7469	0.8496	0.9980	0.8853
CR3SP23	0.8371	0.6460	0.9793	0.7675	1.0000	0.6263	0.8684	0.9326	1.0000	0.9500
CR3SP24	0.8391	0.6329	0.9834	0.7737	1.0000	0.6421	0.9092	0.9508	1.0000	0.9650
CR3SP25	0.8388	0.5509	0.9980	0.7929	1.0000	0.7328	0.9728	1.0000	1.0000	1.0000
CR3SP26	0.8387	0.5464	0.9979	0.7926	1.0000	0.7272	0.9724	1.0000	1.0000	1.0000
CR3SP27	0.8385	0.5218	0.9992	0.8009	1.0000	0.7622	0.9660	1.0000	1.0000	1.0000
CR3SP28	0.8470	0.6872	0.9671	0.7660	0.9986	0.5066	0.7526	0.8439	0.9969	0.8905
CR3SP29	0.8422	0.6263	0.9869	0.7734	1.0000	0.6466	0.9273	0.9595	1.0000	0.9807
CR3SP30	0.8361	0.6046	0.9910	0.7750	1.0000	0.6820	0.9518	0.9902	1.0000	0.9960
CR3SP31	0.8374	0.5520	0.9979	0.7870	1.0000	0.7259	0.9740	0.9999	1.0000	1.0000
CR3SP32	0.8448	0.6783	0.9651	0.7605	0.9994	0.4963	0.7166	0.8759	0.9988	0.8970
CR3SP33	0.8447	0.5091	0.9995	0.8008	1.0000	0.7482	0.9647	1.0000	1.0000	1.0000
SQ2C3BZ	0.8440	0.6692	0.9705	0.7849	0.9999	0.5943	0.8437	0.9248	0.9990	0.9325
SQ2C3BF	0.8339	0.6502	0.9682	0.7784	0.9997	0.5765	0.8450	0.9109	0.9986	0.9182
SQ2C3M	0.8188	0.5566	0.9900	0.7850	1.0000	0.7158	0.9657	0.9986	1.0000	0.9994
SU1C2B	0.8630	0.7425	0.9673	0.8558	0.9939	0.6105	0.8086	0.9512	0.9990	0.9071
SU1C2E	0.8383	0.5923	0.9911	0.8529	1.0000	0.7742	0.9862	1.0000	1.0000	0.9986
TMI1C5B	0.8552	0.6761	0.9819	0.8313	1.0000	0.6959	0.9250	0.9143	1.0000	0.9664
NA1C5B	0.8488	0.7061	0.9580	0.7763	0.9430	0.4552	0.7422	0.7678	0.9817	0.8466

Table C.2 Nuclide-reaction specific *g* index for GBC20 (continued)

CRC state-points	^{241}Am	^{243}Am	^{1}H	^{16}O	^{10}B	^{95}Mo	^{99}Tc	^{101}Ru	^{103}Rh	^{109}Ag[a]
CR3SP1	0.0000	0.0000	0.5548	0.5382	0.6122	0.0000	0.0000	0.0000	0.0000	0.0873
CR3SP2	0.0920	0.2111	0.6468	0.6701	0.4649	0.7423	0.8241	0.8401	0.7525	0.7470
CR3SP3	0.1136	0.8075	0.7089	0.6893	0.3052	0.8412	0.9272	0.9603	0.8543	0.9392
CR3SP4	0.1052	0.5046	0.6346	0.6624	0.4971	0.7974	0.8723	0.9260	0.7920	0.8691
CR3SP5	0.1137	0.5511	0.6223	0.6363	0.5234	0.7715	0.8391	0.9058	0.7498	0.8188
CR3SP6	0.1267	0.9502	0.6969	0.6907	0.3753	0.8279	0.9194	0.9566	0.8345	0.9311
CR3SP7	0.1513	0.9792	0.7050	0.6881	0.3247	0.8634	0.9399	0.9675	0.8696	0.9497
CR3SP8	0.0620	0.4577	0.6236	0.6276	0.5512	0.5955	0.7026	0.7666	0.6108	0.7406
CR3SP9	0.1098	0.9741	0.6945	0.6667	0.3712	0.8367	0.9289	0.9619	0.8515	0.9478
CR3SP10	0.1317	0.9806	0.7065	0.6826	0.3103	0.8567	0.9342	0.9646	0.8678	0.9485
CR3SP11	0.0741	0.2967	0.6168	0.6140	0.6233	0.5497	0.6072	0.6537	0.5409	0.6404
CR3SP12	0.1657	0.9997	0.6851	0.6621	0.3437	0.8951	0.9599	0.9787	0.9027	0.9684
CR3SP13	0.1535	0.8686	0.6223	0.6321	0.6226	0.7728	0.8200	0.9175	0.7423	0.8630
CR3SP14	0.2342	0.9489	0.6531	0.6641	0.5351	0.8350	0.8937	0.9443	0.8198	0.8923
CR3SP15	0.2685	1.0000	0.7014	0.6714	0.2698	0.9313	0.9739	0.9862	0.9271	0.9790
CR3SP16	0.1928	0.7375	0.6057	0.6297	0.6635	0.6651	0.7143	0.8454	0.6183	0.7607
CR3SP17	0.2078	0.9853	0.6746	0.6760	0.4947	0.8388	0.9185	0.9572	0.8349	0.9277
CR3SP18	0.2274	0.9912	0.6828	0.6783	0.4776	0.8612	0.9252	0.9607	0.8543	0.9302
CR3SP19	0.3070	0.9958	0.6868	0.6728	0.4523	0.8918	0.9335	0.9649	0.8746	0.9426
CR3SP20	0.3140	1.0000	0.6947	0.6735	0.3233	0.9288	0.9676	0.9832	0.9116	0.9631
CR3SP21	0.3191	1.0000	0.7121	0.6915	0.3100	0.9313	0.9690	0.9838	0.9155	0.9727
CR3SP22	0.2043	0.7593	0.6081	0.6291	0.7067	0.7121	0.7678	0.8979	0.6611	0.7930
CR3SP23	0.1876	0.9223	0.6340	0.6466	0.6380	0.7726	0.8694	0.9321	0.7593	0.8696
CR3SP24	0.1837	0.9347	0.6466	0.6605	0.6083	0.7864	0.8817	0.9383	0.7757	0.8817
CR3SP25	0.2593	0.9994	0.6903	0.6742	0.4145	0.9009	0.9498	0.9734	0.8911	0.9522
CR3SP26	0.2623	0.9993	0.6914	0.6661	0.4156	0.9019	0.9494	0.9734	0.8909	0.9531
CR3SP27	0.3066	1.0000	0.6988	0.6688	0.3576	0.9357	0.9711	0.9849	0.9203	0.9704
CR3SP28	0.1437	0.7827	0.6107	0.6275	0.7145	0.7359	0.7855	0.9077	0.6790	0.7941
CR3SP29	0.1617	0.9478	0.6454	0.6766	0.5909	0.7971	0.8917	0.9436	0.7852	0.8874
CR3SP30	0.2053	0.9727	0.6551	0.6616	0.5645	0.8403	0.9108	0.9531	0.8305	0.9096
CR3SP31	0.2398	0.9994	0.6825	0.6615	0.4394	0.8916	0.9488	0.9734	0.8771	0.9511
CR3SP32	0.0829	0.8963	0.6063	0.6300	0.7135	0.6919	0.7720	0.9073	0.6523	0.8171
CR3SP33	0.2781	1.0000	0.7130	0.7049	0.3028	0.9430	0.9749	0.9870	0.9282	0.9728
SQ2C3BZ	0.1320	0.8402	0.6363	0.6506	0.6477	0.7713	0.8287	0.9177	0.7446	0.8405
SQ2C3BF	0.1345	0.8406	0.6417	0.6636	0.5737	0.7642	0.8318	0.9082	0.7338	0.8318
SQ2C3M	0.7167	0.9806	0.6795	0.6699	0.3425	0.8769	0.9148	0.9565	0.8516	0.9330
SU1C2B	0.0943	0.4402	0.6600	0.6599	0.5237	0.6197	0.6612	0.7303	0.6147	0.7353
SU1C2E	0.1124	0.9723	0.7018	0.6949	0.2117	0.8293	0.9256	0.9604	0.8395	0.9528
TMI1C5B	0.7787	0.8933	0.6744	0.6894	0.4837	0.8293	0.8813	0.9385	0.8038	0.8646
NA1C5B	0.1144	0.3867	0.6037	0.6247	0.7310	0.6253	0.6383	0.7485	0.5550	0.5855

[a] ^{109}Ag exists in spent fuel and/or control rods.

Table C.2 Nuclide-reaction specific g index for GBC20 (continued)

CRC state-points	^{133}Cs	^{143}Nd	^{145}Nd	^{147}Sm	^{149}Sm	^{150}Sm	^{151}Sm	^{152}Sm	^{153}Eu	^{155}Gd
CR3SP1	0.0000	0.0000	0.0000	0.0000	0.0000	0.0000	0.0000	0.0000	0.0000	0.0000
CR3SP2	0.8067	0.5947	0.7536	0.2665	0.7340	0.5552	0.4803	0.8213	0.5738	0.0661
CR3SP3	0.9118	0.7568	0.8752	0.3693	0.7781	0.7774	0.5707	0.9276	0.8445	0.0154
CR3SP4	0.8484	0.6183	0.7900	0.3618	0.6359	0.6128	0.4616	0.8661	0.7166	0.0385
CR3SP5	0.8172	0.5780	0.7705	0.3634	0.6414	0.5704	0.4292	0.8314	0.6819	0.0554
CR3SP6	0.9020	0.7273	0.8624	0.4186	0.7597	0.7535	0.5492	0.9127	0.8402	0.0177
CR3SP7	0.9268	0.7833	0.8960	0.4761	0.7691	0.8166	0.5961	0.9359	0.8902	0.0197
CR3SP8	0.6902	0.5000	0.6581	0.2147	0.4738	0.4993	0.3237	0.7188	0.5870	0.0254
CR3SP9	0.9135	0.7516	0.8774	0.3505	0.7845	0.7930	0.5784	0.9242	0.8691	0.0186
CR3SP10	0.9202	0.7705	0.8859	0.3911	0.7753	0.8075	0.5931	0.9300	0.8814	0.0270
CR3SP11	0.5956	0.4323	0.5677	0.2231	0.3783	0.4194	0.2732	0.6176	0.4833	0.0302
CR3SP12	0.9505	0.8377	0.9294	0.4976	0.7744	0.8901	0.6402	0.9585	0.9463	0.0181
CR3SP13	0.7950	0.5462	0.7571	0.3634	0.4548	0.5889	0.3377	0.8405	0.7366	0.0691
CR3SP14	0.8711	0.6555	0.8190	0.5458	0.7185	0.6961	0.4879	0.8822	0.8052	0.0824
CR3SP15	0.9679	0.8826	0.9532	0.7417	0.8042	0.9298	0.6797	0.9711	0.9767	0.0307
CR3SP16	0.7005	0.4642	0.6758	0.3718	0.3415	0.4928	0.2753	0.7308	0.6513	0.0782
CR3SP17	0.9007	0.7218	0.8609	0.5650	0.7256	0.7611	0.5473	0.9066	0.8585	0.0239
CR3SP18	0.9090	0.7472	0.8719	0.6141	0.7301	0.7834	0.5686	0.9140	0.8752	0.0400
CR3SP19	0.9190	0.7714	0.8856	0.7516	0.7291	0.8037	0.5810	0.9228	0.8906	0.0903
CR3SP20	0.9595	0.8614	0.9431	0.8344	0.7060	0.9061	0.6617	0.9613	0.9640	0.0237
CR3SP21	0.9615	0.8670	0.9451	0.8442	0.7582	0.9094	0.6651	0.9626	0.9662	0.0294
CR3SP22	0.7444	0.4839	0.7184	0.3973	0.3835	0.5183	0.3042	0.7813	0.6852	0.0875
CR3SP23	0.8407	0.5811	0.7796	0.4435	0.6759	0.6265	0.4496	0.8515	0.7547	0.0146
CR3SP24	0.8550	0.6132	0.8006	0.4661	0.6641	0.6587	0.4803	0.8646	0.7773	0.0128
CR3SP25	0.9387	0.8221	0.9131	0.7133	0.7687	0.8582	0.6259	0.9400	0.9269	0.0527
CR3SP26	0.9379	0.8201	0.9127	0.7144	0.6815	0.8588	0.6323	0.9396	0.9264	0.0473
CR3SP27	0.9642	0.8766	0.9491	0.8122	0.7741	0.9224	0.6824	0.9645	0.9719	0.0316
CR3SP28	0.7577	0.4902	0.7217	0.3854	0.3855	0.5266	0.3137	0.7951	0.6918	0.0476
CR3SP29	0.8670	0.6406	0.8185	0.4998	0.6259	0.6875	0.5009	0.8754	0.7976	0.0117
CR3SP30	0.8916	0.7106	0.8489	0.5991	0.7281	0.7421	0.5421	0.8955	0.8412	0.0404
CR3SP31	0.9365	0.8095	0.9126	0.7212	0.6819	0.8558	0.6289	0.9383	0.9263	0.0197
CR3SP32	0.7451	0.4772	0.7180	0.2614	0.3788	0.5305	0.2894	0.7914	0.6983	0.0191
CR3SP33	0.9687	0.8941	0.9555	0.7702	0.8057	0.9387	0.6999	0.9683	0.9819	0.0431
SQ2C3BZ	0.7982	0.5317	0.7476	0.3654	0.5516	0.6041	0.3750	0.8349	0.7145	0.1222
SQ2C3BF	0.7955	0.5141	0.7404	0.3737	0.3892	0.5843	0.3562	0.8304	0.7028	0.0936
SQ2C3M	0.8964	0.7220	0.8585	0.8758	0.6034	0.8029	0.5466	0.9051	0.8497	0.8133
SU1C2B	0.6558	0.5060	0.6479	0.2501	0.3998	0.5322	0.3091	0.7048	0.5825	0.0721
SU1C2E	0.9082	0.7293	0.8760	0.3495	0.5675	0.8234	0.5522	0.9248	0.8599	0.0194
TMI1C5B	0.8569	0.6302	0.8025	0.8927	0.6328	0.6851	0.4385	0.8717	0.7624	0.9746
NA1C5B	0.6320	0.4186	0.6164	0.3032	0.3709	0.4462	0.2777	0.6399	0.5192	0.1163

Table C.3 Nuclide-reaction specific *g* index for GBC30

CRC state-points	^{234}U	^{235}U	^{236}U	^{238}U	^{238}Pu	^{239}Pu	^{240}Pu	^{241}Pu	^{242}Pu	^{237}Np
CR3SP1	0.9145	0.9820	0.0806	0.9360	0.0000	0.0000	0.0000	0.0000	0.0000	0.0000
CR3SP2	0.8682	0.8492	0.8340	0.9254	0.1219	0.6796	0.6829	0.4268	0.2467	0.3551
CR3SP3	0.8704	0.7674	0.9327	0.9412	0.3216	0.7436	0.8749	0.6894	0.6697	0.5997
CR3SP4	0.8775	0.8487	0.8658	0.9102	0.2081	0.6416	0.7202	0.5142	0.4115	0.4482
CR3SP5	0.8800	0.8697	0.8192	0.9038	0.2115	0.6033	0.6411	0.4668	0.3995	0.4167
CR3SP6	0.8799	0.7935	0.9362	0.9228	0.4201	0.6921	0.8422	0.6649	0.7580	0.6509
CR3SP7	0.8766	0.7577	0.9481	0.9282	0.5439	0.7246	0.8796	0.7532	0.9607	0.7662
CR3SP8	0.8876	0.8922	0.6738	0.9137	0.1695	0.5005	0.5457	0.4250	0.3612	0.3473
CR3SP9	0.8710	0.7621	0.9403	0.9218	0.4775	0.7279	0.8656	0.7409	0.9195	0.7172
CR3SP10	0.8725	0.7483	0.9429	0.9252	0.5113	0.7223	0.8734	0.7457	0.9550	0.7465
CR3SP11	0.8872	0.8769	0.6118	0.8915	0.1274	0.4467	0.4797	0.3541	0.2718	0.2853
CR3SP12	0.8653	0.6963	0.9646	0.9087	0.7013	0.7557	0.9121	0.8463	0.9833	0.8464
CR3SP13	0.8821	0.8377	0.7919	0.8752	0.2834	0.5031	0.6022	0.5334	0.5746	0.4931
CR3SP14	0.8763	0.7905	0.9300	0.8793	0.4300	0.6197	0.7550	0.6270	0.7986	0.6505
CR3SP15	0.8732	0.6686	0.9754	0.9047	0.8794	0.7457	0.9245	0.8722	0.9911	0.8962
CR3SP16	0.8825	0.8352	0.7104	0.8584	0.2355	0.4171	0.4909	0.4168	0.4582	0.4158
CR3SP17	0.8734	0.7406	0.9531	0.8727	0.6018	0.6598	0.8351	0.7134	0.9624	0.7835
CR3SP18	0.8690	0.7240	0.9583	0.8713	0.6471	0.6718	0.8462	0.7339	0.9679	0.8024
CR3SP19	0.8735	0.7243	0.9616	0.8770	0.6944	0.6793	0.8554	0.7454	0.9715	0.8149
CR3SP20	0.8777	0.6738	0.9742	0.8878	0.8828	0.7123	0.9065	0.8381	0.9877	0.8848
CR3SP21	0.8776	0.6683	0.9747	0.8914	0.8903	0.7101	0.9081	0.8397	0.9882	0.8891
CR3SP22	0.8772	0.8278	0.7872	0.8430	0.2488	0.4221	0.5125	0.4207	0.4734	0.4688
CR3SP23	0.8674	0.7871	0.9292	0.8435	0.3719	0.5671	0.6757	0.5529	0.6743	0.6413
CR3SP24	0.8693	0.7742	0.9379	0.8514	0.4182	0.5875	0.7316	0.5835	0.7425	0.6905
CR3SP25	0.8691	0.6893	0.9691	0.8692	0.7869	0.6860	0.8776	0.7856	0.9780	0.8599
CR3SP26	0.8690	0.6840	0.9691	0.8705	0.7894	0.6774	0.8780	0.7813	0.9780	0.8599
CR3SP27	0.8689	0.6594	0.9766	0.8773	0.9203	0.7129	0.9108	0.8502	0.9893	0.9064
CR3SP28	0.8765	0.8254	0.8175	0.8418	0.2635	0.4138	0.5200	0.4228	0.4747	0.4956
CR3SP29	0.8720	0.7672	0.9461	0.8507	0.4780	0.5915	0.7707	0.6080	0.8107	0.7389
CR3SP30	0.8665	0.7459	0.9564	0.8512	0.5884	0.6403	0.8214	0.6797	0.9566	0.7884
CR3SP31	0.8678	0.6905	0.9694	0.8628	0.7994	0.6789	0.8751	0.7818	0.9779	0.8599
CR3SP32	0.8744	0.8164	0.7918	0.8379	0.2869	0.4034	0.4987	0.4715	0.5498	0.5173
CR3SP33	0.8745	0.6461	0.9791	0.8819	0.9473	0.6947	0.9096	0.8497	0.9917	0.9241
SQ2C3BZ	0.8737	0.8122	0.8516	0.8616	0.2937	0.5105	0.6127	0.5207	0.4856	0.5592
SQ2C3BF	0.8644	0.7900	0.8853	0.8571	0.2882	0.4949	0.6433	0.5175	0.5168	0.5654
SQ2C3M	0.8502	0.6939	0.9542	0.8640	0.6322	0.6729	0.8375	0.7091	0.9618	0.8139
SU1C2B	0.8915	0.8836	0.6063	0.9270	0.2017	0.5148	0.5461	0.5083	0.3624	0.3932
SU1C2E	0.8678	0.7368	0.9337	0.9270	0.4967	0.7089	0.8658	0.7681	0.9139	0.7321
TMI1C5B	0.8842	0.8235	0.9141	0.9083	0.3271	0.6297	0.7223	0.4631	0.5606	0.6037
NA1C5B	0.8783	0.8441	0.7038	0.8533	0.1738	0.3681	0.4471	0.3285	0.2726	0.3967

Table C.3 Nuclide-reaction specific *g* index for GBC30 (continued)

CRC state-points	^{241}Am	^{243}Am	^{1}H	^{16}O	^{10}B	^{95}Mo	^{99}Tc	^{101}Ru	^{103}Rh	^{109}Ag[a]
CR3SP1	0.0000	0.0000	0.5623	0.4883	0.6101	0.0000	0.0000	0.0000	0.0000	0.0772
CR3SP2	0.0646	0.0876	0.6578	0.6143	0.4631	0.5519	0.6287	0.5765	0.5911	0.5360
CR3SP3	0.0798	0.3406	0.7268	0.6491	0.3023	0.6794	0.8828	0.8727	0.7566	0.9090
CR3SP4	0.0739	0.2095	0.6485	0.6203	0.4949	0.6085	0.7065	0.6865	0.6370	0.6637
CR3SP5	0.0799	0.2287	0.6344	0.5911	0.5203	0.5811	0.6508	0.6385	0.5877	0.6182
CR3SP6	0.0890	0.5668	0.7085	0.6455	0.3743	0.6751	0.8796	0.9033	0.7347	0.9005
CR3SP7	0.1063	0.8029	0.7238	0.6525	0.3228	0.7825	0.9062	0.9464	0.8258	0.9208
CR3SP8	0.0435	0.1900	0.6295	0.5741	0.5478	0.4352	0.5314	0.5235	0.4723	0.5548
CR3SP9	0.0771	0.7570	0.7124	0.6271	0.3702	0.7027	0.8931	0.9388	0.7875	0.9180
CR3SP10	0.0925	0.8175	0.7175	0.6377	0.3076	0.7688	0.8993	0.9426	0.8264	0.9201
CR3SP11	0.0520	0.1231	0.6306	0.5723	0.6216	0.4003	0.4556	0.4450	0.4145	0.4792
CR3SP12	0.1164	0.9598	0.7089	0.6275	0.3421	0.8505	0.9297	0.9646	0.8634	0.9402
CR3SP13	0.1078	0.3723	0.6294	0.5859	0.6208	0.5917	0.6412	0.6770	0.5837	0.6702
CR3SP14	0.1645	0.6315	0.6683	0.6236	0.5319	0.7722	0.8385	0.8890	0.7547	0.8315
CR3SP15	0.1886	0.9878	0.7212	0.6308	0.2675	0.8868	0.9463	0.9729	0.8891	0.9588
CR3SP16	0.1354	0.3068	0.6234	0.5854	0.6627	0.4886	0.5395	0.5788	0.4764	0.5363
CR3SP17	0.1459	0.9259	0.6926	0.6397	0.4926	0.7973	0.8873	0.9436	0.7986	0.8965
CR3SP18	0.1598	0.9361	0.6999	0.6351	0.4756	0.8199	0.8941	0.9478	0.8178	0.8984
CR3SP19	0.2156	0.9434	0.7075	0.6437	0.4507	0.8483	0.9020	0.9515	0.8367	0.9117
CR3SP20	0.2206	0.9844	0.7209	0.6458	0.3213	0.8845	0.9391	0.9696	0.8731	0.9299
CR3SP21	0.2241	0.9851	0.7356	0.6527	0.3073	0.8873	0.9404	0.9703	0.8774	0.9496
CR3SP22	0.1435	0.3159	0.6201	0.5768	0.7061	0.5331	0.5914	0.6390	0.5107	0.5624
CR3SP23	0.1318	0.5301	0.6419	0.6067	0.6365	0.6271	0.8027	0.8724	0.6249	0.7579
CR3SP24	0.1291	0.6102	0.6595	0.6213	0.6062	0.6721	0.8485	0.9151	0.6731	0.8060
CR3SP25	0.1822	0.9590	0.7137	0.6351	0.4131	0.8573	0.9193	0.9596	0.8536	0.9242
CR3SP26	0.1843	0.9596	0.7188	0.6309	0.4141	0.8582	0.9189	0.9597	0.8535	0.9256
CR3SP27	0.2153	0.9875	0.7225	0.6336	0.3567	0.8924	0.9430	0.9716	0.8829	0.9470
CR3SP28	0.1009	0.3269	0.6194	0.5803	0.7138	0.5585	0.6134	0.6720	0.5251	0.5650
CR3SP29	0.1136	0.7159	0.6579	0.6310	0.5884	0.7029	0.8608	0.9265	0.7037	0.8463
CR3SP30	0.1442	0.9056	0.6713	0.6214	0.5617	0.8012	0.8803	0.9413	0.7960	0.8781
CR3SP31	0.1685	0.9611	0.7020	0.6323	0.4376	0.8485	0.9183	0.9597	0.8395	0.9218
CR3SP32	0.0582	0.4048	0.6162	0.5897	0.7128	0.5138	0.6017	0.6729	0.5032	0.5938
CR3SP33	0.1953	0.9941	0.7291	0.6693	0.2997	0.9011	0.9485	0.9742	0.8909	0.9499
SQ2C3BZ	0.0927	0.3570	0.6427	0.6114	0.6464	0.6084	0.6513	0.6994	0.5880	0.6164
SQ2C3BF	0.0945	0.3719	0.6463	0.6216	0.5705	0.6186	0.6662	0.7184	0.5899	0.6283
SQ2C3M	0.5981	0.9226	0.6959	0.6397	0.3407	0.8354	0.8843	0.9405	0.8165	0.9016
SU1C2B	0.0662	0.1827	0.6643	0.6109	0.5208	0.4560	0.5007	0.4991	0.4778	0.5199
SU1C2E	0.0789	0.7054	0.7204	0.6474	0.2094	0.6658	0.8838	0.9037	0.7282	0.9196
TMI1C5B	0.6860	0.3888	0.6811	0.6297	0.4819	0.7452	0.7572	0.7873	0.6914	0.7248
NA1C5B	0.0804	0.1605	0.6102	0.5744	0.7304	0.4558	0.4787	0.5095	0.4248	0.4072

[a] ^{109}Ag exists in spent fuel and/or control rods.

Table C.3 Nuclide-reaction specific *g* index for GBC30 (continued)

CRC state-points	^{133}Cs	^{143}Nd	^{145}Nd	^{147}Sm	^{149}Sm	^{150}Sm	^{151}Sm	^{152}Sm	^{153}Eu	^{155}Gd
CR3SP1	0.0000	0.0000	0.0000	0.0000	0.0000	0.0000	0.0000	0.0000	0.0000	0.0000
CR3SP2	0.6133	0.4916	0.5695	0.2033	0.7256	0.4107	0.4248	0.6161	0.3745	0.0451
CR3SP3	0.8665	0.6652	0.8200	0.2817	0.7721	0.6350	0.5104	0.8989	0.6769	0.0105
CR3SP4	0.6888	0.5254	0.6475	0.2760	0.6234	0.4643	0.4090	0.7051	0.4773	0.0263
CR3SP5	0.6348	0.4813	0.6001	0.2772	0.6307	0.4244	0.3774	0.6351	0.4493	0.0378
CR3SP6	0.8622	0.6378	0.8136	0.3194	0.7506	0.6225	0.4924	0.8796	0.7174	0.0121
CR3SP7	0.8883	0.6928	0.8462	0.3632	0.7621	0.7019	0.5363	0.9076	0.8112	0.0134
CR3SP8	0.5208	0.4013	0.4908	0.1637	0.4578	0.3625	0.2803	0.5358	0.3828	0.0173
CR3SP9	0.8750	0.6611	0.8284	0.2673	0.7786	0.6754	0.5203	0.8965	0.7875	0.0127
CR3SP10	0.8816	0.6800	0.8366	0.2983	0.7698	0.6930	0.5337	0.9022	0.8021	0.0184
CR3SP11	0.4451	0.3378	0.4179	0.1701	0.3648	0.2979	0.2352	0.4569	0.3125	0.0206
CR3SP12	0.9145	0.7489	0.8814	0.3796	0.7689	0.7940	0.5778	0.9321	0.8711	0.0124
CR3SP13	0.6265	0.4530	0.5970	0.2772	0.4391	0.4465	0.2936	0.6528	0.5206	0.0472
CR3SP14	0.8193	0.5717	0.7726	0.4164	0.7110	0.5726	0.4381	0.8252	0.6924	0.0563
CR3SP15	0.9351	0.7994	0.9087	0.5724	0.7976	0.8415	0.6148	0.9462	0.9123	0.0210
CR3SP16	0.5274	0.3697	0.5024	0.2836	0.3293	0.3567	0.2374	0.5427	0.4261	0.0534
CR3SP17	0.8642	0.6345	0.8140	0.4311	0.7178	0.6583	0.4925	0.8808	0.7851	0.0163
CR3SP18	0.8725	0.6590	0.8246	0.4687	0.7222	0.6852	0.5124	0.8878	0.7999	0.0273
CR3SP19	0.8821	0.6829	0.8375	0.5809	0.7212	0.7065	0.5235	0.8962	0.8146	0.0617
CR3SP20	0.9256	0.7754	0.8980	0.6577	0.6960	0.8128	0.5983	0.9359	0.8953	0.0162
CR3SP21	0.9276	0.7823	0.9000	0.6702	0.7499	0.8167	0.6015	0.9374	0.8985	0.0201
CR3SP22	0.5736	0.3950	0.5507	0.3031	0.3698	0.3808	0.2637	0.5826	0.4588	0.0597
CR3SP23	0.7771	0.5044	0.7397	0.3383	0.6663	0.5082	0.4045	0.7665	0.6333	0.0100
CR3SP24	0.8178	0.5353	0.7600	0.3556	0.6549	0.5507	0.4319	0.8213	0.6883	0.0088
CR3SP25	0.9027	0.7349	0.8656	0.5475	0.7634	0.7610	0.5656	0.9136	0.8519	0.0359
CR3SP26	0.9019	0.7330	0.8653	0.5482	0.6717	0.7618	0.5715	0.9132	0.8517	0.0323
CR3SP27	0.9307	0.7939	0.9041	0.6354	0.7687	0.8335	0.6179	0.9392	0.9071	0.0215
CR3SP28	0.5971	0.4053	0.5727	0.2940	0.3717	0.3915	0.2729	0.6037	0.4746	0.0325
CR3SP29	0.8326	0.5596	0.7757	0.3813	0.6162	0.5867	0.4509	0.8528	0.7308	0.0080
CR3SP30	0.8561	0.6249	0.8034	0.4571	0.7203	0.6465	0.4882	0.8711	0.7709	0.0275
CR3SP31	0.9006	0.7216	0.8653	0.5547	0.6721	0.7589	0.5685	0.9119	0.8517	0.0135
CR3SP32	0.5862	0.3917	0.5654	0.1994	0.3653	0.3975	0.2505	0.5979	0.4967	0.0130
CR3SP33	0.9371	0.8132	0.9130	0.5976	0.7995	0.8550	0.6358	0.9432	0.9208	0.0294
SQ2C3BZ	0.6400	0.4460	0.6165	0.2788	0.5364	0.4729	0.3305	0.6530	0.4978	0.0834
SQ2C3BF	0.6500	0.4355	0.6320	0.2851	0.3754	0.4652	0.3155	0.6735	0.5029	0.0639
SQ2C3M	0.8609	0.6368	0.8129	0.8628	0.5911	0.7079	0.4929	0.8802	0.7792	0.6276
SU1C2B	0.4954	0.4065	0.4842	0.1908	0.3855	0.3910	0.2670	0.5265	0.3809	0.0492
SU1C2E	0.8602	0.6408	0.8274	0.2666	0.5517	0.6991	0.4952	0.8972	0.7427	0.0133
TMI1C5B	0.7447	0.5446	0.7216	0.8770	0.6201	0.5533	0.3887	0.7608	0.5673	0.8335
NA1C5B	0.4720	0.3281	0.4538	0.2313	0.3577	0.3192	0.2398	0.4723	0.3357	0.0794

Table C.4 Nuclide-reaction specific *g* index for GBC40

CRC state-points	^{234}U	^{235}U	^{236}U	^{238}U	^{238}Pu	^{239}Pu	^{240}Pu	^{241}Pu	^{242}Pu	^{237}Np
CR3SP1	0.9136	0.9920	0.0698	0.9533	0.0000	0.0000	0.0000	0.0000	0.0000	0.0000
CR3SP2	0.8653	0.8812	0.7295	0.9428	0.0832	0.6990	0.6449	0.3946	0.1945	0.2775
CR3SP3	0.8670	0.8018	0.8668	0.9564	0.2195	0.7645	0.8592	0.6575	0.5284	0.4750
CR3SP4	0.8760	0.8807	0.7773	0.9273	0.1421	0.6605	0.6820	0.4786	0.3245	0.3503
CR3SP5	0.8791	0.8991	0.7186	0.9221	0.1444	0.6228	0.6077	0.4315	0.3150	0.3257
CR3SP6	0.8773	0.8276	0.8862	0.9411	0.2898	0.7128	0.8106	0.6344	0.5988	0.5166
CR3SP7	0.8732	0.7929	0.9195	0.9458	0.3909	0.7460	0.8712	0.7217	0.7815	0.6172
CR3SP8	0.8867	0.9197	0.5837	0.9309	0.1157	0.5220	0.5229	0.3928	0.2848	0.2715
CR3SP9	0.8681	0.7978	0.9039	0.9395	0.3345	0.7495	0.8548	0.7083	0.7314	0.5718
CR3SP10	0.8694	0.7832	0.9115	0.9428	0.3629	0.7440	0.8649	0.7134	0.7670	0.5979
CR3SP11	0.8870	0.9037	0.5296	0.9104	0.0870	0.4683	0.4597	0.3273	0.2143	0.2230
CR3SP12	0.8632	0.7304	0.9438	0.9264	0.5362	0.7807	0.9056	0.8343	0.9728	0.7865
CR3SP13	0.8822	0.8691	0.6875	0.8955	0.1934	0.5252	0.5785	0.4987	0.4531	0.3854
CR3SP14	0.8763	0.8245	0.8867	0.8993	0.2982	0.6409	0.7221	0.5948	0.6305	0.5147
CR3SP15	0.8719	0.7022	0.9617	0.9235	0.7296	0.7723	0.9183	0.8603	0.9855	0.8567
CR3SP16	0.8826	0.8665	0.6155	0.8783	0.1608	0.4372	0.4704	0.3853	0.3613	0.3250
CR3SP17	0.8734	0.7757	0.9325	0.8920	0.4490	0.6820	0.8224	0.6883	0.8195	0.6771
CR3SP18	0.8691	0.7583	0.9383	0.8912	0.4967	0.6961	0.8376	0.7198	0.8996	0.7398
CR3SP19	0.8735	0.7587	0.9422	0.8968	0.5407	0.7039	0.8470	0.7305	0.9364	0.7596
CR3SP20	0.8777	0.7086	0.9627	0.9070	0.7341	0.7388	0.8999	0.8261	0.9817	0.8464
CR3SP21	0.8776	0.7031	0.9647	0.9109	0.7419	0.7372	0.9018	0.8281	0.9822	0.8512
CR3SP22	0.8776	0.8587	0.6834	0.8634	0.1698	0.4425	0.4912	0.3889	0.3733	0.3664
CR3SP23	0.8677	0.8210	0.9020	0.8637	0.2550	0.5870	0.6454	0.5193	0.5317	0.5045
CR3SP24	0.8694	0.8075	0.9165	0.8718	0.2900	0.6078	0.6962	0.5515	0.5855	0.5468
CR3SP25	0.8692	0.7242	0.9603	0.8891	0.6350	0.7134	0.8711	0.7744	0.9713	0.8238
CR3SP26	0.8692	0.7187	0.9608	0.8904	0.6382	0.7056	0.8714	0.7704	0.9714	0.8240
CR3SP27	0.8691	0.6939	0.9699	0.8979	0.7820	0.7408	0.9050	0.8400	0.9835	0.8697
CR3SP28	0.8770	0.8562	0.7170	0.8622	0.1799	0.4338	0.4983	0.3908	0.3743	0.3873
CR3SP29	0.8721	0.8002	0.9258	0.8713	0.3399	0.6132	0.7324	0.5771	0.6398	0.6024
CR3SP30	0.8668	0.7813	0.9380	0.8719	0.4450	0.6638	0.8096	0.6626	0.7967	0.7299
CR3SP31	0.8680	0.7255	0.9606	0.8826	0.6484	0.7061	0.8686	0.7709	0.9710	0.8240
CR3SP32	0.8751	0.8468	0.6896	0.8578	0.1959	0.4229	0.4779	0.4358	0.4335	0.4044
CR3SP33	0.8746	0.6799	0.9727	0.9019	0.8193	0.7239	0.9039	0.8395	0.9862	0.8875
SQ2C3BZ	0.8742	0.8439	0.7476	0.8815	0.2005	0.5331	0.5845	0.4851	0.3829	0.4377
SQ2C3BF	0.8649	0.8239	0.7932	0.8780	0.1968	0.5173	0.6131	0.4844	0.4075	0.4436
SQ2C3M	0.8516	0.7291	0.9347	0.8850	0.4904	0.6990	0.8291	0.6954	0.9102	0.7742
SU1C2B	0.8895	0.9107	0.5251	0.9456	0.1377	0.5366	0.5233	0.4724	0.2858	0.3085
SU1C2E	0.8651	0.7709	0.8784	0.9445	0.3547	0.7299	0.8515	0.7363	0.7356	0.5931
TMI1C5B	0.8840	0.8560	0.8249	0.9261	0.2233	0.6499	0.6856	0.4280	0.4420	0.4754
NA1C5B	0.8786	0.8749	0.6095	0.8736	0.1186	0.3858	0.4285	0.3037	0.2150	0.3100
g interval	Number of CRCs									
0.9-1.0	1	4	20	19	0	0	5	0	11	0
0.8-0.9	39	18	5	21	1	0	15	6	2	8
0.7-0.8	0	17	6	0	4	16	2	9	5	5
0.6-0.7	0	1	3	0	3	11	7	5	2	3

Table C.4 Nuclide-reaction specific *g* index for GBC40 (continued)

CRC state-points	^{241}Am	^{243}Am	^{1}H	^{16}O	^{10}B	^{95}Mo	^{99}Tc	^{101}Ru	^{103}Rh	^{109}Ag[a]
CR3SP1	0.0000	0.0000	0.5309	0.4593	0.6061	0.0000	0.0000	0.0000	0.0000	0.0725
CR3SP2	0.0560	0.0590	0.6241	0.5959	0.4634	0.4747	0.5237	0.4779	0.5321	0.4605
CR3SP3	0.0691	0.2293	0.6899	0.6307	0.3027	0.5891	0.7572	0.7297	0.6860	0.8256
CR3SP4	0.0640	0.1410	0.6096	0.5979	0.4944	0.5249	0.5902	0.5699	0.5747	0.5764
CR3SP5	0.0691	0.1540	0.5992	0.5613	0.5194	0.5003	0.5426	0.5295	0.5286	0.5395
CR3SP6	0.0770	0.3817	0.6748	0.6216	0.3749	0.5850	0.7605	0.7639	0.6657	0.8129
CR3SP7	0.0920	0.5462	0.6925	0.6255	0.3230	0.6837	0.8541	0.8743	0.7617	0.9121
CR3SP8	0.0377	0.1279	0.6003	0.5433	0.5456	0.3735	0.4408	0.4336	0.4228	0.4841
CR3SP9	0.0667	0.5133	0.6767	0.6054	0.3710	0.6091	0.8166	0.8348	0.7144	0.8942
CR3SP10	0.0801	0.5575	0.6920	0.6227	0.3082	0.6707	0.8362	0.8571	0.7647	0.9116
CR3SP11	0.0451	0.0829	0.5948	0.5380	0.6180	0.3435	0.3778	0.3686	0.3711	0.4195
CR3SP12	0.1007	0.8874	0.6765	0.6104	0.3426	0.8131	0.9120	0.9549	0.8521	0.9307
CR3SP13	0.0933	0.2507	0.5976	0.5564	0.6171	0.5092	0.5337	0.5612	0.5245	0.5771
CR3SP14	0.1424	0.4254	0.6346	0.6010	0.5310	0.6762	0.7103	0.7487	0.6825	0.7404
CR3SP15	0.1633	0.9662	0.7002	0.6125	0.2662	0.8681	0.9307	0.9675	0.8775	0.9511
CR3SP16	0.1173	0.2066	0.5905	0.5615	0.6586	0.4194	0.4475	0.4794	0.4265	0.4560
CR3SP17	0.1264	0.7032	0.6586	0.6137	0.4925	0.7080	0.8610	0.9206	0.7533	0.8794
CR3SP18	0.1383	0.7929	0.6657	0.6129	0.4763	0.7922	0.8755	0.9360	0.8084	0.8904
CR3SP19	0.1867	0.8318	0.6738	0.6105	0.4515	0.8311	0.8839	0.9409	0.8267	0.9033
CR3SP20	0.1910	0.9611	0.6905	0.6172	0.3215	0.8661	0.9231	0.9643	0.8624	0.9176
CR3SP21	0.1940	0.9623	0.7065	0.6331	0.3079	0.8688	0.9248	0.9649	0.8668	0.9418
CR3SP22	0.1242	0.2127	0.5862	0.5438	0.7035	0.4576	0.4906	0.5292	0.4572	0.4781
CR3SP23	0.1141	0.3569	0.6084	0.5821	0.6331	0.5394	0.6775	0.7328	0.5616	0.6743
CR3SP24	0.1117	0.4108	0.6251	0.5957	0.6022	0.5798	0.7329	0.7970	0.6065	0.7177
CR3SP25	0.1577	0.9327	0.6856	0.6190	0.4135	0.8397	0.9041	0.9549	0.8434	0.9155
CR3SP26	0.1595	0.9336	0.6919	0.6132	0.4146	0.8407	0.9037	0.9549	0.8433	0.9173
CR3SP27	0.1864	0.9660	0.6989	0.6143	0.3574	0.8739	0.9277	0.9663	0.8717	0.9390
CR3SP28	0.0874	0.2201	0.5892	0.5448	0.7114	0.4795	0.5090	0.5566	0.4701	0.4802
CR3SP29	0.0983	0.4827	0.6244	0.6103	0.5848	0.6099	0.7817	0.8562	0.6352	0.7567
CR3SP30	0.1248	0.6568	0.6365	0.6070	0.5588	0.7586	0.8617	0.9286	0.7826	0.8603
CR3SP31	0.1458	0.9354	0.6665	0.6078	0.4385	0.8316	0.9032	0.9549	0.8296	0.9126
CR3SP32	0.0504	0.2725	0.5843	0.5587	0.7104	0.4410	0.4992	0.5574	0.4505	0.5059
CR3SP33	0.1691	0.9757	0.7109	0.6516	0.2997	0.8826	0.9333	0.9690	0.8798	0.9420
SQ2C3BZ	0.0803	0.2404	0.6133	0.5863	0.6431	0.5232	0.5419	0.5798	0.5273	0.5248
SQ2C3BF	0.0818	0.2504	0.6175	0.5985	0.5681	0.5346	0.5552	0.5970	0.5302	0.5359
SQ2C3M	0.5280	0.7373	0.6685	0.6116	0.3412	0.8195	0.8655	0.9267	0.8079	0.8944
SU1C2B	0.0573	0.1230	0.6243	0.5797	0.5201	0.3913	0.4154	0.4134	0.4277	0.4425
SU1C2E	0.0683	0.4815	0.6802	0.6070	0.2094	0.5774	0.7622	0.7871	0.6608	0.8355
TMI1C5B	0.6132	0.2617	0.6452	0.6091	0.4819	0.6474	0.6333	0.6541	0.6248	0.6284
NA1C5B	0.0696	0.1081	0.5780	0.5463	0.7279	0.3912	0.3970	0.4220	0.3802	0.3461
g interval	Number of CRCs									
0.9-1.0	0	8	0	0	0	0	9	14	0	12
0.8-0.9	0	2	0	0	0	11	8	4	12	7
0.7-0.8	0	3	3	0	4	3	6	6	5	3
0.6-0.7	1	1	27	23	6	6	2	1	7	2

[a] ^{109}Ag exists in spent fuel and/or control rods.

Table C.4 Nuclide-reaction specific *g* index for GBC40 (continued)

CRC state-points	^{133}Cs	^{143}Nd	^{145}Nd	^{147}Sm	^{149}Sm	^{150}Sm	^{151}Sm	^{152}Sm	^{153}Eu	^{155}Gd
CR3SP1	0.0000	0.0000	0.0000	0.0000	0.0000	0.0000	0.0000	0.0000	0.0000	0.0000
CR3SP2	0.5312	0.4455	0.4912	0.1779	0.7331	0.3537	0.3958	0.5522	0.3059	0.0378
CR3SP3	0.7662	0.6147	0.7210	0.2466	0.7801	0.5646	0.4772	0.8365	0.5607	0.0088
CR3SP4	0.5980	0.4776	0.5603	0.2415	0.6304	0.4033	0.3807	0.6329	0.3899	0.0220
CR3SP5	0.5502	0.4358	0.5180	0.2426	0.6377	0.3659	0.3511	0.5692	0.3670	0.0317
CR3SP6	0.7693	0.5910	0.7290	0.2795	0.7585	0.5532	0.4610	0.8152	0.5947	0.0101
CR3SP7	0.8640	0.6527	0.8139	0.3179	0.7701	0.6355	0.5050	0.8973	0.7131	0.0113
CR3SP8	0.4487	0.3563	0.4200	0.1433	0.4626	0.3122	0.2589	0.4783	0.3126	0.0145
CR3SP9	0.8245	0.6186	0.7761	0.2340	0.7877	0.6063	0.4896	0.8703	0.6675	0.0106
CR3SP10	0.8461	0.6398	0.7955	0.2611	0.7780	0.6259	0.5033	0.8867	0.6945	0.0154
CR3SP11	0.3834	0.2996	0.3576	0.1489	0.3686	0.2566	0.2172	0.4078	0.2553	0.0173
CR3SP12	0.8999	0.7102	0.8618	0.3322	0.7774	0.7457	0.5478	0.9223	0.8413	0.0104
CR3SP13	0.5422	0.4077	0.5139	0.2426	0.4437	0.3862	0.2713	0.5849	0.4255	0.0395
CR3SP14	0.7204	0.5274	0.6808	0.3644	0.7186	0.5050	0.4120	0.7435	0.5721	0.0471
CR3SP15	0.9210	0.7609	0.8891	0.5014	0.8069	0.8036	0.5840	0.9369	0.8824	0.0176
CR3SP16	0.4544	0.3280	0.4300	0.2482	0.3327	0.3072	0.2193	0.4844	0.3480	0.0447
CR3SP17	0.8510	0.5983	0.7973	0.3773	0.7255	0.6055	0.4669	0.8716	0.7329	0.0136
CR3SP18	0.8591	0.6222	0.8075	0.4102	0.7299	0.6355	0.4857	0.8789	0.7721	0.0229
CR3SP19	0.8684	0.6453	0.8196	0.5084	0.7289	0.6559	0.4964	0.8871	0.7877	0.0517
CR3SP20	0.9113	0.7368	0.8784	0.5774	0.7030	0.7749	0.5684	0.9262	0.8661	0.0136
CR3SP21	0.9134	0.7438	0.8805	0.5887	0.7579	0.7788	0.5715	0.9276	0.8692	0.0168
CR3SP22	0.4943	0.3511	0.4715	0.2652	0.3737	0.3280	0.2436	0.5200	0.3748	0.0500
CR3SP23	0.6798	0.4624	0.6489	0.2961	0.6730	0.4453	0.3827	0.6876	0.5201	0.0084
CR3SP24	0.7336	0.4957	0.7036	0.3112	0.6615	0.4864	0.4097	0.7490	0.5696	0.0073
CR3SP25	0.8891	0.6975	0.8472	0.4792	0.7719	0.7246	0.5368	0.9045	0.8241	0.0301
CR3SP26	0.8884	0.6956	0.8470	0.4798	0.6785	0.7256	0.5427	0.9041	0.8239	0.0271
CR3SP27	0.9168	0.7560	0.8849	0.5570	0.7777	0.7958	0.5870	0.9297	0.8777	0.0180
CR3SP28	0.5148	0.3611	0.4905	0.2573	0.3756	0.3372	0.2521	0.5388	0.3877	0.0272
CR3SP29	0.7811	0.5256	0.7511	0.3337	0.6234	0.5247	0.4274	0.8017	0.6225	0.0067
CR3SP30	0.8435	0.5894	0.7876	0.4001	0.7280	0.5986	0.4630	0.8626	0.7359	0.0231
CR3SP31	0.8872	0.6844	0.8470	0.4855	0.6789	0.7226	0.5398	0.9028	0.8240	0.0113
CR3SP32	0.5052	0.3482	0.4842	0.1745	0.3691	0.3426	0.2313	0.5336	0.4057	0.0109
CR3SP33	0.9237	0.7757	0.8944	0.5231	0.8088	0.8185	0.6043	0.9343	0.8922	0.0247
SQ2C3BZ	0.5535	0.4023	0.5308	0.2440	0.5424	0.4120	0.3070	0.5843	0.4066	0.0699
SQ2C3BF	0.5632	0.3941	0.5452	0.2495	0.3794	0.4075	0.2935	0.6034	0.4109	0.0535
SQ2C3M	0.8485	0.6017	0.7971	0.8496	0.5979	0.6612	0.4676	0.8719	0.7469	0.5456
SU1C2B	0.4269	0.3612	0.4146	0.1669	0.3895	0.3368	0.2466	0.4706	0.3111	0.0412
SU1C2E	0.7701	0.5928	0.7619	0.2333	0.5579	0.6363	0.4646	0.8541	0.6251	0.0111
TMI1C5B	0.6469	0.4960	0.6249	0.8263	0.6271	0.4878	0.3615	0.6828	0.4654	0.7493
NA1C5B	0.4066	0.2909	0.3883	0.2024	0.3614	0.2749	0.2215	0.4216	0.2742	0.0665
g interval	Number of CRCs									
0.9-1.0	5	0	0	0	0	0	0	8	0	0
0.8-0.9	12	0	12	2	2	2	0	12	9	0
0.7-0.8	6	16	10	16	16	7	0	2	6	1
0.6-0.7	2	8	3	8	8	8	1	4	4	0

Table C.5 Nuclide-reaction specific *g* index for GBC50

CRC state-points	^{234}U	^{235}U	^{236}U	^{238}U	^{238}Pu	^{239}Pu	^{240}Pu	^{241}Pu	^{242}Pu	^{237}Np
CR3SP1	0.9145	0.9942	0.0633	0.9650	0.0000	0.0000	0.0000	0.0000	0.0000	0.0000
CR3SP2	0.8659	0.8918	0.6626	0.9565	0.0627	0.7069	0.6197	0.3695	0.1663	0.2302
CR3SP3	0.8655	0.8073	0.8080	0.9688	0.1654	0.7727	0.8419	0.6318	0.4518	0.3940
CR3SP4	0.8764	0.8914	0.7065	0.9442	0.1071	0.6684	0.6571	0.4482	0.2774	0.2905
CR3SP5	0.8797	0.9092	0.6528	0.9374	0.1088	0.6306	0.5828	0.4041	0.2693	0.2701
CR3SP6	0.8774	0.8383	0.8260	0.9540	0.2184	0.7210	0.7869	0.6064	0.5120	0.4292
CR3SP7	0.8734	0.8021	0.8614	0.9587	0.2951	0.7542	0.8657	0.6938	0.6694	0.5178
CR3SP8	0.8879	0.9299	0.5299	0.9461	0.0872	0.5286	0.5079	0.3679	0.2435	0.2252
CR3SP9	0.8686	0.8082	0.8428	0.9522	0.2521	0.7575	0.8392	0.6802	0.6263	0.4773
CR3SP10	0.8698	0.7927	0.8518	0.9556	0.2735	0.7526	0.8553	0.6853	0.6569	0.5009
CR3SP11	0.8902	0.9138	0.4808	0.9269	0.0655	0.4746	0.4465	0.3065	0.1833	0.1849
CR3SP12	0.8640	0.7390	0.9239	0.9411	0.4212	0.7921	0.9047	0.8199	0.9609	0.6724
CR3SP13	0.8859	0.8798	0.6243	0.9120	0.1458	0.5322	0.5619	0.4672	0.3874	0.3197
CR3SP14	0.8794	0.8358	0.8259	0.9159	0.2248	0.6483	0.6963	0.5678	0.5391	0.4269
CR3SP15	0.8726	0.7102	0.9433	0.9384	0.6070	0.7841	0.9186	0.8500	0.9806	0.8197
CR3SP16	0.8864	0.8768	0.5587	0.8957	0.1212	0.4431	0.4569	0.3608	0.3089	0.2696
CR3SP17	0.8769	0.7873	0.9089	0.9096	0.3444	0.6902	0.8022	0.6612	0.7018	0.5680
CR3SP18	0.8728	0.7699	0.9198	0.9081	0.3868	0.7067	0.8347	0.6937	0.7746	0.6254
CR3SP19	0.8769	0.7703	0.9240	0.9137	0.4271	0.7141	0.8457	0.7044	0.8089	0.6455
CR3SP20	0.8796	0.7198	0.9441	0.9235	0.6147	0.7510	0.8998	0.8146	0.9748	0.8111
CR3SP21	0.8797	0.7143	0.9460	0.9270	0.6244	0.7495	0.9018	0.8168	0.9762	0.8188
CR3SP22	0.8814	0.8694	0.6205	0.8815	0.1280	0.4484	0.4771	0.3642	0.3191	0.3039
CR3SP23	0.8714	0.8320	0.8423	0.8819	0.1922	0.5949	0.6199	0.4876	0.4546	0.4185
CR3SP24	0.8731	0.8187	0.8712	0.8897	0.2186	0.6160	0.6701	0.5227	0.5006	0.4536
CR3SP25	0.8729	0.7361	0.9420	0.9063	0.5223	0.7263	0.8708	0.7636	0.9617	0.7920
CR3SP26	0.8728	0.7306	0.9425	0.9074	0.5259	0.7187	0.8712	0.7600	0.9619	0.7925
CR3SP27	0.8721	0.7058	0.9558	0.9141	0.6687	0.7548	0.9053	0.8286	0.9800	0.8435
CR3SP28	0.8808	0.8669	0.6510	0.8806	0.1356	0.4396	0.4840	0.3660	0.3201	0.3213
CR3SP29	0.8757	0.8114	0.8978	0.8893	0.2562	0.6214	0.7066	0.5488	0.5470	0.5014
CR3SP30	0.8706	0.7927	0.9199	0.8894	0.3421	0.6737	0.7888	0.6352	0.6817	0.6166
CR3SP31	0.8717	0.7375	0.9423	0.8996	0.5362	0.7191	0.8683	0.7601	0.9614	0.7932
CR3SP32	0.8788	0.8574	0.6261	0.8768	0.1476	0.4286	0.4642	0.4081	0.3706	0.3354
CR3SP33	0.8780	0.6919	0.9653	0.9183	0.7089	0.7370	0.9042	0.8281	0.9829	0.8634
SQ2C3BZ	0.8777	0.8545	0.6790	0.8988	0.1511	0.5399	0.5614	0.4543	0.3274	0.3631
SQ2C3BF	0.8688	0.8345	0.7341	0.8950	0.1483	0.5236	0.5885	0.4542	0.3484	0.3680
SQ2C3M	0.8557	0.7410	0.9168	0.9016	0.3875	0.7116	0.8287	0.6746	0.7879	0.7033
SU1C2B	0.8900	0.9208	0.4767	0.9572	0.1038	0.5430	0.5083	0.4424	0.2443	0.2569
SU1C2E	0.8657	0.7797	0.8191	0.9569	0.2674	0.7382	0.8360	0.7079	0.6340	0.4985
TMI1C5B	0.8861	0.8666	0.7521	0.9418	0.1683	0.6574	0.6606	0.4008	0.3780	0.3944
NA1C5B	0.8824	0.8849	0.5533	0.8913	0.0894	0.3910	0.4162	0.2844	0.1838	0.2572

Table C.5 Nuclide-reaction specific *g* index for GBC50 (continued)

CRC state-points	^{241}Am	^{243}Am	^{1}H	^{16}O	^{10}B	^{95}Mo	^{99}Tc	^{101}Ru	^{103}Rh	^{109}Ag[a]
CR3SP1	0.0000	0.0000	0.5250	0.4376	0.6115	0.0000	0.0000	0.0000	0.0000	0.0699
CR3SP2	0.0509	0.0442	0.6056	0.5603	0.4649	0.4273	0.4742	0.4142	0.4939	0.4178
CR3SP3	0.0629	0.1719	0.6717	0.5892	0.3056	0.5333	0.6905	0.6348	0.6422	0.7692
CR3SP4	0.0582	0.1057	0.5964	0.5590	0.4966	0.4725	0.5353	0.4941	0.5349	0.5260
CR3SP5	0.0629	0.1155	0.5826	0.5266	0.5232	0.4504	0.4913	0.4589	0.4905	0.4946
CR3SP6	0.0701	0.2862	0.6510	0.5865	0.3770	0.5289	0.6936	0.6643	0.6219	0.7573
CR3SP7	0.0837	0.4096	0.6738	0.5865	0.3262	0.6204	0.7815	0.7666	0.7134	0.8665
CR3SP8	0.0343	0.0959	0.5834	0.5134	0.5504	0.3362	0.3991	0.3757	0.3924	0.4439
CR3SP9	0.0607	0.3849	0.6545	0.5623	0.3730	0.5513	0.7448	0.7268	0.6686	0.8357
CR3SP10	0.0729	0.4180	0.6720	0.5827	0.3113	0.6082	0.7635	0.7488	0.7163	0.8612
CR3SP11	0.0410	0.0622	0.5790	0.5102	0.6229	0.3091	0.3422	0.3194	0.3444	0.3866
CR3SP12	0.0916	0.6851	0.6619	0.5680	0.3452	0.7456	0.8982	0.9402	0.8394	0.9255
CR3SP13	0.0849	0.1879	0.5838	0.5238	0.6222	0.4584	0.4833	0.4865	0.4868	0.5232
CR3SP14	0.1296	0.3190	0.6197	0.5604	0.5351	0.6126	0.6464	0.6504	0.6378	0.6887
CR3SP15	0.1485	0.9463	0.6792	0.5747	0.2691	0.8552	0.9231	0.9628	0.8734	0.9465
CR3SP16	0.1066	0.1549	0.5729	0.5253	0.6615	0.3774	0.4052	0.4154	0.3958	0.4106
CR3SP17	0.1149	0.5287	0.6379	0.5805	0.4946	0.6418	0.7981	0.8333	0.7040	0.8226
CR3SP18	0.1258	0.5982	0.6482	0.5733	0.4783	0.7287	0.8482	0.8897	0.7808	0.8713
CR3SP19	0.1698	0.6328	0.6551	0.5775	0.4535	0.8168	0.8653	0.9089	0.8215	0.8989
CR3SP20	0.1737	0.9405	0.6750	0.5816	0.3247	0.8541	0.9156	0.9606	0.8583	0.9111
CR3SP21	0.1765	0.9426	0.6910	0.5959	0.3109	0.8567	0.9172	0.9612	0.8627	0.9367
CR3SP22	0.1130	0.1595	0.5639	0.5223	0.7040	0.4118	0.4443	0.4587	0.4243	0.4304
CR3SP23	0.1038	0.2676	0.5875	0.5469	0.6371	0.4856	0.6152	0.6359	0.5211	0.6288
CR3SP24	0.1016	0.3080	0.6072	0.5591	0.6075	0.5220	0.6666	0.6924	0.5639	0.6684
CR3SP25	0.1434	0.8146	0.6654	0.5762	0.4159	0.8286	0.8963	0.9498	0.8403	0.9113
CR3SP26	0.1451	0.8255	0.6744	0.5767	0.4169	0.8298	0.8962	0.9502	0.8402	0.9130
CR3SP27	0.1696	0.9503	0.6837	0.5736	0.3591	0.8621	0.9204	0.9626	0.8680	0.9341
CR3SP28	0.0795	0.1650	0.5688	0.5195	0.7120	0.4315	0.4609	0.4824	0.4363	0.4323
CR3SP29	0.0894	0.3619	0.6035	0.5760	0.5901	0.5497	0.7119	0.7486	0.5916	0.7042
CR3SP30	0.1135	0.4926	0.6169	0.5595	0.5639	0.6942	0.8126	0.8655	0.7394	0.8058
CR3SP31	0.1326	0.8424	0.6452	0.5694	0.4404	0.8202	0.8957	0.9509	0.8267	0.9082
CR3SP32	0.0458	0.2043	0.5684	0.5272	0.7109	0.3969	0.4520	0.4831	0.4181	0.4563
CR3SP33	0.1538	0.9611	0.6935	0.6043	0.3026	0.8709	0.9264	0.9655	0.8763	0.9369
SQ2C3BZ	0.0730	0.1802	0.5937	0.5448	0.6468	0.4710	0.4907	0.5025	0.4893	0.4724
SQ2C3BF	0.0744	0.1877	0.6022	0.5565	0.5731	0.4813	0.5029	0.5174	0.4920	0.4825
SQ2C3M	0.4812	0.5634	0.6543	0.5711	0.3444	0.8095	0.8495	0.8840	0.8020	0.8681
SU1C2B	0.0521	0.0922	0.6032	0.5563	0.5232	0.3522	0.3761	0.3583	0.3970	0.3984
SU1C2E	0.0622	0.3610	0.6699	0.5895	0.2102	0.5230	0.6956	0.6885	0.6186	0.7703
TMI1C5B	0.5646	0.1962	0.6255	0.5686	0.4835	0.5861	0.5753	0.5677	0.5826	0.5735
NA1C5B	0.0633	0.0810	0.5629	0.5156	0.7287	0.3521	0.3596	0.3657	0.3528	0.3116

[a] ^{109}Ag exists in spent fuel and/or control rods.

Table C.5 Nuclide-reaction specific *g* index for GBC50 (continued)

CRC state-points	^{133}Cs	^{143}Nd	^{145}Nd	^{147}Sm	^{149}Sm	^{150}Sm	^{151}Sm	^{152}Sm	^{153}Eu	^{155}Gd
CR3SP1	0.0000	0.0000	0.0000	0.0000	0.0000	0.0000	0.0000	0.0000	0.0000	0.0000
CR3SP2	0.4818	0.4131	0.4367	0.1618	0.7511	0.3206	0.3788	0.5040	0.2658	0.0333
CR3SP3	0.7008	0.5807	0.6487	0.2243	0.7967	0.5211	0.4577	0.7679	0.4907	0.0077
CR3SP4	0.5439	0.4459	0.5003	0.2197	0.6490	0.3655	0.3644	0.5790	0.3388	0.0194
CR3SP5	0.4992	0.4038	0.4608	0.2207	0.6552	0.3317	0.3355	0.5196	0.3189	0.0279
CR3SP6	0.7034	0.5587	0.6559	0.2543	0.7774	0.5096	0.4424	0.7478	0.5206	0.0089
CR3SP7	0.7926	0.6196	0.7404	0.2892	0.7881	0.5894	0.4852	0.8450	0.6268	0.0099
CR3SP8	0.4069	0.3283	0.3733	0.1303	0.4762	0.2829	0.2464	0.4363	0.2717	0.0128
CR3SP9	0.7546	0.5847	0.7018	0.2129	0.8038	0.5621	0.4700	0.8082	0.5855	0.0093
CR3SP10	0.7752	0.6063	0.7209	0.2375	0.7946	0.5804	0.4836	0.8300	0.6101	0.0136
CR3SP11	0.3477	0.2761	0.3179	0.1354	0.3794	0.2325	0.2068	0.3720	0.2218	0.0152
CR3SP12	0.8904	0.6862	0.8519	0.3023	0.7937	0.7127	0.5306	0.9191	0.8131	0.0091
CR3SP13	0.4916	0.3758	0.4568	0.2207	0.4567	0.3500	0.2583	0.5338	0.3698	0.0348
CR3SP14	0.6571	0.4953	0.6104	0.3316	0.7365	0.4635	0.3947	0.6809	0.4991	0.0415
CR3SP15	0.9122	0.7370	0.8790	0.4562	0.8236	0.7737	0.5667	0.9335	0.8651	0.0155
CR3SP16	0.4120	0.3023	0.3822	0.2258	0.3425	0.2785	0.2088	0.4419	0.3024	0.0394
CR3SP17	0.8079	0.5744	0.7563	0.3433	0.7436	0.5606	0.4525	0.8313	0.6450	0.0120
CR3SP18	0.8484	0.6009	0.7943	0.3732	0.7481	0.5967	0.4718	0.8662	0.7000	0.0201
CR3SP19	0.8589	0.6237	0.8116	0.4625	0.7471	0.6180	0.4821	0.8829	0.7271	0.0455
CR3SP20	0.9022	0.7140	0.8682	0.5255	0.7220	0.7443	0.5518	0.9231	0.8489	0.0119
CR3SP21	0.9045	0.7213	0.8703	0.5360	0.7770	0.7495	0.5548	0.9246	0.8522	0.0148
CR3SP22	0.4482	0.3235	0.4191	0.2413	0.3847	0.2972	0.2319	0.4743	0.3257	0.0440
CR3SP23	0.6187	0.4315	0.5799	0.2694	0.6914	0.4045	0.3678	0.6286	0.4519	0.0074
CR3SP24	0.6690	0.4653	0.6319	0.2832	0.6796	0.4450	0.3956	0.6855	0.4957	0.0065
CR3SP25	0.8802	0.6745	0.8381	0.4359	0.7881	0.6933	0.5216	0.9018	0.8087	0.0265
CR3SP26	0.8796	0.6729	0.8379	0.4365	0.6970	0.6950	0.5275	0.9015	0.8086	0.0238
CR3SP27	0.9083	0.7325	0.8749	0.5067	0.7935	0.7737	0.5703	0.9270	0.8611	0.0159
CR3SP28	0.4667	0.3328	0.4360	0.2341	0.3866	0.3056	0.2400	0.4915	0.3368	0.0240
CR3SP29	0.7137	0.4948	0.6789	0.3036	0.6412	0.4825	0.4148	0.7342	0.5433	0.0059
CR3SP30	0.8197	0.5696	0.7691	0.3640	0.7461	0.5560	0.4498	0.8281	0.6520	0.0203
CR3SP31	0.8784	0.6625	0.8379	0.4417	0.6975	0.6916	0.5247	0.9003	0.8088	0.0099
CR3SP32	0.4581	0.3209	0.4304	0.1587	0.3800	0.3105	0.2202	0.4868	0.3525	0.0096
CR3SP33	0.9152	0.7534	0.8847	0.4759	0.8256	0.7976	0.5879	0.9312	0.8750	0.0217
SQ2C3BZ	0.5019	0.3710	0.4718	0.2220	0.5584	0.3734	0.2929	0.5330	0.3533	0.0615
SQ2C3BF	0.5110	0.3646	0.4853	0.2270	0.3905	0.3702	0.2804	0.5507	0.3571	0.0471
SQ2C3M	0.8384	0.5817	0.7909	0.7933	0.6156	0.6333	0.4544	0.8705	0.6825	0.4908
SU1C2B	0.3871	0.3328	0.3685	0.1519	0.4010	0.3052	0.2348	0.4293	0.2704	0.0363
SU1C2E	0.7049	0.5605	0.6863	0.2123	0.5743	0.5918	0.4461	0.7921	0.5487	0.0098
TMI1C5B	0.5893	0.4648	0.5593	0.7633	0.6456	0.4468	0.3458	0.6252	0.4044	0.6849
NA1C5B	0.3687	0.2681	0.3452	0.1841	0.3720	0.2492	0.2108	0.3846	0.2383	0.0585

Table C.6 Nuclide-reaction specific *g* index for GBC60

CRC state-points	^{234}U	^{235}U	^{236}U	^{238}U	^{238}Pu	^{239}Pu	^{240}Pu	^{241}Pu	^{242}Pu	^{237}Np
CR3SP1	0.9122	0.9976	0.0574	0.9720	0.0000	0.0000	0.0000	0.0000	0.0000	0.0000
CR3SP2	0.8618	0.9150	0.6010	0.9668	0.0466	0.7095	0.5900	0.3409	0.1432	0.1903
CR3SP3	0.8566	0.8281	0.7434	0.9760	0.1229	0.7752	0.8112	0.5981	0.3890	0.3258
CR3SP4	0.8742	0.9139	0.6412	0.9534	0.0795	0.6704	0.6259	0.4135	0.2389	0.2402
CR3SP5	0.8773	0.9312	0.5922	0.9466	0.0808	0.6323	0.5545	0.3728	0.2319	0.2233
CR3SP6	0.8746	0.8636	0.7629	0.9647	0.1622	0.7237	0.7561	0.5734	0.4408	0.3548
CR3SP7	0.8697	0.8256	0.8044	0.9697	0.2192	0.7567	0.8385	0.6599	0.5768	0.4288
CR3SP8	0.8855	0.9490	0.4807	0.9550	0.0648	0.5306	0.4860	0.3394	0.2097	0.1862
CR3SP9	0.8656	0.8324	0.7839	0.9616	0.1873	0.7602	0.8082	0.6472	0.5393	0.3946
CR3SP10	0.8668	0.8177	0.7953	0.9655	0.2032	0.7551	0.8264	0.6518	0.5660	0.4142
CR3SP11	0.8892	0.9359	0.4361	0.9370	0.0487	0.4761	0.4294	0.2828	0.1578	0.1529
CR3SP12	0.8619	0.7621	0.8765	0.9499	0.3143	0.7962	0.8953	0.7878	0.8547	0.5637
CR3SP13	0.8855	0.9015	0.5664	0.9233	0.1083	0.5345	0.5407	0.4311	0.3335	0.2643
CR3SP14	0.8785	0.8599	0.7525	0.9272	0.1670	0.6504	0.6670	0.5322	0.4642	0.3529
CR3SP15	0.8705	0.7322	0.9222	0.9483	0.4761	0.7904	0.9102	0.8322	0.9671	0.7058
CR3SP16	0.8868	0.8977	0.5069	0.9074	0.0900	0.4445	0.4397	0.3329	0.2660	0.2229
CR3SP17	0.8767	0.8129	0.8557	0.9208	0.2559	0.6924	0.7705	0.6268	0.6045	0.4706
CR3SP18	0.8724	0.7967	0.8797	0.9194	0.2876	0.7093	0.8073	0.6601	0.6678	0.5205
CR3SP19	0.8762	0.7971	0.8869	0.9251	0.3193	0.7166	0.8227	0.6700	0.6977	0.5388
CR3SP20	0.8777	0.7448	0.9250	0.9337	0.4842	0.7565	0.8907	0.7950	0.9592	0.6991
CR3SP21	0.8777	0.7390	0.9270	0.9374	0.4937	0.7556	0.8928	0.7981	0.9619	0.7158
CR3SP22	0.8816	0.8915	0.5630	0.8925	0.0951	0.4499	0.4591	0.3360	0.2748	0.2513
CR3SP23	0.8720	0.8554	0.7712	0.8930	0.1427	0.5963	0.5916	0.4499	0.3914	0.3460
CR3SP24	0.8736	0.8443	0.8129	0.9010	0.1624	0.6175	0.6385	0.4833	0.4311	0.3750
CR3SP25	0.8723	0.7626	0.9230	0.9176	0.4027	0.7337	0.8610	0.7444	0.8928	0.6839
CR3SP26	0.8723	0.7569	0.9235	0.9186	0.4061	0.7258	0.8614	0.7414	0.8929	0.6862
CR3SP27	0.8706	0.7309	0.9366	0.9255	0.5401	0.7635	0.8971	0.8141	0.9685	0.7964
CR3SP28	0.8810	0.8896	0.5908	0.8918	0.1007	0.4410	0.4658	0.3377	0.2756	0.2656
CR3SP29	0.8761	0.8368	0.8398	0.9004	0.1903	0.6230	0.6746	0.5108	0.4710	0.4145
CR3SP30	0.8712	0.8175	0.8843	0.9007	0.2541	0.6762	0.7573	0.6009	0.5870	0.5119
CR3SP31	0.8712	0.7640	0.9236	0.9106	0.4161	0.7261	0.8585	0.7416	0.8914	0.6897
CR3SP32	0.8791	0.8814	0.5681	0.8893	0.1096	0.4299	0.4467	0.3765	0.3191	0.2773
CR3SP33	0.8774	0.7177	0.9460	0.9320	0.5812	0.7454	0.8961	0.8134	0.9744	0.8275
SQ2C3BZ	0.8780	0.8787	0.6161	0.9099	0.1122	0.5423	0.5353	0.4191	0.2819	0.3002
SQ2C3BF	0.8693	0.8580	0.6668	0.9087	0.1102	0.5263	0.5614	0.4191	0.3000	0.3043
SQ2C3M	0.8555	0.7671	0.8818	0.9146	0.2901	0.7183	0.8138	0.6411	0.6872	0.5951
SU1C2B	0.8879	0.9432	0.4324	0.9654	0.0771	0.5456	0.4886	0.4081	0.2104	0.2132
SU1C2E	0.8614	0.8043	0.7654	0.9670	0.1986	0.7406	0.8081	0.6748	0.5463	0.4136
TMI1C5B	0.8840	0.8912	0.6829	0.9519	0.1250	0.6595	0.6295	0.3698	0.3254	0.3260
NA1C5B	0.8826	0.9061	0.5019	0.9026	0.0664	0.3923	0.3993	0.2624	0.1582	0.2126

Table C.6 Nuclide-reaction specific *g* index for GBC60 (continued)

CRC state-points	^{241}Am	^{243}Am	^{1}H	^{16}O	^{10}B	^{95}Mo	^{99}Tc	^{101}Ru	^{103}Rh	^{109}Ag[a]
CR3SP1	0.0000	0.0000	0.5383	0.4339	0.6118	0.0000	0.0000	0.0000	0.0000	0.0663
CR3SP2	0.0456	0.0333	0.6230	0.5632	0.4672	0.3851	0.4219	0.3553	0.4537	0.3694
CR3SP3	0.0563	0.1293	0.6954	0.5962	0.3065	0.4811	0.6181	0.5459	0.5943	0.7033
CR3SP4	0.0521	0.0795	0.6111	0.5629	0.4986	0.4258	0.4763	0.4238	0.4913	0.4677
CR3SP5	0.0563	0.0868	0.6046	0.5293	0.5243	0.4059	0.4372	0.3936	0.4505	0.4409
CR3SP6	0.0627	0.2152	0.6766	0.5934	0.3787	0.4766	0.6204	0.5712	0.5752	0.6918
CR3SP7	0.0749	0.3080	0.6943	0.5931	0.3267	0.5626	0.7005	0.6597	0.6620	0.7917
CR3SP8	0.0307	0.0721	0.6030	0.5133	0.5514	0.3030	0.3551	0.3223	0.3604	0.3968
CR3SP9	0.0543	0.2895	0.6799	0.5757	0.3746	0.4973	0.6671	0.6251	0.6188	0.7577
CR3SP10	0.0652	0.3144	0.6944	0.5930	0.3118	0.5510	0.6844	0.6443	0.6645	0.7864
CR3SP11	0.0367	0.0467	0.6020	0.5100	0.6235	0.2786	0.3044	0.2739	0.3163	0.3465
CR3SP12	0.0820	0.5180	0.6790	0.5734	0.3459	0.6784	0.8434	0.8344	0.7852	0.9153
CR3SP13	0.0760	0.1414	0.6010	0.5261	0.6228	0.4131	0.4300	0.4173	0.4471	0.4621
CR3SP14	0.1160	0.2399	0.6326	0.5681	0.5360	0.5537	0.5770	0.5585	0.5891	0.6267
CR3SP15	0.1329	0.7911	0.7022	0.5850	0.2701	0.8071	0.9056	0.9478	0.8595	0.9374
CR3SP16	0.0955	0.1165	0.5911	0.5294	0.6630	0.3402	0.3605	0.3564	0.3636	0.3599
CR3SP17	0.1029	0.3976	0.6581	0.5867	0.4967	0.5805	0.7143	0.7169	0.6516	0.7461
CR3SP18	0.1126	0.4500	0.6669	0.5806	0.4804	0.6616	0.7627	0.7729	0.7238	0.7991
CR3SP19	0.1520	0.4764	0.6746	0.5858	0.4559	0.7516	0.7817	0.7943	0.7748	0.8260
CR3SP20	0.1555	0.7668	0.6935	0.5926	0.3253	0.8267	0.8986	0.9462	0.8430	0.8990
CR3SP21	0.1579	0.7844	0.7074	0.5990	0.3115	0.8319	0.9011	0.9475	0.8511	0.9273
CR3SP22	0.1011	0.1199	0.5868	0.5206	0.7053	0.3711	0.3953	0.3935	0.3898	0.3774
CR3SP23	0.0929	0.2012	0.6099	0.5499	0.6386	0.4376	0.5475	0.5454	0.4787	0.5724
CR3SP24	0.0910	0.2316	0.6213	0.5556	0.6079	0.4704	0.5944	0.5942	0.5179	0.6108
CR3SP25	0.1284	0.6192	0.6843	0.5885	0.4183	0.7988	0.8791	0.9253	0.8292	0.9020
CR3SP26	0.1299	0.6282	0.6922	0.5860	0.4194	0.8027	0.8790	0.9273	0.8298	0.9039
CR3SP27	0.1518	0.8755	0.7042	0.5862	0.3609	0.8433	0.9090	0.9545	0.8569	0.9250
CR3SP28	0.0711	0.1241	0.5838	0.5167	0.7131	0.3889	0.4101	0.4138	0.4007	0.3790
CR3SP29	0.0800	0.2722	0.6238	0.5774	0.5906	0.4953	0.6360	0.6430	0.5438	0.6425
CR3SP30	0.1016	0.3705	0.6379	0.5740	0.5646	0.6289	0.7273	0.7468	0.6843	0.7338
CR3SP31	0.1187	0.6442	0.6688	0.5765	0.4432	0.7730	0.8787	0.9300	0.8000	0.8989
CR3SP32	0.0410	0.1537	0.5830	0.5299	0.7120	0.3577	0.4022	0.4144	0.3841	0.4007
CR3SP33	0.1377	0.9361	0.7167	0.6148	0.3038	0.8522	0.9157	0.9601	0.8650	0.9279
SQ2C3BZ	0.0653	0.1355	0.6190	0.5540	0.6483	0.4244	0.4366	0.4311	0.4494	0.4142
SQ2C3BF	0.0666	0.1412	0.6189	0.5637	0.5739	0.4337	0.4475	0.4438	0.4519	0.4230
SQ2C3M	0.4307	0.4237	0.6681	0.5773	0.3448	0.7807	0.7717	0.7849	0.7670	0.7941
SU1C2B	0.0467	0.0694	0.6268	0.5533	0.5249	0.3175	0.3346	0.3073	0.3646	0.3493
SU1C2E	0.0556	0.2715	0.6879	0.5895	0.2100	0.4722	0.6237	0.5930	0.5729	0.6877
TMI1C5B	0.5067	0.1476	0.6530	0.5766	0.4855	0.5289	0.5121	0.4870	0.5365	0.5077
NA1C5B	0.0566	0.0609	0.5819	0.5136	0.7294	0.3173	0.3199	0.3137	0.3240	0.2732

[a] Ag-109 exists in spent fuel and/or control rods.

Table C.6 Nuclide-reaction specific *g* index for GBC60 (continued)

CRC state-points	^{133}Cs	^{143}Nd	^{145}Nd	^{147}Sm	^{149}Sm	^{150}Sm	^{151}Sm	^{152}Sm	^{153}Eu	^{155}Gd
CR3SP1	0.0000	0.0000	0.0000	0.0000	0.0000	0.0000	0.0000	0.0000	0.0000	0.0000
CR3SP2	0.4286	0.3751	0.3895	0.1463	0.4286	0.7479	0.2849	0.3549	0.4578	0.2274
CR3SP3	0.6287	0.5399	0.5852	0.2028	0.6287	0.7946	0.4698	0.4302	0.7019	0.4207
CR3SP4	0.4840	0.4067	0.4463	0.1986	0.4840	0.6454	0.3248	0.3411	0.5265	0.2899
CR3SP5	0.4442	0.3667	0.4110	0.1995	0.4442	0.6526	0.2947	0.3135	0.4720	0.2729
CR3SP6	0.6304	0.5175	0.5907	0.2299	0.6304	0.7740	0.4587	0.4154	0.6833	0.4465
CR3SP7	0.7118	0.5772	0.6687	0.2614	0.7118	0.7858	0.5352	0.4560	0.7767	0.5411
CR3SP8	0.3620	0.2981	0.3330	0.1178	0.3620	0.4726	0.2514	0.2298	0.3963	0.2325
CR3SP9	0.6773	0.5438	0.6334	0.1924	0.6773	0.8019	0.5083	0.4419	0.7385	0.5045
CR3SP10	0.6958	0.5650	0.6511	0.2147	0.6958	0.7926	0.5262	0.4546	0.7587	0.5264
CR3SP11	0.3093	0.2507	0.2835	0.1224	0.3093	0.3765	0.2066	0.1929	0.3379	0.1898
CR3SP12	0.8513	0.6475	0.8009	0.2733	0.8513	0.7919	0.6547	0.5001	0.9103	0.7125
CR3SP13	0.4374	0.3413	0.4075	0.1995	0.4374	0.4533	0.3111	0.2409	0.4848	0.3164
CR3SP14	0.5875	0.4569	0.5479	0.2998	0.5875	0.7338	0.4132	0.3703	0.6209	0.4270
CR3SP15	0.8989	0.7036	0.8611	0.4124	0.8989	0.8217	0.7310	0.5374	0.9253	0.8380
CR3SP16	0.3666	0.2744	0.3409	0.2042	0.3666	0.3399	0.2474	0.1947	0.4013	0.2588
CR3SP17	0.7248	0.5339	0.6819	0.3103	0.7248	0.7408	0.5078	0.4269	0.7677	0.5558
CR3SP18	0.7727	0.5650	0.7260	0.3374	0.7727	0.7453	0.5408	0.4465	0.8188	0.6039
CR3SP19	0.7923	0.5880	0.7474	0.4182	0.7923	0.7443	0.5620	0.4558	0.8397	0.6288
CR3SP20	0.8890	0.6812	0.8505	0.4751	0.8890	0.7189	0.7016	0.5242	0.9151	0.8195
CR3SP21	0.8914	0.6880	0.8526	0.4846	0.8914	0.7740	0.7076	0.5274	0.9165	0.8263
CR3SP22	0.3988	0.2938	0.3738	0.2182	0.3988	0.3818	0.2641	0.2162	0.4308	0.2787
CR3SP23	0.5510	0.3935	0.5179	0.2435	0.5510	0.6889	0.3595	0.3453	0.5712	0.3867
CR3SP24	0.5973	0.4276	0.5665	0.2560	0.5973	0.6772	0.3958	0.3719	0.6242	0.4242
CR3SP25	0.8678	0.6429	0.8213	0.3941	0.8678	0.7864	0.6516	0.4960	0.8942	0.7614
CR3SP26	0.8672	0.6412	0.8212	0.3946	0.8672	0.6943	0.6537	0.5015	0.8938	0.7645
CR3SP27	0.8957	0.6996	0.8575	0.4581	0.8957	0.7918	0.7328	0.5428	0.9187	0.8368
CR3SP28	0.4153	0.3022	0.3890	0.2116	0.4153	0.3837	0.2716	0.2238	0.4465	0.2882
CR3SP29	0.6385	0.4571	0.6103	0.2745	0.6385	0.6386	0.4318	0.3903	0.6694	0.4651
CR3SP30	0.7371	0.5326	0.6959	0.3291	0.7371	0.7433	0.5032	0.4266	0.7707	0.5613
CR3SP31	0.8662	0.6311	0.8214	0.3993	0.8662	0.6948	0.6504	0.4990	0.8927	0.7658
CR3SP32	0.4076	0.2914	0.3839	0.1435	0.4076	0.3771	0.2759	0.2054	0.4422	0.3017
CR3SP33	0.9027	0.7209	0.8670	0.4303	0.9027	0.8236	0.7619	0.5592	0.9232	0.8511
SQ2C3BZ	0.4466	0.3368	0.4209	0.2007	0.4466	0.5555	0.3318	0.2731	0.4842	0.3024
SQ2C3BF	0.4547	0.3313	0.4329	0.2052	0.4547	0.3875	0.3296	0.2617	0.5002	0.3055
SQ2C3M	0.7815	0.5517	0.7429	0.7267	0.7815	0.6123	0.5887	0.4313	0.8369	0.5930
SU1C2B	0.3444	0.3021	0.3287	0.1373	0.3444	0.3979	0.2712	0.2190	0.3899	0.2313
SU1C2E	0.6334	0.5214	0.6202	0.1919	0.6334	0.5712	0.5400	0.4195	0.7243	0.4734
TMI1C5B	0.5254	0.4262	0.5002	0.6936	0.5254	0.6420	0.3974	0.3235	0.5693	0.3460
NA1C5B	0.3281	0.2434	0.3079	0.1665	0.3281	0.3692	0.2214	0.1966	0.3493	0.2039

Table C.7 Relative standard deviation of k_{eff} due to uncovered sensitivity data for GBC10

Covariance matrix						
nuclide-reaction		with nuclide-reaction		% $\Delta k_{eff}/k_{eff}$ due to this matrix		
u-235	nubar	u-235	nubar	4.19E-01	± 7.53E-05	
u-238	n,gamma	u-238	n,gamma	3.30E-01	± 1.02E-03	
pu-239	nubar	pu-239	nubar	3.16E-01	± 4.32E-05	
h-1	elastic	h-1	elastic	2.00E-01	± 2.47E-02	
pu-240	n,gamma	pu-240	n,gamma	1.88E-01	± 9.36E-04	***
u-238	elastic	u-238	elastic	1.75E-01	± 9.17E-03	***
pu-239	nubar	u-235	nubar	1.72E-01	± 3.22E-05	
pu-239	n,gamma	pu-239	n,gamma	1.47E-01	± 4.31E-04	
pu-239	fission	pu-239	fission	1.18E-01	± 2.41E-04	
u-235	n,gamma	u-235	n,gamma	1.15E-01	± 3.53E-04	
u-235	fission	u-235	fission	1.15E-01	± 2.27E-04	
pu-239	chi	pu-239	chi	9.42E-02	± 4.61E-04	
u-238	fission	u-238	fission	8.28E-02	± 1.33E-04	
pu-239	fission	pu-239	n,gamma	6.27E-02	± 5.57E-04	
h-1	n,gamma	h-1	n,gamma	6.10E-02	± 1.39E-04	
u-238	nubar	u-238	nubar	4.76E-02	± 1.22E-05	
pu-241	nubar	u-235	nubar	4.18E-02	± 8.47E-06	
o-16	n,alpha	o-16	n,alpha	3.48E-02	± 2.44E-04	
pu-241	nubar	pu-241	nubar	3.42E-02	± 5.13E-06	
pu-239	nubar	pu-241	nubar	2.90E-02	± 5.04E-06	
am-241	n,gamma	am-241	n,gamma	2.38E-02	± 6.92E-05	***
sm-149	n,gamma	sm-149	n,gamma	1.89E-02	± 5.25E-05	***
o-16	elastic	o-16	elastic	1.64E-02	± 3.78E-03	
u-238	n,n'	u-238	n,n'	1.49E-02	± 4.64E-03	
nd-143	n,gamma	nd-143	n,gamma	1.39E-02	± 3.21E-05	***
pu-241	n,gamma	pu-241	n,gamma	1.12E-02	± 3.02E-05	
u-238	elastic	u-238	n,gamma	1.03E-02	± 1.54E-03	
sm-151	n,gamma	sm-151	n,gamma	9.39E-03	± 3.32E-05	***
rh-103	n,gamma	rh-103	n,gamma	7.74E-03	± 7.00E-05	***
b-10	n,alpha	b-10	n,alpha	7.61E-03	± 2.49E-05	
pu-241	fission	pu-241	fission	7.35E-03	± 1.24E-05	
u-238	n,n'	u-238	elastic	-7.33E-03	± 2.91E-03	
u-238	n,2n	u-238	n,2n	7.25E-03	± 1.76E-04	
u-236	n,gamma	u-236	n,gamma	7.19E-03	± 1.02E-04	***
pu-240	nubar	u-235	nubar	6.24E-03	± 8.43E-07	
u-238	n,n'	u-238	fission	-6.16E-03	± 3.02E-03	
u-234	n,gamma	u-234	n,gamma	5.70E-03	± 9.80E-05	***
pu-239	fission	u-235	fission	5.61E-03	± 6.07E-06	
o-16	elastic	o-16	n,alpha	5.32E-03	± 9.03E-04	
u-238	n,n'	u-238	n,gamma	5.16E-03	± 1.04E-03	
u-238	chi	u-238	chi	5.12E-03	± 2.80E-04	
nd-145	n,gamma	nd-145	n,gamma	5.12E-03	± 4.23E-05	***
cs-133	n,gamma	cs-133	n,gamma	5.07E-03	± 5.24E-05	***
u-238	n,gamma	b-10	n,alpha	4.86E-03	± 4.07E-04	
pu-239	nubar	pu-240	nubar	4.33E-03	± 5.74E-07	

Table C.7 Relative standard deviation of k_{eff} due to uncovered sensitivity data for GBC10 (continued)

Covariance matrix						
nuclide-reaction		with nuclide-reaction		% $\Delta k_{eff}/k_{eff}$ due to this matrix		
tc-99	n,gamma	tc-99	n,gamma	3.83E-03	± 4.87E-05	***
ru-101	n,gamma	ru-101	n,gamma	3.66E-03	± 3.23E-05	***
u-236	chi	u-236	chi	3.60E-03	± 6.77E-07	*
b-11	elastic	b-11	elastic	3.60E-03	± 4.32E-04	
u-236	nubar	u-236	nubar	3.57E-03	± 1.12E-06	*
pu-240	fission	pu-240	n,gamma	-2.88E-03	± 3.97E-05	
sm-147	n,gamma	sm-147	n,gamma	2.82E-03	± 1.80E-05	***
u-235	chi	u-235	chi	2.56E-03	± 3.88E-02	
sm-152	n,gamma	sm-152	n,gamma	2.25E-03	± 2.25E-05	***
np-237	n,gamma	np-237	n,gamma	2.06E-03	± 9.74E-06	***
u-236	fission	u-236	fission	1.86E-03	± 3.20E-06	***
u-238	n,n'	u-238	n,2n	1.83E-03	± 8.95E-04	
pu-240	fission	u-235	fission	1.80E-03	± 2.19E-06	
sm-150	n,gamma	sm-150	n,gamma	1.50E-03	± 8.02E-06	***
pu-241	fission	pu-241	n,gamma	1.45E-03	± 7.18E-05	
mo-95	n,gamma	mo-95	n,gamma	1.35E-03	± 2.35E-05	***
eu-153	n,gamma	eu-153	n,gamma	1.34E-03	± 6.66E-06	***
pu-242	n,gamma	pu-242	n,gamma	1.19E-03	± 3.16E-05	***
pu-241	fission	u-235	fission	1.17E-03	± 1.30E-06	
pu-240	nubar	pu-241	nubar	1.05E-03	± 1.42E-07	
u-234	chi	u-234	chi	9.27E-04	± 1.74E-07	*
o-16	n,n'	o-16	n,n'	9.26E-04	± 3.55E-04	
u-234	nubar	u-234	nubar	9.20E-04	± 9.45E-07	*
gd-155	n,gamma	gd-155	n,gamma	8.41E-04	± 2.81E-06	
pu-241	chi	pu-241	chi	8.08E-04	± 1.08E-04	
pu-240	fission	pu-240	fission	7.64E-04	± 3.02E-06	
o-16	n,n'	o-16	n,alpha	-7.64E-04	± 2.50E-04	
u-235	elastic	u-235	elastic	7.63E-04	± 2.96E-03	*
am-241	chi	am-241	chi	7.55E-04	± 1.43E-07	*
pu-240	elastic	pu-240	elastic	6.03E-04	± 1.23E-02	*
u-234	fission	u-234	fission	5.93E-04	± 1.92E-06	*
b-10	n,alpha	b-10	elastic	-5.92E-04	± 1.46E-04	
ag-109	n,gamma	ag-109	n,gamma	5.86E-04	± 1.05E-05	***
am-241	fission	u-235	fission	5.55E-04	± 7.02E-07	
u-238	elastic	u-238	fission	-4.40E-04	± 8.48E-05	
o-16	n,gamma	o-16	n,gamma	4.39E-04	± 1.10E-06	***
u-236	elastic	u-236	elastic	4.35E-04	± 4.64E-03	*
am-241	nubar	am-241	nubar	4.12E-04	± 6.19E-08	***
u-235	n,n'	u-235	n,n'	3.96E-04	± 4.91E-04	*
np-237	chi	np-237	chi	3.84E-04	± 7.28E-08	*
np-237	nubar	np-237	nubar	3.84E-04	± 5.99E-08	***
pu-242	fission	u-235	fission	3.18E-04	± 4.24E-07	
pu-240	nubar	pu-240	nubar	2.32E-04	± 3.18E-08	
o-16	elastic	o-16	n,n'	2.31E-04	± 1.03E-03	
pu-238	chi	pu-238	chi	2.15E-04	± 4.05E-08	*

Table C.7 Relative standard deviation of k_{eff} due to uncovered sensitivity data for GBC10 (continued)

Covariance matrix nuclide-reaction		with nuclide-reaction		% $\Delta k_{eff}/k_{eff}$ due to this matrix		
am-241	fission	am-241	fission	1.95E-04	± 4.06E-07	***
eu-151	n,gamma	eu-151	n,gamma	1.93E-04	± 6.77E-07	***
pu-238	n,gamma	pu-238	n,gamma	1.80E-04	± 5.58E-07	***
u-235	n,2n	u-235	n,2n	1.39E-04	± 2.52E-06	*
np-237	fission	np-237	fission	1.32E-04	± 1.48E-07	***
pu-242	nubar	pu-242	nubar	1.15E-04	± 3.98E-07	*
pu-239	elastic	pu-239	elastic	1.14E-04	± 1.91E-05	***
b-10	n,p	b-10	n,p	1.08E-04	± 2.26E-05	*
mo-95	elastic	mo-95	elastic	1.06E-04	± 2.31E-03	*
u-234	elastic	u-234	elastic	1.06E-04	± 3.48E-05	***
o-16	n,p	o-16	n,p	1.00E-04	± 8.11E-06	

* indicates default covariance data.
*** indicates default covariance data used to correct zeros or large values in some groups.

Table C.8 Relative standard deviation of k_{eff} due to uncovered sensitivity data for GBC20

Covariance matrix						
nuclide-reaction		with nuclide-reaction		% $\Delta k_{eff}/k_{eff}$ due to this matrix		
pu-239	nubar	pu-239	nubar	3.92E-01	± 6.44E-05	
pu-240	n,gamma	pu-240	n,gamma	3.52E-01	± 1.37E-03	***
u-235	nubar	u-235	nubar	3.45E-01	± 7.45E-05	
u-238	n,gamma	u-238	n,gamma	3.18E-01	± 8.94E-04	
h-1	elastic	h-1	elastic	2.12E-01	± 2.67E-02	
pu-239	n,gamma	pu-239	n,gamma	1.87E-01	± 5.06E-04	
pu-239	nubar	u-235	nubar	1.76E-01	± 3.83E-05	
u-238	elastic	u-238	elastic	1.73E-01	± 8.14E-03	***
pu-239	fission	pu-239	fission	1.47E-01	± 2.77E-04	
pu-239	chi	pu-239	chi	1.17E-01	± 7.01E-04	
u-235	n,gamma	u-235	n,gamma	1.07E-01	± 2.96E-04	
u-235	fission	u-235	fission	9.99E-02	± 1.73E-04	
pu-241	nubar	pu-241	nubar	9.29E-02	± 1.67E-05	
u-238	fission	u-238	fission	8.28E-02	± 1.25E-04	
pu-239	fission	pu-239	n,gamma	7.51E-02	± 6.63E-04	
am-241	n,gamma	am-241	n,gamma	6.70E-02	± 1.76E-04	***
pu-241	nubar	u-235	nubar	6.35E-02	± 1.49E-05	
h-1	n,gamma	h-1	n,gamma	5.52E-02	± 1.55E-04	
pu-239	nubar	pu-241	nubar	5.38E-02	± 1.09E-05	
u-238	nubar	u-238	nubar	4.73E-02	± 1.48E-05	
o-16	n,alpha	o-16	n,alpha	3.48E-02	± 2.28E-04	
pu-241	n,gamma	pu-241	n,gamma	3.05E-02	± 7.53E-05	
nd-143	n,gamma	nd-143	n,gamma	2.54E-02	± 5.47E-05	***
sm-149	n,gamma	sm-149	n,gamma	2.26E-02	± 6.09E-05	***
pu-241	fission	pu-241	fission	2.08E-02	± 3.08E-05	
o-16	elastic	o-16	elastic	1.92E-02	± 3.53E-03	
u-238	n,n'	u-238	n,n'	1.73E-02	± 4.34E-03	
rh-103	n,gamma	rh-103	n,gamma	1.53E-02	± 1.22E-04	***
sm-151	n,gamma	sm-151	n,gamma	1.27E-02	± 4.33E-05	***
u-236	n,gamma	u-236	n,gamma	1.17E-02	± 1.50E-04	***
u-238	elastic	u-238	n,gamma	1.12E-02	± 1.27E-03	
nd-145	n,gamma	nd-145	n,gamma	1.06E-02	± 8.10E-05	***
cs-133	n,gamma	cs-133	n,gamma	1.00E-02	± 9.10E-05	***
pu-240	nubar	u-235	nubar	8.60E-03	± 1.44E-06	
ru-101	n,gamma	ru-101	n,gamma	8.08E-03	± 6.48E-05	***
u-238	n,n'	u-238	elastic	-7.86E-03	± 2.55E-03	
b-10	n,alpha	b-10	n,alpha	7.58E-03	± 2.41E-05	
tc-99	n,gamma	tc-99	n,gamma	7.56E-03	± 8.48E-05	***
pu-239	nubar	pu-240	nubar	7.28E-03	± 1.22E-06	
u-238	n,2n	u-238	n,2n	7.24E-03	± 1.54E-04	
u-236	chi	u-236	chi	6.91E-03	± 1.59E-06	*
u-238	n,n'	u-238	fission	-6.90E-03	± 2.54E-03	
u-236	nubar	u-236	nubar	6.85E-03	± 2.23E-06	*
pu-239	fission	u-235	fission	6.71E-03	± 6.68E-06	
pu-242	n,gamma	pu-242	n,gamma	6.53E-03	± 1.43E-04	***

Table C.8 Relative standard deviation of k_{eff} due to uncovered sensitivity data for GBC20 (continued)

Covariance matrix						
nuclide-reaction		with nuclide-reaction		% $\Delta k_{eff}/k_{eff}$ due to this matrix		
u-234	n,gamma	u-234	n,gamma	6.09E-03	± 9.17E-05	***
np-237	n,gamma	np-237	n,gamma	5.69E-03	± 2.43E-05	***
o-16	elastic	o-16	n,alpha	5.55E-03	± 8.24E-04	
u-238	n,n'	u-238	n,gamma	5.44E-03	± 8.89E-04	
sm-147	n,gamma	sm-147	n,gamma	5.22E-03	± 3.05E-05	***
u-238	chi	u-238	chi	5.03E-03	± 3.45E-04	
u-238	n,gamma	b-10	n,alpha	4.81E-03	± 3.61E-04	
sm-152	n,gamma	sm-152	n,gamma	4.75E-03	± 4.37E-05	***
pu-240	fission	pu-240	n,gamma	-4.25E-03	± 4.62E-05	
u-235	chi	u-235	chi	4.11E-03	± 2.03E-02	
eu-153	n,gamma	eu-153	n,gamma	3.86E-03	± 1.71E-05	***
u-236	fission	u-236	fission	3.67E-03	± 5.36E-06	***
sm-150	n,gamma	sm-150	n,gamma	3.44E-03	± 1.87E-05	***
b-11	elastic	b-11	elastic	3.23E-03	± 4.34E-04	
mo-95	n,gamma	mo-95	n,gamma	2.71E-03	± 4.23E-05	***
pu-240	fission	u-235	fission	2.71E-03	± 3.00E-06	
pu-240	nubar	pu-241	nubar	2.63E-03	± 4.40E-07	
pu-241	chi	pu-241	chi	2.28E-03	± 3.48E-04	
am-241	chi	am-241	chi	2.28E-03	± 5.27E-07	*
pu-241	fission	u-235	fission	2.06E-03	± 2.06E-06	
u-238	n,n'	u-238	n,2n	1.96E-03	± 7.36E-04	
gd-155	n,gamma	gd-155	n,gamma	1.76E-03	± 5.78E-06	
ag-109	n,gamma	ag-109	n,gamma	1.57E-03	± 2.42E-05	***
pu-240	fission	pu-240	fission	1.54E-03	± 3.05E-06	
pu-241	fission	pu-241	n,gamma	-1.41E-03	± 4.82E-04	
am-241	nubar	am-241	nubar	1.32E-03	± 2.45E-07	***
u-236	elastic	u-236	elastic	1.23E-03	± 6.91E-03	*
pu-238	chi	pu-238	chi	1.15E-03	± 2.66E-07	*
np-237	chi	np-237	chi	1.12E-03	± 2.59E-07	*
np-237	nubar	np-237	nubar	1.12E-03	± 2.14E-07	***
pu-240	elastic	pu-240	elastic	1.06E-03	± 1.03E-02	*
u-234	chi	u-234	chi	1.03E-03	± 2.38E-07	*
u-234	nubar	u-234	nubar	1.03E-03	± 1.01E-06	*
o-16	n,n'	o-16	n,n'	9.98E-04	± 3.24E-04	
am-241	fission	u-235	fission	9.93E-04	± 1.13E-06	
u-235	elastic	u-235	elastic	9.57E-04	± 5.99E-03	*
pu-238	n,gamma	pu-238	n,gamma	9.08E-04	± 2.62E-06	***
o-16	n,n'	o-16	n,alpha	-7.85E-04	± 2.26E-04	
pu-242	fission	u-235	fission	7.82E-04	± 9.12E-07	
pu-242	nubar	pu-242	nubar	6.98E-04	± 2.03E-06	*
u-234	fission	u-234	fission	6.69E-04	± 2.10E-06	*
am-243	n,gamma	am-243	n,gamma	6.12E-04	± 7.15E-06	***
b-10	n,alpha	b-10	elastic	-5.87E-04	± 1.07E-04	
pu-238	nubar	pu-238	nubar	5.52E-04	± 6.34E-08	***

Table C.8 Relative standard deviation of k_{eff} due to uncovered sensitivity data for GBC20 (continued)

Covariance matrix						
nuclide-reaction		with nuclide-reaction		% $\Delta k_{eff}/k_{eff}$ due to this matrix		
am-241	fission	am-241	fission	5.44E-04	± 1.01E-06	***
pu-240	nubar	pu-240	nubar	5.23E-04	± 8.91E-08	
u-235	n,n'	u-235	n,n'	4.96E-04	± 2.56E-04	*
u-238	elastic	u-238	fission	-4.59E-04	± 7.39E-05	
o-16	n,gamma	o-16	n,gamma	3.88E-04	± 1.11E-06	***
np-237	fission	np-237	fission	3.87E-04	± 4.03E-07	***
mo-95	elastic	mo-95	elastic	3.38E-04	± 2.57E-03	*
am-241	fission	am-241	n,gamma	-3.02E-04	± 2.78E-06	
pu-238	fission	pu-238	fission	2.83E-04	± 2.14E-07	***
eu-151	n,gamma	eu-151	n,gamma	2.80E-04	± 9.64E-07	***
o-16	elastic	o-16	n,n'	2.62E-04	± 8.72E-04	
pu-239	elastic	pu-239	elastic	2.08E-04	± 2.58E-05	***
u-234	elastic	u-234	elastic	1.38E-04	± 3.33E-05	***
u-235	n,2n	u-235	n,2n	1.37E-04	± 2.14E-06	*
pu-239	n,n'	pu-239	n,n'	1.37E-04	± 7.27E-05	*
b-10	elastic	b-10	elastic	1.13E-04	± 4.64E-05	***
sm-147	elastic	sm-147	elastic	1.10E-04	± 1.74E-03	*
am-243	nubar	am-243	nubar	1.08E-04	± 3.62E-04	*
b-10	n,p	b-10	n,p	1.08E-04	± 2.11E-05	*
am-243	chi	am-243	chi	1.07E-04	± 2.48E-08	*
o-16	n,p	o-16	n,p	1.06E-04	± 7.48E-06	
pu-242	fission	pu-242	fission	1.06E-04	± 1.11E-07	***

* indicates default covariance data.
*** indicates default covariance data used to correct zeros or large values in some groups.

Table C.9 Relative standard deviation of k_{eff} due to uncovered sensitivity data for GBC30

Covariance matrix						
nuclide-reaction		with nuclide-reaction		% $\Delta k_{eff}/k_{eff}$ due to this matrix		
pu-240	n,gamma	pu-240	n,gamma	4.34E-01	± 1.82E-03	***
pu-239	nubar	pu-239	nubar	4.10E-01	± 5.61E-05	
u-235	nubar	u-235	nubar	3.20E-01	± 5.74E-05	
u-238	n,gamma	u-238	n,gamma	3.10E-01	± 9.46E-04	
h-1	elastic	h-1	elastic	2.14E-01	± 2.56E-02	
pu-239	n,gamma	pu-239	n,gamma	1.99E-01	± 5.86E-04	
pu-239	nubar	u-235	nubar	1.75E-01	± 3.08E-05	
u-238	elastic	u-238	elastic	1.74E-01	± 8.88E-03	***
pu-239	fission	pu-239	fission	1.56E-01	± 3.15E-04	
pu-241	nubar	pu-241	nubar	1.27E-01	± 1.89E-05	
pu-239	chi	pu-239	chi	1.18E-01	± 6.44E-04	
u-235	n,gamma	u-235	n,gamma	1.08E-01	± 3.29E-04	
u-235	fission	u-235	fission	9.73E-02	± 1.70E-04	
am-241	n,gamma	am-241	n,gamma	9.38E-02	± 2.67E-04	***
u-238	fission	u-238	fission	8.26E-02	± 1.35E-04	
pu-239	fission	pu-239	n,gamma	7.63E-02	± 7.96E-04	
pu-241	nubar	u-235	nubar	7.23E-02	± 1.36E-05	
pu-239	nubar	pu-241	nubar	6.48E-02	± 1.07E-05	
h-1	n,gamma	h-1	n,gamma	5.06E-02	± 1.45E-04	
u-238	nubar	u-238	nubar	4.69E-02	± 1.25E-05	
pu-241	n,gamma	pu-241	n,gamma	4.16E-02	± 1.10E-04	
o-16	n,alpha	o-16	n,alpha	3.45E-02	± 2.50E-04	
nd-143	n,gamma	nd-143	n,gamma	3.35E-02	± 7.70E-05	***
pu-241	fission	pu-241	fission	2.94E-02	± 4.59E-05	
u-238	n,n'	u-238	n,n'	2.54E-02	± 4.49E-03	
sm-149	n,gamma	sm-149	n,gamma	2.34E-02	± 6.96E-05	***
o-16	elastic	o-16	elastic	2.18E-02	± 3.66E-03	
rh-103	n,gamma	rh-103	n,gamma	2.03E-02	± 1.77E-04	***
nd-145	n,gamma	nd-145	n,gamma	1.50E-02	± 1.28E-04	***
u-236	n,gamma	u-236	n,gamma	1.47E-02	± 2.05E-04	***
sm-151	n,gamma	sm-151	n,gamma	1.47E-02	± 5.47E-05	***
cs-133	n,gamma	cs-133	n,gamma	1.36E-02	± 1.31E-04	***
ru-101	n,gamma	ru-101	n,gamma	1.20E-02	± 1.05E-04	***
pu-242	n,gamma	pu-242	n,gamma	1.13E-02	± 2.77E-04	***
u-238	elastic	u-238	n,gamma	1.10E-02	± 1.41E-03	
u-238	n,n'	u-238	elastic	-1.04E-02	± 2.38E-03	
tc-99	n,gamma	tc-99	n,gamma	1.01E-02	± 1.22E-04	***
u-236	chi	u-236	chi	9.99E-03	± 1.95E-06	*
u-236	nubar	u-236	nubar	9.91E-03	± 3.05E-06	*
pu-240	nubar	u-235	nubar	9.75E-03	± 1.40E-06	
np-237	n,gamma	np-237	n,gamma	9.52E-03	± 4.48E-05	***
u-238	n,n'	u-238	fission	-9.22E-03	± 2.05E-03	
pu-239	nubar	pu-240	nubar	8.74E-03	± 1.19E-06	
u-235	chi	u-235	chi	8.33E-03	± 7.35E-03	
b-10	n,alpha	b-10	n,alpha	7.62E-03	± 2.79E-05	
pu-239	fission	u-235	fission	7.47E-03	± 7.90E-06	

Table C.9 Relative standard deviation of k_{eff} due to uncovered sensitivity data for GBC30 (continued)

Covariance matrix						
nuclide-reaction		with nuclide-reaction		% $\Delta k_{eff}/k_{eff}$ due to this matrix		
u-238	n,2n	u-238	n,2n	7.43E-03	± 1.67E-04	
sm-147	n,gamma	sm-147	n,gamma	6.97E-03	± 4.45E-05	***
u-234	n,gamma	u-234	n,gamma	6.57E-03	± 1.06E-04	***
sm-152	n,gamma	sm-152	n,gamma	6.56E-03	± 6.78E-05	***
o-16	elastic	o-16	n,alpha	6.21E-03	± 8.09E-04	
eu-153	n,gamma	eu-153	n,gamma	6.19E-03	± 3.04E-05	***
u-238	n,n'	u-238	n,gamma	5.99E-03	± 8.56E-04	
pu-241	fission	pu-241	n,gamma	-5.53E-03	± 2.45E-04	
u-236	fission	u-236	fission	5.43E-03	± 8.18E-06	***
sm-150	n,gamma	sm-150	n,gamma	4.99E-03	± 3.15E-05	***
u-238	n,gamma	b-10	n,alpha	4.78E-03	± 7.76E-04	
pu-240	fission	pu-240	n,gamma	-4.70E-03	± 5.33E-05	
u-238	chi	u-238	chi	4.35E-03	± 3.32E-04	
b-11	elastic	b-11	elastic	4.07E-03	± 5.02E-04	
mo-95	n,gamma	mo-95	n,gamma	3.76E-03	± 6.44E-05	***
pu-240	nubar	pu-241	nubar	3.61E-03	± 5.16E-07	
am-241	chi	am-241	chi	3.38E-03	± 6.64E-07	*
pu-240	fission	u-235	fission	3.27E-03	± 3.88E-06	
pu-241	fission	u-235	fission	2.61E-03	± 2.79E-06	
gd-155	n,gamma	gd-155	n,gamma	2.57E-03	± 9.36E-06	
pu-238	chi	pu-238	chi	2.52E-03	± 4.95E-07	*
pu-241	chi	pu-241	chi	2.45E-03	± 5.12E-04	
ag-109	n,gamma	ag-109	n,gamma	2.29E-03	± 3.86E-05	***
u-236	elastic	u-236	elastic	2.15E-03	± 1.98E-02	*
am-241	nubar	am-241	nubar	2.04E-03	± 3.23E-07	***
pu-240	fission	pu-240	fission	2.00E-03	± 3.29E-06	
np-237	chi	np-237	chi	1.94E-03	± 3.82E-07	*
np-237	nubar	np-237	nubar	1.94E-03	± 3.15E-07	***
u-238	n,n'	u-238	n,2n	1.92E-03	± 8.36E-04	
pu-238	n,gamma	pu-238	n,gamma	1.90E-03	± 5.98E-06	***
am-243	n,gamma	am-243	n,gamma	1.49E-03	± 1.87E-05	***
pu-242	nubar	pu-242	nubar	1.36E-03	± 5.07E-06	*
pu-238	nubar	pu-238	nubar	1.28E-03	± 1.26E-07	***
am-241	fission	u-235	fission	1.28E-03	± 1.54E-06	
u-234	chi	u-234	chi	1.17E-03	± 2.29E-07	*
u-234	nubar	u-234	nubar	1.16E-03	± 1.26E-06	*
pu-240	elastic	pu-240	elastic	1.15E-03	± 3.31E-02	*
pu-242	fission	u-235	fission	1.12E-03	± 1.40E-06	
u-235	elastic	u-235	elastic	1.03E-03	± 1.01E-03	*
o-16	n,n'	o-16	n,n'	9.02E-04	± 3.50E-04	
o-16	n,n'	o-16	n,alpha	-8.24E-04	± 2.49E-04	
am-241	fission	am-241	fission	7.67E-04	± 1.52E-06	***
u-234	fission	u-234	fission	7.64E-04	± 2.68E-06	*
pu-240	nubar	pu-240	nubar	7.15E-04	± 1.04E-07	
np-237	fission	np-237	fission	6.74E-04	± 7.60E-07	***

Table C.9 Relative standard deviation of k_{eff} due to uncovered sensitivity data for GBC30 (continued)

Covariance matrix nuclide-reaction		with nuclide-reaction		% $\Delta k_{eff}/k_{eff}$ due to this matrix		
pu-238	fission	pu-238	fission	6.60E-04	± 5.44E-07	***
u-235	n,n'	u-235	n,n'	6.56E-04	± 1.09E-04	*
b-10	n,alpha	b-10	elastic	-6.52E-04	± 1.50E-04	
mo-95	elastic	mo-95	elastic	4.86E-04	± 9.77E-03	*
u-238	elastic	u-238	fission	-4.65E-04	± 7.98E-05	
am-241	fission	am-241	n,gamma	-4.50E-04	± 4.44E-06	
nd-145	elastic	nd-145	elastic	3.80E-04	± 9.74E-03	*
o-16	n,gamma	o-16	n,gamma	3.50E-04	± 1.05E-06	***
eu-151	n,gamma	eu-151	n,gamma	3.45E-04	± 1.38E-06	***
o-16	elastic	o-16	n,n'	3.34E-04	± 7.26E-04	
am-243	nubar	am-243	nubar	2.76E-04	± 7.71E-04	*
am-243	chi	am-243	chi	2.75E-04	± 5.40E-08	*
pu-239	elastic	pu-239	elastic	2.54E-04	± 3.32E-05	***
pu-239	n,n'	pu-239	n,n'	2.12E-04	± 5.09E-05	*
am-243	fission	am-243	fission	2.12E-04	± 2.27E-07	***
pu-242	fission	pu-242	fission	2.06E-04	± 2.34E-07	***
b-10	elastic	b-10	elastic	2.04E-04	± 5.19E-05	***
sm-147	elastic	sm-147	elastic	1.72E-04	± 1.61E-02	*
u-234	elastic	u-234	elastic	1.67E-04	± 4.10E-05	***
pu-242	elastic	pu-242	elastic	1.67E-04	± 5.89E-05	***
u-236	n,n'	u-236	n,n'	1.64E-04	± 2.79E-05	*
u-235	n,2n	u-235	n,2n	1.50E-04	± 2.40E-06	*
cs-133	elastic	cs-133	elastic	1.35E-04	± 7.81E-04	*
sm-152	elastic	sm-152	elastic	1.28E-04	± 2.95E-04	***
o-16	n,p	o-16	n,p	1.12E-04	± 8.55E-06	
b-10	n,p	b-10	n,p	1.06E-04	± 4.37E-05	*
nd-143	elastic	nd-143	elastic	1.03E-04	± 1.93E-05	***

* indicates default covariance data.
*** indicates default covariance data used to correct zeros or large values in some groups.

Table C.10 Relative standard deviation of k_{eff} due to uncovered sensitivity data for GBC40

Covariance matrix						
nuclide-reaction		with nuclide-reaction		% $\Delta k_{eff}/k_{eff}$ due to this matrix		
pu-240	n,gamma	pu-240	n,gamma	4.61E-01	± 1.79E-03	***
pu-239	nubar	pu-239	nubar	4.07E-01	± 6.22E-05	
u-235	nubar	u-235	nubar	3.16E-01	± 6.33E-05	
u-238	n,gamma	u-238	n,gamma	3.04E-01	± 8.47E-04	
h-1	elastic	h-1	elastic	2.22E-01	± 2.85E-02	
pu-239	n,gamma	pu-239	n,gamma	2.04E-01	± 5.62E-04	
pu-239	nubar	u-235	nubar	1.75E-01	± 3.36E-05	
u-238	elastic	u-238	elastic	1.73E-01	± 7.88E-03	***
pu-239	fission	pu-239	fission	1.55E-01	± 3.00E-04	
pu-241	nubar	pu-241	nubar	1.40E-01	± 2.32E-05	
pu-239	chi	pu-239	chi	1.16E-01	± 7.34E-04	
u-235	n,gamma	u-235	n,gamma	1.16E-01	± 3.18E-04	
am-241	n,gamma	am-241	n,gamma	1.07E-01	± 2.90E-04	***
u-235	fission	u-235	fission	9.84E-02	± 1.63E-04	
u-238	fission	u-238	fission	8.16E-02	± 1.31E-04	
pu-241	nubar	u-235	nubar	7.61E-02	± 1.57E-05	
pu-239	fission	pu-239	n,gamma	7.51E-02	± 7.65E-04	
pu-239	nubar	pu-241	nubar	6.81E-02	± 1.23E-05	
h-1	n,gamma	h-1	n,gamma	4.85E-02	± 1.67E-04	
pu-241	n,gamma	pu-241	n,gamma	4.62E-02	± 1.18E-04	
u-238	nubar	u-238	nubar	4.62E-02	± 1.39E-05	
nd-143	n,gamma	nd-143	n,gamma	3.84E-02	± 8.43E-05	***
pu-241	fission	pu-241	fission	3.30E-02	± 4.89E-05	
u-238	n,n'	u-238	n,n'	2.76E-02	± 4.27E-03	
sm-149	n,gamma	sm-149	n,gamma	2.32E-02	± 6.73E-05	***
rh-103	n,gamma	rh-103	n,gamma	2.30E-02	± 1.78E-04	***
nd-145	n,gamma	nd-145	n,gamma	1.80E-02	± 1.43E-04	***
u-236	n,gamma	u-236	n,gamma	1.70E-02	± 2.15E-04	***
cs-133	n,gamma	cs-133	n,gamma	1.59E-02	± 1.39E-04	***
sm-151	n,gamma	sm-151	n,gamma	1.58E-02	± 5.81E-05	***
ru-101	n,gamma	ru-101	n,gamma	1.45E-02	± 1.18E-04	***
pu-242	n,gamma	pu-242	n,gamma	1.43E-02	± 3.16E-04	***
np-237	n,gamma	np-237	n,gamma	1.25E-02	± 5.33E-05	***
tc-99	n,gamma	tc-99	n,gamma	1.23E-02	± 1.34E-04	***
u-236	chi	u-236	chi	1.23E-02	± 2.73E-06	*
u-236	nubar	u-236	nubar	1.22E-02	± 3.87E-06	*
u-238	n,n'	u-238	elastic	-1.20E-02	± 2.28E-03	
u-238	elastic	u-238	n,gamma	1.15E-02	± 1.21E-03	
u-235	chi	u-235	chi	1.10E-02	± 6.21E-03	
pu-240	nubar	u-235	nubar	1.04E-02	± 1.68E-06	
u-238	n,n'	u-238	fission	-1.00E-02	± 1.80E-03	
pu-239	nubar	pu-240	nubar	9.26E-03	± 1.35E-06	
sm-147	n,gamma	sm-147	n,gamma	8.06E-03	± 4.74E-05	***
pu-239	fission	u-235	fission	8.04E-03	± 8.19E-06	
pu-241	fission	pu-241	n,gamma	-7.94E-03	± 1.94E-04	
eu-153	n,gamma	eu-153	n,gamma	7.78E-03	± 3.48E-05	***

Table C.10 Relative standard deviation of k_{eff} due to uncovered sensitivity data for GBC40 (continued)

Covariance matrix nuclide-reaction		with nuclide-reaction		% $\Delta k_{eff}/k_{eff}$ due to this matrix		
b-10	n,alpha	b-10	n,alpha	7.47E-03	± 2.79E-05	
u-238	n,2n	u-238	n,2n	7.44E-03	± 1.43E-04	
sm-152	n,gamma	sm-152	n,gamma	7.44E-03	± 7.11E-05	***
u-234	n,gamma	u-234	n,gamma	7.25E-03	± 1.05E-04	***
u-236	fission	u-236	fission	6.74E-03	± 9.64E-06	***
sm-150	n,gamma	sm-150	n,gamma	5.92E-03	± 3.61E-05	***
u-238	n,n'	u-238	n,gamma	5.89E-03	± 8.16E-04	
pu-240	fission	pu-240	n,gamma	-4.79E-03	± 4.68E-05	
u-238	n,gamma	b-10	n,alpha	4.71E-03	± 6.36E-04	
mo-95	n,gamma	mo-95	n,gamma	4.43E-03	± 6.89E-05	***
u-238	chi	u-238	chi	4.14E-03	± 3.86E-04	
pu-240	nubar	pu-241	nubar	4.03E-03	± 6.54E-07	
am-241	chi	am-241	chi	3.98E-03	± 8.88E-07	*
b-11	elastic	b-11	elastic	3.81E-03	± 4.95E-04	
pu-238	chi	pu-238	chi	3.80E-03	± 8.48E-07	*
pu-240	fission	u-235	fission	3.63E-03	± 4.12E-06	
gd-155	n,gamma	gd-155	n,gamma	3.07E-03	± 1.11E-05	
pu-241	fission	u-235	fission	2.96E-03	± 3.03E-06	
u-236	elastic	u-236	elastic	2.93E-03	± 1.24E-02	*
pu-238	n,gamma	pu-238	n,gamma	2.79E-03	± 8.61E-06	***
pu-241	chi	pu-241	chi	2.75E-03	± 6.29E-04	
ag-109	n,gamma	ag-109	n,gamma	2.74E-03	± 4.17E-05	***
np-237	chi	np-237	chi	2.59E-03	± 5.79E-07	*
np-237	nubar	np-237	nubar	2.59E-03	± 4.76E-07	***
am-241	nubar	am-241	nubar	2.46E-03	± 4.43E-07	***
am-243	n,gamma	am-243	n,gamma	2.22E-03	± 2.49E-05	***
pu-240	fission	pu-240	fission	2.20E-03	± 2.88E-06	
pu-238	nubar	pu-238	nubar	2.01E-03	± 2.22E-07	***
pu-242	nubar	pu-242	nubar	1.80E-03	± 7.39E-06	*
am-241	fission	u-235	fission	1.47E-03	± 1.69E-06	
pu-240	elastic	pu-240	elastic	1.36E-03	± 8.74E-03	*
pu-242	fission	u-235	fission	1.35E-03	± 1.62E-06	
u-234	chi	u-234	chi	1.30E-03	± 2.88E-07	*
u-234	nubar	u-234	nubar	1.29E-03	± 1.32E-06	*
u-235	elastic	u-235	elastic	1.21E-03	± 7.03E-04	*
u-238	n,n'	u-238	n,2n	1.16E-03	± 1.19E-03	
pu-238	fission	pu-238	fission	1.03E-03	± 8.28E-07	***
np-237	fission	np-237	fission	8.99E-04	± 9.97E-07	***
am-241	fission	am-241	fission	8.65E-04	± 1.63E-06	***
u-234	fission	u-234	fission	8.50E-04	± 2.87E-06	*
u-235	n,n'	u-235	n,n'	8.27E-04	± 1.33E-04	*
pu-240	nubar	pu-240	nubar	8.05E-04	± 1.33E-07	
mo-95	elastic	mo-95	elastic	6.87E-04	± 8.32E-02	*
b-10	n,alpha	b-10	elastic	-6.24E-04	± 7.68E-05	
nd-145	elastic	nd-145	elastic	5.58E-04	± 3.46E-03	*
am-241	fission	am-241	n,gamma	-5.35E-04	± 4.79E-06	

Table C.10 Relative standard deviation of k_{eff} due to uncovered sensitivity data for GBC40 (continued)

Covariance matrix nuclide-reaction		with nuclide-reaction		% $\Delta k_{eff}/k_{eff}$ due to this matrix		
u-238	elastic	u-238	fission	-4.84E-04	± 6.86E-05	
am-243	nubar	am-243	nubar	4.28E-04	± 9.09E-04	*
am-243	chi	am-243	chi	4.26E-04	± 9.52E-08	*
eu-151	n,gamma	eu-151	n,gamma	3.91E-04	± 1.48E-06	***
am-243	fission	am-243	fission	3.29E-04	± 3.48E-07	***
pu-239	elastic	pu-239	elastic	2.93E-04	± 3.26E-05	***
sm-152	elastic	sm-152	elastic	2.87E-04	± 2.00E-04	***
pu-242	elastic	pu-242	elastic	2.86E-04	± 6.84E-05	***
pu-242	fission	pu-242	fission	2.74E-04	± 3.05E-07	***
pu-239	n,n'	pu-239	n,n'	2.50E-04	± 5.38E-05	*
sm-147	elastic	sm-147	elastic	2.15E-04	± 1.36E-03	*
u-236	n,n'	u-236	n,n'	2.13E-04	± 3.46E-05	*
u-234	elastic	u-234	elastic	1.90E-04	± 3.97E-05	***
cs-133	elastic	cs-133	elastic	1.80E-04	± 3.70E-04	*
u-235	n,2n	u-235	n,2n	1.67E-04	± 2.30E-06	*
nd-143	elastic	nd-143	elastic	1.44E-04	± 2.16E-05	***
b-10	elastic	b-10	elastic	1.32E-04	± 5.36E-05	***
ru-101	elastic	ru-101	elastic	1.29E-04	± 3.80E-04	*
tc-99	elastic	tc-99	elastic	1.24E-04	± 1.60E-03	*
sm-150	elastic	sm-150	elastic	1.08E-04	± 1.23E-03	*
b-10	n,p	b-10	n,p	1.05E-04	± 3.59E-05	*

* indicates default covariance data.
*** indicates default covariance data used to correct zeros or large values in some groups.

Table C.11 Relative standard deviation of k_{eff} due to uncovered sensitivity data for GBC50

Covariance matrix						
nuclide-reaction		with nuclide-reaction		% $\Delta k_{eff}/k_{eff}$ due to this matrix		
pu-240	n,gamma	pu-240	n,gamma	4.80E-01	± 1.92E-03	***
pu-239	nubar	pu-239	nubar	4.04E-01	± 5.69E-05	
u-235	nubar	u-235	nubar	3.14E-01	± 5.80E-05	
u-238	n,gamma	u-238	n,gamma	2.98E-01	± 8.25E-04	
h-1	elastic	h-1	elastic	2.23E-01	± 3.30E-02	
pu-239	n,gamma	pu-239	n,gamma	2.03E-01	± 5.65E-04	
pu-239	nubar	u-235	nubar	1.75E-01	± 3.05E-05	
u-238	elastic	u-238	elastic	1.72E-01	± 7.83E-03	***
pu-239	fission	pu-239	fission	1.55E-01	± 3.00E-04	
pu-241	nubar	pu-241	nubar	1.49E-01	± 2.28E-05	
u-235	n,gamma	u-235	n,gamma	1.21E-01	± 3.28E-04	
am-241	n,gamma	am-241	n,gamma	1.16E-01	± 3.21E-04	***
pu-239	chi	pu-239	chi	1.05E-01	± 7.23E-04	
u-235	fission	u-235	fission	1.02E-01	± 1.62E-04	
u-238	fission	u-238	fission	8.06E-02	± 1.32E-04	
pu-241	nubar	u-235	nubar	7.91E-02	± 1.47E-05	
pu-239	fission	pu-239	n,gamma	7.27E-02	± 7.97E-04	
pu-239	nubar	pu-241	nubar	7.04E-02	± 1.16E-05	
pu-241	n,gamma	pu-241	n,gamma	4.92E-02	± 1.28E-04	
h-1	n,gamma	h-1	n,gamma	4.74E-02	± 1.96E-04	
u-238	nubar	u-238	nubar	4.55E-02	± 1.28E-05	
nd-143	n,gamma	nd-143	n,gamma	4.22E-02	± 9.39E-05	***
u-238	n,n'	u-238	n,n'	3.94E-02	± 4.41E-03	
pu-241	fission	pu-241	fission	3.61E-02	± 5.35E-05	
o-16	n,alpha	o-16	n,alpha	3.36E-02	± 2.45E-04	
o-16	elastic	o-16	elastic	2.64E-02	± 3.74E-03	
rh-103	n,gamma	rh-103	n,gamma	2.52E-02	± 1.93E-04	***
sm-149	n,gamma	sm-149	n,gamma	2.25E-02	± 6.77E-05	***
u-235	chi	u-235	chi	2.23E-02	± 2.79E-03	
nd-145	n,gamma	nd-145	n,gamma	2.07E-02	± 1.68E-04	***
u-236	n,gamma	u-236	n,gamma	1.86E-02	± 2.34E-04	***
cs-133	n,gamma	cs-133	n,gamma	1.76E-02	± 1.55E-04	***
ru-101	n,gamma	ru-101	n,gamma	1.68E-02	± 1.36E-04	***
pu-242	n,gamma	pu-242	n,gamma	1.67E-02	± 3.77E-04	***
sm-151	n,gamma	sm-151	n,gamma	1.66E-02	± 6.24E-05	***
np-237	n,gamma	np-237	n,gamma	1.53E-02	± 6.72E-05	***
u-236	chi	u-236	chi	1.45E-02	± 2.98E-06	*
u-238	n,n'	u-238	elastic	-1.45E-02	± 2.46E-03	
u-236	nubar	u-236	nubar	1.44E-02	± 4.51E-06	*
tc-99	n,gamma	tc-99	n,gamma	1.36E-02	± 1.49E-04	***
u-238	n,n'	u-238	fission	-1.16E-02	± 1.55E-03	
u-238	elastic	u-238	n,gamma	1.10E-02	± 1.24E-03	
pu-240	nubar	u-235	nubar	1.09E-02	± 1.65E-06	
pu-241	fission	pu-241	n,gamma	-1.00E-02	± 1.77E-04	
pu-239	nubar	pu-240	nubar	9.67E-03	± 1.31E-06	
eu-153	n,gamma	eu-153	n,gamma	9.16E-03	± 4.14E-05	***

Table C.11 Relative standard deviation of k_{eff} due to uncovered sensitivity data for GBC50 (continued)

Covariance matrix						
nuclide-reaction		with nuclide-reaction		% $\Delta k_{eff}/k_{eff}$ due to this matrix		
sm-147	n,gamma	sm-147	n,gamma	8.96E-03	± 5.29E-05	***
pu-239	fission	u-235	fission	8.56E-03	± 8.88E-06	
sm-152	n,gamma	sm-152	n,gamma	8.29E-03	± 8.15E-05	***
u-236	fission	u-236	fission	8.05E-03	± 1.16E-05	***
u-234	n,gamma	u-234	n,gamma	7.79E-03	± 1.10E-04	***
b-10	n,alpha	b-10	n,alpha	7.45E-03	± 2.86E-05	
u-238	n,2n	u-238	n,2n	7.28E-03	± 1.40E-04	
o-16	elastic	o-16	n,alpha	6.73E-03	± 7.27E-04	
u-238	n,n'	u-238	n,gamma	6.66E-03	± 7.18E-04	
sm-150	n,gamma	sm-150	n,gamma	6.64E-03	± 4.23E-05	***
pu-238	chi	pu-238	chi	5.23E-03	± 1.08E-06	*
mo-95	n,gamma	mo-95	n,gamma	4.96E-03	± 7.63E-05	***
pu-240	fission	pu-240	n,gamma	-4.84E-03	± 4.62E-05	
u-238	n,gamma	b-10	n,alpha	4.66E-03	± 1.40E-03	
am-241	chi	am-241	chi	4.50E-03	± 9.33E-07	*
pu-240	nubar	pu-241	nubar	4.37E-03	± 6.64E-07	
pu-240	fission	u-235	fission	3.94E-03	± 4.59E-06	
pu-238	n,gamma	pu-238	n,gamma	3.70E-03	± 1.19E-05	***
u-236	elastic	u-236	elastic	3.67E-03	± 3.31E-02	*
gd-155	n,gamma	gd-155	n,gamma	3.49E-03	± 1.33E-05	
pu-241	fission	u-235	fission	3.27E-03	± 3.42E-06	
np-237	chi	np-237	chi	3.26E-03	± 6.77E-07	*
np-237	nubar	np-237	nubar	3.26E-03	± 5.61E-07	***
b-11	elastic	b-11	elastic	3.10E-03	± 5.45E-04	
ag-109	n,gamma	ag-109	n,gamma	3.07E-03	± 4.66E-05	***
am-243	n,gamma	am-243	n,gamma	2.98E-03	± 3.43E-05	***
pu-238	nubar	pu-238	nubar	2.86E-03	± 2.96E-07	***
am-241	nubar	am-241	nubar	2.85E-03	± 4.80E-07	***
u-238	chi	u-238	chi	2.56E-03	± 5.49E-04	
pu-240	fission	pu-240	fission	2.37E-03	± 2.86E-06	
pu-242	nubar	pu-242	nubar	2.22E-03	± 1.15E-05	*
am-241	fission	u-235	fission	1.64E-03	± 1.93E-06	
pu-242	fission	u-235	fission	1.55E-03	± 1.94E-06	
u-238	n,n'	u-238	n,2n	1.55E-03	± 8.59E-04	
pu-238	fission	pu-238	fission	1.47E-03	± 1.23E-06	***
pu-241	chi	pu-241	chi	1.46E-03	± 1.23E-03	
u-234	chi	u-234	chi	1.42E-03	± 2.92E-07	*
u-234	nubar	u-234	nubar	1.41E-03	± 1.44E-06	*
pu-240	elastic	pu-240	elastic	1.25E-03	± 2.28E-02	*
u-235	elastic	u-235	elastic	1.22E-03	± 2.23E-03	*
u-235	n,n'	u-235	n,n'	1.18E-03	± 7.72E-03	*
np-237	fission	np-237	fission	1.14E-03	± 1.30E-06	***
mo-95	elastic	mo-95	elastic	9.52E-04	± 2.13E-02	*
am-241	fission	am-241	fission	9.50E-04	± 1.79E-06	***
u-234	fission	u-234	fission	9.34E-04	± 3.21E-06	*

Table C.11 Relative standard deviation of k_{eff} due to uncovered sensitivity data for GBC50 (continued)

Covariance matrix nuclide-reaction		with nuclide-reaction		% $\Delta k_{eff}/k_{eff}$ due to this matrix		
pu-240	nubar	pu-240	nubar	8.81E-04	± 1.37E-07	
am-241	fission	am-241	n,gamma	-6.05E-04	± 5.52E-06	
am-243	nubar	am-243	nubar	5.88E-04	± 1.20E-03	*
am-243	chi	am-243	chi	5.85E-04	± 1.21E-07	*
o-16	n,n'	o-16	n,alpha	-5.67E-04	± 2.70E-04	
b-10	n,alpha	b-10	elastic	-5.53E-04	± 2.78E-04	
nd-145	elastic	nd-145	elastic	5.42E-04	± 1.63E-02	*
u-238	elastic	u-238	fission	-5.22E-04	± 6.31E-05	
am-243	fission	am-243	fission	4.52E-04	± 5.07E-07	***
sm-152	elastic	sm-152	elastic	4.50E-04	± 1.90E-04	***
eu-151	n,gamma	eu-151	n,gamma	4.30E-04	± 1.72E-06	***
o-16	n,n'	o-16	n,n'	4.24E-04	± 2.89E-04	
pu-242	elastic	pu-242	elastic	3.93E-04	± 8.12E-05	***
o-16	elastic	o-16	n,n'	3.90E-04	± 2.22E-03	
u-236	n,n'	u-236	n,n'	3.72E-04	± 4.88E-05	*
pu-239	n,n'	pu-239	n,n'	3.50E-04	± 1.26E-04	*
pu-242	fission	pu-242	fission	3.38E-04	± 3.94E-07	***
pu-239	elastic	pu-239	elastic	3.29E-04	± 3.48E-05	***
o-16	n,gamma	o-16	n,gamma	3.18E-04	± 1.26E-06	***
sm-147	elastic	sm-147	elastic	2.90E-04	± 6.35E-03	*
cs-133	elastic	cs-133	elastic	2.41E-04	± 9.66E-04	*
u-234	elastic	u-234	elastic	1.95E-04	± 4.22E-05	***
u-235	n,2n	u-235	n,2n	1.79E-04	± 2.43E-06	*
nd-143	elastic	nd-143	elastic	1.68E-04	± 2.37E-05	***
tc-99	elastic	tc-99	elastic	1.60E-04	± 2.36E-03	*
ru-101	elastic	ru-101	elastic	1.60E-04	± 4.70E-04	*
sm-150	elastic	sm-150	elastic	1.45E-04	± 2.09E-03	*
b-10	n,p	b-10	n,p	1.05E-04	± 7.67E-05	*
o-16	n,p	o-16	n,p	1.02E-04	± 6.96E-06	

* indicates default covariance data.
*** indicates default covariance data used to correct zeros or large values in some groups.

Table C.12 Relative standard deviation of k_{eff} due to uncovered sensitivity data for GBC60

Covariance matrix nuclide-reaction		with nuclide-reaction		% $\Delta k_{eff}/k_{eff}$ due to this matrix		
pu-240	n,gamma	pu-240	n,gamma	5.06E-01	± 1.57E-03	***
pu-239	nubar	pu-239	nubar	4.07E-01	± 5.45E-05	
u-235	nubar	u-235	nubar	3.06E-01	± 5.36E-05	
u-238	n,gamma	u-238	n,gamma	2.93E-01	± 6.54E-04	
h-1	elastic	h-1	elastic	2.22E-01	± 2.05E-02	
pu-239	n,gamma	pu-239	n,gamma	2.07E-01	± 4.59E-04	
pu-239	nubar	u-235	nubar	1.75E-01	± 2.84E-05	
u-238	elastic	u-238	elastic	1.68E-01	± 5.59E-03	***
pu-241	nubar	pu-241	nubar	1.62E-01	± 2.35E-05	
pu-239	fission	pu-239	fission	1.58E-01	± 2.38E-04	
am-241	n,gamma	am-241	n,gamma	1.29E-01	± 2.70E-04	***
u-235	n,gamma	u-235	n,gamma	1.23E-01	± 2.72E-04	
pu-239	chi	pu-239	chi	1.05E-01	± 7.08E-04	
u-235	fission	u-235	fission	1.02E-01	± 1.21E-04	
pu-241	nubar	u-235	nubar	8.20E-02	± 1.42E-05	
u-238	fission	u-238	fission	8.08E-02	± 9.72E-05	
pu-239	nubar	pu-241	nubar	7.40E-02	± 1.14E-05	
pu-239	fission	pu-239	n,gamma	7.20E-02	± 6.74E-04	
pu-241	n,gamma	pu-241	n,gamma	5.36E-02	± 1.01E-04	
nd-143	n,gamma	nd-143	n,gamma	4.69E-02	± 7.68E-05	***
u-238	nubar	u-238	nubar	4.55E-02	± 1.22E-05	
h-1	n,gamma	h-1	n,gamma	4.48E-02	± 1.19E-04	
pu-241	fission	pu-241	fission	4.01E-02	± 4.48E-05	
u-238	n,n'	u-238	n,n'	3.99E-02	± 3.15E-03	
o-16	n,alpha	o-16	n,alpha	3.33E-02	± 1.85E-04	
rh-103	n,gamma	rh-103	n,gamma	2.76E-02	± 1.70E-04	***
o-16	elastic	o-16	elastic	2.63E-02	± 2.67E-03	
nd-145	n,gamma	nd-145	n,gamma	2.35E-02	± 1.47E-04	***
sm-149	n,gamma	sm-149	n,gamma	2.27E-02	± 4.99E-05	***
u-235	chi	u-235	chi	2.12E-02	± 2.72E-03	
u-236	n,gamma	u-236	n,gamma	2.05E-02	± 2.00E-04	***
cs-133	n,gamma	cs-133	n,gamma	2.00E-02	± 1.34E-04	***
ru-101	n,gamma	ru-101	n,gamma	1.97E-02	± 1.25E-04	***
pu-242	n,gamma	pu-242	n,gamma	1.92E-02	± 3.40E-04	***
np-237	n,gamma	np-237	n,gamma	1.88E-02	± 6.32E-05	***
sm-151	n,gamma	sm-151	n,gamma	1.78E-02	± 4.90E-05	***
u-236	chi	u-236	chi	1.70E-02	± 3.38E-06	*
u-236	nubar	u-236	nubar	1.69E-02	± 4.61E-06	*
tc-99	n,gamma	tc-99	n,gamma	1.54E-02	± 1.29E-04	***
u-238	n,n'	u-238	elastic	-1.52E-02	± 1.58E-03	
pu-241	fission	pu-241	n,gamma	-1.20E-02	± 1.39E-04	
u-238	n,n'	u-238	fission	-1.19E-02	± 1.10E-03	
pu-240	nubar	u-235	nubar	1.13E-02	± 1.66E-06	
u-238	elastic	u-238	n,gamma	1.13E-02	± 8.12E-04	
eu-153	n,gamma	eu-153	n,gamma	1.09E-02	± 3.84E-05	***
pu-239	nubar	pu-240	nubar	1.02E-02	± 1.30E-06	

Table C.12 Relative standard deviation of k_{eff} due to uncovered sensitivity data for GBC60 (continued)

Covariance matrix nuclide-reaction		with nuclide-reaction		% $\Delta k_{eff}/k_{eff}$ due to this matrix		
sm-147	n,gamma	sm-147	n,gamma	1.00E-02	± 4.64E-05	***
u-236	fission	u-236	fission	9.57E-03	± 1.01E-05	***
sm-152	n,gamma	sm-152	n,gamma	9.15E-03	± 6.95E-05	***
pu-239	fission	u-235	fission	9.03E-03	± 6.99E-06	
u-234	n,gamma	u-234	n,gamma	8.09E-03	± 9.26E-05	***
sm-150	n,gamma	sm-150	n,gamma	7.56E-03	± 3.84E-05	***
u-238	n,2n	u-238	n,2n	7.48E-03	± 1.15E-04	
b-10	n,alpha	b-10	n,alpha	7.34E-03	± 2.24E-05	
pu-238	chi	pu-238	chi	7.22E-03	± 1.44E-06	*
o-16	elastic	o-16	n,alpha	6.78E-03	± 5.26E-04	
u-238	n,n'	u-238	n,gamma	6.57E-03	± 5.30E-04	
mo-95	n,gamma	mo-95	n,gamma	5.51E-03	± 6.75E-05	***
am-241	chi	am-241	chi	5.14E-03	± 1.03E-06	*
pu-238	n,gamma	pu-238	n,gamma	4.99E-03	± 1.15E-05	***
pu-240	fission	pu-240	n,gamma	-4.96E-03	± 3.84E-05	
pu-240	nubar	pu-241	nubar	4.81E-03	± 7.04E-07	
u-238	n,gamma	b-10	n,alpha	4.60E-03	± 1.06E-03	
u-236	elastic	u-236	elastic	4.56E-03	± 1.01E-02	*
pu-240	fission	u-235	fission	4.25E-03	± 3.67E-06	
np-237	chi	np-237	chi	4.10E-03	± 8.20E-07	*
np-237	nubar	np-237	nubar	4.10E-03	± 6.77E-07	***
gd-155	n,gamma	gd-155	n,gamma	4.08E-03	± 1.11E-05	
pu-238	nubar	pu-238	nubar	4.04E-03	± 4.03E-07	***
am-243	n,gamma	am-243	n,gamma	3.96E-03	± 3.36E-05	***
pu-241	fission	u-235	fission	3.59E-03	± 2.77E-06	
ag-109	n,gamma	ag-109	n,gamma	3.53E-03	± 4.19E-05	***
am-241	nubar	am-241	nubar	3.32E-03	± 5.38E-07	***
b-11	elastic	b-11	elastic	3.13E-03	± 3.96E-04	
pu-242	nubar	pu-242	nubar	2.77E-03	± 1.76E-05	*
pu-240	fission	pu-240	fission	2.59E-03	± 2.39E-06	
u-238	chi	u-238	chi	2.58E-03	± 5.28E-04	
pu-238	fission	pu-238	fission	2.09E-03	± 1.27E-06	***
am-241	fission	u-235	fission	1.81E-03	± 1.59E-06	
pu-242	fission	u-235	fission	1.78E-03	± 1.62E-06	
u-234	chi	u-234	chi	1.53E-03	± 3.03E-07	*
u-234	nubar	u-234	nubar	1.52E-03	± 1.28E-06	*
np-237	fission	np-237	fission	1.43E-03	± 1.19E-06	***
u-238	n,n'	u-238	n,2n	1.36E-03	± 8.07E-04	
pu-240	elastic	pu-240	elastic	1.34E-03	± 4.49E-03	*
u-235	elastic	u-235	elastic	1.30E-03	± 1.22E-03	*
pu-241	chi	pu-241	chi	1.24E-03	± 1.66E-03	
u-235	n,n'	u-235	n,n'	1.19E-03	± 1.22E-04	*
mo-95	elastic	mo-95	elastic	1.18E-03	± 1.61E-02	*
am-241	fission	am-241	fission	1.06E-03	± 1.51E-06	***
u-234	fission	u-234	fission	1.01E-03	± 2.85E-06	*

Table C.12 Relative standard deviation of k_{eff} due to uncovered sensitivity data for GBC60 (continued)

Covariance matrix						
nuclide-reaction		with nuclide-reaction		% $\Delta k_{eff}/k_{eff}$ due to this matrix		
pu-240	nubar	pu-240	nubar	9.77E-04	± 1.46E-07	
nd-145	elastic	nd-145	elastic	8.51E-04	± 4.21E-03	*
am-243	nubar	am-243	nubar	8.14E-04	± 1.04E-03	*
am-243	chi	am-243	chi	8.10E-04	± 1.62E-07	*
am-241	fission	am-241	n,gamma	-6.85E-04	± 4.83E-06	
am-243	fission	am-243	fission	6.27E-04	± 5.00E-07	***
o-16	n,n'	o-16	n,alpha	-6.11E-04	± 2.32E-04	
o-16	n,n'	o-16	n,n'	5.91E-04	± 2.61E-04	
b-10	n,alpha	b-10	elastic	-5.59E-04	± 8.32E-04	
pu-242	elastic	pu-242	elastic	5.08E-04	± 7.14E-05	***
u-238	elastic	u-238	fission	-5.01E-04	± 4.58E-05	
eu-151	n,gamma	eu-151	n,gamma	4.72E-04	± 1.47E-06	***
sm-152	elastic	sm-152	elastic	4.66E-04	± 1.68E-04	***
u-236	n,n'	u-236	n,n'	4.39E-04	± 1.96E-04	*
pu-242	fission	pu-242	fission	4.24E-04	± 3.55E-07	***
sm-147	elastic	sm-147	elastic	3.76E-04	± 2.16E-03	*
pu-239	n,n'	pu-239	n,n'	3.70E-04	± 2.79E-04	*
pu-239	elastic	pu-239	elastic	3.63E-04	± 2.52E-05	***
o-16	n,gamma	o-16	n,gamma	3.00E-04	± 7.86E-07	***
cs-133	elastic	cs-133	elastic	2.99E-04	± 5.68E-04	*
u-234	elastic	u-234	elastic	2.18E-04	± 3.24E-05	***
nd-143	elastic	nd-143	elastic	2.06E-04	± 2.20E-05	***
ru-101	elastic	ru-101	elastic	2.00E-04	± 8.40E-04	*
tc-99	elastic	tc-99	elastic	1.96E-04	± 3.18E-03	*
sm-150	elastic	sm-150	elastic	1.91E-04	± 3.89E-04	*
u-235	n,2n	u-235	n,2n	1.89E-04	± 2.03E-06	*
b-10	elastic	b-10	elastic	1.80E-04	± 4.46E-05	***
cs-133	n,n'	cs-133	n,n'	1.20E-04	± 2.45E-05	*
o-16	n,p	o-16	n,p	1.11E-04	± 6.13E-06	
ru-101	n,n'	ru-101	n,n'	1.11E-04	± 2.88E-05	*
b-10	n,p	b-10	n,p	1.04E-04	± 6.10E-05	*

* indicates default covariance data.
*** indicates default covariance data used to correct zeros or large values in some groups.

NUREG/CR-6951
ORNL/TM-2006/87
December 2007